Adaptation of energy systems to climate change and water resource constraints

SIMON CHRISTOPHER PARKINSON

B.Sc.E., University of Saskatchewan, 2008

M.A.Sc., University of Victoria, 2011

A dissertation submitted in partial fulfillment of the requirements for the degree of

DOCTOR OF PHILOSOPHY

In the department of

MECHANICAL ENGINEERING

Adaptation of energy systems to climate change and water resource constraints

Simon Christopher Parkinson

B.Sc.E., University of Saskatchewan, 2008

M.A.Sc., University of Victoria, 2011

Supervisory Committee

Prof. Ned Djilali, Supervisor

(Department of Mechanical Engineering)

Prof. Andrew Rowe, Departmental Member

(Department of Mechanical Engineering)

Prof. Tom Gleeson, Outside Member

(Department of Civil Engineering)

Supervisory Committee

Prof. Ned Djilali, Supervisor
(Department of Mechanical Engineering)

Prof. Andrew Rowe, Departmental Member
(Department of Mechanical Engineering)

Prof. Tom Gleeson, Outside Member
(Department of Civil Engineering)

Abstract

This dissertation assesses the long-term technological and policy implications of adapting to water constraints and climate change impacts in the energy sector. Energy systems are increasingly vulnerable to climate change and water resource variability. Yet, the majority of long-term energy infrastructure plans ignore adaptation strategy. New analytical approaches are needed to address the spatial and temporal scales relevant to both climate change and water resources. The research in this dissertation overcomes these challenges with improved engineering-economic modeling. Specifically, the conventional systems-engineering energy technology planning framework is extended to incorporate: (1) robust capacity decisions in the electricity sector in light of impacts from hydro-climatic change and uncertain environmental performance of technology options; (2) an endogenous, spatially-distributed representation of water systems and feedbacks with energy demand; and (3) multi-objective decision-making. The computational modeling framework is applied to four regional case study analyses to quantify previously unaccounted for policy-relevant interactions between water, energy and climate systems. Application of the robust adaptation planning framework to the power system in British Columbia, Canada, reveals technology configurations offering long-term operational flexibility will be needed to ensure reliability under projected climate change impacts to provincial hydropower resources and electricity demand. The imposed flexibility requirements affect the suitability of technology options, and increases the cost of long-term electricity system operation. The case study analysis then focuses on the interaction between groundwater conservation and concurrent policy aimed at reducing electricity sector carbon emissions in the water-stressed country of Saudi Arabia. Application of the novel water-energy infrastructure planning framework reveals that transitioning away from non-renewable groundwater use by the year 2050 could increase national electricity demand by more than 40 % relative to 2010 conditions, and require investments similar to strategies aimed at transitioning away from fossil fuels in the electricity sector. The research in this dissertation demonstrates the crucial need for regional planners to account for adaptation to climate change and water resource constraints when developing long-term energy strategy.

Contents

List of Figures

List of Tables

Acknowledgements

I thank Ned Djilali for providing me with the guidance needed to complete this PhD. Ned's support and collaboration enabled me to explore exciting new research ideas while fulfilling my academic requirements efficiently.

I thank Keywan Riahi and Volker Krey for hosting me at the International Institute for Applied Systems Analysis. This opportunity allowed me to access important data and contribute to an active research program with a global perspective.

I thank Andrew Rowe and Tom Gleeson for providing detailed feedback regarding the direction of my research.

I thank Pat Wagner, Gardina Kartasasmita, Pauline Shepherd, Sue Walton and Susan Wignall for the administrative support.

I am very fortunate to have such an amazing family that provided me with support and inspiration throughout my journey.

Funding from the Natural Sciences & Engineering Research Council of Canada is gratefully acknowledged.

Chapter 1

Introduction

1.1 Motivation

Water plays a key role in the supply of energy in many regions globally, primarily for thermal power plant cooling, fuel processing and hydropower generation [1]. Constraints on the availability of water resources in these regions therefore pose risks to the reliable supply of energy. At the same time, a significant amount of energy is required to extract, treat and distribute water resources [2]. Constraints on the supply of water services therefore pose risks of additional energy requirements. Moreover, energy and water are required for meeting the development goals of societies. These interdependencies promote coordinated planning of water and energy systems.

Additional energy system planning challenges are posed by climate change. Projections of future climate under a range of possible greenhouse gas emission pathways indicate that a 1 to 2 °C increase in global mean temperature change is likely by mid-century, with concurrent large-scale shifts in global precipitation patterns and water resource availability [3]. Energy infrastructure developed this decade is likely to operate until mid-century, making these assets vulnerable to projected hydro-climatic change [4, 5]. Moreover, technology investments impart long-term structural inertia into the entire energy supply chain that can impact technology decisions for many decades to come [6]. To ensure long-term reliability of energy systems, it is essential that regional planners integrate climate change adaptation into system development strategy.

Adaptation here refers to the anticipation of effects from climate change and water contraints, and taking the appropriate measures to reduce foreseen damages or maximize any opportunities during system design. Adaptation measures from a systems engineering perspective include modifications to the operation of existing assets or transformation in the integrated system structure through development and decomissioning of technologies. Although energy sector adaptation strategy addressing both climate change and water resource constraints is an increasingly urgent issue facing regional planners, it is not included in the majority of long-term energy infrastructure plans. New analytical approaches are needed to address the complex challenge of assessing energy systems at spatial and temporal scales relevant to both climate change and water resources. The research presented in this dissertation seeks to provide insight into how these challenges can be overcome by exploring alternative formulations of the long-term energy planning model. Specifically, this research focuses on improving the endogenous representation of water supply systems in energy optimization models and addressing long-term uncertainty due to climate change during system design. The improved systems analysis tools are applied in this dissertation to assess the long-term technological and policy implications of adapting to water constraints and climate change impacts in the energy sector.

1.2 Previous work

1.2.1 Assessing energy sector transformation pathways

Computational models have emerged as important tools for assessing the benefits of different transformation strategies in the energy sector [7–9]. These tools focus on assessing potential transformations in the context of different performance criteria, such as reliability, costs and environmental impacts. Mathematical programming enables modeling development scenarios that optimize system performance. Such frameworks are also commonly referred to as engineering-economic models due to the usual focus on minimizing system production costs.

Infrastructure development decisions are tackled with models that optimize system capacity. Capacity decisions incorporate both the size and location of new technologies, and are key design parameters for regional planners due to the relationship with geographical constraints, investment costs and long-term structural inertia of the supply systems [6]. Moreover, capacity decisions are crucial from the perspective of adaptation strategy due to the opportunity to embed adaptation measures during infrastructure development. Strategizing capacity decisions is also commonly referred to as capacity expansion planning, but may also entail reductions in system capacity in situations where reduced demands are projected. Due to the impact on long-term structural inertia, capacity decisions are usually assessed over multi-decadal time periods.

A large body of previous work demonstrates application of mathematical programming models to the assessment of long-term energy transitions. The majority of this work focuses on the economic impacts of low-carbon energy pathways [10], although the scope of similar models are being increasingly broadened to enable analysis of co-benefits such as reducing air pollution and increasing energy security [11].

1.2.2 Water-energy nexus analysis

A number of previous studies demonstrate the risks posed to water resources by regional low-carbon energy transitions. Specific concern surrounds increased development of bioenergy, and the potential use of irrigated crops as energy feedstock. Global analysis with an integrated model of the energy-land-climate system estimates that the scale of future bioenergy expansion consistent with deep global decarbonization can be supported primarily with rainfed crops [12]. Nonetheless, any precipitation incorporated into the feedstock biomass will be significant, and becomes unavailable for downstream purposes such as ground and surface water recharge [13]. Downscaled decarbonization scenarios for the United States indicate increased risk of regional water stress due to potential bioenergy expansion that could exceed the anticipated water impacts of more extreme climate change [14]. This previous research demonstrates the importance of assessing water constraints during the formulation of climate change mitigation strategies involving bioenergy.

Low-carbon transitions including electric power generated with thermal processes could also lead to increased stress on water resources due to the potential water demand for process cooling [15–20]. Alternative cooling technologies can significantly reduce cooling water demand, but are also more expensive. The costs of transitioning the existing electricity supply to cooling systems with zero freshwater use was considered for the United States using spatially-explicit cost functions for alternative cooling technologies [21]. The analysis suggests the transition would cost \$3.53/MWh or less than 4% of recently reported average electricity prices in the United States [22]. Several other studies have examined the impact of water availability on the development of the energy sector by adding explicit constraints to an optimal infrastructure planning model [23, 24]. Optimal dispatch of water and electricity supply systems has also been proposed for integrated thermal power plants and desalination systems prevalent in the Middle East and North Africa (MENA) region [25], and for river-cooled thermal power generation in the United States [26, 27]. Other approaches dynamically link electricity generation planning to physical water constraints derived with water resource assessment models [28–33].

Previous work further demonstrates the risks posed to energy systems by future water supply transitions. Recent long-term analysis of different cities in the United States quantifies the potential electricity sector emissions directly attributed to water supply development using projections of water sector energy use and pre-defined regional electricity supply scenarios [34]. Similar analyses for regions in the Middle East and China at a relatively coarse spatial and temporal resolution integrates water and energy supply planning decisions with an optimization model covering both sectors [35–37]. This type of *hard-linked* optimization framework was also considered in its basic form much earlier [28, 29], and allows identification of coupled regional infrastructure pathways that simultaneously balance energy and water sustainability objectives. Similar research underscores the importance of geography due to water distribution-related energy demand [31, 38–40]. These studies demonstrate that spatially-explicit cost functions are required to parameterize the water and energy interactions in regional capacity expansion models.

1.2.3 Quantifying impacts of climate change

Climate is a key driver of energy supply and demand. Previous research explored impacts of warming temperatures on building energy demand and generally highlight geographic variability due to the differential effects on cooling and heating requirements [41–44]. Projections of sea-level rise under alternative global climate scenarios have also been used to assess the vulnerability of existing power plants in the United States [45]. Hydrological modeling under alternative climate scenarios has further been explored at local, regional and global scales to estimate the impact of climate change on the magnitude and timing of hydropower potential [30, 46–48]. The analyses suggest mixed outcomes, with some regions expected to benefit under projected increases in precipitation and shifts in seasonal snowpack. Likewise, projections of streamflow and stream temperature have been used to estimate climate change impacts on the efficiency and availability of river-cooled thermal generation [49–53]. Moving towards air cooling technology will reduce hydro-climatic vulnerabilities, but comes with additional tradeoffs in terms of energy efficiency and investment cost. Recent analysis for a water stressed region in Northern China indicates the transition to air cooling technology over the past two decades has resulted in a 1 % increase in national electricity sector carbon emissions [54]. Climate change will also impact wind patterns, cloud cover and ocean conditions, and the implications for the performance of wind, solar and ocean energy technologies have been considered in different regional case studies by employing regional climate models [55–57]. Finally, variations in air temperature impact the electrical properties of materials, and these implications of climate warming have been previously assessed for electricity transmission technologies [58].

These studies (among others) highlight the importance of including climate change impacts into long-term energy strategy, and further provide a wealth of techniques and data useful in impacts quantification. However, most previous studies neglect impacts during long-term energy system planning. These decisions are critical from the perspective of adaptation strategy, due to the opportunities to modify system design [59]. Integrated analyses of the operational impact of climate change on energy systems has been assessed in quite some detail for hydropower systems using hydro-economic models [60–63]. Recent analyses with energy-economic models are further quantifying the broader anticipated impact on electricity prices [30, 64–66]. Less explored is the opportunity to incorporate climate change impacts into the regional capacity planning process. This approach embeds adaptive capacity into system design. The implications have been discussed for Brazil [67] and the northwestern United States [68], where hydropower resources represent the majority of total electricity supply. These previous studies apply long-term optimization models to examine least-cost regional energy system adaptation pathways. Similarly, adaptation of Macedonia's energy system to climate change-driven shifts in demand was investigated using an optimization modeling framework [69]. An optimization approach was further investigated in the US for electricity generation planning under impacts of climate change on thermal power generation [31].

Integrated analyses of development pathways for the island of Mauritius and the Sacramento Valley in California demonstrate a new framework that combines two models used extensively for climate change impact and adaptation planning [70, 71]. The integrated framework soft-links existing tools in the sense that the output from each model is used as inputs for the other sector models. The feed-forward process is repeated until strategies simulated by the framework reach an acceptable level of convergence. Simultaneous optimization of decision-making across sectors (i.e., hard-linking) is more desirable, as less sensitivity analysis is required to identify scenarios that balance unified objectives [29, 35, 72].

1.2.4 Key limitations

Very few long-term assessments of climate change mitigation include representation of climate change impacts, even though some impacts are projected to occur regardless of mitigation measures taken [73]. This prevents estimating the avoided cost of adaptation, which could reduce the apparent cost of mitigation in situations where climate change causes detrimental impacts to system performance. Long-term energy scenarios should be designed to reflect that global policies aimed at reducing emissions are likely to reduce the magnitude of climate change impacts on energy systems.

Climate change is highly uncertain and thus it is further essential that energy infrastructure be designed acknowledging that it will need to cope with a range of hydro-climatic conditions [74]. Previous studies that incorporate climate change impacts into the energy technology planning process are limited because of the focus on a specific climate outcome. Planning models should internalize risks and opportunities associated with alternative scenarios to identify a long-term system configuration resilient to climate change uncertainty [74]. Li et al. [75] explored robust optimization as a tool for system planning under climate change impact risks to electricity supply technologies. Further important aspects are hydrological changes, and the ability to represent feedbacks with physical climate and water constraints.

Additional modeling of water constraints under alternative climate scenarios and an endogenous representation of the water supply systems will provide the capabilities to assess energy system performance across a broader range of future operational conditions. Greater spatial detail than that typically used in regional energy planning is needed to resolve physical water constraints and the energy demand resulting from water supply and distribution. Moreover, conflicting performance metrics across water and energy will necessitate application of multi-criteria model analysis methods. Such tools will support analysis of tradeoffs between all relevant objectives, and interactive exploration of diverse trade-off solutions across multiple objectives. Despite the potential to apply this type of tool to effectively model coupled economic-environmental decision-making [76], application of multi-criteria methods to the integrated planning of energy and water systems has been limited to cooling technology choices in the power sector [77].

1.3 Objectives and outline

The objective of this dissertation is to assess the technological and policy implications of adapting to water constraints and climate change impacts in the energy sector. Improved computational analysis tools are developed for this purpose. Specifically, the conventional systems-engineering energy technology planning framework is enhanced to incorporate: (1) robust capacity decisions in the electricity sector in light of impacts from hydro-climatic change and uncertain environmental performance of technology options; (2) an endogenous, spatially-distributed representation of water systems and feedbacks with energy demand; and (3) multi-objective optimization capabilities. The enhanced modeling tools are demonstrated within four case studies to assess regionally-specific issues surrounding energy sector adaptation to climate change and water constraints.

In chapter 2, the robust adaptation framework is applied to examine the potential impact of climate change on electricity generation planning in British Columbia, Canada.

Adaptation strategy is crucial in this region, mainly due to the large contribution of hydropower resources to regional electricity supply. The model is then extended in chapter 3 to consider uncertain environmental performance of technology options, and is applied to examine system design implications of policies that avoid electricity resource options with uncertain greenhouse gas emissions intensity. The scenario analysis developed for this chapter integrates climate change mitigation and adaptation assessment by stategically linking electricity demand, resource availability and carbon emissions projections.

In chapter 4, the framework incorporating an improved representation of water supply operations and capacity investment is used to examine how groundwater and climate sustainability objectives can be balanced in the water-stressed country of Saudi Arabia. These objectives are selected as the focus for the analysis due to the anticipated challenges in balancing future socioeconomic development with aspirations surrounding global climate stewardship and national food security. The former is a concern due to increasingly stringent global climate change policy, and the fact that more than half of the current power generation fleet in Saudi Arabia burns carbon-intensive crude oil [78]. Fulfilling national food security ambitions locally in Saudi Arabia's harsh desert environment requires industrial-scale irrigation, and has driven widespread over-exploitation of regional groundwater resources, leading to concerns regarding long-term supply sustainability [79]. A modified version of the reference point methodology is applied in chapter 5 to enhance the integrated water-energy supply planning model with multi-objective optimization capabilities.

Demand projections represent a critical input to the water and energy supply modeling approaches applied in this dissertation. The Saudi Arabia case study analysis develops a set of unique national demand projections consistent with the most recent global change scenarios. A further contribution to modeling demand projections is presented in Appendix A, and applied to map global impacts of climate change and human development on municipal water demand.

Chapter 2

Robust response to hydro-climatic change in electricity generation planning[1]

[1]The body of this chapter was published in S. Parkinson and N. Djilali, *Climatic Change* 130 (4), 475-489, 2015, and is reproduced with the permission of Springer. SP and ND conceived and designed the study. SP performed the analysis, drafted the initial manuscript, and finalized the published version. ND contributed to the refinement of further manuscript drafts.

Preamble

An electricity generation planning framework incorporating adaptation to hydro-climatic change is presented. The planning framework internalizes risks and opportunities associated with alternative hydro-climate scenarios to identify a long-term system configuration robust to uncertainty. The implications of a robust response to hydro-climatic change are demonstrated for the electricity system in British Columbia (BC), Canada. Adaptation strategy is crucial in this region, mainly due to the large contribution of hydropower resources to regional electricity supply. Analysis of results from basin-scale hydrologic models driven with downscaled global climate data suggest that shifts in regional streamflow characteristics by the year 2050 are likely to increase BCs annual hydropower potential by more than 10 %. These effects combined with an estimated decrease in electricity demand by 2 % due to warmer temperatures, could provide an additional 11 TWh of annual energy. Uncertainties in these projected climate impacts indicate technology configurations offering significant long-term operational flexibility will be needed to ensure system reliability. Results from the regional long-term electricity generation model incorporating adaptive capacity show the significant shifts required in the non-hydro capacity mix to ensure system robustness cause an increase in cumulative operating costs of between 1 and 7 %. Analysis of technology configurations involving high-penetrations of wind generation highlights interactions between flexibility requirements occurring over multiple temporal scales.

2.1 Introduction

Under current global development trends, fundamental changes in the climate system are projected this century [3]. The implications for infrastructure are substantial [80], including widespread impacts on energy systems [5]. Adaptation strategy is an increasingly urgent issue: energy technology investments made today impart long-term structural inertia into the entire energy supply chain [6].

A number of previous studies quantify impacts of climate change on energy systems [5, 81, 82]. For instance, projected hydrologic changes are expected to shift the timing and magnitude of hydropower potential across Europe [46–48]. Increased streamflow temperatures under climate-warming are further capable of reducing the efficiency and availability of the region's river-cooled thermal generation [51, 52]. Integrated analyses of hydrologic impacts suggest important feedbacks into European electricity prices [30, 32, 64, 65]. In California, climate-warming is likely to trigger increased demand for cooling that is expected to increase the electricity system peak load carrying requirement by 6-20% [58, 83]. Corresponding shifts in the seasonal availability of the state's hydropower resources is further expected to affect regional electricity prices [61, 84]. In North America's Columbia River basin, climate change impact on electricity resources has been assessed in some detail, including: combined analysis of both hydropower and demand impacts in the US portion of the basin [43, 68]; and operational strategies for the integrated multinational hydropower system [60].

These studies (among others) highlight the importance of including climate change impacts into long-term energy system development plans, and further provide a wealth of techniques and data useful in impacts quantification. However, most previous studies neglect impacts during the long-term planning of infrastructure capacity. The need to incorporate climate change impacts into the regional capacity planning process has been discussed for Brazil, where hydropower resources supply approximately 80% of electricity demand [67]. The study develops a long-term optimization model to examine national energy system adaptation pathways. Similarly, adaptation of Macedonia's energy system to climate change-driven shifts in demand was investigated using an optimization modeling framework [69]. An optimization approach was further investigated in the US for electricity generation planning under impacts of climate change on thermoelectric generation [31].

Climate change is highly uncertain and thus infrastructure should be designed acknowledging that it will need to cope with a range of climate conditions [74]. Previous studies that incorporate climate change impacts into the capacity planning process are limited because of the focus on a specific climate outcome. In the current study, a robust optimization approach to capacity planning under climate change is proposed. The framework internalizes risks and opportunities associated with alternative scenarios to identify a long-term system configuration robust to uncertainty. The approach is similar to that recently proposed in [75], although the current study integrates combined hydrologic and climate uncertainties into the analysis. The framework is demonstrated for the electricity system in British Columbia, Canada, where adaptation strategy is especially crucial: the existing system contains a large portion of climate-sensitive supply (hydropower) and demand (heating and cooling technologies).

2.2 Methodology

Optimization models are commonly applied tools in long-term energy planning analysis [6, 85–87]. These models enable representation of physical and institutional processes as algebraic relationships, and identification of solutions that optimize an overarching objective (e.g., minimization of total system costs). Long-term planning models are typically deterministic in the sense that perfect foresight over a future planning horizon is assumed. Incorporating impacts of hydro-climatic change into these models presents a challenge: projections of both future climate [88], and hydrology are highly uncertain [89].

Uncertainties surrounding future hydro-climate are integrated into the conventional deterministic analysis using the framework depicted in Fig. (2.1). The methodology relies on regional hydro-climate scenarios generated from a large number of coupled modeling experiments. By incorporating a wide range of models and results into the analysis, the scenario space captures uncertainty across available projections. Many previous studies focus on the generation of hydro-climate ensemble projections (e.g., [89–93]), with a brief methodological overview provided here. At the global-scale, general circulation models (GCM) investigate the evolution of climate variables under specified long-range emission or radiative forcing scenarios [94,95]. Current GCMs lack the spatial and temporal resolution needed for hydrologic impact assessment, with downscaling tools applied to transform GCM results into a desired frame of reference. When driven with the downscaled climate parameters, hydrologic models generate concurrent projections of hydrologic variables, such as streamflow and groundwater recharge.

By quantifying effects of the alternative hydro-climate scenarios on electricity system performance, concurrent electricity impact scenarios are generated. The distribution of projected impacts is then used to parameterize design constraints in an electricity gen-

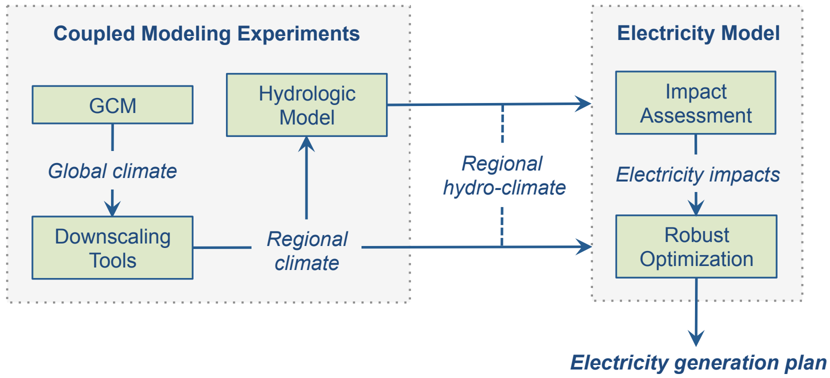

Figure 2.1: Framework for incorporating hydro-climatic change into the electricity generation plan.

eration planning model. This model solves for the least-cost operational trajectory of the electricity system at a seasonal time-step, including investment decisions in new and existing generation and interregional transmission capacity. A robust optimization formulation is chosen for the planning model because it enables proactive consideration of scenario-based uncertainties in large-scale system design studies[2] [101]. In robust optimization, optimal design (capacity) and control (activity) variables are determined based on calculated performance across a number of alternative scenarios. By including climate change impact scenarios in the analysis, robust optimization reveals system designs resilient to uncertainties in climate change projections [74, 75].

In the current study, we extend the robust optimization approach to include hydrologic impacts of climate change. We further impart increased stringency into the system's design by requiring feasibility across all electricity impact scenarios included in the analysis (i.e., the model is *solution robust* [101]). This choice of model formulation enables our analysis to highlight long-term capacity implications of hydro-climate uncertainty. The objective function in this case minimizes the weighted sum of each scenario's total cost. The weights are inferred from the frequency distribution associated with the hydro-climate

[2] Alternative methods for addressing uncertainty in long-term energy planning analysis include stochastic programming [96, 97], mini-max optimization [98], real-options [99], and hybrid approaches [100]

ensemble. This objective favours a technology portfolio that performs best under projections occurring most frequently in the coupled modeling experiments[3]. The mathematical formulation of the model is provided in the Supplementary Information.

2.3 Application: British Columbia, Canada

The proposed energy system adaptation framework is applied to British Columbia's (BC) electricity system. To resolve long-term climate change impacts, a planning horizon of 2010-2050 is chosen for the analysis. The region is an ideal place to apply the planning framework due to its strong linkage to the hydrologic cycle: provincially-operated hydropower resources currently service more than 90% of BC's annual electricity demand, with seasonal surplus further generating significant export revenue within inter-regional electricity markets [103]. BC's heating and cooling end-use sector is also sensitive to changes in climate, and is a major contributor to electricity demand in the province [104]. Our analysis specifically focuses on impacts and uncertainties surrounding hydropower potential and electricity demand, as these effects are expected to dominate regionally. A comprehensive assessment would account for other vulnerabilities (e.g., wind potential, transmission systems, thermoelectric efficiency, etc.), and will be addressed in future research.

2.3.1 Hydro-climate scenarios

Results from analysis by the Pacific Climate Impacts Consortium (PCIC) parameterize the hydro-climate scenarios applied in the case study. PCIC generated an ensemble of 23 downscaled climate projections for BC, from 8 GCMs run under the B1, A1B and A2 global emissions scenarios [94, 105, 106]. The downscaled climate parameters were

[3] A limitation of this approach is that the climate ensemble distribution is not a true probability distribution but instead an expert judgment with respect to potential future climatic conditions [102]. Nonetheless, this is currently the best representation of future conditions regional planners have access to, and thus is used to parameterize the scenario probability space.

then applied to hydrologic models of several key provincial freshwater basins[4] [93]. The models are found to outperform other approaches at predicting historical conditions [108]. The large number of scenarios considered also helps to estimate the range of future hydro-climate uncertainty.

The specific hydro-climate scenarios considered in the current study are the seasonal streamflow and temperature anomaly distributions projected by PCIC for 2041-2070 trends relative to observed 1961-1990 trends [93,108]. These changes are assumed to accumulate linearly over a 1990-2050 period (i.e., some changes are assumed to have occurred by the model base year of 2010). The data is provided in the Supplementary Information, with overall trends summarized here. Climate warming is observed across PCIC's downscaled regional projections. An increased precipitation trend is seen in most seasons and annually, with notably drier conditions observed in the summer. Perennial warming triggers earlier spring snowmelt, which combined with an increasing precipitation trend, is expected to make more run-off available in the winter and spring seasons. Less snowpack combined with warmer and drier summer conditions are expected to reduce summer run-off in many provincial basins. Projected hydro-climatic conditions differ regionally, with some locations displaying greater uncertainty than others. For a thorough breakdown, readers are directed to [93].

2.3.2 Electricity impact scenarios

The approach taken to quantify climate change impacts to hydropower potential is similar to that seen in other recent assessments [30, 47]. Hydropower potential is calculated considering the potential energy E in available streamflow V:

$$E = \rho g h V \tag{2.1}$$

The potential depends on the site-specific hydraulic head h. The parameters g and ρ represent the acceleration due to gravity and water density respectively. Historical streamflow data is merged with the anomalies estimated by PCIC to generate impact scenarios at

[4] For the hydrologic analysis, PCIC applied a modified version of the Variable Infiltration Capacity (VIC) model [107].

hydroelectric facilities throughout the province. The spatial distribution of the stations included in the study is provided in Fig. (2.2). Historically, these sites on average produce about 90% of hydropower in the province. The remaining 10% consists mainly of small-scale distributed systems, and due to data limitations is represented in the model as an aggregated resource that follows an average seasonal inflow trajectory. Facility-level technical data used to parameterize this model is obtained from various regional water-use planning documents [109–115], and is summarized in the Supplementary Information.

For climate impacts to electricity demand, the model identification process typically involves regression analysis of historical time-series data [81], and we developed a BC-specific model applying a similar approach. Hourly aggregate electricity demand data for the province over the 2012-2013 period was obtained from the regional balancing area authority [116]. Concurrent hourly temperature data was obtained from a number of climate measurement stations [117]. To better capture spatial temperature variability within the analysis, a population-weighted regional temperature trajectory was generated [118]. Four stations were selected based on their proximity to the following population centres: Vancouver, Victoria, Kelowna, and Prince George. The contribution of each station towards the weighted average follows the regional distribution in [119]. Daily averages and peaks of the combined dataset were calculated and applied within a least-squares analysis to identify polynomials of various order[5]. For daily averages, business and non-business days are separated, to account for known correlations overlooked in the regression analysis. Cubic polynomials are found to provide adjusted R^2 values ranging from 0.90-0.92. The data and fitted models are provided in the Supplementary information. Seasonal demand requirements for each hydro-climate scenario were then synthesized by applying the derived statistical model to shift a baseline load forecast. The baseline trajectory is obtained from the regional balancing area authority's recent long-term resource plan[6] [104].

[5] A limitation of this approach is that it neglects structural changes in the end-use technology mix that would likely accompany a warmer climate (i.e., increased market penetration of cooling technology). Although empirical models that capture these effects have been proposed for air conditioners [41], they are unable to account for the complex interaction with other emerging technologies, such as heat pumps. This can be addressed in future work by incorporating end-use technology investment decisions into the long-term planning problem. Neglecting structural change effects means our estimates likely underestimate climate change impacts to summer electricity demand.

[6] The baseline load trajectory is further shifted by known annual energy entitlements that hydropower

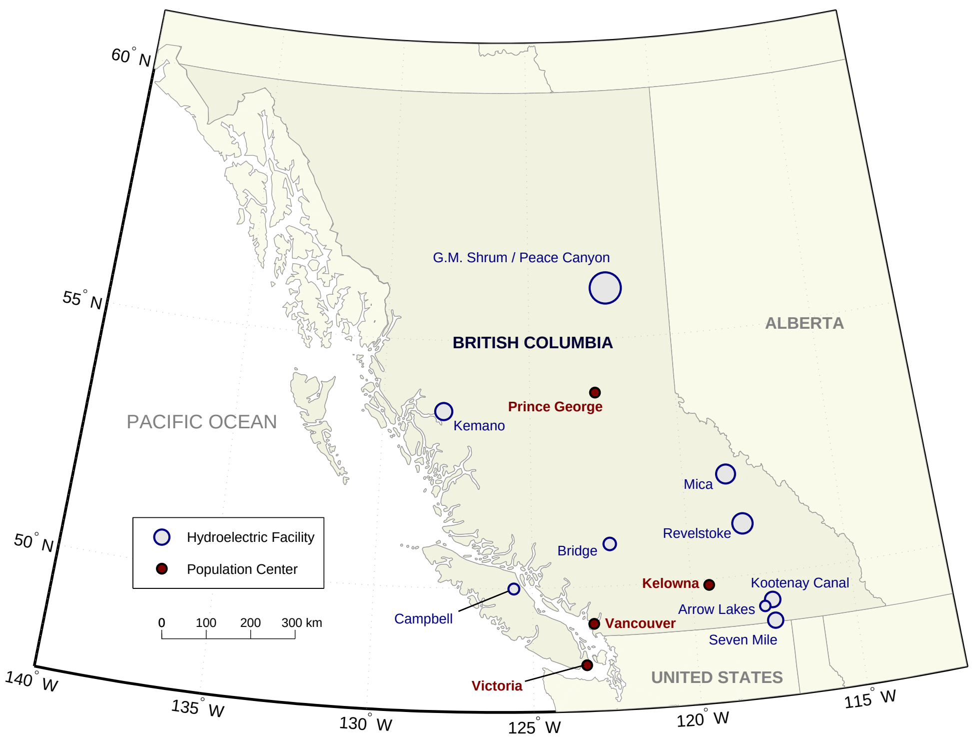

Figure 2.2: Spatial distribution of hydroelectric facilities and population centers included in the study. The diameter of the hydroelectric facility marker is proportional to the contribution of that station to aggregate provincial energy production (all depicted sites together represent approximately 90%). Some of the mapped facilities represent aggregations, as operations are already synchronized or insufficient data was available. This includes: Kootenay Canal, which also considers Corra Lynn, Upper / Lower Boddington, South Slocan and Brilliant capacity; Seven Mile, which also considers Waneta capacity; Bridge, which also considers Seton and Walden capacity; and Campbell, which consists of Stratchcona, Ladore and John Hart capacity.

Future baseline seasonality trends are assumed to follow historical trends.

2.3.3 Technology and policy assumptions

Considering the importance of hydropower generation in BC, specific attention is paid to the representation of these technologies in the model. Streamflow management is integrated into the optimization model as a water balance constraint at individual hydroelectric facilities. Streamflow can be directed through the turbines, stored (if available), or spilled. The cascading nature of large-scale facilities with seasonal storage opportunities is respected. Long-term reservoir sustainability is assured by constraining the initial level in each winter to be the same. Other water demands at the reservoirs included in the model are minimal, and are excluded from the analysis. The model considers planned hydroelectric capacity upgrades, as well as assumed addition of a new 1,100 MW facility in 2020 [120]. The model excludes expansion of the existing large-scale hydropower system beyond that planned. Facility-level technical data used to parameterize the hydropower system is provided in the Supplementary Information.

Other generation technologies considered in the BC electricity model follow the recent assessment of resource options performed by the provincial balancing area authority[7] [120]. This includes the following fossil fuel technologies: single-cycle natural gas turbines (SCGT), combined-cycle natural gas turbines (CCGT), and distributed natural gas cogeneration. The model further considers the following renewable energy technologies: two types of wind technology (offshore and onshore), wave, tidal, geothermal, small-scale run-of-river (RoR), and three types of bioenergy technology. The model can also choose from two technologies that help balance supply and demand: pumped storage and demand response[8] (DR). Renewable energy technologies are considered non-dispatchable, with

---

resources incorporated into the model currently provides.

[7]Nuclear and coal generation technologies are excluded from the analysis. Neither is considered a viable option in BC due to the province's no-nuclear, low-carbon energy policy. Carbon capture and storage technology is also excluded from the analysis due to uncertainties surrounding its performance and regulation in the province.

[8]Demand response here refers to a technology that enables the shifting of load over periods ranging from minutes to hours. This is different from long-term demand impacts of efficiency investments and price response, which are included in the baseline load forecast [104].

energy contributions determined by a seasonal capacity factor. To enable consideration of short-term operating issues at a seasonal time-step, specific capacity and flexibility reserve constraints are imposed in the model. The mathematical formulation can be found in the Supplementary Information.

Interregional transmission links included in the model are corridors south to the United States (US) and east to Alberta (AB). The model allows for expansion of each corridor up to a maxmimum of 4,000 MW. Current provincial energy policy strives for electricity self-sufficiency[9] [120]. This strategy is integrated into the model by prescribing that imports never exceed 5% of annual electricity consumption. This enables some importing of electricity for services such as balancing and peak support that is likely to occur regardless of the provincial self-sufficiency policy. Based on this constraint, transmission expansion in the model is driven by the desire to export electricity.

Existing generation and transmission capacities are obtained from a number of sources [119–122]. Cost of renewable generation, distributed cogeneration and pumped storage are represented as different resource grades fitted to supply curves derived by the provincial balancing area authority [120]. For each technology category, the supply curves rank spatially-distributed projects based on levelized cost of supplying electricity ($/MWh). The supply curves also limit technology expansion, as only cost-effective projects are included. SCGT, CCGT and transmission expansion costs, as well as natural gas and trade prices are estimated from [119]. A supply curve for DR technology is estimated from [123]. Current levels of provincial climate policy are assumed over the modeled time-horizon (i.e., a carbon price of $30 per tonne of CO_2-equivalent), which impacts the operating costs of technology options that incur emissions. Technology costs, including natural gas and trade prices, are held at a constant rate over time. Tradeoffs between climate adaptation and concurrent climate and technology uncertainties is the topic of a companion paper [124].

The model is applied within two policy scenarios. The first enables the system to expand within conventional bounds, and the second explores system configurations free of natural gas generation. The latter scenario reflects the commitment of BC to a low-carbon

[9] BC contains significant natural gas resources and thus it is assumed that use of these resources does not jeopardize self-sufficiency goals.

energy future through fulfillment of capacity requirements with renewable resources [120].

2.4 Results

Key results of the impacts analysis are summarized in Fig. (2.3). The model estimates that average future streamflow conditions bring approximately 9 TWh of additional hydropower potential by 2050 (an 11% increase)[10]. Significant seasonal variability exists; much of the increased potential comes in the spring (MAM), while a deficit is observed in the summer (JJA). On the demand-side, reductions in heating overshadow modest increases in summer cooling. Mean future temperature conditions are found to decrease both average and peak demand (not shown) by 2%[11]. Overall, the net effect of climate change on BC's electricity system is dominated by the change in hydropower potential, and translates to an increase of approximately 11 TWh of available energy by 2050 (equivalent to a 38% decrease in the supply-demand energy gap). The variations in seasonal impacts are of a similar magnitude, and underscore the importance of including climate change uncertainty into the planning analysis.

Results from the regional electricity system model are provided in Fig. (2.4). Depicted is the optimal installed capacity in 2050, excluding the large-scale hydropower system, for the two natural gas policy scenarios. To examine the implications of planning problem formulation, the capacity mix was obtained under five different climate change adaptation strategies. The *base* strategy neglects projected hydro-climatic change, and considers only one scenario characterized by baseline trajectories (i.e., no impacts). The *minimum*, *average*, and *maximum* strategies also consider a single scenario, characterized by the corresponding level of electricity impacts depicted in Fig. (2.3) (i.e., the 5th, 50th, and 95th percentiles). Finally, there is the *robust* strategy, which considers the minimum, average, and maximum electricity impact scenarios in the proposed robust optimization framework[12]. This range covers 90% of the ensemble distribution (from the 5th to 95th

[10] Hydropower impacts calculated for BC are of similar magnitude as those estimated for Nordic Europe [30, 47]. The results do not consider limitations imposed by existing hydropower capacity, which must accommodate the new conditions. This aspect is explored in the optimization model.

[11] Demand impacts calculated for BC compare well with those estimated for Canada [42].

[12] The robust objective function scenario weights are inferred from the percentiles, which in this case

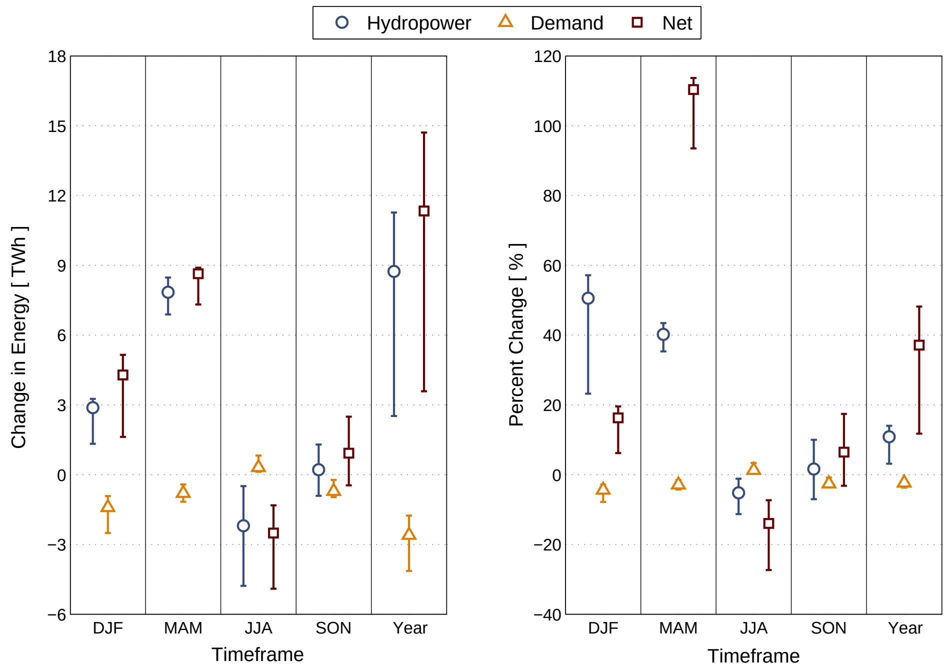

Figure 2.3: Estimated impact of hydro-climatic change on average electricity demand and average hydropower potential in the year 2050. Left: change in energy versus the baseline (no climate change); Right: percent change in energy versus the baseline. The marker represents the impacts obtained under the mean (50th percentile) trajectory from the hydro-climate ensemble distribution, with the whiskers extending to the results obtained under the minimum (5th percentile) and maximum (95th percentile) trajectories. Net impacts represent hydropower less demand. DJF = December, January, February; MAM = March, April, May; JJA = June, July, August; SON = September, October, November.

percentile), meaning the robust configuration will remain reliable across a wide range in projected conditions.

The modeled impacts to hydropower and demand translate to noticeable shifts in the trajectory of the non-hydro capacity mix. In each case, the excess energy made available by climate change displaces capacity expansion. Naturally, the robust strategy consistently requires more capacity than the average and maximum cases since it yields a portfolio that it is capable of adapting to the extreme case (minimum climate change). The robust strategy therefore places a high value on operational flexibility. For instance, when natural gas is included as an electricity resource option, more efficient CCGT capacity adopted under the minimum adaptation strategy is displaced by less efficient SCGT capacity in the robust case, even though both strategies face equivalent capacity requirements (i.e., the supply-demand gap is at its greatest in the minimum impacts case, which is the limiting factor within the robust problem formulation). This effect is observed because CCGT capacity is modeled with a much higher minimum utilization rate than SCGT capacity, and thus is less flexible when it comes to adapting to the projected range in future hydro-climatic conditions.

When natural gas is excluded as an electricity resource option, wind and pumped storage technology are combined to provide adaptive capacity. Tab. (1) presents the percent change in cumulative trade when moving from the deterministic to robust case for each natural gas and electricity impact scenario. It can be seen that increased exploitation of non-dispatchable wind resources when natural gas is excluded significantly increases interregional exports under the average and maximum impact scenarios. This is because wind resources are over-developed in the robust strategy to provide redundancy needed in the extreme case (minimum impacts). In the other electricity impact scenarios, the interregional transmission system provides a sink for the excess wind generation. If transmission was unavailable, expanded storage options would be needed to prevent wind curtailment.

The cost of embedding adaptive capacity into the electricity system is also compared to the deterministic cases in Tab.(1). Presented is the percent increase in total discounted costs when moving from the deterministic to robust strategy for each natural gas and elec-

translates to a normalized value of 0.08 for both the maximum (95th percentile) and minimum (5th percentile) impact cases, and 0.84 for the average (50th percentile) case.

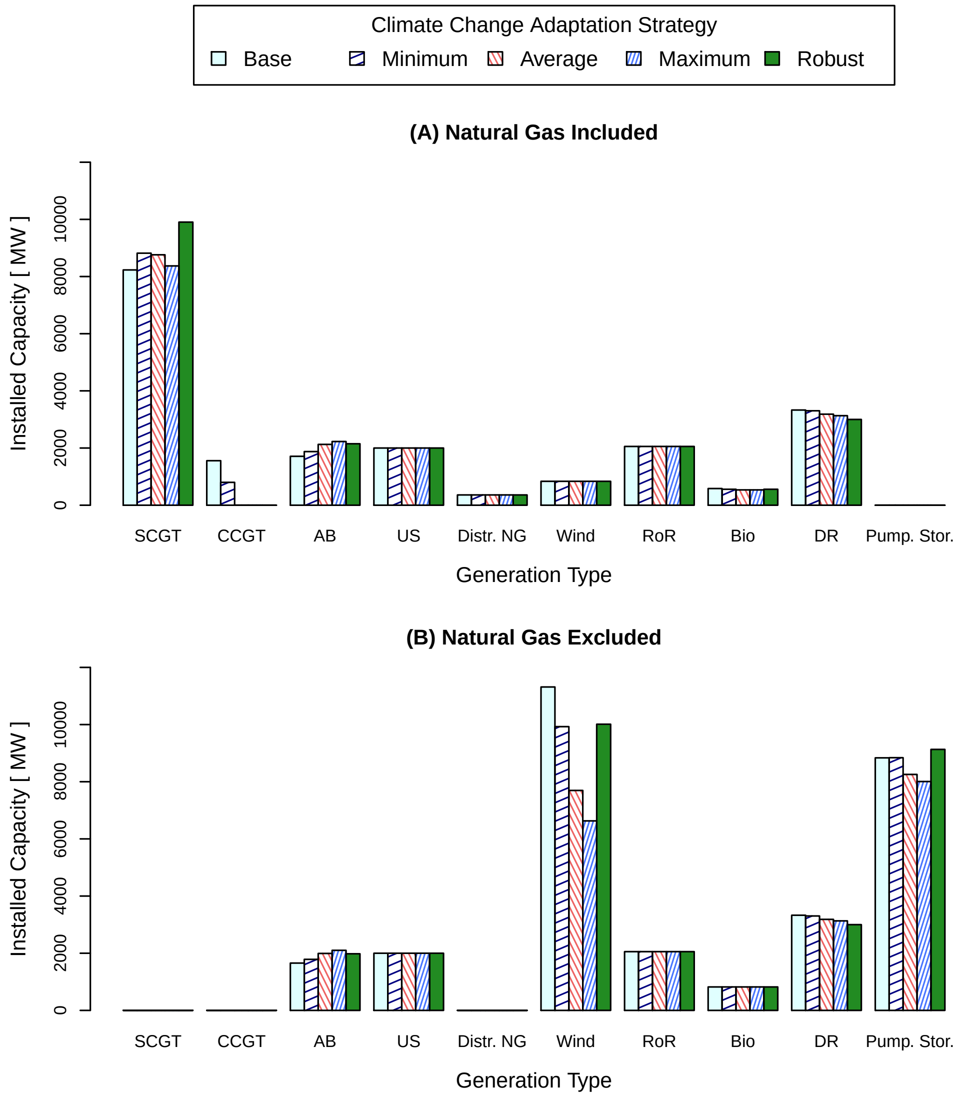

Figure 2.4: Accumulated capacity (excluding large-scale hydropower) in 2050 for each climate change adaptation strategy and natural gas policy scenario. SCGT = single-cycle natural gas; CCGT = combined-cycle natural gas; AB / US = AB / US transmission capacity; Distr. NG = distributed cogeneration; RoR = small-scale run-of-river; Bio = bioenergy; DR = demand response; Pump Stor. = pumped storage.

	Electricity Impact Scenario		
	Minimuim	Average	Maximum
Cumulative Trade			
Natural Gas Included	5.6 %	10.6 %	10.3 %
Natural Gas Excluded	0.8 %	47.8 %	59.2 %
Discounted Cost			
Natural Gas Included	0.7 %	1.8 %	2.6 %
Natural Gas Excluded	0.6 %	4.6 %	6.6 %

Table 2.1: Percent increase in cumulative trade and discounted costs when moving from the deterministic to robust energy strategy for each natural gas and electricity impact scenario (positive trade values indicate a net increase in exports).

tricity impact scenario. The robust strategy increases cumulative operating costs between 0.7 and 6.6%, depending on the natural gas policy assumed and hydro-climate trajectory. The difference in cost between the natural gas scenarios is driven by available technology; if natural gas is excluded, other more costly options must provide capacity (i.e., wind and pumped storage). For BC, the smallest difference in cost is observed under minimum electricity impacts. This is because the minimum scenario determines capacity requirements within the robust problem formulation. For systems that experience a capacity deficit under hydro-climatic change–the opposite of what is predicted here for BC–the trends would be reversed.

For climate change, most of the impacts are likely to occur in the second half of the century. Although robustness was assessed in the view of average conditions to mid-century, path-dependency in the electricity system makes the period after 2050 relevant. Regional climate projections do suggest the direction of change continues post 2050, which would likely cause further impacts to hydropower potential and electricity demand in BC. Focusing on a robust response in 2050 is therefore likely to place the system on a direction well-suited for further climate adaptation. Potentially concerning, however, is the growth in BC's summer electricity demand and reductions in late summer water availability under climate change, which could drive capacity shortages if conditions are strained in the future. This outcome represents a divergence from trends, which may threaten the ability of the 2050 configuration to adapt in the longer term. Future work should consider implications of these effects by exploring electricity pathway response to century-scale planning horizons. A recursive planning model might be better at reflecting the decadal practices widely applied in today's electric power sector.

2.5 Conclusion

Given the long lead times required for deploying any new infrastructure, and the inertia technology decisions impart into the entire energy supply chain, protecting the electricity system from hydro-climatic change should be an integral part of long-term system planning. Uncertainties surrounding impacts of hydro-climatic change pose risks to electricity strategy developed deterministically. Planning for resilience is one way to hedge against these risks, by ensuring the system remains reliable across a range of possible outcomes. The robust optimization modeling framework presented in this paper addresses the issue of uncertain adaptation planning in the electricity sector by providing an approach to identify generation portfolios that contain sufficient adaptive capacity to handle a range of future hydro-climatic conditions.

Implications of a robust response to hydro-climatic change in the electricity sector was demonstrated for the western Canadian province of British Columbia. Climate change impact scenarios were initially generated considering the seasonal effects of projected streamflow changes on hydropower potential and the senstivity of seasonal demand to shifts in temperature. The results suggest climate change could be beneficial; warming temperatures reduce both peak and average demands, and increased precipitation enhances hydropower potential. These combined effects narrow the future supply-demand gap, reducing capacity expansion requirements. The wide range in quantifed impacts is, however, a complicating issue. Application of the robust planning framework reveals technology configurations offering significant long-term operational flexibility will be needed to ensure reliability. The imposed flexibility requirements effect the suitability of technology options, and increases the cost of long-term electricity system operation.

Although the analysis is specifically focused on BC, some of the conclusions have broader relevance, and the methodology can be readily extended to other regional jurisdictions. Particularly concerning are electricity systems that display a strong linkage to the hydrologic cycle, and where climate change impacts degrade system performance (the opposite of what is projected here for BC). In these situations, the need for flexible adaptive capacity adds to the costs of deteriorating operational conditions under climate change. This has implications for mitigation strategy, where simultaneously adapting to climate change could affect options for reducing emissions. The results of this study demonstrate how wind energy technology paired with storage and/or interregional transmission could provide mitigation and adaptation co-benefits. In this case, interactions between flexibility requirements occurring over short- and long-term scales are found to be important drivers of technology investment.

Climate impacts in this paper were assessed in the view of average conditions at mid-century. Yet, the majority of climate change impacts are likely to occur in the second half of the century, and because development of the electricity system is highly path-dependent, the period after 2050 may be relevant to our analysis.Much more uncertainty surrounds climate conditions after 2050, further exacerbating the long-term planning challenges. Attempting to preserve robustness across a scenario-space bridging century-scale climate uncertainty is impractical with the stringent system reliability constraints used in this study. Future work could consider implications of longer-term effects by exploring alternative formulations of the optimization framework.

Chapter 3

Long-term energy planning with uncertain environmental performance metrics[1]

[1]The body of this chapter was published in S. Parkinson and N. Djilali, *Applied Energy* 147, 402-412, 2015, and is reproduced with the permission of Elsevier. The model analysis is an extension of the framework presented in chapter 2. SP and ND conceived and designed the study. SP performed the analysis, drafted the initial manuscript, and finalized the published version. ND contributed to the refinement of further manuscript drafts.

Preamble

Environmental performance (EP) uncertainties span a number of energy technology options, and pose planning risk when the energy system is subject to environmental constraints. This paper presents two approaches to integrating EP uncertainty into the long-term energy planning framework. The methodologies consider stochastic EP metrics across multiple energy technology options, and produce a development strategy that hedges against the risk of exceeding environmental targets. Both methods are compated within a case study of emission-constrained electricity generation planning in British Columbia, Canada. The analysis provides important insight into model formulation and the interactions with concurrent environmental policy uncertainties. EP risk is found to be particularly important in situations where environmental constraints become increasingly stringent. Model results indicate allocation of a modest risk premium in these situations can provide valuable hedging against EP risk.

3.1 Introduction

Environmental resources are increasingly strained, with technological transitions in the energy sector sought to provide relief [125]. For long-term planners, policies that constrain the environmental impact of energy systems drive the need to rank technology options based on environmental performance (EP). Common EP metrics include the rate at which a technology emits greenhouse gases and other air pollutants [126], or consumes land and water resources [17, 127].

Accurate EP quantification at the technology-level requires detailed knowledge of the end-use demands, location of implementation, and the supply chain that enables technology operation [128, 129]. The large-scale, spatially-distributed nature of modern energy systems means long-term planners often lack computational resources to perform analysis at the necessary resolution. Although lifecycle studies quantify EP uncertainty, long-term energy scenarios–developed to inform long-term planners–are typically generated with models operated under deterministic conditions. This approach poses risk when the planner must secure environmental targets: if technology is developed under the precondition it provides a certain level of EP, only to find out later it was overestimated, unforeseen changes to the energy strategy may be required. Potential measures include pre-mature retirement of capacity: a fate projected for much of the global coal-powered electricity generation under climate stabilization policy [130]. These ‘lock-in’ effects are costly, and caused by the lengthy planning period and lifecycle associated with energy infrastructure, and the resulting inertia technology decisions impart into the entire energy supply chain [6]. To avoid similar energy pathways, opportunities to mitigate EP risk should be considered within the long-term energy planning framework.

A number of previous studies tackle the issue of risk in long-term energy system planning. Uncertainties covered span a number of different components, including: technology costs and availability [23,87,96,131–133]; technological learning rates [134–136]; renewable resource availability and demand [137]; climate policy [98,138,139]; climate sensitivity [140–142]; or a combination thereof [97,99,100,143–150]. Relatively few studies, however, examine implications of EP risk. Technology efficiency scenarios were explored within a stochastic planning framework [151,152]. Uncertain technology efficiency and emission factors were also addressed within a multi-criteria analysis [153]. The issue of natural gas lifecycle emissions uncertainty was incorporated within a stochastic planning model [154]. This recent study demonstrates the importance of including uncertain EP into the long-term planning analysis, by quantifying the potential benefits of upstream emission controls on climate change mitigation costs.

The current study presents two approaches to integrating EP uncertainty into the environmentally constrained long-term energy planning framework. The methodologies consider stochastic EP metrics across multiple technology options, and produce a development strategy that hedges against the risk of exceeding associated environmental targets. The models are applied to a case study of emission-constrained electricity generation planning in western Canada. The analysis provides important insight into model formulation and the interactions with concurrent environmental policy uncertainties.

3.2 Methodology

Mathematical programming is a frequently applied tool for resource planning analysis that enables representation of physical and institutional processes as a series of algebraic relationships and identification of solutions that optimize some overarching objective. Due to the large number of relationships requiring representation, linear models are typical in long-range energy planning studies [7–9]. A conventional linear programming problem is represented by the following set of equations:

$$\mathbf{Min} \sum_{j} \left(c_j \cdot x_j \right) \tag{3.1a}$$

$$\mathbf{s.t.} \sum_{j} \left(a_{i,j} \cdot x_j \right) \leq b_i \ \forall \ i \tag{3.1b}$$

$$x_j \geq 0 \ \forall \ j \tag{3.1c}$$

The objective of the problem is to find the solution vector $\mathbf{x}$ (with elements x_j) that minimizes the function defined in (3.1a), subject to the constraints given in (3.1b) and (3.1c). For long-term energy planning, the solution vector represents the capacity and activity of energy technologies over the time horizon of interest. The objective is typically economic, and coefficients c_j therefore transform the solution vector into expenditures and revenue. The performance of individual technologies is represented by the technical input-output coefficients $a_{i,j}$. These parameters determine the amount of constrained resource i consumed or provided by decision j. The total amount of constrained resource i available or demanded is given by b. Energy-related constraints include service requirements, fuel availability and capacity levels. Environmental constraints are also of increasing concern to energy planning, and can be represented by using the input-output coefficients to link development and operation of technologies to specific environmental impacts. An example is the inclusion of emission factors and emission constraints to explore system configurations that ensure an emissions-level that remains below a desired target.

The linear programming model in its current form is deterministic, and therefore its utility in studying EP uncertainty is limited. Deterministic scenario analysis is an option; however, this strategy requires multiple model runs and a skilled analyst to identify robustness across the solution space [96]. Another method is to hedge against potential risks through explicit representation of uncertainties within the original problem framework. One way of incorporating risk-hedging within the mathematical programming framework is to define a measure of risk R that inflates the original deterministic objective function [155]. The risk measure can be parameterized based on the total absolute deviation from the expected value, obtained based on successive draws from a known probability space [156]. Risk-hedging against EP uncertainties requires a different tactic, as these uncertainties concern the technical input-output coefficients. A similar approach translates the risk measure to the technical constraints [157, 158]. Formulation of a linear programming problem with risky input-output coefficients can be represented by the following system of equations:

$$\mathbf{Min} \sum_j \left(c_j \cdot x_j \right) \tag{3.2a}$$

$$\mathbf{s.t.} \sum_j \left(\bar{a}_{i,j} \cdot x_j \right) + \Phi_i \cdot R_i \leq b_i \;\; \forall \;\; i \tag{3.2b}$$

$$\sum_j \left[\left(a_{i,j,k} - \bar{a}_{i,j} \right) \cdot x_j \right] - \left(r^+_{i,k} - r^-_{i,k} \right) = 0 \;\; \forall \;\; i,k \tag{3.2c}$$

$$\frac{1}{N} \cdot \sum_k r^+_{i,k} - R_i = 0 \;\; \forall \;\; i \tag{3.2d}$$

$$x_j, R_i, r^+_{i,k}, r^-_{i,k} \geq 0 \;\; \forall \;\; i,j,k \tag{3.2e}$$

The mathematical programming model now considers stochastic technical coefficients $a_{i,j,k}$, which are included in the model as N realizations of the assumed uncertainty distributions. The subscript k denotes the particular realization of the stochastic coefficients included in the model. Constraint (3.2b) contains the risk term $\Phi \cdot R_i$, which is added to the technical performance obtained under the expected value of the input-output coefficients $\bar{a}_{i,j}$. The risk term inflates resource usage above the expected value, and essentially provides a reserve margin. Following Messner et al. [96], the mean positive deviation from the expected value parameterizes the risk measure in (3.2d). The positive value is chosen to reflect that underestimating technical performance is more risky than overestimation[2]. Constraint (3.2c) computes the deviations obtained under each realization k of the stochastic technical coefficients. The deviations are broken into positive and negative components $r^{+}_{i,k}$ and $r^{-}_{i,k}$ to preserve linearity. The parameter Φ is the risk aversion parameter, and its utility is sensitivity analysis of results, namely to varying decision-maker attitudes towards technical performance risk. The formulation allows for impact-specific risk aversion parameters to be specified, enabling preferential weighting of resource constraints.

A drawback of the above approach is the abstract nature of the risk aversion parameter and the expected difficulty in eliciting an appropriate value from non-technical decision-makers. These individuals are typically interested in understanding tradeoffs between cost and risk reduction. An alternative approach based on available budgetary constraints is therefore proposed here, and is similar to that described in [150]. In this formulation, a risk premium quantifies the decision-maker's willingness to safeguard the energy system from technical performance uncertainty. Risk is then minimized subject to expected total system costs. The formulation of this linear programming problem is given by:

[2]Arguably, both positive and negative risk should be penalized, as both impact the strategy costs at the expected (average) parameter values. This type of formulation can be achieved by defining a non-linear risk measure (e.g., linear-quadratic risk). Options are discussed in greater detail in [150]. The energy models explored in this paper implement linear solvers and thus this work is limited to linear programming solutions.

$$\textbf{Min} \sum_i \left(\phi_i \cdot R_i \right) \tag{3.3a}$$

$$\textbf{s.t.} \sum_j \left(c_j \cdot x_j \right) \leq \left(1 + \mu \right) \cdot C^{det} \tag{3.3b}$$

$$\sum_j \left(\bar{a}_{i,j} \cdot x_j \right) \leq b_i \ \forall \ i \tag{3.3c}$$

$$\sum_j \left[\left(a_{i,j,k} - \bar{a}_{i,j} \right) \cdot x_j \right] - \left(r^+_{i,k} - r^-_{i,k} \right) = 0 \ \forall \ i,k \tag{3.3d}$$

$$\frac{1}{N} \cdot \sum_k r^+_{i,k} - R_i = 0 \ \forall \ i \tag{3.3e}$$

$$x_j, R_i, r^+_{i,k}, r^-_{i,k} \geq 0 \ \forall \ i,j,k \tag{3.3f}$$

In this model, risks occurring across different resources are weighted within the objective function by coefficients ϕ. Similar to the risk aversion parameter, these coefficients allow certain technical performance risks to be preferentially mitigated. A risk premium μ is defined, and represents the fraction of total cost in absence of uncertainty the decision-maker is willing to pay for hedging expenditures. The total cost in absence of uncertainty C^{det} is equivalent to the deterministic solution obtained under the expected values of technical performance.

A key difference between the two risk-hedging approaches is that the focus is strictly risk minimization in the risk premium formulation, whereas reductions in both average resource use and performance risk can contribute to satisfying the reserve margin imposed in the risk aversion parameter approach. Both formulations benefit from relatively straightforward implementation, provided the analyst is able to accurately parameterize the uncertainty distributions. The models are also able to address a number of technical performance uncertainties concurrently and could be combined with alternative risk formulations to examine sources of uncertainty throughout the problem structure (i.e., in the objective function or right-hand side constraints).

3.3 Case study

3.3.1 Emission-constrained electricity generation planning in BC

The modeling approaches presented in the previous section were applied to a case study and demonstrates the implications of including EP uncertainty into the long-term energy planning framework. The focus of the study is emission-constrained electricity generation planning in the western Canadian province of British Columbia. The province is an ideal test case for the following reasons: (i) policy-makers have historically demonstrated a commitment to reducing environmental risks, as illustrated by their implementation of a progressive carbon tax and a low-carbon energy policy [159]; (ii) although hydropower currently provides more than 90% of provincial electricity needs, significant capacity shortfalls are expected in the coming years [159]; (iii) resource options with uncertain lifecycle impacts, such as natural gas, forest bioenergy and electricity imports, are expected to play an increasing role in the regional electricity mix [119, 120].

The proposed EP risk-hedging approaches are integrated into an existing BC long-term electricity generation planning framework. The original framework is a deterministic linear systems-engineering optimization model, and thus it is possible to translate all model equations into a form equivalent to (3.1). The following section describes salient features of the existing BC model, with the mathematical formulation provided in the appendix. Parameterizing the risk metrics in terms of an emissions constraint requires generation of technology-specific emission factor uncertainty distributions, with the procedure applied described in section (3.3.3). All technical input-output coefficients other than emission factors are assumed fixed (i.e., deterministic). The corresponding constraints therefore reduce to the conventional linear programming form given by (3.1b). It will be the topic of future work to explore potential tradeoffs between risks occurring across multiple environmental resources (e.g., water use and CO_2 emissions).

3.3.2 Existing BC model description

The existing BC electricity capacity planning model solves for the least-cost operational trajectory of the electricity system at a seasonal time-step, over a planning horizon spanning the years 2010-2050. The decisions include investments in new generation and interregional transmission capacity. Considering the importance of hydroelectric power in the provincial electricity mix, specific attention is paid to the representation of these resources in the model. Streamflow management is integrated into the optimization model by considering the water balance at individual hydroelectric facilities. The cascading nature of large-scale facilities with seasonal storage opportunities is respected. Simplifications are made at smaller stations where operations are already synchronized (i.e., cascading run-of-river systems), or when insufficient data is available. The model includes planned hydroelectric capacity upgrades, as well as assumed addition of a new 1,100 MW facility in 2020 [120].

Other technologies considered in the model follow the recent assessment of resource cost competitiveness performed by the provincial balancing area authority [120]. This includes the following fossil-fuelled generation types: single-cycle natural gas turbines (SCGT), combined-cycle natural gas turbines (CCGT) and distributed natural gas cogeneration. The model further considers the following renewable energy resource types: onshore wind, offshore wind, wave, tidal, geothermal, small-scale run-of-river, biogas, and forest bioenergy. Pumped storage, and load control[3] technolologies are also incorporated into the model. Renewable energy resource costs are modeled as long-term energy contracts with independent producers; the costs of which are represented as different resource grades fitted to the supply curves derived by the provincial balancing area authority [120]. These supply curves also limit distributed resource expansion, as only cost-effective projects are included. Distributed resources are assumed non-dispatchable, with energy contributions determined by a seasonal capacity factor.

Interregional transmission included in the model are corridors south to the United States (US) and east to Alberta (AB). The model allows for expansion of each interregional transmission corridor up to a maximum of 4,000 MW. Current provincial energy policy takes a strong stance on self-sufficiency [120]. This strategy is integrated into the model by prescribing that imports never exceed 5% of annual electricity consumption.

[3]Load control refers to a technology that enables the shifting of load over periods ranging from minutes to hours. A supply curve for this technology is estimated from [123]. For more information on how this technology as well as pumped storage are integrated into the modeling framework, readers are directed to [160].

This enables some importing of electricity (e.g., ancillary services) that is likely to occur regardless of the provincial energy security policy. Based on this constraint, transmission expansion is mainly driven by the desire to export energy.

3.3.3 Emission factor uncertainty distributions

The Intergovernmental Panel on Climate Change performed a review of lifecycle emissions from electricity generation technology [126], and the uncertainties estimates are used to parameterize many of the CO_2 emission factor distributions in the current study. Lognormal distributions are fitted to the range of reported values[4]. Specific attention is, however, paid to forest bioenergy and natural gas technologies, as well as electricity imports.

The carbon benefit of forest bioenergy may be overestimated, even in situations where waste forest management residues are the only source of feedstock [161, 162]. Nevertheless, research also indicates potential benefits of utilizing residues from degraded forests, particularly those from the vast areas of British Columbia affected by mountain pine beetle [161]. A lognormal distribution is defined to model the uncertainty of forest bioenergy emissions, with the mean representing the value currently proposed by the province for emissions analysis [163].

Similar controversy has centered on natural gas. In particular, upstream methane leakage at unconventional extraction sites remains highly uncertain [164], and has the potential to offset carbon benefits typically associated with the movement from coal to gas in the electricity system [165, 166]. We utilize the range in lifecycle impacts of natural gas reported in [129, 165, 167] to model the emission uncertainty as a lognormal distribution.

Finally, BC's electricity imports come from one of the largest interconnected systems on the planet. This network contains a diverse range of both carbon-intensive and low-carbon generation technologies. The actual mixture differs substantially based on time-

[4]Lifecycle impacts incorporate electricity used during construction, and thus some double-counting of emissions is likely to occur by implementing lifecycle values within the analysis. However, part of the construction process may take place outside the region in question (e.g., component manufacturing) and could be associated with emissions from sources outside the electricity system (e.g., emissions from direct fuel- or land-use). This in itself is an uncertainty that should also be considered in the analysis.

of-day and season, although it is typical to assume an average Pacific Northwestern US electricity emission factor for US imports and an average AB electricity emission factor for AB imports [163]. For US imports, the uncertainty distributions are defined based on the range put forward in [168]. For AB imports, less uncertainty is assumed due to the relative size of the system and the high-prevalence of carbon-intensive generation technology.

The emission factor distributions implemented in the model are depicted in Fig.(3.1). These distributions are sampled to estimate the carbon risk associated with a given technology strategy. Latin hypercube sampling has been shown to produce better convergence than conventional random sampling methods in stochastic energy system optimization modeling [150], and thus is implemented to estimate the risk function under a finite number of samples. A suitable sample size is identified in the appendix. Correlation between the emission factor distributions is unaccounted for, except in the case of natural gas technologies. In these cases, the same natural gas emission factor distribution is assumed (i.e., perfectly correlated), with the rate of natural gas use determined by a technology-specific average conversion efficiency.

3.3.4 Scenarios

The model is applied within three scenarios to highlight the interactions between stochastic emission factors and global climate policy uncertainties. The scenarios reflect potential conditions under which energy planning will take place over the coming decades. To mimic the scenario space implemented by BC's regional electricity system planner (i.e., the balancing area authority), the scenarios are interpreted from the most recent provincial electricity resource plan [104, 108, 120, 169]. The scenarios dictate the level of demand as well as the carbon intensity of electricity imports. The scenarios are further extended to incorporate impacts of climate change. This enables the scenario space to address climate change mitigation and adaptation simultaneously. The scenarios are described below.

- **Scenario (A)**. Business-as-usual scenario. No global climate change policy beyond current levels resulting in a lack of change in the average carbon intensity of Western Interconnection electricity imports. Maximum global climate change impacts are realized and limited electrification of the transport and heating sectors occurs.

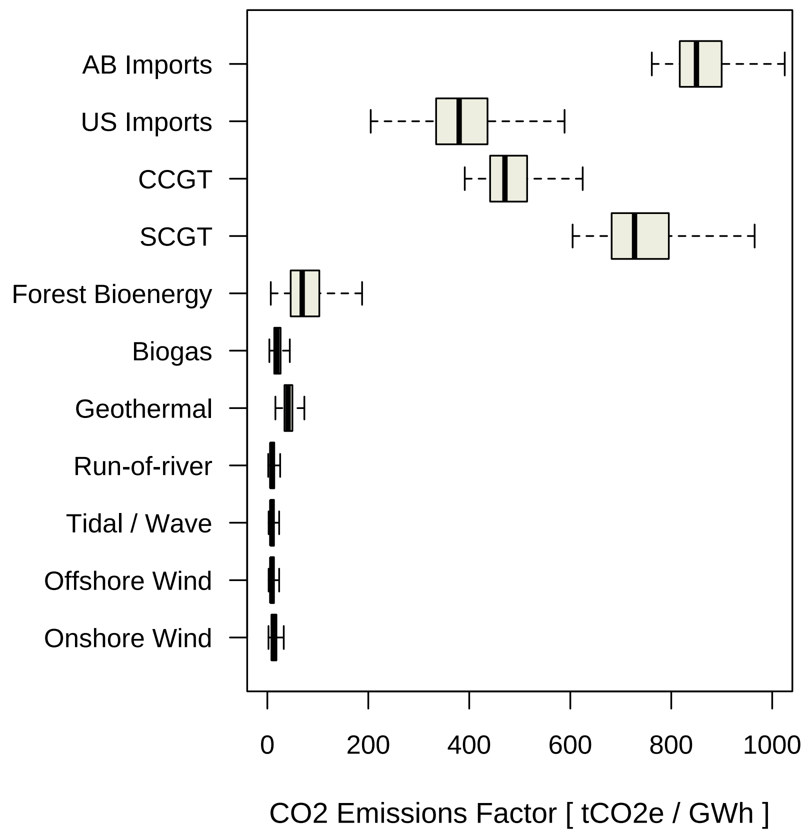

Figure 3.1: Emission factor distributions assumed in the risk-hedging version of the BC long-term energy planning model. The unit is metric tons of CO_2 equivalent (tCO2e) per GWh of electricity produced. The distribution for pumped storage technology (not shown) is drawn from the same distribution as run-of-river. The edge of the box represents the 25th and 75th percentiles with the whiskers extending to 1.5 times the interquartile range.

- **Scenario (B)**. Middle-of-the-road scenario. Moderate global climate change policy beyond current levels is implemented resulting in a 30% decrease in the average carbon intensity of Western Interconnection electricity imports by 2050. Mean global climate change impacts are realized and medium-scale electrification of the transport and heating sectors occurs.

- **Scenario (C)**. Climate stabilization scenario. Ambitious global climate change policy beyond current levels is implemented resulting in an 80% decrease in the average carbon intensity of Western Interconnection electricity imports by 2050. Minimum global climate change impacts are realized and large-scale electrification of the transport and heating sectors occurs.

Concurrent cumulative CO_2 emission caps are imposed by coupling the scenarios to carbon price trajectories developed by the regional balancing area authority [169]. The carbon price is equivalent to the shadow price of an emission constraint, and thus is interchangeable with an emission cap. To obtain the emission constraint, the model is initially run deterministically (i.e., assuming average emission factors) under a given carbon price trajectory. The cumulative emissions from this scenario are then used to constrain the stochastic model. The carbon intensity of imports is also related to the climate policy scenarios. To model each case, the emission reductions for electricity imports defined within the storyline are assumed to accumulate linearly, with the emission factors then scaled accordingly.

The scenario parameters introduced above are depicted in Fig.(3.2). Increases in demand under more stringent climate policy is driven by electrification of end-use services traditionally met with fossil fuels (e.g., transport and heating) [104]. Demands incorporate efficiency programs, price effects, and transmission losses [104], as well as climate change impacts [160]. Climate change is expected to translate to net benefits for BC's electricity system; gains in hydropower potential and reductions in demand are projected under a warming climate [160]. The jump in hydropower potential in 2020 is the result of assumed development of a new 1,100 MW facility[5] [120].

[5]Hydropower potential represents the raw resource and does not consider limitations imposed by existing hydropower capacity. These constraints are imposed in the optimization model.

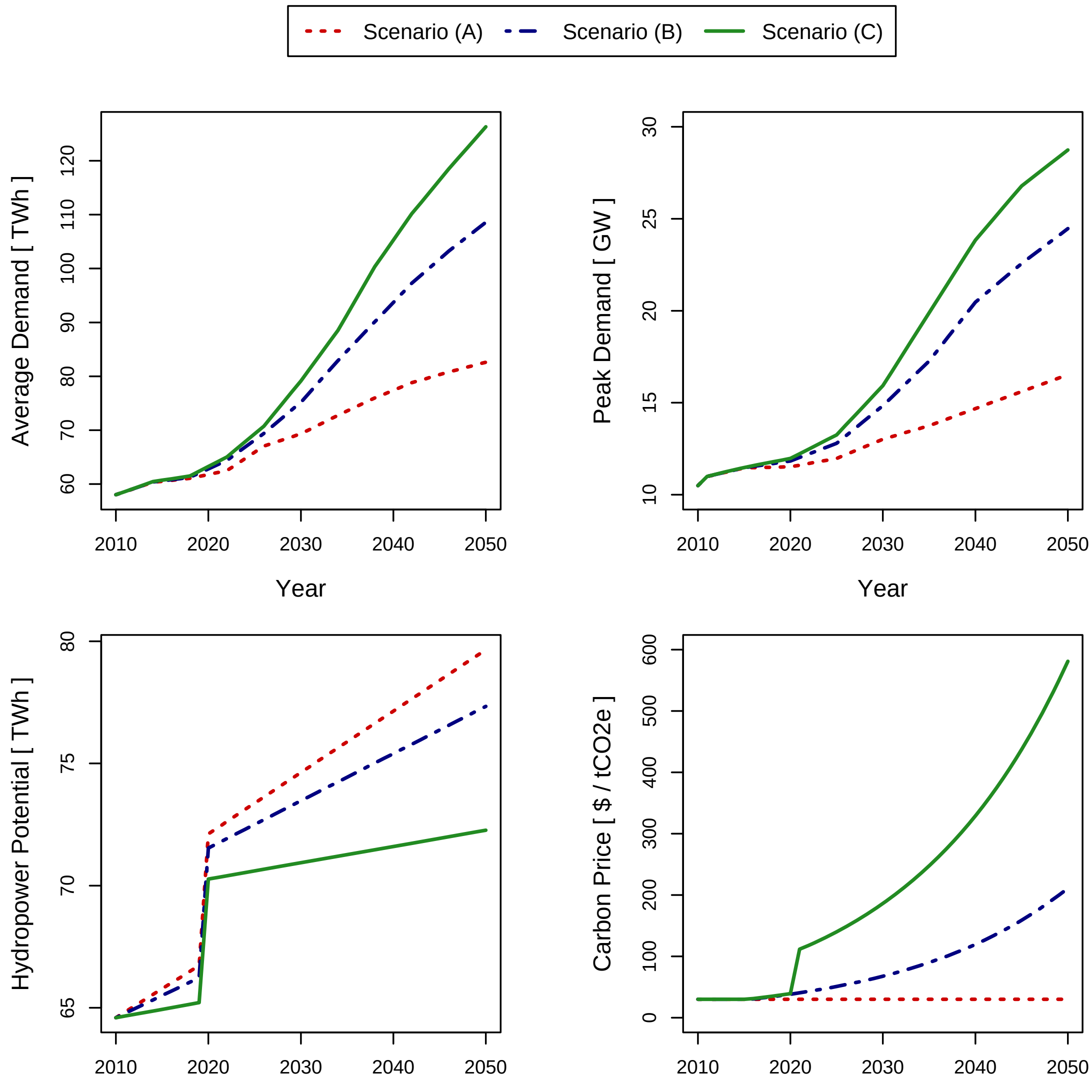

Figure 3.2: Average annual demand, average annual peak demand, average annual hydropower potential, and carbon price trajectories for each scenario implemented in the BC long-term energy planning model.

3.4 Results

The model is initially run deterministically, applying (3.1) with expected (average) emission factors. This step is needed to obtain the emission and cost constraints for the stochastic analysis. The results are provided in Tab.(1). Costs steadily increase with the level of climate policy defined in the scenario storyline. In scenario (C), the largest future supply-demand gap occurs due to a combination of widespread heating and transport electrification, accompanied by only modest gains in hydropower potential under climate change. A high carbon price trajectory dictates that significant investment into abatement measures already occurs in scenario (C). In scenario (A), low demand growth combined with an unambitious carbon price trajectory causes less pressure for future low-carbon capacity to be incorporated into the electricity system. Much of the load growth in this case is offset by combined climate change impacts to hydropower potential and heating demand. Although slightly more ambitious climate policy is proposed in scenario (B), the emissions from the electricity system increase with respect to scenario (A). Nevertheless, this analysis neglects tradeoffs implicit in the scenario storyline; heating and transport electrification displaces fossil fuels from final energy demand, but these carbon benefits are unaccounted for.

	Climate Policy Scenario		
	(A)	(B)	(C)
Cost [$\times 10^9$ \$ CAD (2010)]	51	76	105
Emissions [$\times 10^6$ tCO2e]	173	240	90

Table 3.1: Baseline emissions and costs obtained under the average emission factors.

For the stochastic analysis, each scenario was run over a range of risk aversion parameters (0 to 5) and risk premiums (0 to 5%). This enables the analysis to capture results sensitivity to potential environmental risk attitudes.

The capacity and cumulative energy mixtures[6] in 2050 obtained under the risk aver-

[6]The mixture represents the portion of each technology included in the aggregate. The energy mixture is the cumulative output over the simulation horizon (2010-2050). The capacity mixture is a snapshot of conditions in 2050.

sion parameter formulation are provided in Fig.(3.3). Initial conditions (i.e., for the year 2010) are also provided for reference[7]. Scenario (A) is relatively insensitive to the risk aversion parameters tested. The emissions reserve imposed by this formulation primarily pushes distributed natural gas cogeneration from the energy mixture. Impacts are slightly more pronounced in scenario (B), where increased risk aversion displaces SCGT generation from the capacity portfolio. In scenario (C), forest bioenergy and US imports are displaced from the energy mixture as the risk aversion parameter is increased, with additional onshore wind and geothermal entering the mix. Minor impact on the final capacity portfolio is observed in scenario (C), indicating the majority of risk is mitigated during the 2010-2050 transition (i.e., by limiting the activity of risky technologies over the simulated horizon or by investing in lower risk technologies earlier).

Capacity and energy mixtures obtained under the risk premium formulation are provided in Fig.(3.4). In this case, scenarios (A) and (B) undergo significant changes as the risk premium is increased. Natural gas and forest bioenergy technologies, as well as electricity imports are displaced. Interestingly, in scenario (C) more forest bioenergy is pushed out of the energy mix than electricity imports: the opposite of what is seen in the risk aversion parameter approach.

To help understand these results, the relationship obtained between total costs and risk parameterization is provided in Fig.(3.5). Costs increase non-uniformly in the risk aversion parameter approach. In scenarios (A) and (B), the least impact on costs is observed because more low-cost abatement measures remain in the baseline capacity configurations. This means it costs less to provide the emissions reserve margin imposed by the risk aversion parameter. Most of the low cost abatement measures have already been tapped in scenario (C); therefore, costs increase significantly with risk aversion. For the risk premium approach, the increase in cost is equivalent to the risk parameterization, and thus both quantities are interchangeable. Overall, more risk hedging expenditures are incurred in the risk premium approach, leading to greater impact on the energy and capacity mixtures. These results highlight a key aspect of the risk aversion parameter approach:

[7]The model results show that existing natural gas capacity contributes a negligible amount of energy to the initial mixture. This results from the assumed initial conditions, which includes a carbon price of $30 per tCO2e and enough hydropower potential to fulfill most of the energy requirements. Under these conditions, natural gas generation is less appealling than the other existing resources and thus is left primarily idle.

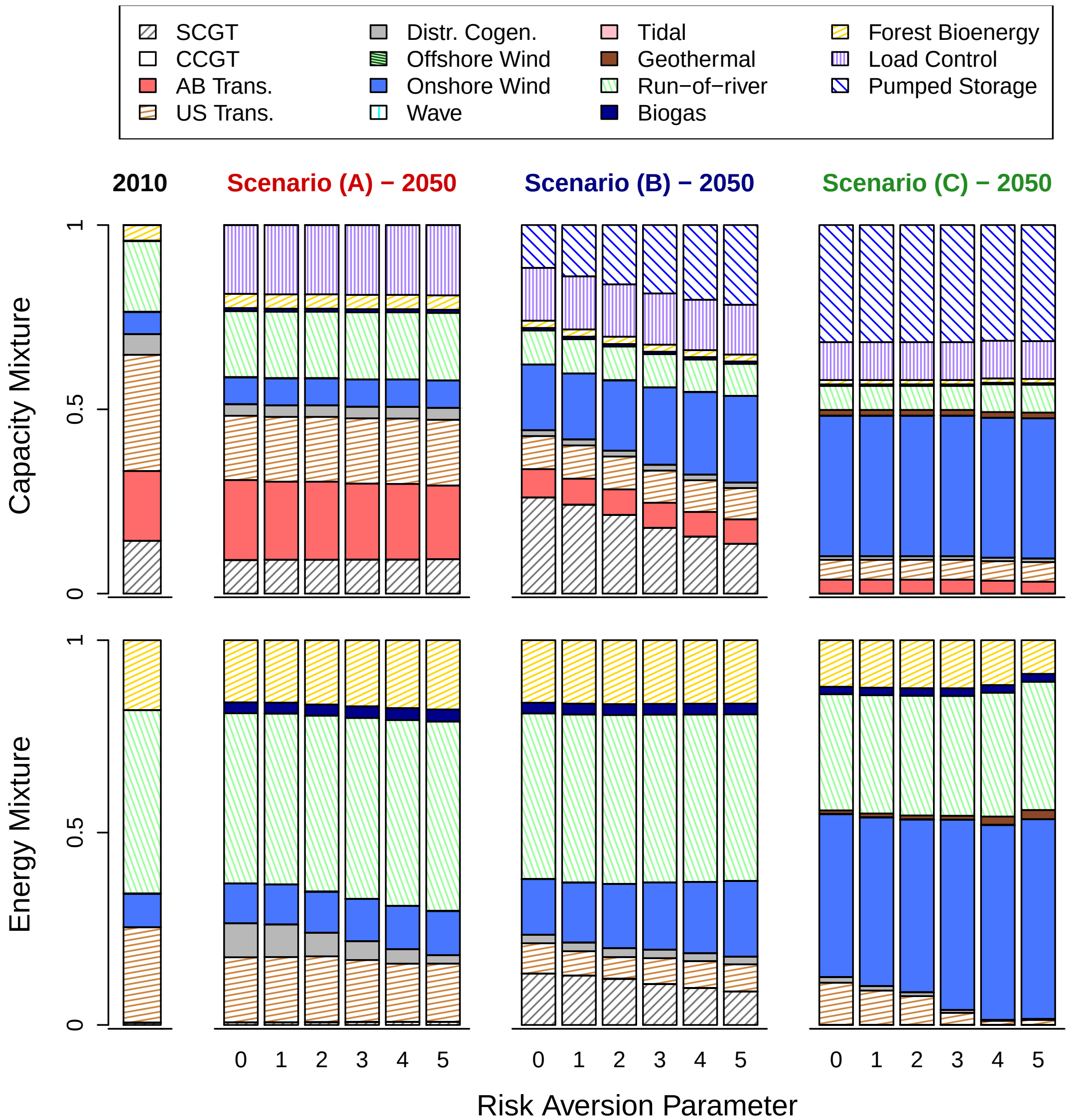

Figure 3.3: Sensitivity of the optimal capacity and energy mixtures in 2050 to the risk aversion parameter. The energy and capacity levels differ across each scenario and are depicted in Fig.(3.2).

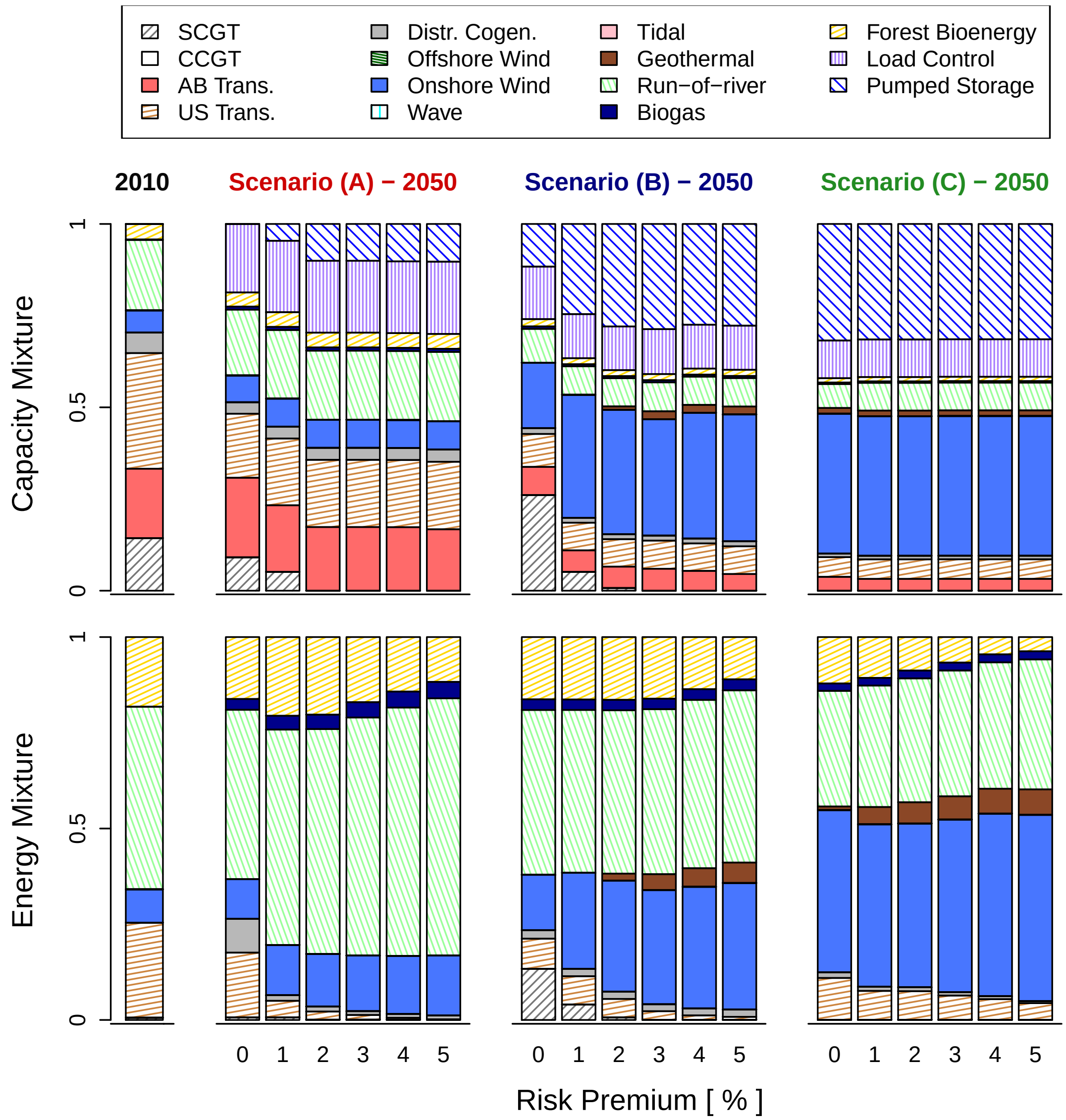

Figure 3.4: Sensitivity of the optimal capacity and energy mixtures in 2050 to the risk premium. The energy and capacity levels differ across each scenario and are depicted in Fig.(3.2).

sensitivity analysis is required to identify a given level of risk hedging expenditure.

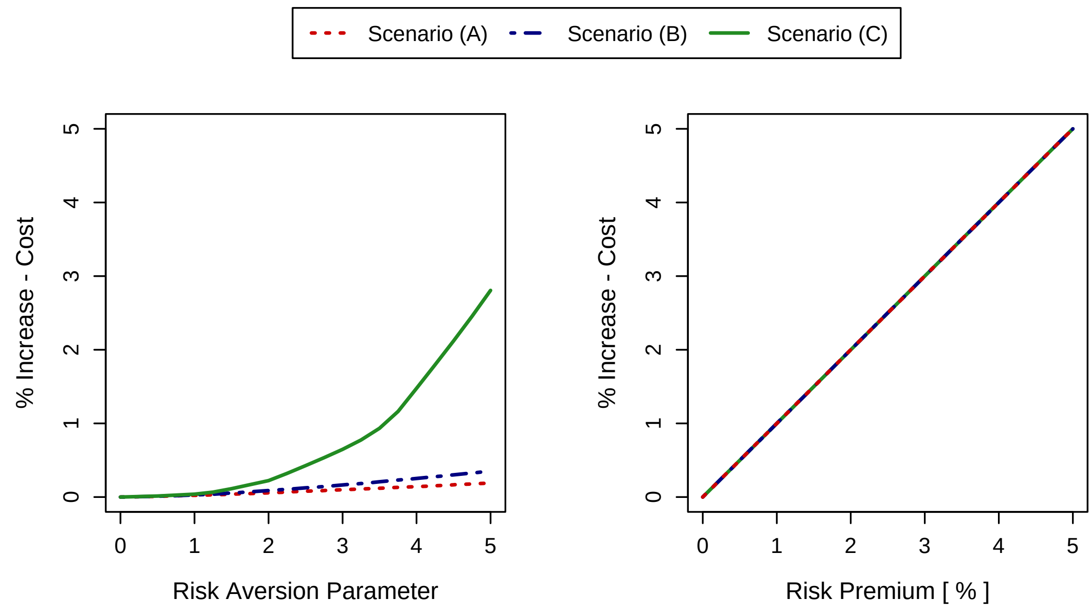

Figure 3.5: Relationship between risk parameterization and total system costs.

The primary purpose of including EP uncertainty into the long-term planning framework is to provide a way to hedge against environmental impact risk. To explore risk implications of the hedging expenditures, the cumulative emissions associated with the identified strategies were calculated under each stochastic realization of the emission factors. The distribution of results obtained for each risk parameterization are depicted in Fig.(3.6) as the percent change in baseline CO_2 emissions. The baseline represents the cumulative emissions calculated deterministically, or more specifically the cumulative emissions cap imposed on the electricity system. A percent change greater than zero therefore indicates a situation where the emission constraint is exceeded. A modest risk premium provides significant hedging against exceedance risks. For example, in scenario (C) a risk premium of 1% reduces the probability of exceedance from 45% to 4%, representing an 89% decrease. In all scenarios, risk-hedging investments reduce expected emissions.

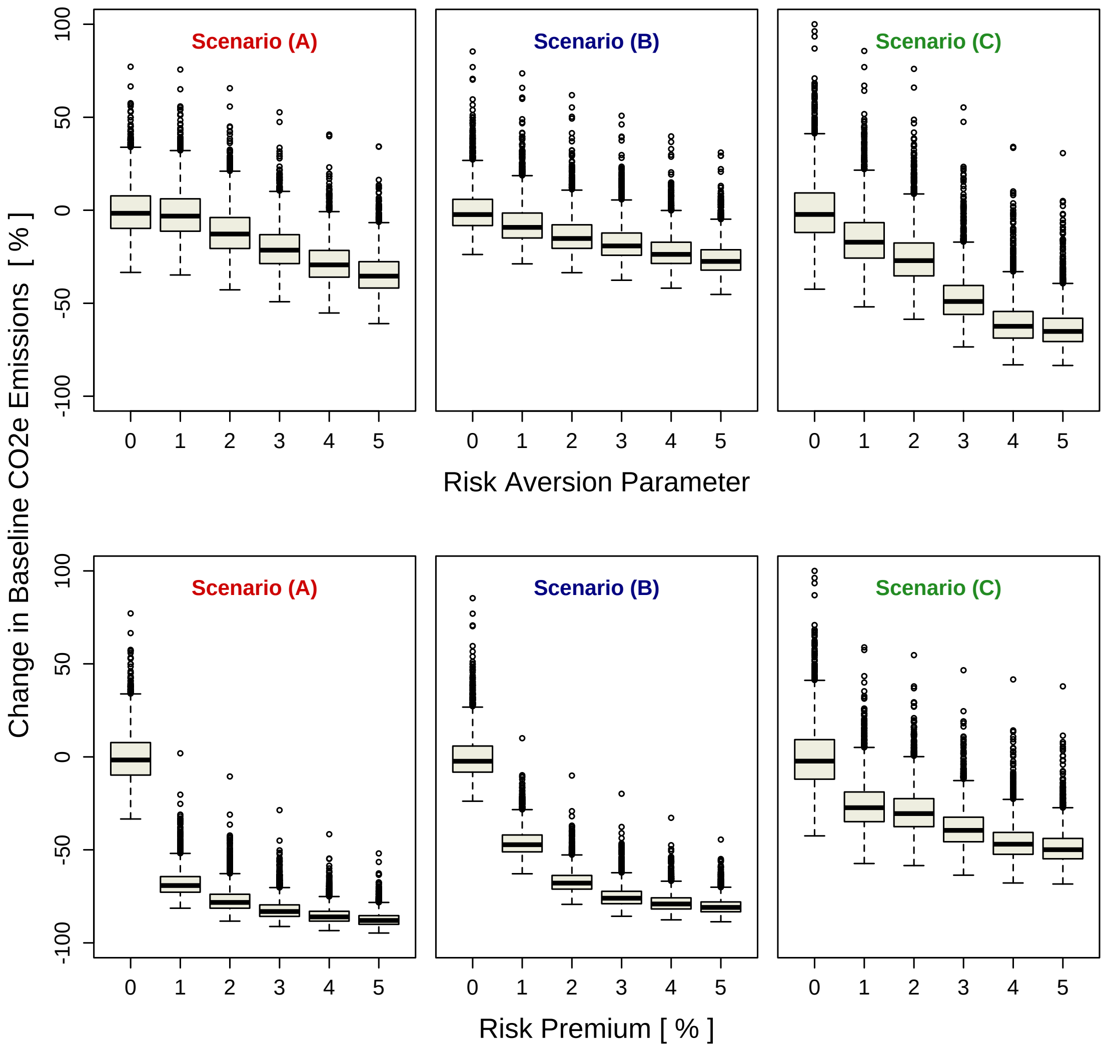

Figure 3.6: Impact of risk aversion parameter and risk premium on the CO_2 emissions uncertainty. Results are presented as distributions of percent change in baseline CO_2 emissions. The distributions are obtained by calculating the emissions associated with each stochastic realization of the emission factors. The baseline is the cumulative CO_2 emissions calculated under expected performance parameters, and corresponds to the emissions constraint imposed in each scenario. The edge of the box represents the 25th and 75th percentiles with the whiskers extending to 1.5 times the interquartile range. The outliers extend to the most extreme outcomes.

3.5 Conclusions

Deployment of energy technology under specified environmental impact constraints poses investment risk due to the uncertaintes in environmental performance. One way to safeguard the system from this risk is to hedge against it within the long-term development plan. The methodologies proposed in this paper provide such a procedure, by integrating stochastic EP metrics into the conventional long-term energy modeling framework.

The risk aversion parameter approach hedges against EP risk by holding a reserve margin. This reserve can be provided by either reductions in the expected environmental impact or the associated performance risk. The methodology brings some challenges in interpretation, due to the abstract nature of the risk aversion parameter and the need for its elicitation from often non-technical policy-makers. Furthermore, the risk aversion parameter approach requires sensitivity analysis to identify similar risk hedging expenditures within different modeling cases. Alternatively, the risk premium approach sets the available risk hedging budget from the onset. This enables quick comparison of risk across alternative model scenarios and is easier to interpret from a non-expert perspective. However, the focus in the risk premium approach is on risk minimization, meaning the model neglects potential opportunities to hold performance risk by reducing expected systemic environmental impacts.

When EP risk hedging is applied to British Columbia's electricity system, the results capture expected attitudes towards certain technologies that would otherwise be difficult to model. This includes the displacement of natural gas, forest bioenergy and interregional imports. Alternative methods might involve limiting the expansion or activity of these technologies with explicit constraints. The risk-hedging methodologies achieve these results under more formal conditions and allow identification of tradeoffs between technology options that might be difficult to identify within a scenario analysis. These qualities benefit the planning process, as the risk-hedging model is more transparent and robust than conventional deterministic designs.

Performance risk-hedging impacts both the timing and magnitude of technology investment, although activity limitation also provides opportunities for risk reduction. Incorporating EP risk into the planning framework is most valuable when decision-makers face stringent environmental constraints. In these situations, many of the low-cost environmental impact abatement measures would be part of the original deterministic agenda, making tradeoffs between risk hedging and technology selection potentially expensive. The model results indicate allocation of a modest risk premium in these situations provides valuable risk reduction, and thereby helps to safeguard against the possibility of exceeding environmental targets.

Chapter 4

Impacts of groundwater constraints on Saudi Arabia's low-carbon electricity supply strategy[1]

[1]The body of this chapter was published in S. Parkinson et al., *Environmental Science & Technology* 50(4), 1653-1662, 2016, and is reproduced with the permission of the American Chemical Society. SP and ND conceived and designed the study. SP performed the analysis, drafted the initial manuscript, and finalized the published version. Other authors contributed data and to the refinement of further manuscript drafts.

Preamble

Balancing groundwater depletion, socioeconomic development and food security in Saudi Arabia will require policy that promotes expansion of unconventional freshwater supply options, such as wastewater recycling and desalination. As these processes consume more electricity than conventional freshwater supply technologies, Saudi Arabia's electricity system is vulnerable to groundwater conservation policy. This paper examines strategies for adapting to long-term groundwater constraints in Saudi Arabia's freshwater and electricity supply sectors with an integrated modeling framework. The approach combines electricity and freshwater supply planning models across provinces to provide an improved representation of coupled infrastructure systems. The tool is applied to study the interaction between policy aimed at a complete phase-out of non-renewable groundwater extraction and concurrent policy aimed at achieving deep reductions in electricity sector carbon emissions. We find that transitioning away from non-renewable groundwater use by the year 2050 could increase electricity demand by more than 40 % relative to 2010 conditions, and require investments similar to strategies aimed at transitioning away from fossil fuels in the electricity sector. Higher electricity demands under groundwater constraints reduce flexibility of supply-side options in the electricity sector to limit carbon emissions, making it more expensive to fulfill climate sustainability objectives. The results of this analysis underscore the importance of integrated long-term planning approaches for Saudi Arabia's electricity and freshwater supply systems.

4.1 Introduction

Located on the Arabian Peninsula in Western Asia, the Kingdom of Saudi Arabia is a rapidly expanding economy of more than 28 million people. From 1990 to 2010, the average income in Saudi Arabia nearly doubled [170], and was accompanied by an average annual increase in urban electricity and freshwater demand of 7 and 3 % respectively [78, 171]. With similar demographic trends projected moving forward [172, 173], there is concern surrounding increased consumption. The additional strain on the region's existing infrastructure will require expanded electricity and freshwater supply capacity [171, 174, 175]. A key challenge facing regional planners is identification of a cost-effective and sustainable long-term development strategy.

Compared to most other nations, Saudi Arabia contains relatively little exploitable surface water, and relies primarily on groundwater resources for its freshwater supply [171]. Annual groundwater withdrawals of approximately 18 km^3 exceed the estimated national renewable groundwater resource of 0.8 to 2.2 km^3, and are rapidly depleting long-term aquifer storage in the region [79,171,176,177]. To mitigate the risk of freshwater scarcity, the country has developed more seawater desalination capacity than any other nation globally [177, 178]. Wastewater recycling also plays an important role in managing the region's freshwater challenges [177, 179]. As desalination and wastewater recycling requires more electricity than conventional groundwater and surface water supply technologies [180, 181], expanding capacity to balance groundwater constraints and urban growth will impact the regional electricity supply.

The bulk of electricity generation in Saudi Arabia is from oil burning thermal plants (53 % in 2010 [78]) that are carbon intensive. Increased electricity demand from the water sector thus exacerbates climate change risks. The region has abundant untapped renewable energy resources in the form of favorable solar, wind, and geothermal energy potentials [182–188]. To meet increasing demands while decreasing carbon emissions, national energy policy calls for the development of over 50 GW of new renewable electricity generation capacity by 2040 [189, 190]. Increased operational flexibility will support legislated solar and wind power integration, and is an electricity service market well-suited for an electrified freshwater supply [191–193]. Thermal power plants can also require large amounts of freshwater for cooling and steam production [194], although regional freshwater scarcity has prompted implementation of alternative seawater and air cooling technologies throughout Saudi Arabia [195–197]. Trade-offs with conventional freshwater cooling systems include increased implementation and maintenance costs, and reduced power generation efficiency [198–200].

The existing linkages between Saudi Arabia's electricity and freshwater strategies, and the pressing need for a transition towards a more sustainable pathway, make an integrated electricity-freshwater supply strategy essential. A number of previous studies highlight co-benefits of systems integration. Analysis of regional technology deployment strategies find that solar-assisted desalination is already cost-effective in many locations throughout Saudi Arabia for the combined supply of low-carbon electricity and freshwater services [183, 186]. Opportunities to enhance operational efficiencies in coupled electricity-water supply systems through combined management have also been investigated for similar arid regions in the Middle East [25, 191]. Recent analysis has also focused on the climate impacts of various water supply options in the US under pre-defined electricity supply scenarios [34]. Less explored are the interactions between electricity and freshwater systems during the planning of regional infrastructure capacity (supply technologies and networks). These investment decisions are important from the viewpoint of policy, as electricity and water supply infrastructures last for many decades and introduce structural inertia into the long-term development pathway [6]. This quality of energy and water infrastructure requires prospective analysis of development strategies over decadal timescales [6, 79].

Optimization models have emerged as key planning tools that enable system designers to explore long-term development pathways and the tradeoffs among technology options [201, 202]. Many regional jurisdictions employ optimization models to develop integrated resource plans [203], and yet few combine long-term energy and water supply planning despite potential synergies. For example, previous research demonstrates that water supply planning models are sensitive to energy prices [29, 201, 204], and likewise electricity generation planning models are sensitive to water constraints [23, 24, 28, 30, 70], and water-related energy demand [39, 174, 193]. Recent analysis of the Middle East region and China at a relatively coarse spatial and temporal resolution demonstrates the insights from and benefits of co-optimizing electricity and freshwater supply planning decisions [35–37]. This type of *hard-linked* optimization framework allows identification of pathways that hedge against undesirable interactions between electricity and freshwater systems, and provides a platform to explore technology portfolios that simultaneously balance energy and water sustainability objectives. Similar research underscores the importance of geography due to water distribution-related energy costs [39]. These spatial effects are particularly important to consider in the case of Saudi Arabia because of the inland urban population lacking direct access to desalination opportunities available on the coast.

In this paper, we develop a modeling framework that co-optimizes electricity and freshwater supply planning decisions across spatially-distributed regions to provide an improved representation of feedbacks between coupled infrastructure systems. The tool is applied to study impacts of groundwater management on the structure of the electricity system and the potential interplay with strategies aimed at reducing electricity sector climate impacts through deployment of low-carbon power generation. Results of this analysis provide important insight into the potential cost of policies and characteristics of technology portfolios that enable a transition towards a more sustainable system.

4.2 Methods

We explore the interaction between long-term groundwater constraints and climate change mitigation objectives with a linear systems-engineering optimization model. We provide an overview of the salient features of the model in this section; the mathematical details are given in the Supplementary Information (section S1 to S3). The modeling framework explicitly represents key electricity and water supply technologies in Saudi Arabia. Each technology is modeled as a linear input-output process where the consumption of resources and production of services are defined by average conversion factors. Technologies are coupled to form a closed system by accounting for the physical balance of resources across the modeled supply-chain. A cost-optimization model calibrated to the existing national electricity and freshwater supply systems is then used to identify future infrastructure investments under projections of future demand and technology costs. The framework is applied across a number of scenarios to explore sensitivities to different national policy levers and model parameterizations.

4.2.1 Integrated systems modeling

The integrated systems model developed for the analysis is depicted in Figure (4.1). The supply systems are mapped as a series of electricity and water flows between technologies. The system boundary is defined such that hydro-climate data is used to parameterize water resource constraints, including the availability of surface water, groundwater and precipitation. Sector demand projections parameterize supply requirements. The water supply technologies included are reverse osmosis (RO) desalination, multi-stage flash (MSF) desalination, rainwater harvesting, groundwater withdrawals, and surface water withdrawals. These technologies convert raw water resources (seawater, precipitation, groundwater and surface water) into freshwater suitable for consumption within the different end-use sectors (agriculture, industrial and domestic). Water storage technologies included are surface reservoirs and potable water storage at end-use. Wastewater recycling is also included in the analysis, and enables upgrading of wastewater to potable quality. Water supply technologies interact with the electricity system through electricity intensity factors (e.g., kWh per m^3 of potable water produced). The cost and energy intensity of water supply technologies are parameterized to include pre-treatment and local distribution (Supplementary Information, Table S4) [180,181,205]. Thermal energy requirements for MSF desalination technologies are also included and are supplied with the estimated excess heat from co-located thermal power generation, which is a common practice at modern combined-cycle plants in Saudi Arabia today [206].

Modeling of the electricity supply system parallels that of the water supply, and considers a number of different power plant technologies. Fossil fuel technologies (oil or natural gas) included are single- and combined-cycle steam turbines, and combustion turbines. We exclude carbon capture and storage technologies due to uncertainties surrounding costs and performance. Coal is also excluded due to its high emission intensity and expected impact on regional energy security (international imports would be required). Low-carbon technologies considered include nuclear, municipal waste-to-energy, geothermal, onshore wind, solar photovoltaic (PV), and concentrating solar power (CSP) with and without thermal storage. Thermal power plants (including CSP) are further distinguished by cooling technology to enable feedbacks to the water supply system. Once-through and closed-loop cooling systems utilizing freshwater are considered in the analysis, as well as air-cooled and seawater-cooled once-through systems. The volume of water withdrawn and the associated wastewater return flow is defined based on average water intensity factors (i.e., m^3 of water per kWh generated) [20]. The choice of cooling system affects operating efficiency and investment costs [198–200], and these characteristics are explicitly included in the analysis by defining unique parameters for each type of cooling technology.

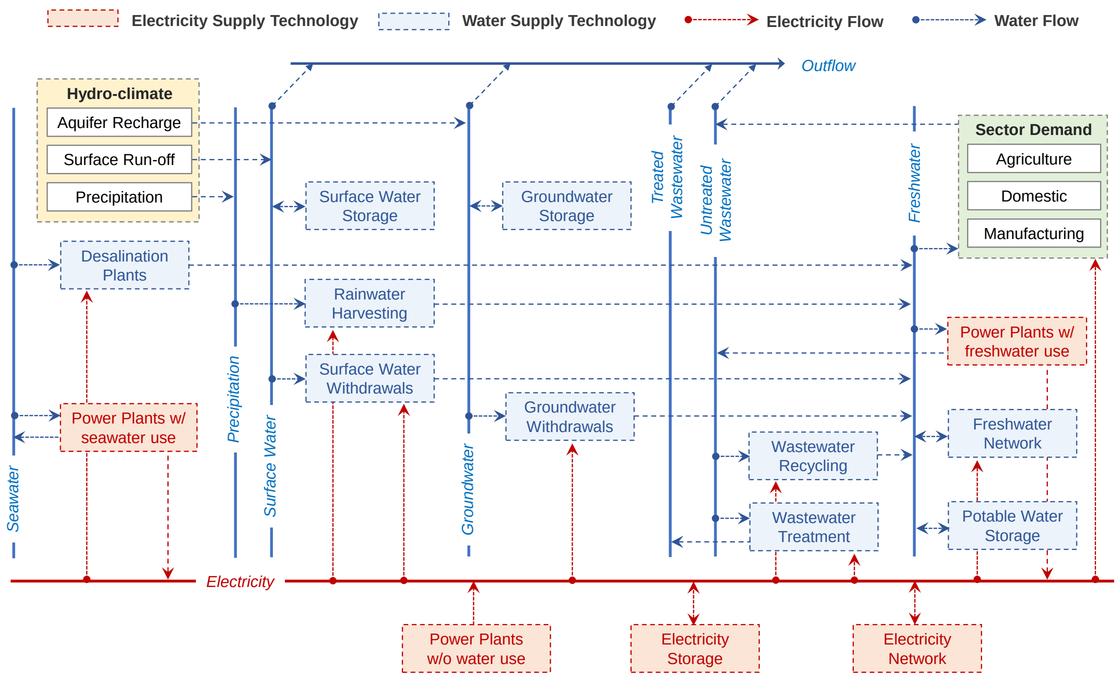

Figure 4.1: Integrated modeling of electricity and water supply systems. The systems are mapped as a series of flows between technologies. Each technology is modeled as a linear input-output process where the consumption of resources and production of services are defined by average conversion factors. Technologies are coupled to form a closed system by accounting for the physical balance of electricity and water flows across the modeled supply-chain. The system boundary is defined such that existing hydro-climate data is used to parameterize water resource constraints, including the availability of surface water, groundwater and precipitation. Exogenous sector demand projections parameterize supply requirements. The integrated system is represented in each province, with the network technologies allowing flow and trade of electricity and freshwater between provinces.

Constraints on peak and flexibility requirements of the electricity technology portfolio are defined to reflect operating constraints occurring between model periods (Supplementary Information, section S1) [207]. We also distinguish flexible and base-load power plant operational modes to account for different operating costs and scheduling procedures that accompany flexible operation [208]. Short-term electricity storage and load control technologies are also included in the analysis, and interact with the system by providing peak and flexibility reserve capacity [209]. The potential for load control is dynamically linked to the total demand for electricity, allowing increased demand from the water sector to contribute to load control capabilities. The load control technologies are different from end-use conservation measures, which are addressed in the scenario analysis.

Long-distance transport of electricity and water is important to consider when comparing options for supply development [38, 40, 210]. We incorporate spatial effects by disaggregating the study region into the 13 provincial administrative regions (Supplementary Information, Figure S6). We chose this level of spatial disaggregation due to limited input data and computational efficiency. Expandable electricity and freshwater transmission between regions is included in the model with a simplified transport representation (i.e., the capacity of a network pathway is defined as a maximum amount of water or electricity that can be transferred over a given model period). Transmission losses are included (Supplementary Information, Table S7). Energy for interprovincial water conveyance is estimated based on a recent analysis of long-distance desalination transport in the United States [211], and incorporates vertical and horizontal components of expected energy use (Supplementary Information, S1.2). Distances and elevations between regions are inferred based on the locations of major provincial cities, with primary road transport connecting these cities used as a proxy for candidate network pathways. Elevation distances are calculated based on the altitude of major cities and do not incorporate the cumulative elevation change.

Although the majority of Saudi Arabia's population resides in urban areas (82 % in 2010 [170]), there remains a significant rural population. These individuals often lack access to the urban electricity and water supply infrastructures. We model the rural technologies separately to reflect these differences, with limitations set on the availability and cost of options. Rural electricity technologies considered in the model include diesel generators, solar PV and battery storage systems. For freshwater, rural areas are assumed to have access to groundwater, rainwater harvesting, and wastewater recycling technologies [212]. Anticipated urbanization is included in the demand projections, allowing the analysis to address future migration towards urban areas. Electricity and freshwater trade between rural and urban areas is excluded.

4.2.2 Optimization

Optimization methods are used to solve for the capacity (design) and output (activity) of technologies included in the model (Supplementary Information, section S1). The objective of the optimization is to minimize cumulative discounted costs of water and electricity supply systems over the planning horizon, with technology investment, fixed/variable O&M, and fuel costs considered in the system cost accounting. This type of cost optimization model is common in national infrastructure planning [202, 203], and could be extended to include risk metrics or multi-objective formulations. Similar to the approach proposed in Dubreuil et al (2013) [35], we represent both water and electricity supply technologies and solve for the design and activity variables simultaneously. Climate and groundwater objectives are modeled as constraints on carbon emissions and groundwater withdrawals. A planning horizon of 2010 to 2050 in 5-year segments is selected for the analysis to explore impacts of national policy and path-dependency on technology deployment. Each modeled year is broken into monthly time-slices to enable treatment of seasonal effects, such as the potential mismatch between available supply and demand. Intertemporal optimization is used to solve for each time-step concurrently.

4.2.3 Parameterization

A significant amount of input data is required to parameterize the model, and is detailed in the Supplementary Information (section S2). We specifically calibrate the model to existing conditions by identifying the capacity, vintage, and location of existing and committed infrastructure from regional planning documents and recent resource assessments [174, 177, 180, 195, 196, 213–215]. Cost and performance data for supply technologies are taken from a number of recent technology assessments [20, 123, 180, 181, 205, 212, 216–221].

Future fuel costs are estimated using domestic prices from a previous regional planning study [174], and growth rates for the Middle East North Africa (MENA) region projected from a global integrated assessment model [222]. Due to regional water scarcity and lack of data, we assume that all thermal power generation in 2010 located in coastal regions are seawater-cooled and all thermal generation in 2010 located inland are air-cooled. Technical documentation for large-scale plants support this assumption [195–197].

4.2.4 Demand projections

Demands for electricity and water from the coupled supply technologies are endogenous to the cost-optimization model. Limited data is available to parameterize the diverse set of technologies and consumers existing in the domestic, agriculture and manufacturing sectors. We therefore treat these demands as exogenous and define a number of scenarios to explore uncertainties surrounding conservation potential. Econometric models linking socioeconomic development to consumption are typically used to generate exogenous electricity and freshwater demand projections [174, 183, 203], and we apply a similar approach to generate demands for Saudi Arabia. The demand models estimate agriculture, manufacturing and domestic electricity and freshwater consumption based on projected population, urbanization, GDP and rate of technological change (i.e., improved efficiency over time). The model identification process and parameterization is summarized in the Supplementary Information (section S3). Corresponding wastewater volumes from the industrial and domestic sectors are estimated with national consumption efficiencies (the fraction of water withdrawn that is consumed) from a previous global analysis [223].

For the projections, we use population, urbanization, and GDP trajectories aligned with the shared socioeconomic pathways (SSP) [172, 173, 224, 225]. We specifically focus on the SSP2 scenario, a mid-range case reflecting a continuation of current trends (moderate sustainability policy and technology shifts). Although SSP2 is a moderate scenario (globally), in the specific case of Saudi Arabia it corresponds to substantial population and economic activity growth [172, 173]. We utilize the quantitative SSP scenario data to generate a reference national-level electricity and freshwater demand trajectory for each sector (agriculture, manufacturing, and domestic) out to 2050. The results are depicted in

Figure (4.2) and project an average annual growth rate for urban electricity demand of 3 %. The trajectories are more conservative than other recent projections [189], and suggest the existing renewable energy deployment strategy (50 GW by 2040) will accommodate load growth and not reduce aggregate electricity sector emissions.

Water demands remain relatively constant reflecting large reductions in per capita irrigation. Nevertheless, desalination would be needed to support the reference agriculture demand under aggressive groundwater conservation, which represents a significant and costly transformation pathway. Similar development has occurred in Spain and Israel, where the desalinated seawater enables production of high-value fruits and vegetables in areas facing water scarcity [226]. Recent analysis of Saudi Arabia's agricultural policy suggests a shift towards increased production of similar crops to promote national food security [227]. It therefore seems likely that Saudi Arabia would consider large-scale seawater desalination as a potential supply option for irrigation.

When desalinated seawater or recycled wastewater is used for irrigation, additional care must be taken to replace nutrients stripped during the treatment process that are important for soil quality [228,229]. These additional costs are excluded from the assessment due to lack of data.

The estimated national domestic and industrial demands are downscaled to the provincial level based on the population distribution, whereas agriculture demands are disaggregated following the historical provincial distribution [230]. Future monthly domestic electricity demands are decomposed based on historical trends [189]. Domestic and irrigation water demands are broken into monthly components based on the estimated monthly average soil moisture deficit, which is calculated across 1/4 degree grid cells and weighted based on population for domestic demands [231].

4.2.5 Scenarios

The model is applied across a number of scenarios to explore: (1) tradeoffs and synergies between groundwater and climate policy; and (2) sensitivity to uncertainties in model parameterization. The impact of national groundwater policy on the electricity and freshwater supply systems is explored by varying the allowable annual extraction in each model

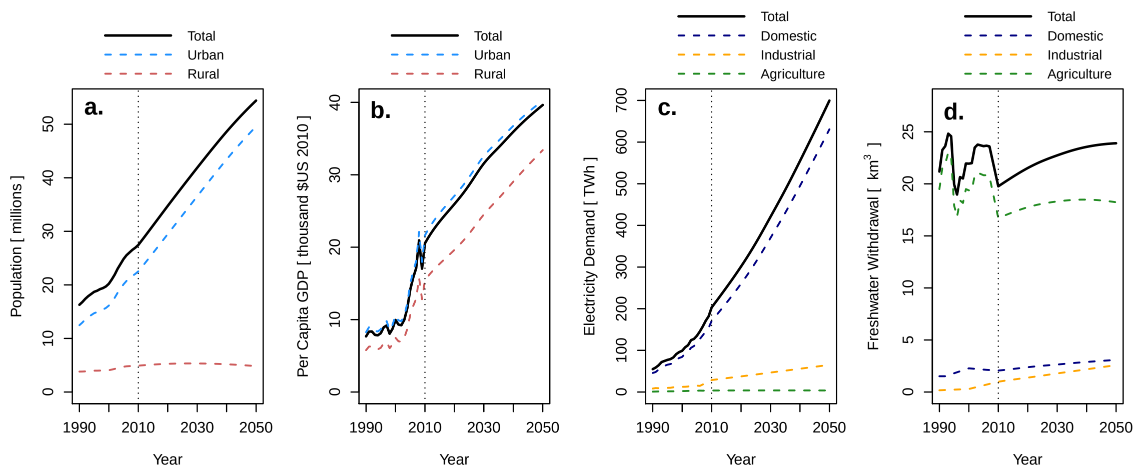

Figure 4.2: National socioeconomic and demand projections for the SSP2 scenario. a. Population; b. Per capita GDP; c. Electricity demand; and d. Freshwater withdrawal. Industrial demands exclude electricity for desalination and cooling water for thermoelectric generation.

region. It is estimated that at current extraction rates approximately 50 years of fossil groundwater remains in Saudi Arabia [180, 232], although estimates vary widely across the literature [177]. We initially explore the mid-century timeframe by constraining the allowable extraction in each region along a linear trajectory that results in national annual groundwater withdrawals reducing from 18 km^3 in 2010 to 1.6 km^3 in 2050 (i.e., a 91 % reduction). This would correspond to an annual extraction rate in 2050 that falls within estimates of the renewable recharge [177, 230]. This also corresponds to a depletion of remaining non-renewable groundwater reserves of approximately 330 km^3 by 2050, which is within recent estimates of the available resource [177]. It is important to note that further investigation into the distributed aquifer response via long-term hydrogeological modeling should be pursued to fully understand the implications for groundwater sustainability [79, 233].

We also explore potential interplays with increasingly ambitious climate policy. Limiting 21st century climate change to 2 °C over pre-industrial levels will require widespread transformation of the electricity system [222]. We construct scenarios for Saudi Arabia by simulating stringent mitigation policies that are constrained to achieve an 80 % reduction in cumulative carbon emissions as compared to unconstrained conditions by the year 2050. Sensitivity to simultaneous groundwater and climate objectives are then examined by simulating different combinations of increasingly stringent policy scenarios. Each policy objective is varied between a baseline (0 % fulfillment) and a 100 % fulfillment case in increments of 50 %. As groundwater is already overexploited, the baseline constrains withdrawals to 2010 levels. The results of this analysis provide insight into how costs and technology deployment patterns vary based on groundwater and climate policy ambition.

To investigate results sensitivity to uncertain model parameters, the cost-optimization model is applied across the scenarios listed in Table (4.1). The *Reference* scenario considers average performance parameters and the exogenous demands depicted in Figure (4.2). Uncertainties surrounding the scale of the available groundwater resource are explored by parameterizing a conservative scenario that shifts the 91 % reduction target to the year 2030. An additional scenario considers a 50 % capital cost subsidy to renewable electricity generation, and is meant to reflect a situation where market conditions are improved with external financial support. The remaining scenarios explore demand uncertainties. Although the reference demand trajectories include improvements in energy efficiency, advanced conservation scenarios are defined to reflect uncertainties surrounding technological change, price response, and end-use behaviour (Supplementary Information, Figures S2 and S3). Exogenous demands in the advanced conservation scenarios decrease 40 % by the year 2050 relative to the reference scenario. This represents a potential for water and electricity conservation similar to that identified in recent analyses [39, 180, 234, 235]. The potential impacts of alternative food import policies on national irrigation withdrawals are also important to consider due to the fraction of total freshwater demand applied for irrigation. We explore a scenario investigating the potential for increased food imports to displace unconventional water resource expansion by simulating a 50 % reduction in irrigation withdrawals by 2050 (Supplementary Information, Figure S4). The electricity intensity of water supply technologies is also uncertain, and we explore the potential for enhanced performance to impact the results by including a scenario parameterized with the lowest energy intensities from the literature (Supplementary Information, Table S4). Finally, we combine all conservation measures and efficient water supply assumptions to generate an *Optimistic* development scenario (Supplementary Information, Figure S5).

Scenario	Model implementation
Reference	Reference demand trajectories. Performance / cost parameters follow averages from the literature.
2030 groundwater target	The groundwater target year is shifted from 2050 to 2030.
Low-cost renewables	Investment costs for renewables are reduced by 50% relative to the reference scenario.
Water conservation	Exogenous freshwater demands are reduced by 40 % in 2050 relative to the reference scenario.
Electricity conservation	Exogenous electricity demands are reduced by 40 % in 2050 relative to the reference scenario.
Increased food imports	Agriculture freshwater withdrawals are reduced by 50 % relative to the reference scenario.
Efficient water supply	Water supply technologies set to the lowest energy intensity from the literature.
Optimistic	Electricity and water conservation, increased food imports and efficient water supply.

Table 4.1: Summary of scenarios explored in the analysis.

All scenarios include Saudi Arabia's existing renewable energy deployment strategy that involves integration of over 50 GW of renewable power generation by 2040. The strategy includes the following technology-specific targets: 25 GW of CSP, 16 GW of solar PV, 9 GW of wind, 3 GW of waste-to-energy, and 1 GW of geothermal [189]. We model this policy by constraining the capacity from the associated technologies to exceed an annual deployment target in each simulated year. The target capacity development represents a linear trajectory fitted between current levels and the 2040 goal.

4.3 Results

We initially focus on analyzing the implications of simultaneous groundwater and emission constraints on supply and network technology development for the *Reference* scenario. Depicted in Figure (4.3) are the optimal supply mixes and network technology capacities aggregated to the national-scale for the year 2050 across the groundwater and climate policy objectives simulated. Provincial results are included in the Supplementary Information (section S4.2).

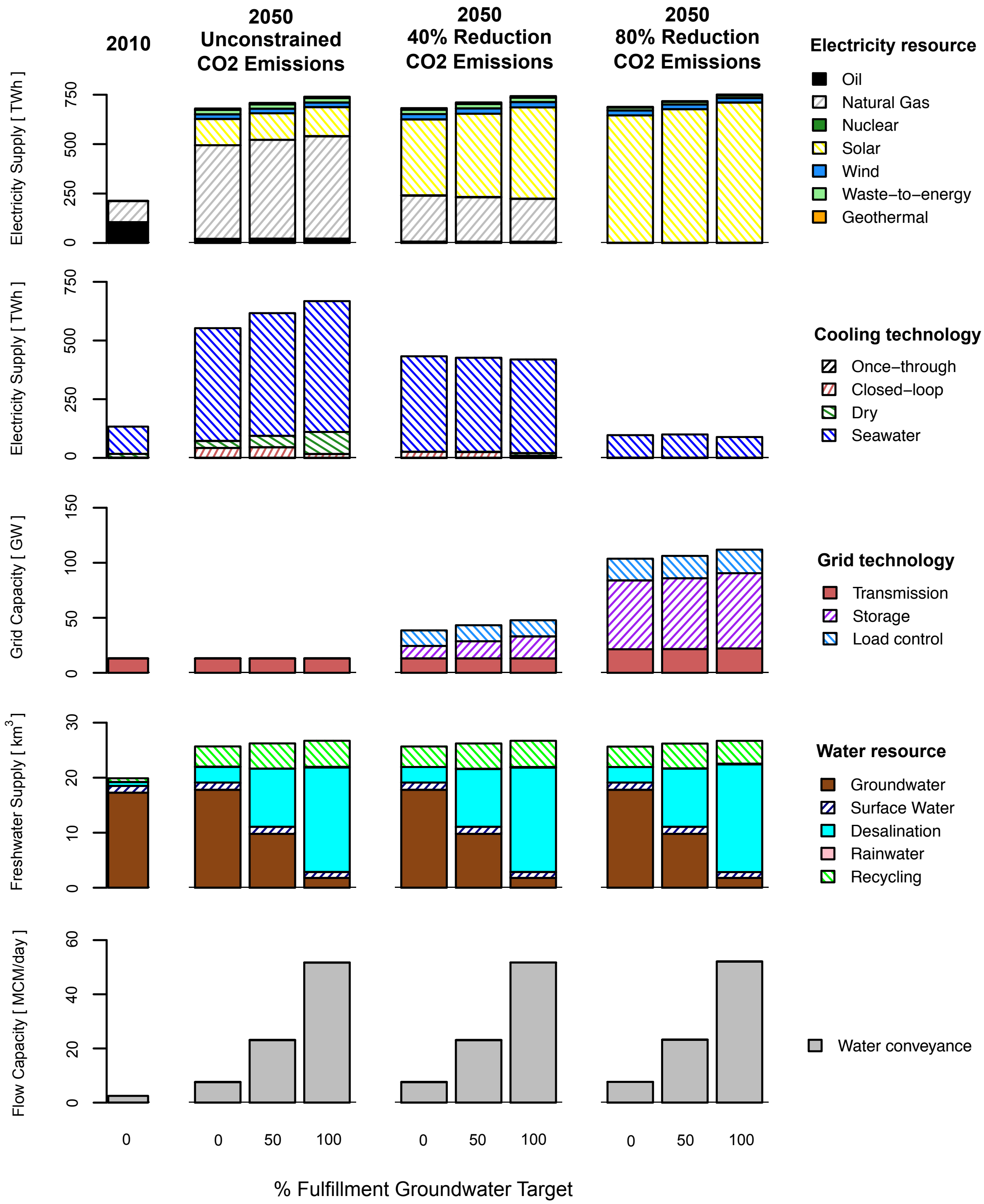

Figure 4.3: Optimal supply mixes and network technology capacities aggregated to the national-scale for the year 2050 across the groundwater and climate policy objectives investigated. The groundwater target represents a 91 % reduction in annual groundwater withdrawals in 2050 relative to 2010.

The rapid growth in electricity demand and retirement of existing units results in a complete redesign of the electricity generation portfolio. When carbon emissions are unconstrained, combined-cycle natural gas plants make-up the largest portion of new capacity due to the relatively low investment cost. The capacity is deployed primarily in coastal regions to access seawater for cooling. A relatively small amount of capacity employing closed-loop freshwater cooling is also deployed in Asir: a province lacking coastlines but with a relatively high per capita availability of surface water resources. Air-cooled combined-cycle generation and combustion turbines are deployed in the remaining provinces to help support load growth without expanding transmission. Existing renewable energy policy (50 GW of installed capacity by 2040) results in wind, geothermal, solar PV and CSP expansion. The CSP capacity is deployed in coastal regions due to the accessibility of seawater for cooling. Rural areas combine diesel generators with PV capacity to meet the stagnating demand growth anticipated under the SSP2 urbanization scenario. The constraint on groundwater withdrawals in the reference case to remain at or below 2010 levels results in an increase in wastewater recycling and desalination capacity, and expansion of the water conveyance infrastructure beyond 2010 levels is needed to transport desalinated water inland.

Policy that reduces cumulative carbon emissions in 2050 by 80 % relative to the unconstrained scenario triggers an electricity system transformation. All regions rapidly deploy solar technologies to reduce emissions, and utilize a combination of conventional storage and load control technologies to maintain system reliability. PV technology expands particularly quickly under the parameterized cost improvements. Seawater withdrawals reduce significantly under PV expansion due to the displacement of seawater-cooled thermal generation. Electricity transmission capacity is reinforced to support matching seasonal solar and load coincidence across provinces. The electricity system transformation is found to have a relatively modest impact on the structure of the water supply. The largest difference compared to the unconstrained emissions case is a small increase in wastewater recycling.

Policy that reduces annual groundwater withdrawals in 2050 by 91 % relative to 2010 results in a significant transformation of the water supply system. RO desalination capacity expands rapidly in coastal provinces, and all regions utilize available wastewater for recycling. The interprovincial water network is developed more extensively to support inland transfer of desalinated water from coastal regions, and a greater volume of water must be produced to overcome distribution losses. The regional distribution of electricity technologies shift towards increased capacity of power generation in coastal regions where desalination occurs. The increased electricity demand from desalination and water conveyance impacts the electricity transmission configuration, with larger capacity corridors developed between regions connecting high-quality inland solar energy resources with coastal desalination opportunities. More investment into load control technologies also occurs due to greater resource availability accompanying the increased water sector electricity demand.

In the baseline scenario (no emissions or groundwater reduction targets), water sector electricity use increases from 15 TWh in 2010 to 22 TWh in 2050 (3 % of total national electricity demand). The majority of water sector electricity use in this case is from groundwater (11 TWh), with the remaining balance mainly attributed to desalination (6 TWh), recycling (3 TWh) and conveyance (2 TWh). Electricity requirements increase rapidly with stringency of the groundwater constraint. In the scenario where groundwater withdrawals are reduced by 91 % in 2050, the freshwater supply sector represents 12 % (92 TWh) of total final electricity demand. For perspective, this represents more than 40 % of the total national electricity demand in 2010. The majority of increased electricity use comes from desalination (67 TWh), water conveyance (19 TWh) and wastewater recycling (4 TWh), with groundwater electricity demand dropping significantly (1 TWh). The freshwater allocated to the electricity system is less intuitive. Most freshwater is used in the unconstrained emissions scenario to support closed-loop cooled natural gas generation located inland, with a small amount persisting in the intermediate scenario despite increasingly stringent groundwater constraints. Nevertheless, freshwater allocated to the electricity sector in the most extreme case represents less than 1 % of projected national demand across all sectors in 2050, suggesting a relatively minor role in future freshwater supply requirements.

Transitioning to 100 % fulfillment of the groundwater conservation objective without climate policy results in costs increasing 46 % compared to the baseline scenario. Under 2010 groundwater withdrawals, reducing cumulative carbon emissions by 80 % increases discounted costs by 51 %. Combining the 91 % groundwater reduction and the 80 % emission reduction policies results in costs increasing by 101 %. The main challenge under combined policy objectives is the need to simultaneously increase electricity supply capacity to allow for increased electricity demand due to desalination, wastewater recycling and water conveyance, while decreasing carbon intensity to maintain cumulative electricity sector carbon emissions. It is important to note that some of the benefits and costs associated with these scenarios are excluded (e.g., conservation measures, climate damages, reduced air pollution, avoided water shortages, etc.).

Further sensitivity analysis is performed by examining the results obtained across the different scenarios listed in Table (4.1). We specifically explore uncertainties surrounding future costs by varying the technology cost assumptions across a suitable range identified in the literature (Supplementary Information, Table S9) [220]. Figure (4.4) depicts the percent change in discounted system costs relative to the unconstrained baseline scenario (i.e., no cumulative emissions constraint, groundwater extraction limited to 2010 rates, reference demand trajectories, and average cost / performance parameters for technologies). System costs increase in the reference scenario between 79 to 149 % relative to the unconstrained scenario. Nuclear generation expands when the least optimistic technology costs are assumed due to the slow cost improvement for solar generation and advanced grid technologies (load control and storage). Major cost savings are achieved in the ”Low-cost renewables” scenario. PV and CSP become more attractive as a generating option, and expand across all regions to prevent transmission development despite the geographic diversity modeled between provinces. When the groundwater target year is shifted to a more conservative 2030 fulfillment timeframe, investment into unconventional water resource options is accelerated earlier in the planning horizon, leading to large increases in system costs. The scenarios involving reduced demands achieve significant savings, while the enhanced water supply performance scenario displays less impact. The ”Optimistic” scenario, combining the conservation and efficient water supply parameterizations, results in a supply portfolio that costs 11 to 65 % more than the unconstrained case, thus representing considerable savings when compared to the costs obtained for the reference scenario.

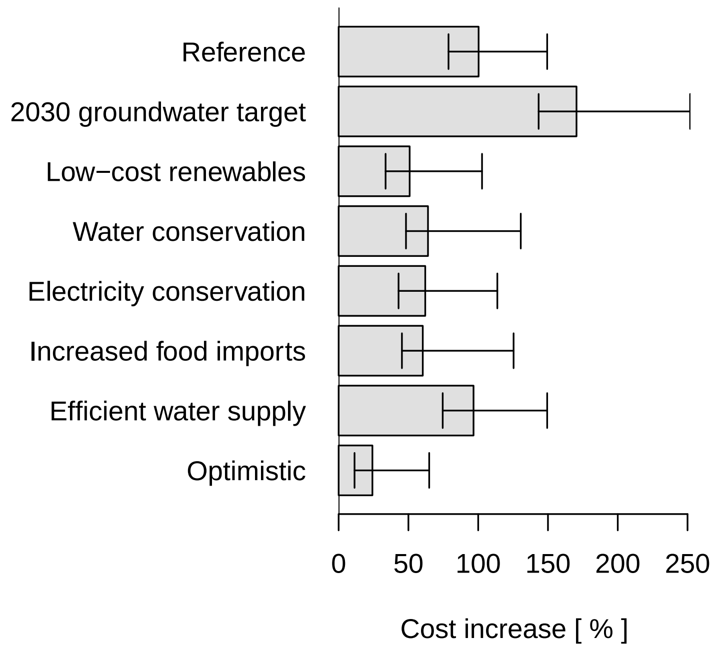

Figure 4.4: Sensitivity to technology cost parameterization for the scenarios listed in Table (4.1). The horizontal bars represent results obtained with average cost parameters. The error bars span the results obtained with the minimum and maximum cost parameters. Each scenario considers 100 % fulfillment of the groundwater and climate objectives (91 % reduction in groundwater withdrawals and 80 % reduction in cumulative carbon emissions). The cost increase is calculated as a percent change relative to the unconstrained baseline scenario (i.e., no cumulative emissions constraint, groundwater extraction limited to 2010 rates, reference demand trajectories and average cost / performance parameters for technologies).

4.4 Discussion

Many parts of the world face increasing groundwater stress that will necessitate the deployment of alternative electricity-intensive water infrastructure, such as desalination, wastewater recycling, and long-distance water transfers. Saudi Arabia is one of the most severely constrained jurisdictions in this respect and provides a challenging case study for exploring tradeoffs between electricity and freshwater systems. In this paper, we developed a new modeling framework that hard-links electricity and freshwater investment decisions across provinces to provide an improved representation of feedbacks between coupled infrastructure systems. The framework was applied to explore impacts of groundwater constraints on the structure of electricity and freshwater supply in Saudi Arabia, and the potential interplay with climate policy aimed at reducing electricity sector carbon emissions.

Our results suggest that strategies aimed at achieving deep reductions in non-renewable groundwater extraction will lead to fundamental changes in regional electricity system design. Large-scale expansion of desalination and regional water distribution capacity emerges as a critical infrastructure solution enabling displacement of groundwater withdrawals while supporting growth in urban freshwater demand. The required infrastructure increases water sector electricity-intensity and migrates electricity demand from distributed groundwater pumping stations to coastal desalination plants. The reconfiguration of demand benefits thermal generation, due to the ability to co-locate with desalination plants and access seawater for cooling. Protecting coastal ecosystems from the increased industrial activity (e.g., thermal water pollution) will pose additional constraints to technology development that were unexplored in this analysis, and important to address in future research.

Our results further suggest that strategies aimed at mitigating non-renewable groundwater extraction are likely to require similar investment as strategies aimed at limiting fossil fuel use in the electricity sector. The increased water supply costs follow from the required ramp-up in desalination and water distribution investments. When emission constraints are also considered, we find that higher electricity demands under groundwater constraints reduce flexibility of supply-side options in the electricity sector to limit carbon emissions. The need to simultaneously increase electricity supply capacity while reducing carbon intensity make it more expensive to fulfill climate change mitigation objectives under groundwater constraints. The integrated planning framework incorporating investment and operation across provinces is crucial to identifying these tradeoffs, and underscores the importance of a systems perspective when assessing suitability of supply options across the electricity-water nexus.

Results incorporating optimistic demand projections indicate the significant potential for end-use conservation to enable a low-cost transition away from non-renewable groundwater use and towards a low-carbon electricity system. Potential policy instruments targeting demand reductions include increased prices or end-use efficiency standards. Our assessment also demonstrates the sensitivity of the optimal system configuration to uncertainties surrounding groundwater constraints and technology costs. To provide further insight into robust strategies, future work should consider endogenous representations of these key uncertainties in the optimization model. Finally, the importance of agricultural policy suggests the framework would benefit from incorporating land-use decisions. This approach would enable consideration of adaptive land management to address concerns surrounding desalination and national food security.

Chapter 5

Multi-criteria infrastructure planning for integrated water-energy systems[1]

[1]The body of this chapter was submitted for publication, and is reproduced with the permission of Elsevier. The analysis extends the modeling framework developed in chapter 4. Simon Parkinson, Marek Makowski and Ned Djilali conceived and designed the study. SP performed the analysis, drafted the initial manuscript, and finalized the published version. Marek Makowski provided software for the computations and assistance with the analysis. Other authors contributed data and to the refinement of further manuscript drafts.

Preamble

Sustainable development objectives surrounding water and energy systems are interdependent, and yet the associated performance metrics are often distinct. Regional planners tasked with designing future supply systems therefore require multi-criteria analysis methods and tools to determine a suitable combination of technologies and scale of investments. This paper presents a flexible and interactive multi-criteria model analysis framework and its application to long-term energy and freshwater supply planning at national or regional scales. The framework incorporates a linear systems-engineering model of the coupled supply technologies and intra-regional transmission networks. The applied multi-criteria analysis approach enables the interactive specification of diverse decision-making preferences for disparate criteria, and leads to learning on trade-offs between the resulting criteria values of the corresponding Pareto-optimal solutions. A case study of the water-stressed nation of Saudi Arabia explores diverse, simultaneously attainable goals for conflicting objectives such as cost, water and climate sustainability, and reveals the corresponding integrated system configurations that remain ambitious from both an economic and environmental perspective.

5.1 Introduction

Water plays a key role in the supply of energy in many regions globally, primarily for thermal power plant cooling and hydropower generation [236]. Constraints on the availability of water resources in these regions therefore pose risks to energy service reliability. At the same time, a significant amount of energy is required to extract, treat and distribute freshwater resources [2]. Constraints on the supply of freshwater services therefore pose risks of additional energy requirements. Moreover, energy and freshwater are required for meeting the development goals of societies. These interdependencies promote integrated planning of water and energy infrastructure systems.

Infrastructure here refers to the technologies or processes that enable supply of energy and water services to consumers. Planners tasked with designing regional energy and freshwater infrastructures are faced with a plethora of technologies and a wide variety of economic, social and environmental conditions, which make it difficult to decide which technologies to invest in and promote, and in what order. The optimal combination of technologies and level of investments will be difficult to determine without appropriate analysis methods and tools. From this perspective, mathematical programming models have provided critical decision support by enabling planners to identify system designs that perform well under anticipated operational conditions [6, 8, 9, 201, 237, 238].

Previous studies explored impacts of water constraints on energy system operation by coupling water supply and electricity generation dispatch models [25, 30, 32, 239, 240]. Several other previous studies note the importance of future capacity decisions (the size and location of technologies) in terms of enabling effective adaptation to future water constraints, and examined the impact of water availability on the development of regional power systems by adding explicit water constraints to an optimal infrastructure planning model [23,24,28,31,67,241]. Water constraints are found to primarily cause a shift towards water-efficient cooling technology for thermal power generation, as well as increased siting in regions with greater access to water availability [31]. Increased hydrologic variability under climate change was also found to cause further long-term capacity challenges in regions where hydropower plays an important role in electricity supply [67, 160]. A key limitation of these previous analyses of water constraints is the inability to incorporate feedbacks from future water supply development, which will impact the availability of water for energy and water-related energy demand. To reconcile development interdependencies, a number of other studies link freshwater and energy infrastructure planning models directly [29, 35, 37, 39, 70]. This approach enables modeling of system configurations that adapt to undesirable interactions between water and energy during infrastructure development.

Most previous coupled planning models focus on identifying system configurations that minimize costs or maximize consumer surplus. Yet, there are often other social or environmental objectives of concern to regional decision-makers and stakeholders, thus requiring a more integrated approach to assessing system performance [242]. Metrics of interest include limiting greenhouse gas emissions and air pollution, and securing food, water and energy resources. Previous analyses addressed such objectives as constraints, values of which were explored using parametric optimization [11, 23, 37, 241]. Parametrization of constraints requires not only skilled analysts but also specification of a large number of optimization problems, many of which are either infeasible or result in dominated (inefficient) solutions. Multi-criteria analysis (MCA) of discrete alternatives can be applied to the results of parametric model optimization [11], but such a two-stage process is by far less effective than a direct linking of the model with the MCA tool. Another popular approach is based on weighted-sum criteria aggregation into a composite goal function. This approach has, however, serious shortcomings [243], e.g.,: (1) in some situations the same solution is returned even if substantial changes are made to the weights; (2) many efficient solutions[2] cannot be obtained by varying the weights; and (3) increasing a weight does not guarantee improvement of the corresponding criterion value.

In this context, MCA methods offer an improvement to traditional optimization approaches, as illustrated by a sample of applications relevant to the case study presented in this paper [244–247]. MCA supports analysis of tradeoffs between all relevant objectives, and interactive exploration of diverse efficient solutions across multiple objectives. Despite the potential to apply this type of methodology and tools to effectively model coupled economic-environmental decision-making [76], application of MCA to the integrated planning of energy and water systems has been limited to cooling technology choices in the power sector [77].

This paper presents a novel systems analysis tool for integrated regional planning of energy and freshwater supply systems. The framework incorporates a multi-objective decision support system to enable analysis of long-term infrastructure strategies that balance economic, energy and water sustainability objectives. The integrated decision support framework is demonstrated within a case study of the water-stressed nation of Saudi Arabia. The results of the analysis provide important insight into model formulation and the scale of tradeoffs between environmental and human development objectives in the case study region.

[2]Solutions are called efficient or Pareto-optimal if there exists no other solution for which at least one criterion can be made better without sacrificing performance of the criteria.

5.2 Methodology

This section presents the approach for coupled water-energy supply planning and its integration with the MCA methods and tools. The framework is based around a water-energy infrastructure planning model developed previously for Saudi Arabia [241]. Previous research with this framework demonstrated that transitioning away from nonrenewable groundwater use by the year 2050 in Saudi Arabia could increase electricity demand by more than 40% relative to 2010, due to rapid development of desalination and water conveyance infrastructure, and require investments similar to strategies aimed at transitioning away from fossil fuels in the electricity sector. These results highlight the need to incorporate multiple policy objectives into system design, and is the key feature of the enhanced MCA tool proposed in the current study. Following a description of the mathematical model for coupled water-energy supply planning, we discuss its integration with the applied MCA methodology. Finally, we describe the input data and scenarios explored in the case study demonstrating model application.

5.2.1 A core model for water-energy infrastructure development

The planning challenge dealt with in this paper is the sustainable long-term development of water and energy systems. These decisions are typically made at national or regional-scales, and encompass choices surrounding the capacity of existing and future infrastructure. Capacity decisions are key design parameters for energy and water supply planners due to the relationship with geographical constraints, investment costs and long-term structural inertia of the supply systems [6]. Capacity choices incorporate both the size and location of new technologies, as well as the operational management (activity) of the technologies over the planning horizon. Strategizing capacity decisions is also commonly referred to as capacity expansion planning, but may also entail reductions in system capacity in situations where reduced demands are projected. Due to the impact on long-term structural inertia, capacity decisions are usually assessed over multi-decadal time periods. Performance criteria of primary concern include service reliability, end-use prices and environmental impacts.

Water and energy resource potentials represent an important input to any capacity planning approach, and vary significantly across resources, time and geographic location. Transporting water and energy from one location to another also requires massive investment in network infrastructure, with long-distance water conveyance presenting further interdependencies due to the energy required for pumping. Planning models incorporating spatially resolved infrastructure systems will be needed to understand the implications of local constraints and transmission for long-term development strategy [21, 38–40, 210]. Yet, there is also a need to maintain an adequate temporal resolution in order to capture operational constraints occurring primarily in the electricity sector [33]. Moreover, spatial units typical in water resource management are geophysically-based and do not necessarily align with administrative units typical in energy supply planning (e.g., national, provincial, utility, etc.). The spatial mismatch may require disaggregation of spatial decision-making units in order to converge on a common resolution across energy and water systems [248]. The added complexity will be additionally demanding to accommodate in mathematical models containing an already diverse range of technologies and processes. Maintaining a careful balance between spatial and temporal scales when developing integrated water-energy models for long-term planning purposes is thus a critical challenge for regional planners, and scoping will depend on the specific research question (e.g., transmission expansion, emissions mitigation, groundwater depletion, etc.) and characteristics of the study region (interconnectivity of basins/aquifers, population density, income-level, etc.).

In this paper, we adapt the Saudi Arabia Electricity-Water Planning model (SEWP): an integrated supply planning framework that incorporates simulataneous capacity decisions in the water and electric power sectors. The framework includes a diverse range of technologies including most power generation types (e.g., natural gas combined-cycle, concentrating solar power, etc.) and water supply technologies (e.g., groundwater extraction, desalination, wastewater recycling, etc.). Thermal power plants are further distinguished by cooling technology (e.g., once-through, recirculating, etc.). The study region is broken into the 13 provincial administrative regions, with expandable electricity and freshwater transmission between provinces included in the capacity planning decisions. To explore impacts of national policy and path-dependency on technology deployment, SEWP focuses on a planning horizon of 2010 to 2050 in 5-year segments, with each time-step solved concurrently. Each modeled year is broken into monthly timeslices to enable treatment of seasonal effects, such as the potential mismatch between available supply and demand. For computationaly efficiency, the current version of SEWP considers linear relantionships between variables. Although designed specifically for application to infrastructure planning in Saudi Arabia, the approach is readily adaptable to other regional situations.

SEWP ensures a physical representation of resource conversion across a set of R resources, I spatially distributed regions, and T temporally distributed decision making intervals. For each resource $r \in R$, location $i \in I$ and time-step $t \in T$, the managed supply must exceed the exogenous demand:

$$Q(r,i,t) + \Delta S(r,i,t) \geq D(r,i,t) \tag{5.1}$$

where Q is the managed flow from supply technologies, ΔS is the managed flow from storage, and D is the exogenous demand. The managed flow from supply technologies includes consumption and production of different energy and water resources at the technology-level, and can be modeled consistently using appropriate functional relationships that link technology activity to net resource availability. SEWP considers a diverse set of P technologies capable of operating in a set of O operational modes, and calculates the managed flow of resource $r \in R$ from a specific technology $p \in P$ using input activity ratios ε^{in} and output activity ratios ε^{out}. The activity ratios represent the average rate at which a certain technology consumes or produces a certain resource per unit of activity-level. Operational modes are distinguished to enable representation of diverse operating costs and efficiencies for a single technology type. To allow for spatial transfers of water and electricity via conveyance or transmission infrastructure, net resource flows in each region $i \in I$ incorporates inputs produced and consumed in that region, as well as from other regions $j \in I$. Summing across regions, modes and technologies yields the managed flow for each resource in each region and time step:

$$Q(r,i,t) = \sum_{p,o,j} \left[\varepsilon^{out}(r,p,o,j,i,t) \cdot x(p,o,j,t) - \varepsilon^{in}(r,p,o,i,j,t) \cdot x(p,o,i,t) \right] \tag{5.2}$$

where x is the activity-level of a specific technology. The change in storage-level is equivalent to the difference between the levels across decision-making intervals:

$$\Delta S(r,i,t) = s(r,i,t) - s(r,i,t+1) \tag{5.3}$$

where s is the storage-level. Surface water reservoirs and potable storage at end-use are the only between-month storage technologies currently included in SEWP. Level-dependent losses are important for surface water reservoirs (evaporation is proportional to surface area), and can be accounted for using linearized area-volume relationships [249]. Saudi Arabia contains relatively little exploitable surface water and associated storage, and for this reason, volume-dependent losses are neglected. Due to uncertainties surrounding the scale of the resource and complexities of hydro-geological modeling, groundwater storage is incorporated into SEWP as a model criteria (section 5.2.2).

The activity-level of each technology is constrained in SEWP by the available capacity:

$$\phi(p,i,t) \cdot z(p,i,t) - \sum_{o} \sigma(p,o,i,t) \cdot x(p,o,i,t) \geq 0 \tag{5.4}$$

where z is the installed capacity, ϕ is the fraction of installed capacity that is available (or the capacity factor), and σ is the rate at which a particular operational mode utilizes capacity. Certain operational modes are allowed to consume more capacity than others in the model to reflect e.g., capacity impacts of scheduling flexible reserve generation in the electricity sector [250]. SEWP includes incremental capacity expansion decisions u that alleviate capacity constraints. Incremental capacity retirements w are also modeled as decision variables to allow representation of finite technology lifecycles. The installed capacity of a particular technology is given by:

$$z(p,i,t) - z(p,i,t+1) + u(p,i,t) - w(p,i,t) = 0 \tag{5.5}$$

Likewise, storage capacity c constrains storage levels, incremental new storage capacity b can be used to alleviate constraints on storage levels, and incremental storage retirements

d reduce installed storage capacity:

$$\psi(r,i,t) \cdot c(r,i,t) - s(r,i,t) \geq 0 \tag{5.6}$$

$$c(r,i,t) - c(r,i,t+1) + b(r,i,t) - d(r,i,t) = 0 \tag{5.7}$$

where ψ is the fraction of installed storage capacity that is active. In the case reported in this paper, capacities are modeled by continuous variables. The authors are aware that integer variables enable modeling the effects of reduced unit costs with increasing unit size (i.e., economies-of-scale), which provides insight into the benefits of distributed or centralized supply configurations [210]. However, the choice of continuous variables is justified by two arguments. First, the obtained capacity values usually provide a good approximation. Second, and most importantly, due to the model size its mixed-integer formulation would require qualitatively more computational resources.

Upper and lower bounds are further imposed on the capacity and activity variables to reflect e.g., resource availability, excess supply and existing infrastructure. Other additional contraints address operational policies such as technology retirements, inter-annual reservoir sustainability and electricity system flexibility. A detailed account of these relationships can be found elsewhere [241], and for brevity are not repeated here.

5.2.2 Multi-criteria model analysis

A vector of outcome variables $\mathbf{y}$ can be used for measuring various consequences of the simulated development strategy in SEWP. Outcome variables are often named differently (e.g. criteria, objectives, goals, metrics, performance indices, etc.). A vector of algebraic relations $\mathbf{F}$ are defined that convert decisions variables to outcomes:

$$\mathbf{y} = \mathbf{F}(\mathbf{v}) \ , \ \mathbf{v} \in V_o \tag{5.8}$$

where $\mathbf{v}$ is the vector of model decision-variables (the activity and capacity of the technologies introduced in the previous section), and V_0 is the set of feasible solutions (admissible due to the physical and logical constraints introduced in the previous section).

Past application of SEWP focused on a single objective: minimize total discounted system costs over the planning horizon. This formulation requires a unique specification of a goal function that adequately represents system cost. Capital and operational cost parameters for each technology are input to SEWP and multplied by the corresponding capacity or activity variable to estimate the cost contribution. Discounting is then used to translate future costs into an estimated present value. In the single-objective formulation, preferences for outcomes, including available budget, requires a re-definition of the set of feasible solutions V_0 by V_1: $V_1 = V_0 \cap \mathbf{P}$, where $\mathbf{P}$ is the set of outcomes conforming to the decision-making preferences. In some cases the preferences are too ambitious, e.g., tight constraints on the budget actually shrinks the set of feasible solutions to a small subset (which ignores many possibly interesting solutions), or even results in an empty set V_1, which in turn makes the underlying optimization problem infeasible.

Alternatively, preferences for multiple objectives might be obtained based on linear weighted-sum criteria aggregation into a composite goal function. This approach has the serious shortcomings mentioned in the introductory section [243]. In this paper, an achievement scalarizing function (ASF) serves as the goal function in the mathematical programming analysis built on the core model described in the previous section. The ASF is defined through criteria achievement functions (CAFs) specified for each objective independently. The role of the CAFs is to provide a common measure for criteria performance, typically defined in different metrics and scales. We utilize a modified version of the reference point methodology [76,251], where each CAF is parametrized by two values specified by the user, namely aspiration and reservation levels, which correspond to the criterion values that are desired and worst acceptable, respectively. In this context, a CAF for the k-th criterion is denoted by:

$$u_k = f_k(q_k, \bar{q}_k, \underline{q}_k), \tag{5.9}$$

where $f_k(\cdot)$ is a strictly monotone concave function (decreasing for minimized, and increasing for maximized criteria, respectively), and $q_k, \bar{q}_k, \underline{q}_k$ are the criterion value, aspiration, and reservation levels, respectively. Values of q_k are defined by the corresponding outcome variables of the analyzed core model (i.e., $q_k = y_k$). The $f_k(\cdot)$ are usually defined as piece-wise linear functions with linear segments determined by the utopia, aspiration, reservation, and nadir values [252]. The utopia point **U** is defined by a vector composed of the best values of all considered criteria. Utopia components are easily computed through the so-called *selfish* optimizations (i.e., optimizing each criterion separately). The nadir point **N** is defined by the worst values of the criteria within the Pareto-set. The piece-wise linear functions represent the human values related to satisfaction and regret, and also have a nice mathematical property; namely, the underlying multi-criteria optimization model remains linear for linear core models. A correctly implemented multi-criteria model analysis framework does not impose any restrictions on the feasibility of the aspiration and reservation values, other than two exceptions: (1) the reservation is lower/higher than aspiration for minimized/maximized criterion, respectively; and (2) the aspiration and reservation values are between the corresponding utopia and nadir values.

The CAF values have a very easy and intuitive interpretation in terms of the degree of satisfaction from the corresponding value of the criterion. Values of 1 and 0 indicate that the value of the criterion exactly meets the aspiration and reservation values, respectively. CAF values between 0 and 1 can be interpreted as the degree of satisfaction of the criterion value, i.e., to what extent this value is close to the aspiration level and far away from the reservation level. These interpretations correspond to the interpretation of the membership function from fuzzy set theory [252]. In fact, the CAF extends the membership function concept because the CAF also takes negative values (for criteria values worse than the reservation), and values greater than one (for criteria values better than the aspiration). This extension is necessary for proper handling of any $\bar{q}_k$ and $\underline{q}_k$, which in turn frees the users from concerns regarding attainability of the considered aspiration and reservation levels.

The ASF is defined by:

$$\mathscr{S} = \min_{k \in K_a} (u_k) + \frac{\varepsilon}{K} \cdot \sum_{k=1}^{K} u_k \tag{5.10}$$

where K_a is the subset of active criteria, u_k are defined by (5.9), and ε is a small positive number. The first term causes improvement of the worst performing (in terms of the corresponding CAF) criterion. The second term assures that the optimal solution provided for maximization of the ASF is indeed Pareto-optimal [76, 253]. Maximization of (5.10) for $\mathbf{v} \in V_o$ generates a properly efficient solution aligned with the user's criteria preferences.

Implementation of the MCA methods described in this paper is accomplished with the Integrated Modeling Environment Project's online Multiple Criteria Model Analysis (MCMA) framework [254]. The approach is outlined in E.1.

5.2.3 Case study

The focus of the Saudi Arabia case study analysis are infrastructure strategies that are efficient at simultaneously minimizing investment costs, groundwater extraction and carbon dioxide (CO_2) emissions. These objectives are selected as the focus for the analysis due to the anticipated challenges in balancing future socioeconomic development with aspirations surrounding global climate stewardship and national food security. The former is a concern due to increasingly stringent global climate change policy, and the fact that more than half of the current power generation fleet in Saudi Arabia burns extremely carbon-intensive crude oil [78]. Fulfilling national food security ambitions locally in Saudi Arabia's harsh desert environment requires industrial-scale irrigation, and has driven widespread over-exploitation of regional groundwater resources, leading to concerns regarding long-term supply sustainability [79]. Cost, groundwater criteria is accounted for in the SEWP model by tracking the corresponding cumulative value over the planning horizon (2010-2050) and over all sub-national regions (13 provinces).

The case study in this paper demonstrates the analytical efficiency of a multi-objective framing to long-term planning models of water and energy supply systems, and is applied within a scenario analysis involving interactive specification of the criteria aspiration and reservation levels. Relative levels of ambition across the disparate objectives are defined by normalizing the range between the nadir and utopia values for each criteria, and separating the normalized values into three intervals: *Ambitious* (+++), *Moderate* (++), and *Relaxed* (+). The *Ambitious* criteria interval has the aspiration and reservation levels near the utopia point, whereas the *Relaxed* interval converges on the nadir. Scenarios involving a combination of these aspiration and reservation categories are initially defined to explore trade-offs between sustainability objectives. Following the initial assessment, a sensitivity analysis is performed in which approximately 100 model iterations are explored (i.e., criteria preferences specified by diverse combinations of the aspiration and reservation levels).

Technology performance and demands for electricity and water occurring in the agricultural, municipal and manufacturing sectors are key inputs to the MCA framework. The analysis in this paper focuses on a single technology performance scenario; sensitivity of the SEWP model to these assumptions were explored previously [241]. Exogenous demands from each sector are generated with quantitative socioeconomic projections that follow the Shared Socioeconomic Pathways (SSP) [255]. National population and per capita GDP increase more than two-fold by 2050 in the mid-range (SSP2) scenario [172, 173, 225]. Previously derived sector-specific econometric models linking population and GDP to freshwater and electricity demand are used to convert the SSP data into provincial demand trajectories [241]. Moderate levels of end-use technological change are included, and reflect expected efficiency improvements driven by technological innovation. The SSP2 scenario results in modeled national electricity demands (other than for water supply) increasing from approximately 200 TWh in 2010 to more than 700 TWh in 2050. Freshwater demands (other than for power supply) increase less dramatically, from 21 km^3 in 2010 to 25 km^3 in 2050, due to anticipated impacts of existing national agricultural policy [227]. A detailed account of the input data used to parameterize the model, including an assessment of existing infrastructure, can be found in [241].

5.3 Results

5.3.1 Impact of multiple criteria on system cost

This section presents key results of the scenario analysis with specific focus on the impacts of the MCA enhancements on system cost in the SEWP model. To highlight system boundaries, the scenario analysis initially involves exploration of the utopia solutions, and then moves to adjusting the aspiration and reservation levels to explore compromise solutions. Outcomes for each criteria for a select range of aspiration and reservation levels obtained through interactive scenario analysis are presented in Table 5.1. The relationship between the criteria for the selected scenarios are also plotted in Figure 5.1, where results are indexed to the respective criteria outcome obtained in the cost-minimization solution.

Scenario name	Criteria ambition-level			Criteria reservation ($\underline{q}$), aspiration ($\overline{q}$) and outcome (q) Cost [$\times 10^{12}$ USD]			CO_2 [$\times 10^9$ metric tons]			GW [$\times 10^3$ km^3]		
	Cost	CO_2	GW	$\underline{q}$	$\overline{q}$	q	$\underline{q}$	$\overline{q}$	q	$\underline{q}$	$\overline{q}$	q
Cost selfish	(+++)	(-)	(-)	1.04	0.24	0.24	-	-	8.32	-	-	1.26
CO_2 selfish	(-)	(+++)	(-)	-	-	1.25	3.51	0.46	0.46	-	-	0.21
GW selfish	(-)	(-)	(+++)	-	-	2.17	-	-	4.04	0.39	0.03	0.03
GW-CO_2 ambitious	(+)	(+++)	(+++)	2.05	0.24	0.81	2.75	0.46	1.18	0.30	0.03	0.12
Cost-CO_2 ambitious	(+++)	(+++)	(+)	0.84	0.24	0.53	2.66	0.46	1.52	0.84	0.03	0.42
Cost-GW ambitious	(+++)	(+)	(+++)	0.84	0.24	0.56	7.31	0.46	4.07	0.30	0.03	0.17
CO_2 ambitious	(++)	(+++)	(++)	2.05	0.24	0.69	2.75	0.46	1.04	0.84	0.03	0.23
GW ambitious	(++)	(++)	(+++)	2.05	0.24	0.74	7.31	0.46	2.37	0.30	0.03	0.11
Cost ambitious	(+++)	(++)	(++)	0.84	0.24	0.47	7.31	0.46	3.04	0.95	0.03	0.38
Cost-GW-CO_2	(+++)	(+)	(++)	0.84	0.24	0.50	7.31	0.46	3.40	0.64	0.03	0.29
Cost-CO_2-GW	(+++)	(++)	(+)	0.84	0.24	0.49	5.03	0.46	2.32	0.95	0.03	0.41
All criteria ambitious	(+++)	(+++)	(+++)	0.48	0.24	0.62	1.38	0.46	1.89	0.15	0.03	0.22

Table 5.1: Parameterization of the decision-making preferences (aspiration and reservation levels) and the corresponding MCA results for the preliminary scenarios investigated. Each scenario is identified based on its level of ambition with respect to cost, CO_2 and groundwater (GW) objectives. Relative levels of ambition across the disparate objectives are defined by normalizing the range between the nadir and utopia values for each criteria, and separating the normalized values into three intervals: *Ambitious* (+++), *Moderate* (++), and *Relaxed* (+); *inactive* criteria are marked by (-). The *Ambitious* criteria interval has the aspiration and reservation levels near the utopia values, whereas the *Relaxed* interval converges on the nadir.

We find largest cost trade-offs in this preliminary analysis for the groundwater selfish scenario. Under the parameterized technology costs, this scenario represents a discounted system cost that is more than 8 times the cost-minimization (cost selfish) solution. In fact, the cost selfish solution corresponds to the groundwater nadir outcome, highlighting the direct trade-offs between these objectives. The CO_2 selfish solution is also more than 6 times expensive than the cost-minimization solution; however, this scenario also achieves groundwater co-benefits, as indicated by the 80% drop in cumulative groundwater extraction compared to the cost-minimization solution (Figure 5.1). Varying the criteria aspiration and reservation levels across the other scenarios listed in Table 5.1 reveals that the largest costs are incurred when fulfilling the stringent CO_2 and groundwater preferences,

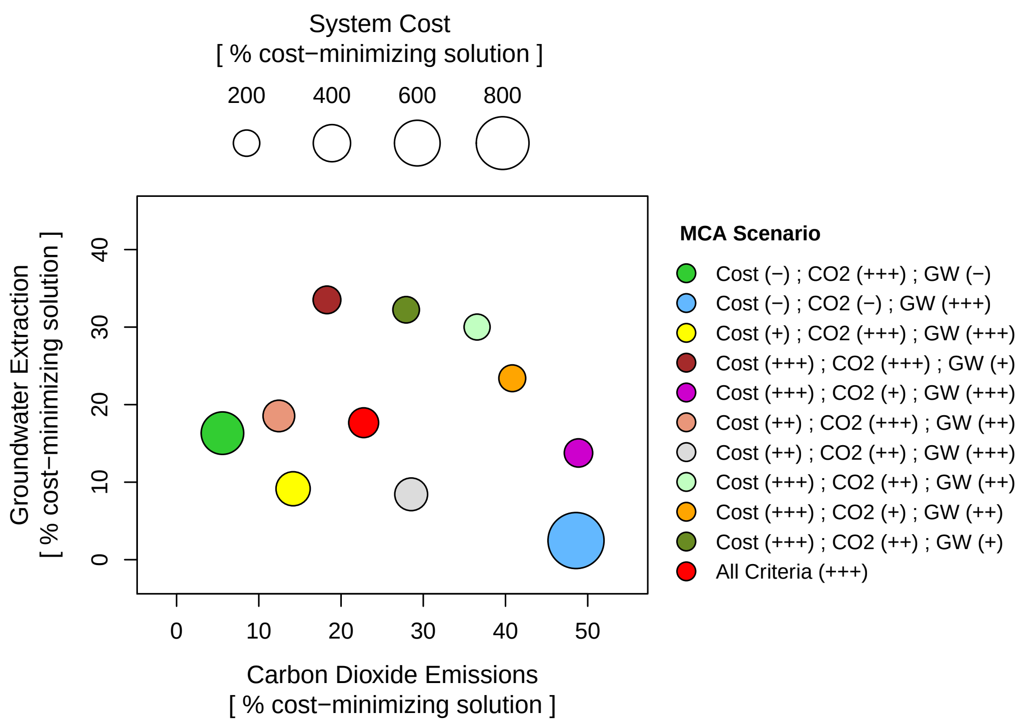

Figure 5.1: System cost, groundwater extraction and CO_2 emission outcomes obtained for the scenarios listed in Table 5.1. The marker area is proportional to the discounted system cost. Results are indexed to the respective criteria outcome obtained in the cost-minimization solution.

and that a slightly relaxed criteria preference can achieve significant cost savings while remaining ambitious from an environmental perspective. For example, when all criteria are set to relatively ambitious preferences (i.e., the 'all criteria ambitious' scenario), the MCA model seeks a Pareto-optimal solution that is relatively balanced across objectives. The discounted system cost in this solution is only 2.5 times the cost-minimization outcome, but simultaneously achieves deep reductions in cumulative groundwater extraction (more than 80% reduction versus the cost-minimization outcome) and cumulative CO_2 emissions (more than 75% reduction versus the cost-minimization outcome). Further relaxing the cost preferences (i.e., the 'GW-CO_2 ambitious' scenario) results in a system that is 3.4 times more expensive than the cost-minimization solution, but achieves a further 10% reduction in cumulative groundwater extraction and CO_2 emissions. The level of mitigation in this latter scenario is likely required to avoid local groundwater shortages [177], and achieve national electricity sector contributions to global climate stabilization [222].

5.3.2 Impact of criteria preferences on system configuration

Impacts of the criteria settings on the provincial-level technology build-out for selected scenarios are provided in Figure 5.2. Depicted is the optimal annual electricity and freshwater supply mix in each region, as well as the interprovincial transfers and demand-levels. The cost-minimization solution (Figure 5.2a) involves expansion of relatively low-cost combined-cycle natural gas generation, with existing renewable energy policy driving development of 50 GW of mostly solar generation capacity. Groundwater withdrawals are left unconstrained in the cost-minimization model, and under the parameterized costs dominate the future water supply mix and displace existing interprovincial desalination transfers. Moreover, in the cost-minimization solution thermal power plants employ once-through freshwater cooling systems due to the low investment cost and lack of concern surrounding groundwater sustainability. The modeled extraction across sectors in this scenario likely exceeds available aquifer storage [177].

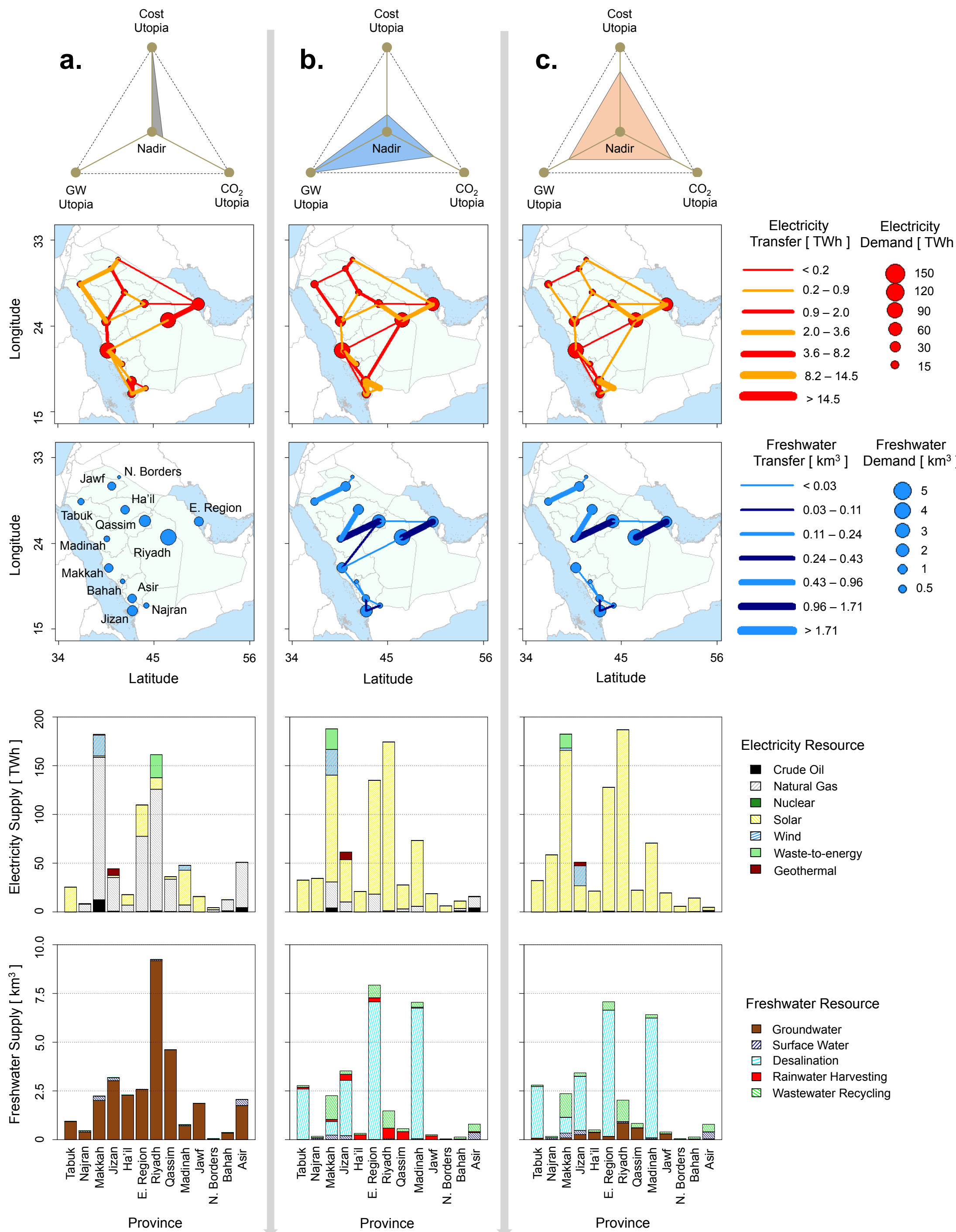

Figure 5.2: Provincial electricity and freshwater supply in 2050 for three of the MCA scenarios listed in Table 5.1. a. Cost selfish (minimization) solution; b. Groundwater (GW) selfish solution; c. All criteria ambitious solution. The top row depicts the criteria outcomes in relation to the Utopia and Nadir points. Row two and three from the top depict the annual freshwater and electricity transfers between provinces, as well as the scale of annual demand. The bottom two rows depict the supply mix from the different resources.

In the groundwater selfish solution (Figure 5.2b) costs are more than 8 times the cost-minimization solution due to the rapid expansion of desalination, wastewater recycling and rainwater harvesting, and corresponding development of highly integrated interprovincial conveyance networks to meet water demands located inland. The increased electricity load from the water sector technologies increases aggregate national electricity demand in 2050 by 12% compared to the cost-minimization solution, and additional electricity sector capacity is developed to meet these requirements. Deep reductions in technology costs projected later in the simulation horizon combined with a lack of water requirements results in solar PV dominating the 2050 electricity supply mix in the groundwater selfish solution, and large-scale investment into electricity storage and load control capacity enables this transition (not depicted).

Similar characteristics of the 2050 supply mix are apparent when all criteria are set to ambitious preferences (Figure 5.2c). The push to reduce costs in this scenario results in a slower transition away from groundwater extraction and CO_2 emissions, and enables groundwater and fossil fuel generation to continue to provide services in areas facing costly infrastructure constraints. For example, inland provinces continue to extract groundwater in the 'all criteria ambitious' scenario to displace investment in rainwater harvesting and conveyance infrastructure, and fossil fueled power plants are operated to provide flexibility to displace investment in storage technology and transmission upgrades.

5.3.3 Sensitivity analysis

The sensitivity analysis involved over 100 model iterations (i.e., preferences specified by diverse combinations of the aspiration and reservation levels). Each of the identified Pareto-optimal solution has a certain trade-off (compromise) between criteria values. However, in decision-making practice extreme solutions (i.e., solutions with very good values for some criteria and very bad for the other criteria) are rarely accepted. As an example of exploration of criteria trade-offs we examine the iterations presented in Figure 5.3. The solutions are sorted by increasing cost.

Similar to the preliminary analysis, solutions with low cost have very high levels of CO_2 emissions and groundwater extraction. For a relatively small increase of cost one

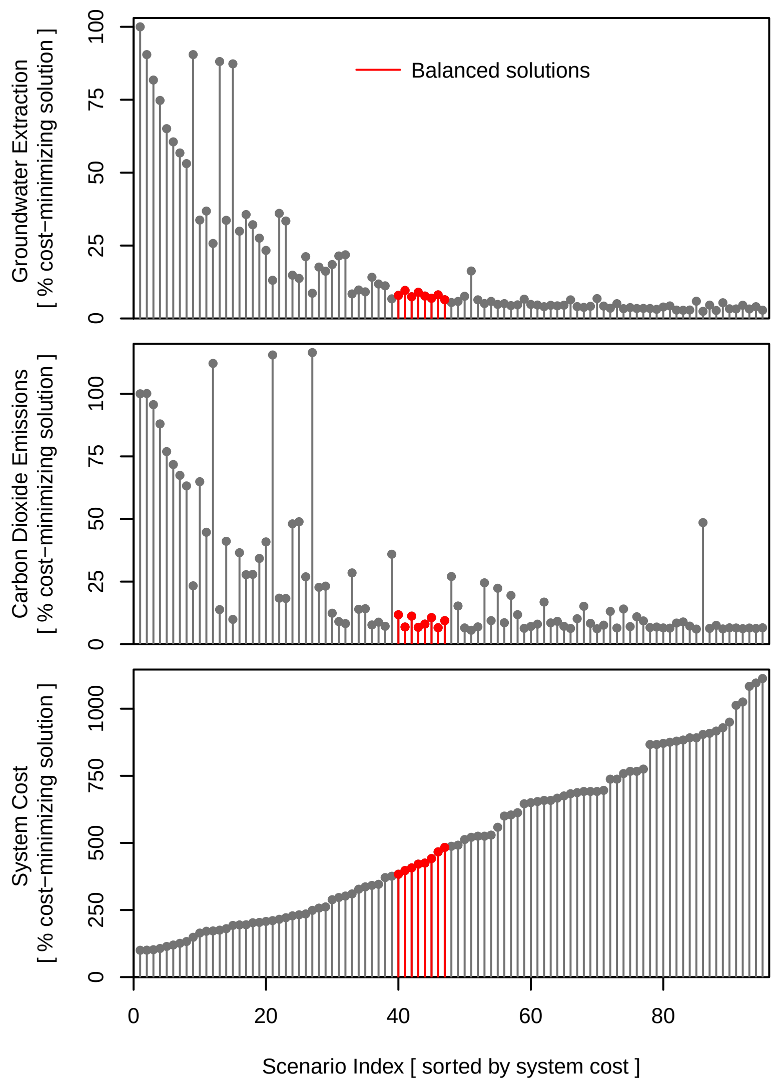

Figure 5.3: Criteria outcomes for the extended scenario analysis and identification of potential balanced solutions. Results are indexed to the respective criteria outcome obtained in the cost-minimization solution.

can achieve substantial reduction to the other two criteria, although such reductions are not monotone for both criteria. On the other hand, solutions with very low levels of CO_2 and water are very expensive. Such an illustration of various Pareto-efficient solutions provides a good basis for selecting a subset of the Pareto-frontier for further exploration. Such a selection depends on the preferences of actual decision-makers, who decide on the actual available budget and the goals for other criteria. The role of the MCA is to help them identify goals for all criteria that are simultaneously attainable.

For example, solutions in the region marked as *balanced solutions* might be considered as having good compromises between the criteria values, as each of them achieves relatively ambitious outcomes for both groundwater and CO_2 with relatively moderate impact on costs. Mitigation costs increase rapidly for more expensive solutions with relatively little improvement over the other criteria, and can therefore be deemed cost-prohibitive. Balanced solutions display similar system configurations in 2050 as in (Figure 5.2c), but are distinct with respect to implementation time. Largest cost savings are found to accompany balanced solutions that wait longest to transition away from groundwater.

5.4 Conclusion

Water and energy systems are increasingly interdependent, and will benefit from integrated long-term development strategy. Diverse performance criteria across development objectives necessitate multi-criteria assessment methods and tools. This paper presented a multi-criteria model analysis framework for long-term energy and water supply planning at national or regional scales. The framework incorporates a linear systems-engineering model of the coupled supply technologies and intra-regional transmission networks. A modified version of the reference point methodology enables interactive specification of decision-making preferences for disparate sustainability criteria, and convergence on a Pareto-optimal solution reflecting the relative criteria ambition-levels. Scenarios involving a combination of economic, climate and groundwater sustainability preferences were explored in the context of national planning in Saudi Arabia to demonstrate the performance of the novel analysis framework, as well as to quantify criteria trade-offs specific to the case study region.

Application of the integrated modeling framework in the case study region demonstrates important tradeoffs between diverse sustainability criteria. Similar to previous research [241], we find that policy objectives in Saudi Arabia for 2050 that reduce cumulative groundwater extraction and electricity sector CO_2 emissions to levels likely needed to avoid local groundwater shortages and meet global climate stabilization targets are associated with a significant increase in system investment costs. However, the MCA framework in this paper goes further by revealing a suite of trade-off solutions that remain nearly ambitious at much lower costs. These savings would impact the affordability of water and energy services in the rapidly developing nation of Saudi Arabia.

Our results further demonstrate that a conventional linear systems-engineering model used to identify optimal capacity expansion policies and investment strategies for integrated water-energy systems can be efficiently converted into a multi-objective framework using a generic transformation algorithm. Overall, the MCA framing is found to require approximately the same computational effort to solve each scenario as the single-objective framing, with the added benefits of significant analytical efficiency in terms of long-term performance assessment due to the capabilities in balancing multiple development objectives. It is therefore recommended that similar MCA methods become widespread in long-term water-energy infrastructure planning.

The scope of model applications in this paper focuses mainly on the electricity sector. Future work should consider expanding the system boundaries to allow assessment from resource extraction through to end-use services. This would allow mapping the impacts from a more comprehensive set of technologies to energy and water sustainability metrics of interest. An important issue to address in this context is the linking of surface and groundwater management, which was simplified in the analysis due to surface water scarcity in the case study region. Moreover, the effects of other criteria important to regional planners (e.g., air pollution, energy security, investment risk, etc.) on the optimal development strategy should be explored to fully highlight potential trade-offs or synergies. The general MCA framework proposed in this paper can readily be adapted to include these features, and will be the topic of future research.

Chapter 6

Summary and contributions

The anticipated climate and water resource variability around the world this century will pose challenges to future energy systems. One way to adapt is to hedge against climate and water vulnerabilities within long-term regional infrastructure plans. This dissertation assesses the technological and policy implications, and presents integrated optimization methods for the adaptation of regional energy systems to climate change and water constraints. A hard-linked, spatially-resolved representation of water and energy supply capacity planning is derived to study the interaction between sustainable groundwater management and concurrent policy aimed at reducing electricity sector carbon emissions in the groundwater-stressed country of Saudi Arabia. Additionally, an optimal electricity generation planning model incorporating a robust response to climate change impacts to hydropower and demand is derived to quantify the cost of climate change adaptation in the hydro-dominated electricity mixture of western Canada.

6.1 Key findings

The results of this research demonstrate a crucial need for regional planners to account for adaptation to climate change and water constraints when developing long-term energy strategy. Of particular concern are energy systems with a strong linkage to the hydrological cycle or regions that face challenges in securing freshwater resources. Key findings of this research broadly applicable to energy systems planning include:

- Water supply and resource constraints can reduce the availability of supply-side options in the energy sector and increase energy demand, making it more expensive to fulfill climate sustainability objectives.
- Adequate quantification of water constraints requires greater spatial resolution than that typically seen in regional energy modeling.
- Adapting to uncertainties surrounding future hydro-climatic change will require embedding increased operational flexibility into energy system design.
- A conventional linear systems-engineering model used to identify optimal capacity expansion policies and investment strategies for integrated water-energy systems can be efficiently converted into a multi-objective framework using a generic transformation algorithm.

These general observations are consistent with previous research on water constraints and climate change adaptation in the energy sector [30, 35, 39, 67].

In addition to the integrated modeling and optimization, novel contributions of this research emerge from the regional case studies. Specifically, the analysis provides important insight into the potential direction and magnitude of a number of environmental and economic parameters important to regional policy-makers:

- British Columbia (BC), Canada:
  - Climate change has the potential to increase provincal hydropower potential in 2050 by more than 10 %, and reduce annual electricity demand by about 2 %.
  - Adapting to the uncertainties in the hydro-climatic projections requires operational flexibility and could increase long-term electricity supply costs by more than 3%.
  - Allocating a modest risk premium of 1 % of total investment costs during electricity generation planning can provide significant hedging against the risk of natural gas and bionenergy emissions performance uncertainty.

- Saudi Arabia
  - Transitioning away from non-renewable groundwater use in Saudi Arabia could incur costs similar as the transition away from fossil fuels in the electricity sector.
  - The use of desalination, wastewater recycling and distribution to displace groundwater use in Saudi Arabia has the potential to increase electricity demand by 40 % in 2050 relative to 2010.

6.2 Future work

Future work should consider expanding the system boundaries to allow assessment from energy resource extraction to end-use services. This would allow mapping the impacts from a more comprehensive set of technologies to energy and water sustainability metrics of interest. Moreover, the applications rely on pre-defined earth-system scenarios, whereas operationalizing the earth-system components of the model (hydrology and regional climate) would provide a better tool for updated analysis. An important issue to address in this context is the linking of surface and groundwater management across wide geographic areas. Network effects occur due to users and resources distributed along rivers and aquifers, and will complicate the use of conventional optimization methods. The need to model non-linear water quality indicators such as water temperature in order to accurately estimate power plant cooling requirements introduces further complexity [49]. Reduced form approaches representing water temperature and allocation are likely needed to ensure the analysis remains manageable from a computational perspective.

Finally, as land-use plays an essential role in global greenhouse gas emissions and water use, it would be very informative to further consider modeling endogenous land-use decision-making. This would allow adaptive response of the agricultural and forestry sectors in the model (and associated water and energy use) to tradeoffs between food security, ecosystems and climate change. A challenge is deriving suitable economic representations of agricultural exports into the future, due to dependence on the evolution of international markets. Integrated assessment models incorporating energy, water, land-use and climate provide a potential tool to assess global synergies and tradeoffs across sectors [256], but currently lack the spatial and temporal detail to explore endogenous water constraints in the energy sector. Thus, a crucial area of future work is the development of improved methods to incorporate spatial water constraints into global integrated assessment models [257].

Appendix A

Climate and human development impacts on municipal water demand: A spatially-explicit global modeling framework[1]

[1]The body of this chapter was published as S. Parkinson et al., *Environmental Modelling & Software* 8: 266-278, 2016, and is reproduced with the permission of Elsevier. The approach is applied in chapters 4 and 5 to generate demand scenarios for the case study analysis. SP conceived of and performed the analysis, and drafted the initial manuscript. Other co-authors contributed data sources and to the refinement of updated manuscript drafts.

Preamble

Municipal water systems provide crucial services for human well-being, and will undergo a major transformation this century following global technological, socioeconomic and environmental changes. Future demand scenarios integrating these drivers over multi-decadal planning horizons are needed to develop effective adaptation strategy. This paper presents a new long-term scenario modeling framework that projects future daily municipal water demand at a 1/8° global spatial resolution. The methodology incorporates improved representations of important demand drivers such as urbanization and climate change. The framework is applied across multiple future socioeconomic and climate scenarios to explore municipal water demand uncertainties over the 21st century. The scenario analysis reveals that achieving a low-carbon development pathway can potentially reduce global municipal water demands in 2060 by 2 to 4 %, although the timing and scale of impacts vary significantly with geographic location.

A.1 Introduction

Global hydrological models (GHM) provide a virtual environment to explore the impacts of long-term development pathways on water resources and the effectiveness of policy [256, 258–262]. As the quality and magnitude of water resources varies with geography, GHMs incorporating spatially-resolved water demand projections have been crucial in the assessment of future water challenges, such as resource scarcity and ecosystem quality [263, 264]. Municipal water systems extract and distribute water for direct use by the population and play an important role in the global hydrological cycle, representing 12 to 14 % of total water withdrawn globally for human purposes in 2010 [223, 265]. Most GHMs incorporating municipal water demand estimate average per capita trends at the national-level, and then downscale to a finer resolution by assuming national trends hold within countries [223, 256, 261, 266]. Yet, historical observations suggest that per capita municipal water demand within countries varies spatially, mostly due to a combination of local climate conditions, economic status and urban form [267–270]. Furthermore, global models applied for future projections assume a static population distribution and are therefore unable to represent the sub-national spatial demand variability that will accompany projected urbanization.

Also less explored at the global-scale are the potential impacts of future climate change on municipal water demand. The direct climate sensitivity arises in the municipal sector from the freshwater used for municipal irrigation [267, 271–276]. Municipal irrigation includes water to support household and municipal landscaping (e.g., turf grass and gardens), and outdoor water features (e.g., swimming pools and fountains). Municipal irrigation represents more than 50 % of total municipal water demand in many regions of the United States [268], and could play a key role in meeting future urban food requirements [277] and mitigating urban heat island effects [278]. Future variations in urban climate will affect water requirements of vegetation as well as the rate of evaporation from outdoor water features. Understanding the scale of climate change impacts on municipal water demand will provide insight into suitable adaptation strategy and the potential water co-benefits of global climate change mitigation policy.

The objective of this paper is to provide a new approach to developing long-term global municipal water demand scenarios. A spatially-explicit modeling framework is proposed that incorporates enhanced representations of human migration, economic development and climate sensitivity. The framework is applied across multiple future human development and climate scenarios to explore the impact of coupled climate-development trajectories on municipal water demand uncertainties over the 21st century. The results provide important insight into model formulation and the potential water co-benefits in the municipal sector of policy targeting climate change mitigation.

A.2 Methods

A.2.1 Overview

Combined impacts of climate change and human development on municipal water demand are assessed at the global-level with the computational framework depicted in figure (A.1). The approach involves mapping per capita demand on a gridded representation of the earth's surface (i.e., a raster). The per capita water demand in each grid-cell is modeled as a function of a number of spatially-explicit indicators including projected income, population density, climate and historical observations. Per capita demand is then multiplied by spatial projections of population to estimate aggregate municipal water requirements in each grid-cell. The methodology utilizes spatially-explicit, quantitative interpretations of the most recent global change scenarios as a basis for the projections: the Shared Socioeconomic Pathways (SSP) [224], and the Representative Concentration Pathways (RCP) [95].

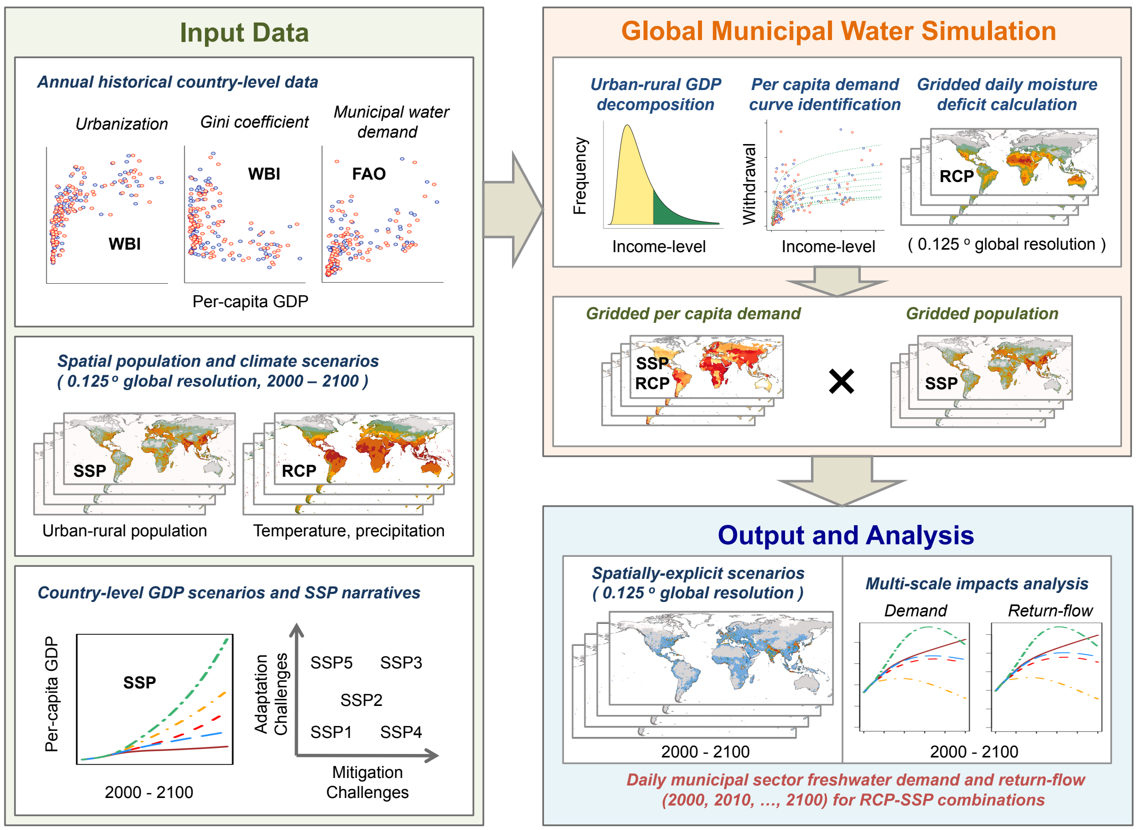

Figure A.1: Framework for assessing global impacts of human development and climate change on municipal water demand. FAO = Food & Agriculture Organization of the United Nations [230]. WBI = World Bank Indicators [170]. SSP = Shared Socioeconomic Pathway. RCP = Representative Concentration Pathway.

A key output of the analysis is therefore a new harmonized dataset well-suited for further application in global integrated assessment models (IAMs). Increasingly, global IAMs are being adapted with GHMs to examine the interplay between long-term economic development, water constraints and climate change mitigation [256, 279]. Global IAMs incorporating future water constraints must project the scale of demand from different end-use sectors in order to devise economic responses at scales relevant to water system transformations. The simulated water demands from the municipal sector will aid in the quantification of constraints on water availability for land-use and energy, which are the historical focus of global IAMs used to study climate change mitigation [10].

Demand scenarios are computed at a 1/8° spatial resolution (grid cells approximately 14 km x 14 km near the equator) and out to the year 2100 to align with the downscaled SSP and RCP datasets. The spatial resolution also ensures that parameterized demand sensitivities to population density are captured. Urban and rural populations are modeled separately in the framework to feature diversity in per capita demand stemming from differences in economic status, urban form and local climate conditions. A temporal downscaling approach enables generation of the demand scenarios at a daily time-scale. The daily time-scale is investigated to capture anticipated effects of changing socioeconomic and climatic conditions on extreme (peak) demand events important to water supply reliability [280]. Spatially-explicit validation of the modeling framework is currently limited due to the absence of suitable historical data. We alternatively calibrate the model to observed national data and use demand projections from other global models to evaluate the reliability of model results.

We use the term *municipal water demand* in this paper to refer to the volume of water that is needed in a particular location to fulfill useful end-use services in the municipal sector. We emphasize the definition here to differentiate the modeled water volumes from withdrawals, which often occur at locations other than end-use due to the reach of urban water infrastructure [264]. A separate analysis is required to parameterize corresponding scenarios for water supply e.g., with a hydro-economic model including investment decisions for alternative water supply options (reservoirs, wastewater recycling, desalination, etc.) [238, 241]. Hydro-economic models are able to quantify economic tradeoffs between upstream and downstream users, as well as economic impacts of conjunctive management of different sources. Future water prices can be simulated with a hydro-economic model and used to parameterize an expected response from municipal consumers [281]. In this context, the demand scenarios presented in this paper provide a useful reference point for analysis of additional responses to future water availability.

A.2.2 Income effects

Previous studies highlight that as household income increases, demand for water from the municipal sector increases because part of this new income is spent on increasingly water-intensive end-uses [267, 270, 282]. However, as income continues to rise, per capita demand for water increases less proportionally, due to eventual saturation of useful services [259]. This suggests a non-linear relationship between household income and municipal sector water demand, and we propose an empirical model capturing these characteristics.

The lack of comprehensive consumer income and water use data makes identifying household-level models on a global-scale impractical. At the national-level, the Food & Agriculture Organization of the United Nations (FAO) provides estimates of aggregate municipal sector water demand [230]. Concurrent observations of GDP are further available from organizations such as the World Bank [170]. Consequently, per capita GDP has been widely applied as a surrogate for average income in national-level municipal sector water demand models [183, 223, 259, 266, 283–285]. Yet, the non-linear demand response to income changes expected at the household-level means consumers respond differently depending on their current income-level. Therefore, aggregating the response of households following non-linear demand curves to average income changes should involve treatment of the income distribution [286].

The effects of income inequality are included in the demand model applied in this paper following the formulation proposed in [286]. The approach takes advantage of the observation that income distributions typically follow a log-normal shape [287]. Under the assumption of log-normality it is possible to consider average annual per capita demand Ω as a function of both per capita GDP g and the variance of the income distribution ν, by replacing the assumed arithmetic mean income (i.e., per capita GDP) with the geometric mean in a conventional semi-logarithmic demand model [286]:

$$\Omega(y) = \alpha(y) + \beta(y) \cdot \left[\ln g(y) - \frac{\nu(y)}{2} \right] \tag{A.1}$$

where α and β are model coefficients, and y denotes year. The Gini coefficient can be used to estimate the variance of the income distribution under the assumption of log-normality [288], and historical values are available for most countries [170]. A similar approach for municipal energy consumption utilized the Gini coefficient to project demands associated with different income quintiles [289]. In the approach applied here, when two countries with the same average per capita GDP are compared, the country with less income inequality will have the higher per capita water demand (i.e., aggregate demand elasticity with respect to income inequality is less than one). Previous analysis suggests the inclusion of the income inequality term has a relatively minor impact on demand levels; however, for long-term projections the effects of income inequality are likely important because of impacts on the rate of demand growth and interplay with long-term technological progress [286].

All parameters in (A.1) can be estimated for a number of countries in the base-year, making it possible to calculate the model coefficients at the national-scale using e.g., regression. Figure (A.2) depicts the results of a least-squares cross-sectional regression analysis utilizing data from 2000 and 2005 for 105 countries. The r-squared values are 0.56 and 0.55 respectively, and compare well with similar analysis of this dataset [284, 290]. Differences in the socioeconomic standing and consumption characteristics between urban and rural populations within countries are ubiquitous [291], and suggests the model should distinguish between population groups. We assume that in the base-year urban and rural populations within countries display different average income-levels but follow similar national demand curves (i.e., equivalent α and β). The national urban and rural demand curves are then calibrated based on gridded socioeconomic and climate indicators (section A.2.4).

Cultural preferences and existing water policies (e.g., water price) represent other key determinants of municipal water demand [270], but are difficult to include in the modeling framework due to a lack of comprehensive global data. Previous analysis at the house-

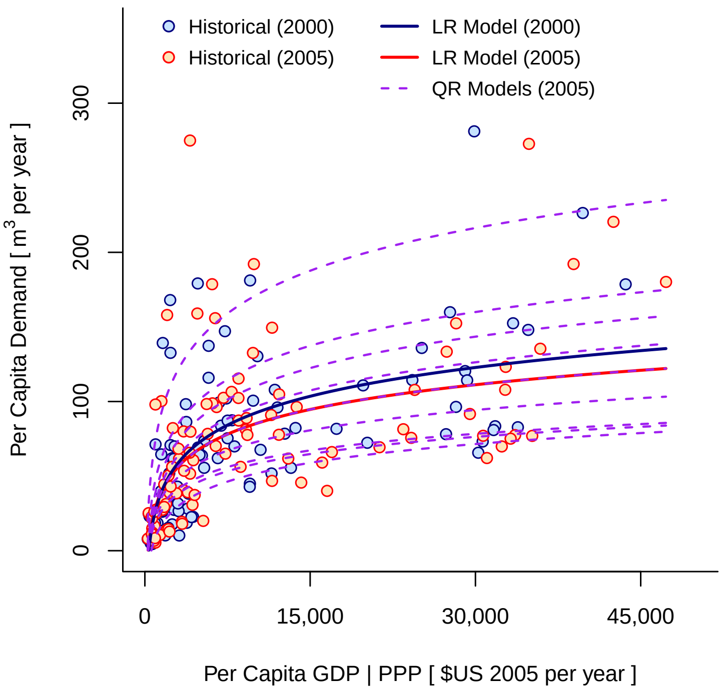

Figure A.2: FAO Aquastat data for 105 countries, the results of the least-squares cross-sectional regression analysis for 2000 and 2005, and decile demand curves fit to the FAO Aquastat data for the year 2005. LR = least-squares regression; QR = quantile regression.

hold level used agent-based models to integrate behavioral and social drivers of water demand [292]. Other global modeling approaches have incorporated water prices into the analysis by combining a number of separate country-level data sources [284]. These data sources often cover only part of a country's population, and include costs for wastewater treatment. Instead, the model in this study emphasizes a combination of path-dependency and long-term convergence at the national-scale to reflect inertia of the existing systems and associated policies and behaviors that impact long-term municipal water use, such as water pricing and cultural preferences.

The model accounts for path-dependency and the wide-range in observed historical per capita demands at the national-scale by identifying an ensemble of demand curves. The curves are estimated using quantile regression with (A.1). The quantile regression analysis specifies ten unique demand curves (or decile curves) representing the best fit solutions to ten equal increments of the cross-sectional data ordered from lowest to highest [293]. The decile curves fit to the FAO data for the year 2005 are also depicted in Figure (A.2). In the initial simulation year, countries are associated with a best-fit decile curve based on historical FAO data trends from 2000 to 2010. Countries lacking historical data are assumed to follow a regional average, with the regionalization following the breakdown used in similar previous global scenario modeling [294]. Convergence towards the identified decile curve is assumed over time using the following scaling factor:

$$\gamma(y) = 1 + \gamma_o \cdot e^{-\lambda \cdot y} \tag{A.2}$$

where γ_o is the fractional difference between the base year observation, and the best-fit decile curve estimated with (A.1). The parameter λ governs the convergence speed. By exploring the response to different convergence speeds and levels, as well convergence to alternative decile curves, the simulation framework can incorporate scenario-specific assumptions surrounding behavior and policy. For example, behavioral changes implicit in the scenario narrative (section A.2.6) that are expected to reduce long-term water use intensity are represented in the framework by selecting a lower decile curve for convergence. The use of decile curves bounds the projections to lie within the historically-observed range of per capita demand intensities. Combining this constraint with the convergence rules enables a diverse number of plausible demand trajectories to be generated. The decile curves do not cover all possible future policy regimes, and therefore alternative demand trajectories outside the simulated range are a possibility.

A.2.3 Technological change

Technological change is a dynamic effect apparent in the long-term development of municipal water systems [223], and refers to the observed improvements in the efficiency of resource use caused by long-term technological innovation [295]. The emergence of technological change is represented in the demand curves by scaling the model coefficients α and β in (A.9) by an annual improvement factor, with assumptions embedded in the scenario narratives (section A.2.6). It is expected that technological change will occur most rapidly in countries that spend more on technology research, and historical spending levels typically correlate with income-level [170]. We reflect this quality using the sigmoid curve depicted in figure (A.3) to model accelerated technological change as an annual improvement in water intensity ε that increases with average income. The frontier technological change rate (ε_{max}) is interpreted from previous long-term scenario studies [223, 259, 284], with the minimum rate (ε_{min}) assumed to be half the frontier value. Curve parameters are updated in each simulation year to reflect changes in the global GDP distribution. Scenarios involving a reduction in between country income inequality therefore lead to harmonization of technological change rates in the model.

Technological change is calculated at the national-scale in each simulated year using the projected intensity improvements:

$$\eta(y) = \prod_{t=1}^{y} [1 - \varepsilon(y)] \tag{A.3}$$

where η is the cumulative intensity improvement. Combining the path-dependency and technological change parameters yields the following form for the model coefficients:

$$\alpha(y) = \alpha_o \cdot \gamma(y) \cdot \eta(y) \tag{A.4}$$

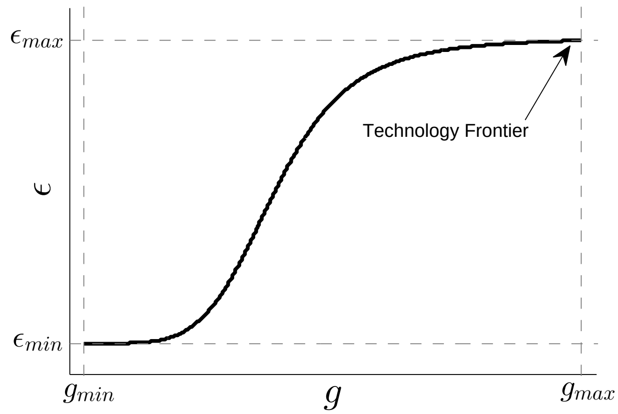

Figure A.3: Graphical depiction of the implemented technology frontier approach to technological change, where ε is the compound annual efficiency increase and g is per capita GDP.

$$\beta(y) = \beta_o \cdot \gamma(y) \cdot \eta(y) \tag{A.5}$$

where α_o and β_o denote the coefficients identified in the base year using quantile regression with (A.1).

A.2.4 Climate and population density

Local climate conditions affect the amount of moisture needed to sustain vegetation grown in urban environments. Evaporative losses from swimming pools and fountains are also enhanced under increasingly arid conditions. The soil moisture deficit is an empirical hydro-climatic indicator describing the amount of freshwater needed to sustain moisture levels in a particular location, and is routinely applied to estimate irrigation requirements under data limitations [296, 297]. Previous studies investigating the linkage between local climate and municipal water demand highlight the relationship between observed municipal irrigation and the calculated soil moisture deficit [267, 268, 271, 272, 298, 299]. Following the results of these previous studies, we integrate climate sensitivity into the global model by accounting for changes in the moisture deficit under alternative climate scenarios.

Initially, municipal irrigation demands Ω_i are disaggregated from the national demands estimated by (A.1). A parameter μ representing the fraction of total demand used for municipal irrigation is defined:

$$\Omega_i(y) = \mu_i(y) \cdot \Omega(y) \tag{A.6}$$

Previous observations suggest that μ increases with household income [267,268,300]. For example, survey of households in Eastern Africa show that municipal irrigation makes up a small fraction (about 1%) of total water demand in very low-income rural households, whereas nearby urban areas able to afford piped access apply an average of 10 % of total demand towards municipal irrigation [269]. Previous research in China and Brazil also identifies similar differences between the fraction of total demand used for municipal irrigation and income-level [301, 302]. We model the observed income effect on municipal irrigation penetration with the sigmoid curve ψ depicted in Figure (A.4a). The stylized curve increases from a minimum of 1 %, which occurs at the average per capita GDP estimated for rural Sub-Saharan Africa in 2010, to a saturation level at an average per capita GDP equivalent to the United States in 2010. The saturation level is calibrated based on geographical sensitivities to the moisture deficit observed in North America [268]. Specifically, we fit a linear function ϕ between the estimated annual average moisture deficit m_a and observed municipal irrigation (Figure (A.4b)), and results compare well with similar analysis in Mayer et al (1999) [268]. Combining the income and climate sensitivity terms yields the estimated fraction of total demand used for municipal irrigation (i.e., $\mu = \psi \cdot \phi$).

Further spatial and temporal downscaling of the municipal irrigation demands is achieved by assuming proportionality with changes in the simulated daily moisture deficit. A similar approach to temporal disaggregation was proposed in [261], but was based on the monthly temperature distribution. A proportional relationship between changes in irrigation volumes and the moisture deficit was also previously used to estimate the impact of climate change on agricultural systems in the United States [275] and globally [297]. As the demand curves applied in this paper are calibrated from national-level averages, spatial variations in municipal irrigation due to climate are taken relative to the population-weighted mean annual moisture deficit M_o:

$$M_o = \frac{1}{N_c} \cdot \sum_c [\, \hat{p}\,(c, y_o) \cdot m_a(c, y_o)\,] \tag{A.7}$$

where c denotes grid-cell, N_c is the number of grid-cells, $\hat{p}$ is the normalized population (i.e., grid-cell population divided by total national population), and y_o is the first year in the simulation horizon. The population-weighted moisture deficit in the initial year is also used to estimate the maximum penetration of municipal irrigation (i.e., $\phi = \phi(M_o)$). This choice ensures a consistent representation of non-irrigation demands under varying climate. Spatial and temporal variations in municipal irrigation due to climate variability are reflected by the fractional change in the moisture deficit δ_m:

$$\delta_m\,(c, y, t) = \chi(c, y) \cdot \left[\frac{m\,(c, y, t)}{M_o} - 1 \right] \tag{A.8}$$

where m represents the daily moisture deficit, and t represents the sub-annual time-slicing (daily). A scaling factor χ is applied to the gridded daily moisture deficit to reflect reduced per capita irrigable area with increasing population density. This urban form effect has been observed e.g., in China, where municipal irrigation plays a minor role in dense urban areas [303], but is prevalent in lower income rural municipalities [301]. These observations contradict the assumed relationship between income and municipal irrigation, and follow from reduced availability of outdoor area in dense urban cities. We estimated an inverse sigmoid function $\chi = \xi\,(d)$, where d is population density, to reflect the anticipated impacts of urban form on municipal irrigable area. The stylized curve is depicted in Figure (A.4c). Population density is calculated as the total grid-cell population divided by the raster grid-cell area. Assuming the non-irrigation demand is spread evenly across the population and year, the following functional form for per capita municipal water demand ω is obtained at the grid-scale:

$$\omega\,(c, y, t) = \Omega(y) \cdot [\, 1 + \mu_i\,(y) \cdot \delta_m\,(c, y, t)\,] \tag{A.9}$$

We calculate the moisture deficit at the daily time-scale as the difference between po-

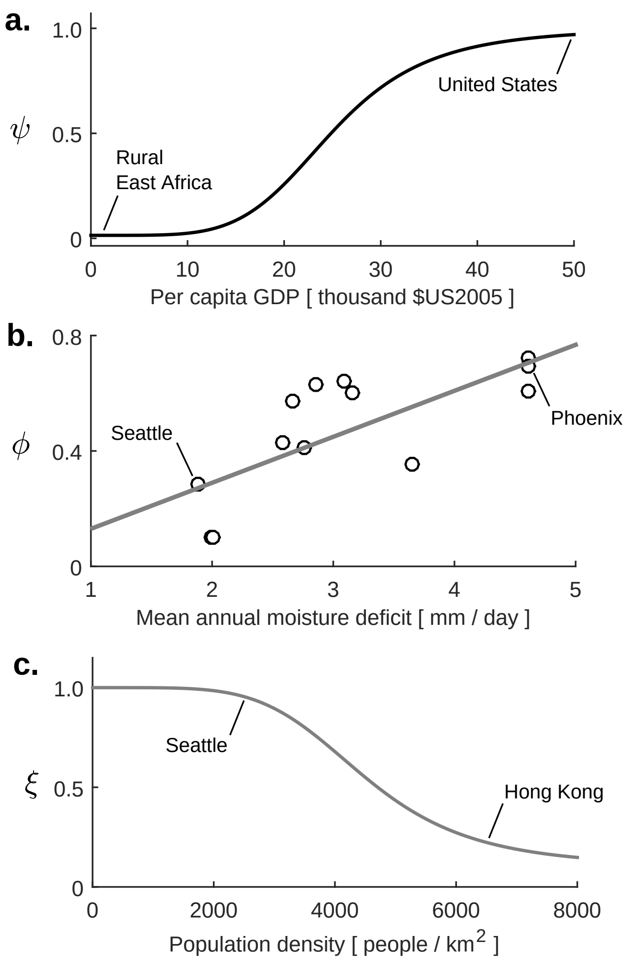

Figure A.4: Stylized models for representing demand sensitivities to climate and urban form: a. Municipal irrigation utilization (ψ) as a function of per capita GDP; b. Maximum penetration of municipal irrigation into national demand (ϕ) as a function of mean annual moisture deficit, and observed values for a number of cities in North America [268]; and c. Municipal irrigable area indicator ξ as a function of population density.

tential evapotranspiration v and effective precipitation e :

$$m(c,y,t) = v(c,y,t) - e(c,y,t) \tag{A.10}$$

Effective precipitation is calculated following the methodology described in [296] and [297], and the modified daily Hargreaves method is used to calculate potential evapotranspiration [304]. Evapotranspiration rates vary across vegetation types, although we currently assume a constant vegetation index due to a lack of historical urban vegetation data at the global-scale.

The proposed methodology represents a simplified way of modeling climate and urban form sensitivities. Basing the response of municipal irrigation on changes in the moisture deficit is somewhat analogous to the use of heating and cooling degree days in the estimation of climate change impacts on the municipal energy sector [42]. There are a number of limitations, including uncertainties surrounding assumptions that municipal irrigation demands scale linearly with changes in the moisture deficit. Detailed physical modeling will provide a more accurate representation of the water impacts of urban form [305], but is currently too data intensive to consider in global-scale analysis. The lack of irrigated vegetation in dense urban areas is also a contributor to the urban heat island effect [278], and the current version of the model does not account for impacts of urban irrigation on local climate conditions.

A.2.5 Return-flow

The return-flow from the municipal water sector provides an indication of the potential wastewater volume produced over a given timeframe. Following previous studies [223] the return flow is quantified by subtracting consumptive demand (the amount of water demanded that will not be returned to the source) from total demand. Consumptive demand is estimated with country-level efficiencies taken from the WaterGAP model [223]. The consumption efficiencies are then assumed to converge towards a maximum of 92 % under the process of long-term technological change. The maximum possible efficiency is meant to represent constraints on the amount of municipal water that must be consumed (e.g., for transpiration and other evaporative losses), and is selected based on the highest observed historical level [223]. Convergence rates align with assumptions for supply efficiency, and are described in greater detail in the following section.

A.2.6 Human development scenarios

The shared socioeconomic pathways (SSP) represent the most recent socioeconomic scenarios implemented in long-term global change modeling. The scenarios consist of qualitative narratives and quantitative projections for economic growth, technology, and demographic characteristics, and are specifically tailored to span the range of expected challenges faced when mitigating and adapting to climate change [224]. The five SSP narratives are briefly described below, with a detailed description provided in [255].

- SSP1 (Sustainability): The world transitions towards a more sustainable path, with specific focus on the environment. Population growth is low, economic development is high, and inequalities decrease both between and within countries.

- SSP2 (Business-as-usual): Countries proceed on a social, economic, and technological pathway that follows historical patterns. Population growth and economic development is in the mid-range of the projections.

- SSP3 (Regional rivalry): Countries increasingly focus on domestic and regional issues. Economic development is slow, consumption is material-intensive, and inequalities persist or worsen over time. Population growth is low in high-income countries and high in emerging countries.

- SSP4 (Inequality): Inequality worsens both within and between countries. Economic growth is moderate in high-income and middle-income countries, while low-income countries lag behind. Global population growth is moderate, driven by high fertility in emerging countries.

- SSP5 (Fossil fueled development): The world transitions toward a more fossil fuel intensive path, with relatively little action on avoiding potential global environmental impacts, due to a perceived tradeoff with economic development. Global population growth is low, driven by reduced fertility in the developing world, economic development is high, and inequalities reduce both between and within countries.

The SSP narratives provide important guidance on assumptions surrounding technological change, behavior and income inequality. For example, the conditions expected in SSP1 are likely to translate into sustainable and inclusive water development strategies. The focus on sustainability is expected to drive rapid technological change that combined with long-term behavioral shifts, would lead to long-term reductions in per capita municipal water demand. Conversely, limited concern and action on issues in SSP5 is expected to correlate with widespread increases in per capita intensity, although rapid technological change accompanying high-income levels will help to offset increased supply requirements.

Table (1) summarizes the translation of the SSP narratives to the model parameterization. Convergence towards different demand curves is stipulated to reflect the differences in behavior and policies implicit in the SSP narratives. For example, sustainable end-use behavior and policies assumed in SSP1 are simulated by having countries converge towards one of the lower decile curves. Following [294], we further utilize the scenario narratives to disaggregate urban-rural average income trajectories, by assuming income convergence to different levels at different rates (Appendix A). For instance, to reflect inequalities implicit in the narratives, urban-rural incomes in SSP3 and 4 are assumed to converge the slowest.

The quantitative SSP data applied in this work includes the GDP and population projections for 184 countries. Population projections come from the Wittengenstein Centre for Demography's long-term population model, which generates national-level population estimates out to 2100 based on assumptions surrounding future age, sex and educational composition [172]. Urbanization dynamics have also been estimated under SSP-specific assumptions surrounding urbanization rates [225]. National-level GDP scenarios (in purchasing power parity) come from the Organization for Economic Co-operation and Development's (OECD) Environmental Growth model, which is based on a convergence process and places emphasis on the following key drivers: population, total factor productivity, physical capital, employment and human capital, and energy resources [173].

Parameter	*Socioeconomic Scenario*				
	SSP1	SSP2	SSP3	SSP4	SSP5
Per capita demand decile curve	30th	30-70th	50-90th	40-90th	90th
Frontier technological change rate	1.00 %	0.50 %	0.25 %	0.25 %	1.00 %
Urban-rural IR convergence level	5 %	10 %	20 %	20 %	5 %
National Gini convergence level	0.25	-	0.60	0.60	0.25
Convergence year	2110	2120	2130	2130	2110

Table A.1: Translation of the qualitative SSP narratives to the quantitative water modeling parameterization. For per capita demand decile curves, entries with a range in values indicate divergence across countries. For example, in SSP4 developing economies converge to a lower decile curve, with advanced economies converging to higher levels. Technological change rates are estimated from [223] and [284]. Urban-rural income ratio (IR) convergence modeled after [294]. Decile curve and Gini convergence are interpreted from the SSP narratives. For SSP2, the Gini coefficients remain at the estimated 2010 level over the projections.

Spatial population scenarios are a key component of the analysis, and we apply the dataset described in [306] to represent the national-level urban and rural population projections at a $1/8^\circ$ spatial-scale. The downscaling approach applied in [306] utilizes a gravity-based population model to capture important spatial effects of urbanization, including densification and urban sprawl. Further improvements over previous approaches include refined treatment of protected areas and boundary effects, and a procedure for estimating model parameters from historic trends [307]. The spatial population scenarios are a potential source of uncertainty, as small area (grid-cell) projections of long-term population change are subject to a variety of assumptions regarding vital rates, migration, as well as population response to the socio-economic drivers of spatial change. The GDP pathways are also broken into urban and rural components and downscaled to the corresponding $1/8^\circ$ spatial-scale following the procedures described in Appendix A.

A.2.7 Climate scenarios

For climate, we utilize the most recent scenarios applied in the global climate modeling community, the RCPs [95]. Downscaled, bias-corrected ensemble results from five global climate models participating in the Coupled Model Intercomparison 5 (CMIP5) project are included in our analysis [308, 309]: MIROC-ESM-CHEM, IPSL-CM5A-LR, HadGEM2-ES, NorESM1-M and GFDL-ESM2M. The downscaled data was obtained from the Inter-sectoral Impacts Model Intercomparison Project (ISI-MIP) database[2] [310]. These data are generated at a $1/2°$ spatial-scale, and we downscale to $1/8°$ using bi-linear interpolation. We decided to utilize this simple downscaling approach to enable better treatment of the effects of population density at the $1/8°$ spatial scale, which would be less pronounced if the population data was aggregated to $1/2°$. Challenges associated with developing higher resolution downscaled climate parameters for projecting hydrologic indicators is discussed recently in [311], and overcoming these challenges is beyond the scope of this paper.

A.3 Results

This section presents key results of the global assessment, with specific focus on spatial, temporal, and scenario-specific dimensions of the analysis. We initially assess the relative importance of socioeconomic drivers by exploring results sensitivity to the SSPs. Effects of non-stationary climate conditions are then incorporated by examining results under SSP-RCP scenario combinations.

A.3.1 National-level

Figure (A.5) depicts the modeled urban and rural demand curves obtained at the national-level under stationary base-year climate for a sample of eight representative countries. The national demand curves trace the per capita water demand as a function of per capita GDP (income) over the simulation horizon (2000 to 2100). Municipal water demand in

[2]The data is produced up to 2099, and to simplify the modeling we assume these conditions hold in the year 2100.

emerging economies (China, India, Egypt, Nigeria and Brazil) initially increases rapidly across all scenarios due to high elasticity at low-incomes. The model projects relatively steady per capita demand in developed economies (Germany, US, and Japan) across most scenarios due to the assumed saturation of useful water services at high-income levels. Base year per capita demand in Germany is relatively low compared to other advanced economies, and as the SSP5 scenario is parameterized to converge towards the 90th percentile global trend curve, significant demand growth occurs in Germany in this scenario. Conversely, the sustainability-oriented behavioral and policy changes assumed implicit in the SSP1 narrative lead to significant reductions in per capita water demand across all nations (convergence towards the 30th percentile global trend curve), with the results particularly prevalent in the US, which currently experiences some of the highest per capita demand levels globally.

Technological change is included in the results depicted in Figure (A.5), and helps offset increases in water demand with increasing incomes. The impacts are most prevalent in SSP1 and 5, where a reduction in water demand intensity can be seen as countries transition to higher income-levels. Lower technological change rates occur in SSP3 and 4. These differences affect the long-term trajectory in the US, where per capita demands excluding technological change in SSP4 and 5 are similar but diverge significantly when technological change is considered. The GDP downscaling procedure places more wealth in urban areas, with the effects observed in the results as a difference between the urban and rural trajectories in the base year. Rural per capita demands are observed to exceed urban demands at similar income-levels because rural technological change lags behind urban areas based on the parameterized relationship with income-level. In SSP1 and 5, the urban-rural incomes converge more quickly, both within and between nations, leading to similar end-of-century per capita demands globally. Alternatively, in SSP3 and 4, where the most inequality is assumed, the trajectories remain more divergent over the simulation horizon.

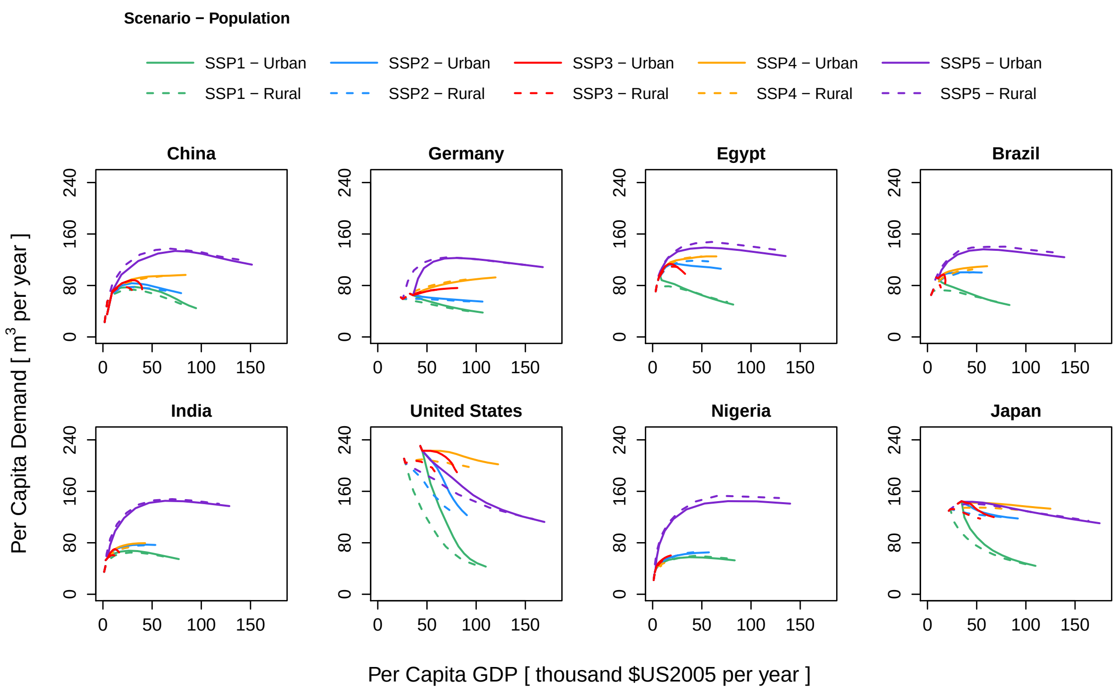

Figure A.5: Modeled urban and rural demand curves obtained at the national-scale under constant climate for a sample of eight representative countries. The demand curves trace the per capita water demand trajectory as a function of per capita GDP over the simulation horizon (2000 - 2100) for SSP1 - 5, and include scenario-specific effects of technological change.

A.3.2 Grid-level

The demand curves estimated at the national-scale are downscaled to the grid-level with Eq.(A.9). Results of the spatially-explicit analysis are summarized in Figure (A.6). Depicted is the mean annual municipal water demand across the SSPs, in the years 2010, 2040 and 2070, under stationary base-year climate conditions. The most significant growth in municipal sector water demand is anticipated to occur between 2010 and 2060, and to take place mainly in South Asia, China, and Sub-Saharan Africa. Economic growth is projected in these regions across many of the SSPs [173], which under the identified demand model (high elasticity at low-incomes), significantly increases per capita water demand. Concurrent to the economic development is an increasing population, which is expected to peak in these regions across most scenarios (excluding SSP3) around 2070 [172]. A combination of reduced fertility rates and saturation of useful municipal water services occurs as urban areas transition towards higher income-levels, and leads to long-term reductions in per capita demand.

Further mapped in Figure (A.7) is the coefficient of variation (CoV) calculated across the SSPs as the maximum range divided by the mean. The spatial distribution largely follows country delineation due to the parameterized national demand curves. The largest variability occurs in locations with a combination of uncertainties surrounding both demand intensity and population. For example, variability is particularly prevalent in the Tibetan Plateau region of Southwest China mainly due to uncertainties surrounding urbanization levels and its effect on the distributed rural population in this region. Most locations display a range of results across the SSPs that is greater than the ensemble mean value (i.e., CoV > 1), indicating a high-degree of sensitivity to socioeconomic uncertainties. As expected, much more uncertainty surrounds end-of-century conditions compared to mid-century conditions.

Scenario-specific results are highlighted for Nigeria in Figure (A.7). The economic growth and urbanization projected for this emerging African economy across the SSPs results in rapid growth in urban water demands across all scenarios. The SSP5 scenario displays the most growth due to the assumed transition towards water-intensive societies and the scale of the projected GDP expansion relative to the other SSPs. Conversely, the

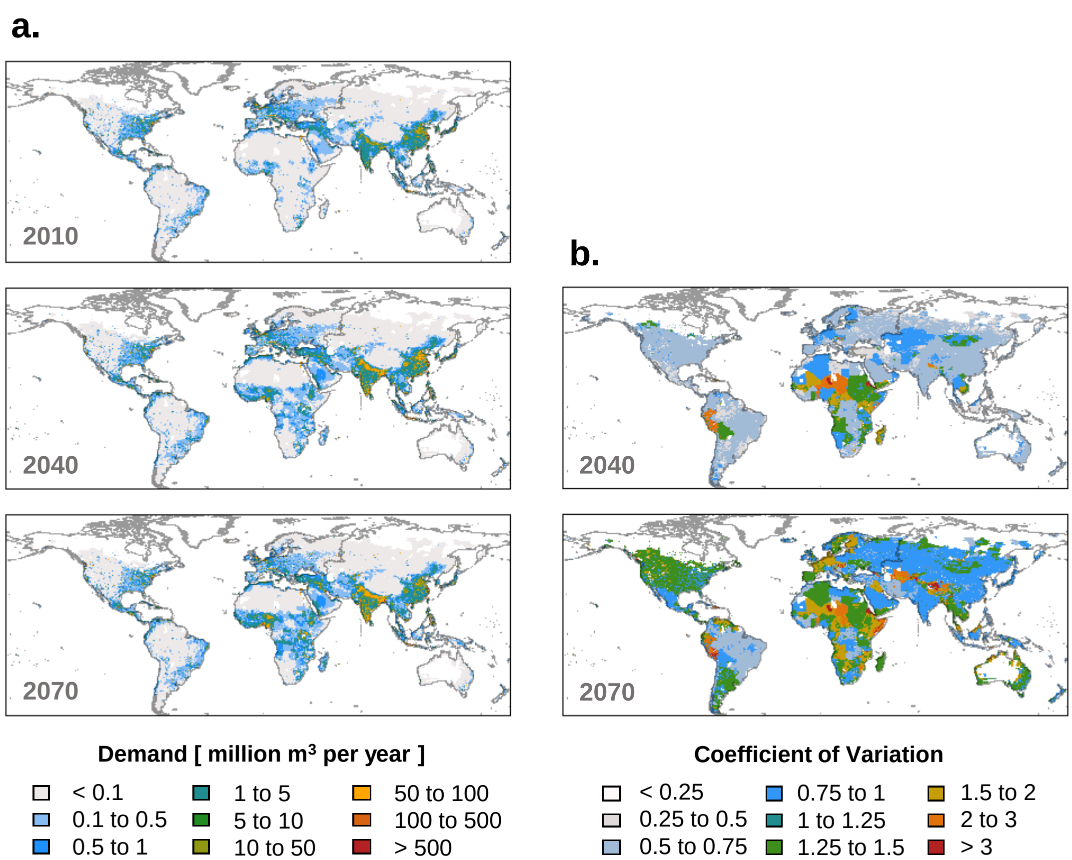

Figure A.6: Mean and coefficient of variation (CoV) of the spatially-explicit global municipal water demands obtained across the SSPs. In the calculation of the CoV, we utilize the maximum range across the scenarios divided by the mean value.

sustainability-oriented policy and behavioral measures expected in SSP1 lead to significantly lower water requirements. SSP2 and 3 display somewhat similar demand patterns, but the per capita demand in SSP3 is less due to slower income growth. In the end, the reduced per capita usage in SSP3 ends up being offset by increased population. Similar results are obtained for other emerging economies throughout Sub-Saharan Africa, as well as in Latin America and Asia.

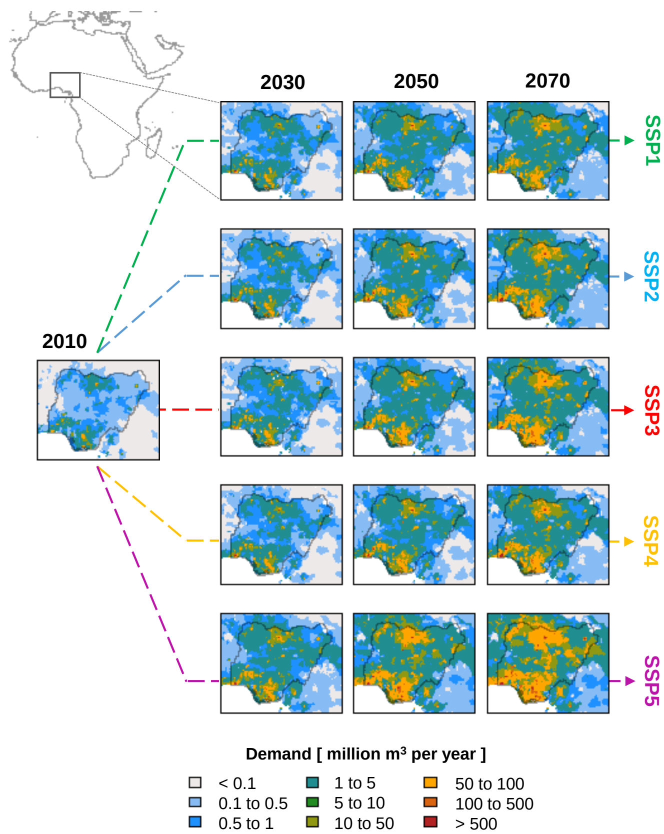

Figure A.7: Spatially-explicit municipal water demand scenarios for Nigeria across the SSPs.

A.3.3 Global

Aggregating the water requirements at the grid-scale yields an estimate of total global municipal water demand. Annual results are presented in Figure (A.8), along with the calculations for consumption and return-flow. In SSP1 we find that by 2070, global municipal water use reduces compared to current levels. The largest reductions are expected in consumptive demand due to a combination of improved supply and end-use efficiencies. At the high-end of the projections, we find that SSP3 and 5 lead to end-of-century requirements more than doubling from the current level. Peak water demand is expected to occur in SSP5 in the year 2070, and represents a municipal water requirement nearly three times the current level. Results from three similar models for the SSP2 socioeconomic scenario are also depicted in Figure (A.8). Our assessment appears to yield a global estimate for SSP2 that compares well with the H08 model [266, 312], but is lower than the WaterGAP [312] and PCR-GLOBWB [261] models, as well as a similar business-as-usual scenario explored with the GCAM model [284].

A.3.4 Impacts of climate change

We focus on the municipal water implications of the RCP2.6 and 8.5 climate scenarios to capture the largest range of uncertainties in radiative forcing under future greenhouse gas emissions. The RCP8.5 scenario represents a fossil fuel intensive global development pathway that results in an increase in end-of-century radiative forcing of 8.5 W/m^2 relative to pre-industrial levels and extreme climate change [313]. The RCP2.6 scenario represents a low-carbon development pathway associated with a 2.6 W/m^2 increase in radiative forcing and a high probability of limiting global mean temperature change over the 21st century to 2°C [314]. The use of the extreme climate scenarios restricts the socioeconomic scenarios that can be explored to SSP3 and 5, as these are the only cases likely to produce emission pathways consistent with a 2.6 and 8.5 W/m^2 radiative forcing. Even SSP3 may be incapable of providing the economic input commensurate with a 8.5 W/m^2 world; nonetheless, we decided to analyze the pathway to explore the different challenges to adaptation with SSP5.

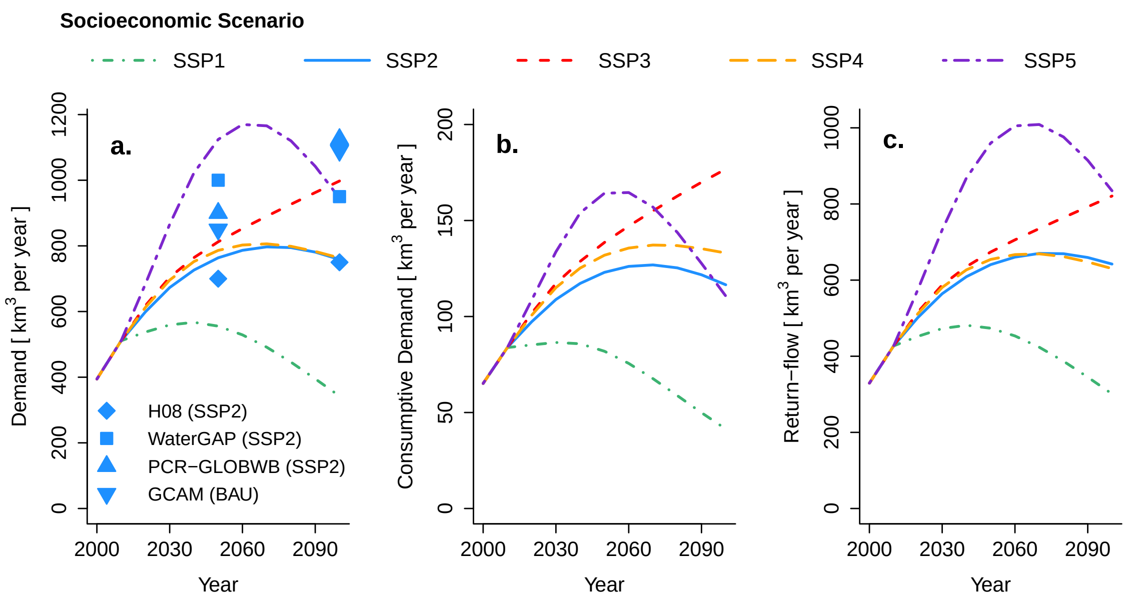

Figure A.8: Annual results aggregated to the global-scale for: a. Demand; b Consumptive demand; and c. Return-flow. For comparison, global results from similar models [H08 [266], PCR-GLOBWB [261] and WaterGAP [312]] available for the SSP2 socioeconomic scenario are included in the results for demand. Also included is the business-as-usual (BAU) scenario from the GCAM model [284].

Average and peak demand

To highlight the vulnerability of municipal water supply systems to climate change, we examined impacts to both average and peak daily demand requirements. The peak daily requirements are closely related to the required capacity of water supply and distribution infrastructure, and are therefore an important aspect of long-term planning. We estimated the peak daily water demand in each grid-cell as the 95th percentile of the annual time-series. The long-term response of the climate to different emission pathways means the climate scenarios vary little until mid-century [95], and to capture these longer-term effects while accommodating uncertainties surrounding the long-term evolution of the climate system, we focus on the average impacts obtained over the 2050 to 2080 period.

Figure (A.9) depicts the mapped difference in global municipal water demand between RCP8.5 and RCP2.6. In most locations, RCP8.5 (extreme climate change) results in relatively modest increases in average annual municipal water demand, although in some instances (e.g., Indonesia), demand in fact decreases. This decrease is due to wetter conditions in RCP8.5 reducing the need for municipal irrigation. Spatial precipitation patterns vary significantly across climate models, and will affect the results depending on the selected model (in this case we used the ensemble). The analysis suggests that achieving the RCP2.6 scenario (minimum climate change) would reduce aggregate annual global municipal water demand in comparison to the RCP8.5 scenario (maximum climate change) by 2 % in the SSP3 scenario, and by 4 % in the SSP5 scenario.

Benefits of climate change mitigation (i.e., achieving RCP2.6 opposed to RCP8.5) differ spatially. Figure (A.10) depicts the percent change in average and peak demand for SSP3 and 5 as a cumulative spatial distribution calculated across inhabited grid-cells. The change is calculated relative to results obtained under static base-year climate conditions. We find that in the RCP8.5 scenario that 95% of locations experience a change in average demand between -1 to 10 %, and a change in peak demand between 0 to 12 %. More than half of inhabited grid-cells in the RCP8.5 scenario see an increase in peak daily demand of 4 %. The range in climate impacts is reduced substantially in the SSP3 scenario: 95% of locations experience both peak and average demand increases of only 0 to 6%, with a mean value of less than 1%. Similar distributions are obtained when the gridded impacts

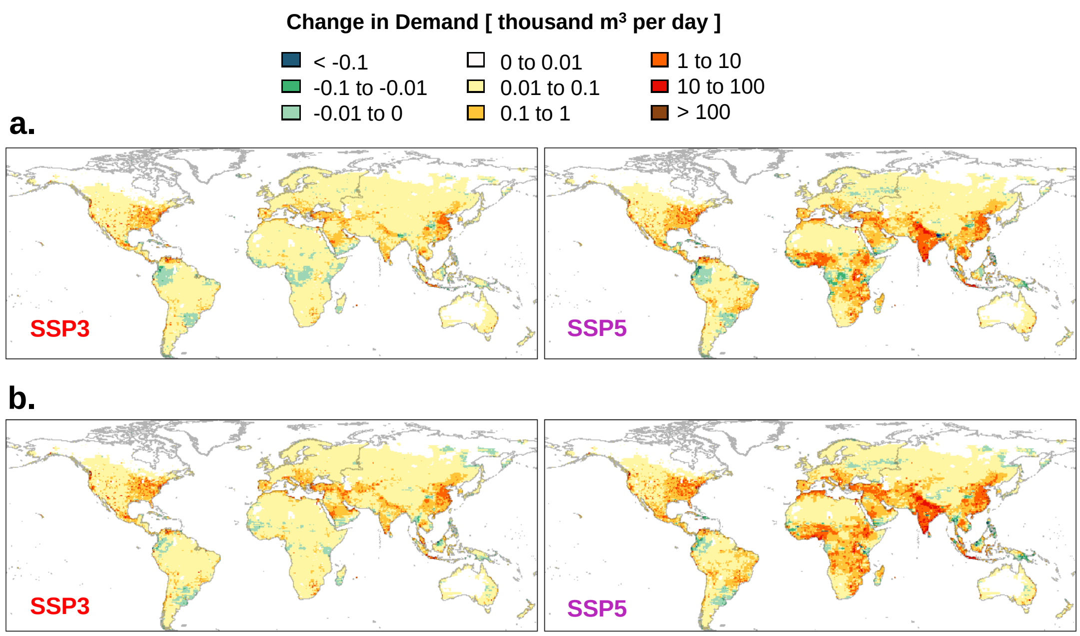

Figure A.9: Mapped change in municipal water demand in RCP8.5 relative to RCP2.6. The changes are averaged over the 2050 to 2080 period. a. Annual average demand; and b. Peak daily demand.

are weighted by population.

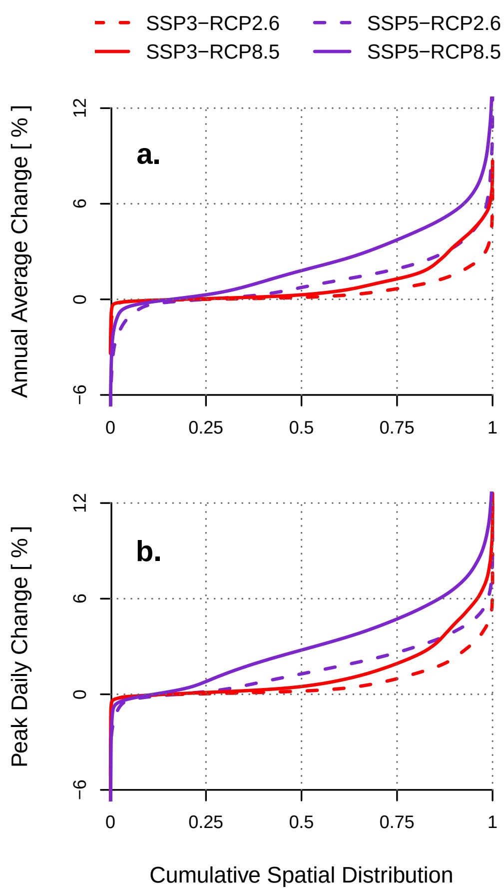

Figure A.10: Spatial distribution of climate change impacts on municipal water demand over the 2050 to 2080 period. The change is calculated relative to the results obtained under stationary baseyear climate conditions, and is averaged across the three decades. a. Annual average demand and b. Peak daily demand.

A.4 Discussion and conclusion

The municipal water sector provides crucial services for human well-being and will experience significant growth under the projected socioeconomic change in many regions globally. The municipal water sector is also directly vulnerable to the effects of climate change due to the large volumes of water used for municipal irrigation. This paper has assessed, for the first time, coupled climate-development impacts on global municipal water demand. A new modeling framework incorporating enhanced representations of human migration, income inequality, population density and climate sensitivity was developed for this task. The framework was applied to generate global municipal water demand scenarios over the 21st century aligned with the most recent global change scenarios at a 0.125° spatial resolution.

Model results suggest that socioeconomic changes will be the most important driver of shifts in future municipal water demand, with a wide range in outcomes obtained across the scenarios investigated. The least water-intensive scenario (SSP1) results in global municipal water demand decreasing at an average rate of 0.1 % per year over the 21st century, whereas the most water-intensive case (SSP5) results in demands increasing at a rate of 0.9 % annually. All scenarios investigated involve rapid demand growth in urban areas of emerging economies (0.7 to 1.7 % increase per year), whereas demand-levels in high-income regions remain relatively constant or decrease (-0.7 to 0.5 % increase per year). The scale of growth and levels of uncertainty observed across the results for emerging economies suggest a critical need for infrastructure development strategies that incorporate long-term flexibility.

Climate sensitivities were incorporated into the global modeling framework using an empirical hydro-climatic metric encapsulating local water availability (the moisture deficit). Results obtained under non-stationary climate conditions suggest that half of all inhabited locations may experience peak municipal water demands 2 to 4 % higher under a fossil fuel intensive global emission scenario (RCP8.5) relative to demand consistent with the emission scenario displaying a high probability of stabilizing global mean temperature change over the 21st century at 2°C (RCP2.6). The outcome means there are moderate freshwater co-benefits of climate change mitigation policy anticipated in the municipal sector that are additional to estimates from previous integrated assessments.

Comparing the non-stationary climate results across the SSP3 and 5 socioeconomic scenarios indicates that in terms of municipal water demands, SSP5 is much more vulnerable to the effects of climate change. Differences between the scenarios are largest in

Sub-Saharan Africa and India. These results follow from the assumptions surrounding sensitivity of municipal irrigation to both changes in climate and socioeconomic development. In SSP3, slower income growth in emerging economies result in less municipal irrigation and therefore lower climate sensitivity, whereas in SSP5, rapid income growth results in a higher-penetration of municipal irrigation and therefore increased climate change vulnerability. Although the population in SSP5 appears more vulnerable than in SSP3, it is better equipped for adaptation due to significantly higher-incomes and less inequality.

Systematic validation of the modeling framework is currently limited by our ability to test its long-term performance due to the absence of spatially-explicit historical data. Global results were compared with four similar modeling frameworks harmonized to similar national data-sets, and it was found that our calculations fall on the low-end of previous estimates. The reason is likely due to the semi-logarithmic form assumed in the demand model, and what this implies for demand elasticity at higher-incomes. Incorporation of income distribution effects in the model developed in this paper also leads to reduced demand projections, due to the impact on perceived average income-level in the aggregated household demand model. Overall, the income-demand relationship has a strong impact on the results, and this causal link could in fact be less pronounced. Other local drivers, such as institutional stability, cultural trends, policies and infrastructure could not be taken into account due to lack of globally comprehensive data sets. These areas are important for future work aiming to explain a greater range of the historical data.

A.5 Supplementary material: GDP downscaling

National GDP projections are initially disaggregated into urban and rural average incomes in the base-year (2010). We make the assumption that per capita GDP in purchasing power parity is equivalent to per capita income at the national-scale. The national per capita GDP is then related to the urban and rural components through the following relationship:

$$g_n = u \cdot g_u + (1-u) \cdot g_r \tag{A.11}$$

where u is the urbanization rate (fraction of national population that is urban), g_n is average per capita GDP (income) across the national population, and g_u and g_r denote the urban and rural values respectively. The GDP projections are disaggregated into the urban and rural components following the procedure described in Grübler et al. (2007) [294]. The approach relies on the observation that residents in urban areas typically have higher incomes [291]. To reflect the income inequality between urban and rural populations, we take advantage of the fact that income is typically distributed lognormally across a population [287], and that in the base-year (2010) the top income quintile (i.e., top 20%) always resides in urban areas [294].

We identify the average per capita GDP of the national income quintiles using the income Lorenz curve L. The Lorenz curve is estimated based on the shape of the lognormal distribution [288]:

$$L(x) = \Phi\left[\Phi^{-1}(x) - \sigma\right] \tag{A.12}$$

where x is the percentile associated with a given income quantile, σ is the standard deviation of the income distribution, and Φ denotes the cumulative normal distribution function. Under the assumption of lognormality, the standard deviation is estimated with the following relationship [288]:

$$\sigma = \sqrt{2} \cdot \Phi^{-1}\left(\frac{\pi + 1}{2}\right) \tag{A.13}$$

where π is the Gini coefficient. Historical observations of the Gini coefficient are available for most countries from the World Bank, and are applied in this study to parameterize income inequality in the base-year. For countries lacking historical observations, we utilize a regional average.

Assuming the bottom four national income quintiles incorporating both urban and rural residents split the income evenly (i.e., everything but the GDP represented by the top quintile), we identify the average rural per capita GDP using the value of the Lorenz curve at the top income quintile:

$$g_r = g_n \cdot \frac{L(x)}{x} \tag{A.14}$$

where $x = 0.8$ for the top income quintile. Once calculated, the rural per capita GDP is inserted into (1) to calculate the corresponding urban-level. Without further information on the sub-national distribution of income-levels[3], we assume that the identified urban and rural per capita GDPs do not vary across grid-cells within countries.

In future years, national Gini coefficients are assumed to converge or diverge towards the qualitative inequality trends implicit in the scenario narratives (Table 1, main text). For example, in SSP1 and 5, inclusive development leads to widespread reductions in inequalities, and we reflect these conditions by having Gini coefficients converge towards a relatively low value of 0.29 by the end of the century (close to the level currently seen in Sweden and Denmark). Conversely, in SSP 3 and 4, which contain explicit narratives describing increased inequality, we set convergent values to 0.6 (close to the level currently seen in South Africa). To account for institutional inertia, we analyzed decadal observations for OECD countries to identify a distribution of historical rates of change and then set a maximum rate of inequality change to the 50th percentile value (0.15 % per year).

The model formulation requires estimates of the urban and rural Gini coefficient. Empirical studies show that differences between urban and rural income inequality exist in countries such as India, where in the 90s, the rural Gini was typically about 20 % less than the urban Gini [316]. In China, the urban and rural Gini coefficients from 1978 to 2002 trace a similar path [317]. Without detailed information on the historical trajectories of all countries we simplify the analysis by assuming that the urban and rural population groups display equivalent Gini coefficients, and identify a common value that ensures consistency with the national-level and the decomposed average income levels. The Theil index is an alternative inequality metric that can be readily decomposed into urban and rural components [318]. Under income distribution lognormality, the Theil index is approximately equal to half the variance $\nu = \sigma^2$ [319]. Based on the Theil decomposition described in [318], we obtain the following relationship between the national income standard deviation (ν_n) and the urban-rural value (ν_{ur}):

$$\nu_{ur} = \nu_n + 2 \cdot \{\, u \cdot \ln(\kappa) - \ln[\, 1 + u \cdot (\kappa - 1)\,]\,\} \tag{A.15}$$

[3] The GECON dataset provides sub-national spatial information on the distribution of GDP [315]. Calculating gridded per capita GDP with the GECON and SSP population datasets results in extreme outcomes because some rural areas with low population have high industrial output. The spatial GDP in GECON is a better metric for production intensity, not consumption in the municipal sector.

where κ is the urban-rural average income ratio. Corresponding urban-rural Gini coefficients can be identified with (A.13). Following the analysis in [294], the urban-rural average income ratio is assumed to converge over time at the scenario-specific rates in Table 1 of the main text. This feature allows the simulation framework to incorporate expected income effects implicit in the scenario narrative, such as inclusive development strategies that reduce income inequalities across a population.

Software/data availability

The gridded municipal water demand scenarios described in this paper are available upon request from the corresponding author (S.C. Parkinson: scp@uvic.ca).

Acknowledgements

The Coupled Model Intercomparison Project Phase 5 (CMIP5) and the Inter-Sectoral Impact Model Intercomparison Project (ISIMIP) is acknowledged for providing the global climate model output for this study. SCP was supported in part by a post-graduate scholarship from the Natural Sciences & Engineering Research Council of Canada. ND acknowledges with thanks partial funding of this project by the Deanship of Scientific Research (DSR), King Abdulaziz University, Jeddah, under grant no. (1-135-36-HiCi).

Appendix B

Supplementary material: Robust response to hydro-climatic change in electricity generation planning

List and description of symbols

Sets

c	Scenario
g	Resource grade
l	Interregional transmission link
p	Power plant type
r	Managed rivers or aggregated basins
s	Season in year
y	Year in simulation horizon

Parameters

α	Seasonal storage recharge frequency
β	Discount rate
δ	Seasonal time-step duration
ε	Hydroelectric streamflow-to-energy conversion coefficient
η	Energy conversion efficiency
ϕ^E	Capacity / availability factor
ϕ^F	Flexibility factor
ϕ^P	Peak load carrying capability factor
ψ^C	Fixed costs coefficient
ψ^I	Import price coefficient
ψ^N	Capital costs coefficient
ψ^V	Variable costs coefficient
ψ^X	Export price coefficient

τ	Minimum storage discharge time
d^{avg}	Seasonal average energy demand
d^{flex}	Flexible reserve demand
d^{peak}	Seasonal peak capacity demand
v^{nat}	Natural streamflow into hydroelectric facility
w	Objective function weighting

Variables

C	Installed capacity
D	Volume of streamflow in seasonal reservoir storage
D^{+}	Volume of streamflow into seasonal reservoir storage
D^{-}	Volume of streamflow out of seasonal reservoir storage
E	Electricity produced
I	Imported electrcicity
N	New capacity
R	Retired capacity
S	Volume of streamflow spilled
T	Total annual cost of system operation
V	Volume of streamflow passed through hydroelectric turbines
X	Exported electricity

B.1 Hydro-climate scenarios

Tab. (1) provides the climate scenario data included in the study. Presented are the seasonal ranges in provincial temperature and precipitation anomalies projected by the Pacific Climate Impacts Consortium (PCIC) for 2041-2070 trends relative to observed 1961-1990 trends [106]. Climate warming is observed across the ensemble distribution. An increased precipitation trend is seen in most seasons and annually, although drier conditions are expected in the summer.

Climate Parameter	Winter (DJF)	Spring (MAM)	Summer (JJA)	Fall (SON)	Year
Temperature [°C]	2.6 (0.6, 3.6)	2.1 (1.1, 3.2)	2.6 (1.4, 4.4)	2.2 (1.3, 3.9)	2.4 (1.4, 3.7)
Precipitation [%]	13 (5, 26)	12 (0, 19)	-3 (-21, 5)	13 (1, 27)	9 (0, 18)

Table B.1: Regional mean temperature and precipitation anomalies projected for 2041-2070 trends relative to observed 1961-1990 trends. The 5th and 95th percentile of the annual ensemble distribution are provided in brackets. Adapted from: [106].

Corresponding distributions in streamflow impacts modeled by PCIC using the VIC hydrologic model at a number of major provincial hydroelectric reservoirs are provided in Tab. (2). Perennial warming triggers earlier spring snowmelt, which combined with an increasing precipitation trend, is expected to make more run-off available in the winter and spring seasons. Warmer and drier summer conditions lead to reduced summer run-off in many of the managed basins.

B.2 Climate-sensitive electricity demand model

The data and fitted models for the electricity demand model are depicted in Fig.B.1. Cubic polynomials are found to provide adjusted R^2 values ranging from 0.90-0.92. Coefficients from the regression analysis are provided in Tab.(B.2).

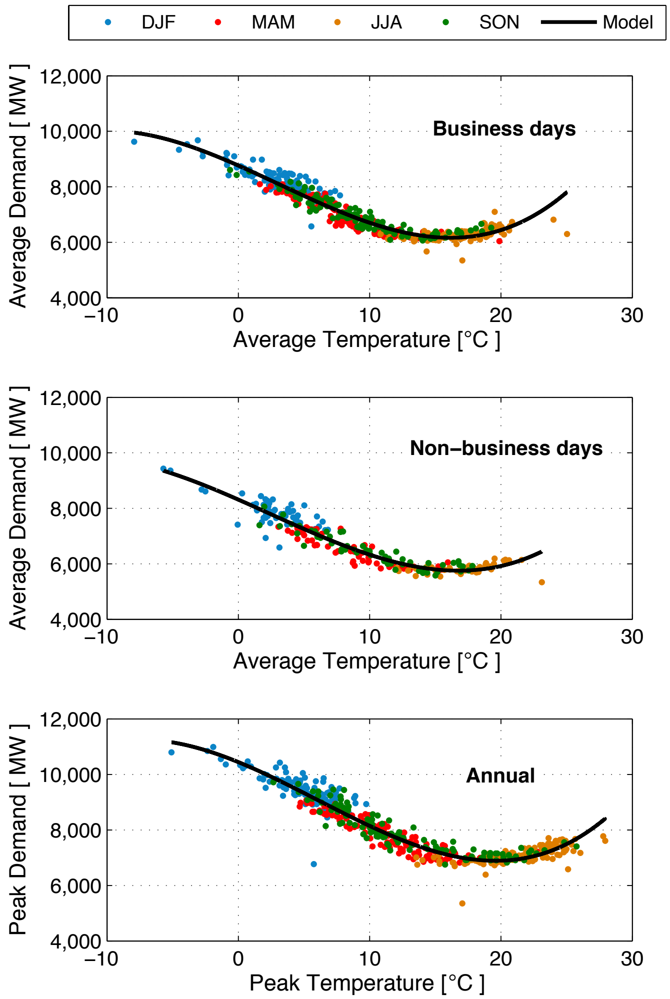

Figure B.1: Sensitivity of regional electricity demand to weighted outdoor air temperature at the daily timescale and the corresponding cubic polynomial model fit.

Basin	Winter (DJF)	Spring (MAM)	Summer (JJA)	Fall (SON)	Year
Kinbasket [%]	53 (14, 104)	77 (75, 68)	9 (5, 11)	2 (-9, 15)	17 (10, 24)
Revelstoke [%]	91 (24, 132)	79 (84, 63)	-2 (-7, 4)	-1 (-20, 21)	12 (2, 23)
Arrow Lakes [%]	111 (60, 115)	53 (54, 57)	-7 (-14, 0)	-3 (-16, 18)	9 (-1, 21)
Williston [%]	78 (25, 64)	61 (46, 55)	-15 (-28, -7)	5 (-5, 13)	11 (-7, 19)
Kootenay [%]	86 (72, 101)	38 (37, 46)	-18 (-31, -12)	-4 (-27, 17)	6 (-5, 16)
Strathcona [%]	52 (45, 42)	6 (-10, 13)	-64 (-68, -43)	10 (8, 12)	1 (-10, 8)

Table B.2: Mean natural inflow (run-off) anomalies projected for 2041-2070 trends relative to observed 1961-1990 trends at major provincial hydroelectric reservoirs. The 5th and 95th percentile of the annual ensemble distribution are provided in brackets. Adapted from: [108].

B.3 Climate-sensitive hydropower model

Climate change impact to BC's hydropower potential is quantified by explicitly considering the streamflow balance at existing facilities. The spatial distribution of the stations included in the study is provided in Fig. (2.2). Historically, these sites on average produce about 90% of hydropower in the province. The remaining 10% of hydroelectric capacity consists mainly of small-scale distributed systems, and due to data limitations is represented in the model as an aggregated resource that follows an average seasonal inflow trajectory. The approach taken to quantify hydropower potential is similar to that seen in other recent climate change impact assessments [30, 47]. Hydropower potential is calculated considering the potential energy E in available streamflow V:

$$E = \rho g h V \tag{B.1}$$

The potential depends on the site-specific hydraulic head h. The parameters g and ρ represent the acceleration due to gravity and water density respectively.

Facility technical data implemented in the model is summarized in Tab.(B.3). The parameters are calibrated such that each plant's baseline trajectory aligns with the historical

Time-series	Polynomial Coefficients				Adj. R^2
	a_0	a_1	a_2	a_3	
Average Demand					
Business days	8765.9841	-209.1196	-4.0521	0.4347	0.9221
Non-business days	8314.1203	-208.0120	-2.5101	0.3464	0.9002
Peak Demand					
Annual	10442.7920	-193.3393	-8.0773	0.4435	0.9147

Table B.3: Coefficients and adjusted R^2 for fitted polynomials $y = a_o + a_1 x + a_2 x^2 + a_3 x^3$, where y is aggregate provincial electricity demand and x is the population-weighted provincial temperature trajectory.

long-term energy performance reported in the literature. The model includes planned hydroelectric capacity upgrades, as well as the addition of a new 1,100 MW plant on the Peace River (the so-called Site C, downstream from the G.M. Shrum and Peace Canyon projects). The remaining 10% of hydroelectric capacity consists mainly of small-scale distributed systems, and is represented in the model as an aggregated resource that follows an average seasonal inflow trajectory.

Streamflow projections at the Seven Mile, Kemano, and Bridge project locations are not covered in the PCIC study. To include these stations in the study at hand, we take advantage of the consistency observed in the direction of projected streamflow changes. Missing project inflow anomalies are inferred from those available based on how historical seasonal inflow patterns and predicted future climate trends compare. Future climate conditions at project locations were taken from PCIC's sub-regional database [320]. The results of this mainly qualitative analysis couple the following stations inflow anomaly distributions: Seven Mile and Kootenay Canal; Bridge and Mica; and Kemano and Revelstoke.

River	Facility	Reservoir	Capacity [MW]	Head [m]	Active Storage [Mm^3]	Annual Inflow [Mm^3]	Seasonal Inflow Fraction DJF	MAM	JJA	SON	Annual Energy [GWh]	Planned Expansion [MW] (Year)	Sources
Columbia	Mica	Kinbasket	1,805	197	14,800	18,196	0.05	0.17	0.63	0.15	8,562	1,000 (2015)	[109, 120, 122]
Columbia	Revelstoke	Revelstoke	2,480	160	1,850	7,442	0.05	0.22	0.57	0.16	9,496	500 (2021)	[109, 120, 122]
Columbia	Arrow Lakes	Arrow Lakes	185	10	8,760	11,195	0.16	0.39	0.32	0.13	767	-	[109, 321]
Peace	G.M. Shrum	Williston	2,730	190	39,472	34,059	0.07	0.25	0.51	0.17	16,477	220 (2025)	[110, 119, 120, 122]
Peace	Peace Canyon	Dinosaur	728	50	25	-	-	-	-	-	4,054	-	[110, 119, 120, 122]
Peace	Site C	Site C	-	60	25	-	-	-	-	-	-	1,100 (2020)	[119]
Nechako	Kemano	Nechako	1,000	700	3,400	4,081	0.05	0.29	0.50	0.16	7,271	-	[114, 115, 119]
Pend D'Oreille	Seven Mile	Seven Mile	1,298	123	46	17,660	0.17	0.33	0.30	0.20	5,327	335 (2015)	[111, 120, 121]
Kootenay	Kootenay Canal	-	1,030	194	-	11,639	0.06	0.29	0.55	0.10	5,533	-	[93, 111, 120, 121]
Bridge	Bridge	Carpenter	583	325	1,732	3,500	0.06	0.15	0.62	0.17	2,793	-	[113, 121, 122]
Campbell	Campbell	Strathcona	240	160	767	3,130	0.12	0.34	0.39	0.15	1,230	-	[112]

Table B.4: Technical data used to parameterize the hydroelectric facilities included in the analysis. Hydraulic heads have been calibrated such that the historical inflow data matches the reported annual energy performance. Parameterizations that represent the characteristics of multiple projects aggregated together include: Kootenay Canal, which also considers Corra Lynn, Upper / Lower Boddington, South Slocan and Brilliant capacity; Seven Mile, which also considers Waneta capacity; Bridge, which also considers Seton and Walden capacity; and Campbell, which consists of Stratchcona, Ladore and John Hart capacity.

B.4 Robust electricity generation planning model

Model equations

A dynamic optimization model is developed to examine impacts of hydro-climate uncertainty on the electricity generation planning process. The model is linear and solves for the least-cost operational trajectory of the electricity system at a seasonal time-step. This includes investment decisions in new generation and interregional transmission capacity. Interrseasonal capacity and flexibility constraints are imposed to relfect short-term operating requirements. The model is written in the GNU Mathematical Programming Language (GMPL) and solved with the GNU Linear Programming Kit (GLPK) [322].

Objective

The formulation specifically incorporates climate-resilience into the optimal technology portfolio using a form of robust optimization. Robust optimization is chosen because it is an effective method for pro-actively handling scenario-based uncertainties in large-scale system design problems[1] [101]. In robust optimization, optimal design (capacity) and control (activity) variables are determined based on calculated performance across a number of alternative scenarios. By including climate change impact scenarios in the analysis, robust optimization reveals system designs resilient to uncertainties in climate change projections [75].

In the current study, we extend the robust optimization approach to include hydrologic impacts of climate change. We further impart increased stringency into the system's design by requiring feasibility across all electricity impact scenarios included in the analysis (i.e., the model is *solution robust* [101]). This choice of model formulation enables our analysis to explore long-term capacity implications of climate-resilience. The objective function in this case minimizes the weighted sum of each scenario's total cost.

$$\textbf{Min} \sum_{c} w_c Z_c \tag{B.2}$$

The weights are inferred from the frequency distribution associated with the hydro-climate ensemble used to generate each impact scenario included in the robust set. This objective favours a technology portfolio that performs best under projections occurring most frequently in the coupled modeling experiments.

Economics

Total discounted cost of each climate scenario included in the analysis is given by:

$$Z_c = \sum_{y} T_{c,y} \left(1+\beta\right)^{-y} \tag{B.3}$$

[1] Alternative methods for addressing uncertainty long-term energy planning analysis include stochastic linear programming [96, 97], mini-max optimization [98], real-options [99], and hybrid approaches [100]

Annual costs are comprised of investments in new capacity, and the operation and maintenance of existing infrastructure:

$$
\begin{aligned}
T_{c,y} = \sum_{p,g,s} \left(\psi^N_{p,g,y} N_{p,g,y} + \psi^C_{p,g,y} C_{p,g,y} + \psi^V_{p,g,y} E_{c,p,g,s,y} \right) + \\
\sum_{l,s} \left(\psi^N_{l,y} N_{l,y} + \psi^C_{l,y} C_{l,y} + \psi^I_{l,y} I_{c,l,s,y} - \psi^X_{l,y} X_{c,l,s,y} \right)
\end{aligned}
\tag{B.4}
$$

In the above equation, variable costs include fuel and emissions. Note that activity variables are scenario-dependent while capacity variables are scenario invariant; this ensures the capacity is robust.

Electricity

To ensure consistent service, electricity production is constrained to always be greater than or equal to consumption:

$$
\sum_{p,g} E_{c,p,g,s,y} + \sum_{l} (I_{c,l,s,y} - X_{c,l,s,y}) \geq d^{avg}_{c,s,y} \tag{B.5}
$$

The activity of each generation-type is constrained by its installed capacity and seasonal availability (i.e., capacity factor):

$$
E_{c,p,g,s,y} \leq \phi^E_{p,g,s,y} C_{p,g,y} \, \delta \tag{B.6}
$$

Likewise, imports and exports are constrained by installed transmission capacity:

$$
I_{c,l,s,y} + X_{c,l,s,y} \leq C_{l,y} \, \delta \tag{B.7}
$$

To resolve peak capacity constraints, seasonal peak demand is considered separately from average requirements:

$$
\sum_{p \in P_1, g} \phi^P_{p,g} C_{p,g,y} + \sum_{p \in P_2, g} \phi^P_{p,g} E_{c,p,g,s,y} \, \delta^{-1} \geq d^{peak}_{c,s,y} \tag{B.8}
$$

The model considers all dispatchable technologies (set P_1) to contribute to peak requirements based on the installed level, whereas non-dispatchable technologies (set P_2) contribute based on their average energy output. The peak requirements include a 10% buffer for reserve.

Flexibility constraints are also incorporated into the model using the methodology described in [207]. The flexibility requirement is defined based on the level of energy demand:

$$\sum_{p,g} \phi^F_{p,g} E_{c,p,g,s,y} \geq d^{flex}_{c,s,y} \tag{B.9}$$

Technologies are then defined to contribute to flexible capacity differently based on average performance expectations. For instance, SCGT plants provide positive flexible capacity while wind technologies provide negative flexible capacity.

To meet future demand requirements, new capacity must be developed. The accumulated capacity in each year is given by:

$$C_{p,g,y} = C_{p,g,y-1} + N_{p,g,y-1} - R_{p,g,y-1} \tag{B.10}$$

$$C_{l,y} = C_{l,y-1} + N_{l,y-1} - R_{l,y-1} \tag{B.11}$$

Pumped storage technology included in the model requires special treatment. Intertemporal dispatch is set exogeneously, by defining a set number of recharge intervals per season and a minimum discharge time. To simplify the modeling, seasonal storage is disallowed (seasonal storage opportunities are addressed in the hydrologic model). Due to efficiency losses, the storage unit represents net seasonal energy consumption:

$$E_{c,p,g,s,y} = C_{p,g,y}\, \tau \left(\eta^2 - 1\right) \alpha \tag{B.12}$$

The operational strategy for a typical pumped storage technology described in [323] is used to parameterize the storage model.

Demand response (DR) is also included in the model, and refers to a technology that enables the shifting of load over periods ranging from minutes to hours. This is different from long-term demand impacts of efficiency investments and price response, which are included in the baseline load forecast [104]. These resources contribute to peak load and flexible capacity, but do not effect energy demand. Resource grades for DR are estimated from the supply curve in [123], which is then multiplied by a factor of 2 to represent potential costs in 2025. The supply curve limits DR to a maximum of 10% of peak demand. Both storage and DR capacity expansion is enabled in the model post-2025.

For hydropower technologies coupled to streamflow, water passed through the hydroelectric turbines produces energy at a rate proportional to the site-specific conversion efficiency (product of turbine efficiency, acceleration due to gravity, water density and hydraulic head):

$$E_{c,p,g,s,y} = \sum_r \varepsilon_{p,s,y} V_{c,r,p,s,y} \tag{B.13}$$

Other energy-related constraints on the model include minimum infrastructure utilization rates, maximum growth rates, maximum installed capacity constraints (e.g., renewable resource availability), and non-negativity constraints.

Streamflow

Hydrologic constraints are represented within the long-term planning problem by explicitly considering streamflow balance at most of the provincial large-scale hydroelectric stations. At upstream stations this balance is modeled by:

$$V_{c,r,p,s,y} + S_{c,r,p,s,y} + D^{+}_{c,r,p,s,y} - D^{-}_{c,r,p,s,y} = v^{nat}_{c,r,p,s,y} \tag{B.14}$$

For rivers that contain projects in a cascading configuration, the regulated outflow from upstream projects must be considered in the downstream project balance:

$$V_{c,r,p,s,y} - V_{c,r,p-1,s,y} + S_{c,r,p,s,y} - S_{c,r,p-1,s,y} + D^{+}_{c,r,p,s,y} - D^{-}_{c,r,p,s,y} = v^{nat}_{c,r,p,s,y} \tag{B.15}$$

The total amount of active water in storage is determined by:

$$D_{c,r,p,s,y} = D_{c,r,p,s-1,y} + D^{+}_{c,r,p,s-1,y} - D^{-}_{c,r,p,s-1,y} \tag{B.16}$$

This formulation neglects reservoir and downstream transport losses (e.g., reservoir evaporation), although the model parameters are specifically calibrated to help account for potential errors.

For the Mica facility, seasonal pumped storage opportunities are considered, and an extra variable is added to the upstream and downstream water balance that represents the volume pumped from downstream to upstream. If developed, energy required for pumping is determined using the hydropower equation from above.

Streamflow management variables are further constrained by prescribed capacities and to remain non-negative. Seasonal minimum / maximum (ecological) flow requirements are also respected. Finally, reservoir sustainability is assured by constraining the initial level in each winter to be the same.

Appendix C

Supplementary material: Long-term energy planning with uncertain environmental performance metrics

C.1 Formulation of the existing BC electricity planning model

The existing BC electricity planning model is linear and solves for the least-cost operational trajectory of the electricity system at a seasonal time-step. The model is written in the GNU Mathematical Programming Language (GMPL) and solved with the GNU Linear Programming Kit (GLPK) [322]. Model formulation is in Appendix B.4.

C.2 Stochastic sampling sensitivity

Risk is parameterized by estimating the shape of the uncertain performance distributions. This is done by drawing a finite number of random samples from a defined probability distribution. To test stability of solutions to the emission factor distribution sample size, a modified version of the convergence criteria proposed in [150] was applied. A 1-norm convergence criteria Δ is calculated, and describes the distance between two objective functions C obtained under alternative realizations of the stochastic distributions a and b. The difference is then compared to the relative magnitude of the solutions, namely:

$$\Delta_{a,b} = \frac{|C_a - C_b|}{C_a + C_b} \tag{C.1}$$

The model was run with different sample sizes with the 1-norm criteria computed to test for convergence. It was found that the risk aversion parameter approach produces the most volatile response at the highest risk parameter tested (Φ = 5). Results of the analysis are depicted for this case in Fig(C.1). It can be seen that solutions provide adequate

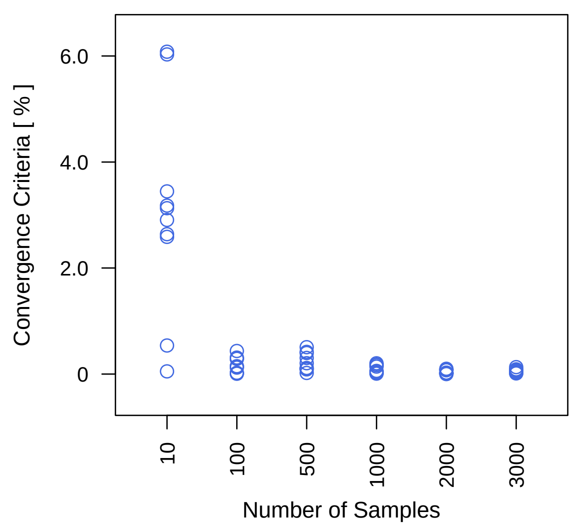

Figure C.1: Objective function convergence obtained under different number of samples drawn from the stochastic emission factor distributions.

convergence when $N = 3000$. This sample size was applied in all remaining model runs.

Appendix D

Supplementary material: Impacts of groundwater constraints on Saudi Arabia's low-carbon electricity supply strategy

List and description of symbols

Sets

c Carrier

m Month

m_f Final month (December)

m_i Initial month (January)

o Supply technology operational mode

r Region

rr Alternative region

s Storage technology

t Supply technology

y Year in simulation horizon

y_{end} Final year in simulation horizon

Parameters

α^{tech} Capacity used by activity in a specific operating mode

β^{tech} Maximum capacity available for an activity in a specific operating mode

δ Discount rate

$\varepsilon^{net,in}$ Input activity ratio for network technology

$\varepsilon^{net,out}$ Output activity ratio for network technology

$\varepsilon^{sto,in}$ Input activity ratio for storage technology

$\varepsilon^{sto,out}$ Output activity ratio for storage technology

ε^{tech} Input/output activity ratio for supply technology

γ^{net} Network technology fixed costs

γ^{sto}	Storage technology fixed costs
γ^{tech}	Supply technology fixed costs
μ	Minimum run-time fraction for supply technologies.
ϕ^{net}	Capacity or load factor of network technology
ϕ^{sto}	Capacity or load factor of storage technology
ϕ^{tech}	Capacity or load factor of supply technology
π^{tech}	Supply technology fuel costs
ψ^{net}	Network technology investment costs
ψ^{sto}	Storage technology investment costs
ψ^{tech}	Supply technology investment costs
D	Exogenous demand
l	Lifetime of infrastructure

Variables

N	Total consumption/production of all network technologies in a region
S	Total consumption/production of all storage technologies in a region
T	Total consumption/production of all supply technologies in a region
x^{net}	Network technology activity
$x^{sto,in}$	Storage technology input activity
$x^{sto,level}$	Amount stored in storage technology
$x^{sto,out}$	Storage technology output activity
x^{tech}	Supply technology activity
Z	Cumulative discounted cost over the simulation horizon
Z^{fix}	Total fixed costs

Z^{inv}	Total investment costs
$z^{net,new}$	New network technology capacity
$z^{net,ret}$	Retired network technology capacity
z^{net}	Existing network technology capacity
$z^{sto,new}$	New storage technology capacity
$z^{sto,ret}$	Retired storage technology capacity
z^{sto}	Existing storage technology capacity
$z^{tech,new}$	New supply technology capacity
$z^{tech,ret}$	Retired supply technology capacity
z^{tech}	Existing supply technology capacity
Z^{tot}	Total annual cost
Z^{var}	Total variable costs

D.1 Mathematical formulation of the planning model

This section presents the mathematical formulation of the supply planning model, as well as the sub-models used to estimate technology performance. The nonmenclature details the parameters and variables, with the model equations then defined.

D.1.1 Objective

The objective of the optimization is to identify the design (capacity) and activity variables of technology options included in the model that minimize the total discounted cost over the simulation horizon. The discounted cost is calculated as the annual cost of operation multiplied by the discount factor. The discount factor is weighted to reflect the multi-year decision-making (i.e., inter-temporal optimization across 5-year time steps). This yields the following objective function formulation:

$$\textbf{Min } Z = \sum_{y} \left(\delta_y \cdot Z_y^{tot} \right) \tag{D.1}$$

The model solves for the optimal variables subject to the constraints detailed below.

D.1.2 Resource balance with network flow and storage

To ensure demands are met, supply of each carrier within each region is constrained to be greater than the demand for the carrier in that region.

$$T_{r,c,y,m} + S_{r,c,y,m} + N_{r,c,y,m} \geq D_{r,c,y,m} \; \forall \; r,c,y,m \tag{D.2}$$

Carriers considered in the model are depicted in Figure (1) of the main text. Exogenous demands are defined for electricity, freshwater, and wastewater. Wastewater from the domestic and manufacturing sectors defined in this way are negative due to the contribution to resource availability.

Total consumption / production of carriers in each region by supply technologies is calculated with average conversion coefficients. These coefficients relate the activity of supply technologies to the consumption or production of a specific carrier (e.g., m^3 of water per kWh of electricity produced). Multiplying the activity of each technology by its activity ratio yields the total amount consumed or produced by a technology over the model period (1 month). These technology-level results are summed across the portfolio included to quantify the total transformation in each region:

$$T_{r,c,y,m} = \sum_{t,o} \varepsilon^{tech}_{t,c,o} \cdot x^{tech}_{r,t,o,y,m} \;\forall\; r,c,y,m \tag{D.3}$$

We model electricity supply technologies across multiple operational modes to account for the effects of flexibility requirements, which are described in greater detail below.

A similar approach is used for storage technologies. Surface reservoirs and potable water storage at end-use are considered options for storing water between months. The need to track the storage level dynamically is addressed by breaking the storage activity into input and output components:

$$S_{r,c,y,m} = \sum_{s} \left(\varepsilon^{sto,out}_{s,c} \cdot x^{sto,out}_{r,s,y,m} - \varepsilon^{sto,in}_{s,c} \cdot x^{sto,in}_{r,s,y,m} \right) \;\forall\; r,c,y,m \tag{D.4}$$

Likewise, the total supply or consumption by network technologies are calculated by summing the total input and outputs across potential transmission pathways:

$$N_{r,c,y,m} = \sum_{rr,n} \left(\varepsilon^{net,out}_{rr,r,c,n} \cdot x^{net}_{rr,r,n,y,m} - \varepsilon^{net,in}_{r,rr,c,n} \cdot x^{net}_{r,rr,n,y,m} \right) \;\forall\; r,c,y,m \tag{D.5}$$

Network losses are incorporated in the framework, including energy use for water pumping with the procedure used to identify the network parameters detailed below.

For seasonal storage technologies, the level must also be balanced across time-periods. To ensure long-term sustainability of surface water reservoirs and prevent pre-filling of new storage investments (i.e., conservation of energy) we constrain the level at the end of the year to be equivalent to the initial value. These assumptions yield the following constraints:

$$x^{sto,level}_{r,s,y,m+1} = x^{sto,level}_{r,s,y,m} + x^{sto,in}_{r,s,y,m} - x^{sto,out}_{r,s,y,m} \;\forall\; r,s,y,m < m_f \tag{D.6}$$

$$x^{sto,level}_{r,s,y,m_f} + x^{sto,in}_{r,s,y,m_f} - x^{sto,out}_{r,s,y,m_f} = x^{sto,level}_{r,s,y,m_i} \;\forall\, r,s,y \tag{D.7}$$

D.1.3 Capacity adequacy

Operating flexibly impacts the efficiency and cost of power plants [208], and we distinguish between two operational modes for plants included to capture effects within the long-term modeling framework. The first mode represents steady or base-load operation, with the second mode representing flexible or load-following mode. Plants operating in load-following mode must be scheduled in advance, with the scheduled capacity required to move in both incremental and decremental directions to balance under and over forecast errors. This scheduling effect reduces the capacity available from power plants operating as a flexibility reserve. The scheduling impacts are emulated in the model by stipulating that power provided by power plants operating flexibly consumes twice the capacity as when it operates in base-load operation (i.e., capacity to move up or down is maintained in the flexible mode to account for scheduling). These assumptions yield the following capacity constraints for supply technologies:

$$\sum_{o} \left(\alpha^{tech}_{t,o} \cdot x^{tech}_{r,t,o,y,m} \right) \leq \phi^{tech}_{r,t,m} \cdot z^{tech}_{r,t,y} \;\forall\, r,t,y,m \tag{D.8}$$

$$\alpha^{tech}_{t,o} \cdot x^{tech}_{r,t,o,y,m} \leq \beta^{tech}_{t,o} \cdot \phi^{tech}_{r,t,m} \cdot z^{tech}_{r,t,y} \;\forall\, r,t,y,m \tag{D.9}$$

The load factor varies across months to reflect the variability of wind and solar generation. Water supply technologies are only considered to operate in a single operational mode with capacity usage assumed to scale one-to-one with activity.

To mitigate capacity constraints, new investments in capacity can be made in the model. Capacity retirements also accompany the decommissioning of ageing infrastructure. The capacity available in each year is therefore updated based on a balance of new investments and retirements:

$$z^{tech}_{r,t,y+1} = z^{tech}_{r,t,y} + z^{tech,new}_{r,t,y} + z^{tech,ret}_{r,t,y} \;\forall\, r,t,y < y_{end} \tag{D.10}$$

Forced retirements follow from a constraint on the lifetime of infrastructure:

$$z^{tech,ret}_{r,t,y+l_t} \geq z^{tech,new}_{r,t,y} \;\forall\, r,t,y < y_{end} - l_t \tag{D.11}$$

Similar capacity constraints are defined for storage:

$$x^{sto,level}_{r,s,y,m} \;\leq\; \phi^{sto}_{s} \cdot z^{sto}_{r,s,y} \;\forall\, r,s,y,m \tag{D.12}$$

$$z^{sto}_{r,s,y+1} = z^{sto}_{r,s,y} + z^{sto,new}_{r,s,y} + z^{sto,ret}_{r,s,y} \;\forall\, r,s,y < y_{end} \tag{D.13}$$

$$z^{sto,ret}_{r,s,y+l_s} \geq z^{sto,new}_{r,s,y} \;\forall\, r,t,y < y_{end} - l_s \tag{D.14}$$

For network technologies we reflect the bi-directional flow on possible pathways by constraining capacity in either direction to be equivalent and then divide the investment and operating costs equally between the pathways:

$$x^{net}_{r,rr,n,y,m} + x^{net}_{rr,r,n,y,m} \;\leq\; \phi^{net}_{n} \cdot z^{net}_{r,rr,n,y} \;\forall\, r,rr,n,y,m \tag{D.15}$$

$$z^{net}_{r,rr,n,y} = z^{net}_{rr,r,n,y} \;\forall\, r,rr,n,y \tag{D.16}$$

$$z^{net}_{r,rr,n,y+1} = z^{net}_{r,rr,n,y} + z^{net,new}_{r,rr,n,y} + z^{net,ret}_{r,rr,n,y} \;\forall\, r,rr,n,y < y_{end} \tag{D.17}$$

The current version of the model does not consider retirement of network technology or surface water reservoirs due to the selected simulation horizon (2050) and the long lifetimes typically associated with the infrastructure.

Minimum run requirements are included in the model to prevent fossil generation capacity contributing to reserve requirements without operating. We prescribed that the annual activity from power plants exceed 1% of installed capacity.

$$\sum_{o,m} x^{tech}_{r,t,o,y,m} \geq \mu \cdot z^{tech}_{r,t,y} \;\forall\, r,t,y \tag{D.18}$$

D.1.4 Cost accounting

Total costs of electricity and water system operation are calculated in each year by summing the investment, fixed and variable costs associated with each technology option:

$$Z_y^{tot} = Z_y^{inv} + Z_y^{fix} + Z_y^{var} \ \forall \ y \tag{D.19}$$

The investment costs are calculated based on the new capacity and no salvage value for retirements are currently considered.

$$Z_y^{inv} = \sum_{r,t} \left(\psi_{t,y}^{tech} \cdot z_{r,t,y}^{tech,new} \right) + \sum_{r,s} \left(\psi_{s,y}^{sto} \cdot z_{r,s,y}^{sto,new} \right) + \sum_{r,rr,y} \left(\psi_{n,r,rr,y}^{net} \cdot z_{r,rr,n,y}^{net,new} \right) \ \forall \ y \tag{D.20}$$

Similarly, fixed costs are calculated based on existing capacity:

$$Z_y^{fix} = \sum_{r,t} \left(\gamma_{t,y}^{tech} \cdot z_{r,t,y}^{tech} \right) + \sum_{r,s} \left(\gamma_{s,y}^{sto} \cdot z_{r,s,y}^{sto} \right) + \sum_{r,rr,y} \left(\gamma_{n,y}^{net} \cdot z_{r,rr,n,y}^{net} \right) \ \forall \ y \tag{D.21}$$

We only consider variable costs for supply technologies. Different costs are assumed for the operating modes to account for the cost of operating flexibly, and include fuel costs.

$$Z_y^{var} = \sum_{r,t,o,m} \left(\pi_{t,o,y}^{tech} \cdot x_{r,t,o,y,m}^{tech} \right) \ \forall \ y \tag{D.22}$$

D.1.5 Short-term electricity storage

Inter-temporal dispatch of short-term electricity storage is set exogenously, by defining a set number of recharge intervals per season and a minimum discharge time. Due to efficiency losses, the storage unit represents net seasonal energy consumption:

$$d = z \cdot \tau \cdot \left(\eta^2 - 1 \right) \cdot \xi \tag{D.23}$$

where d is the total electricity consumption, z is the installed capacity, τ is the minimum storage discharge time, η is the one-way storage efficiency, and ξ is the number of recharge intervals per season.The operational strategy for a typical pumped storage technology used for short-term purposes described in [218] is used to parameterize the storage model.

D.1.6 Energy for water conveyance

Energy requirements for water conveyance are parameterized after the analysis in [211]. The Darcy-Weisbach equation is used to estimate head losses due to turbulent flow in the pipeline:

$$h_f = f \cdot \frac{v^2}{2g} \cdot \frac{\Delta L}{D} \tag{D.24}$$

where h_f is the head loss due to friction, g is the acceleration due to gravity, f is the friction factor, ΔL is the pipe length, v is the average fluid velocity, and D is the inside pipe diameter. We utilize the parameters described in [211] to estimate an average energy input per km of horizontal conveyance. For vertical pumping we consider the energy needed to lift an equivalent volume of water:

$$p = \rho \cdot g \cdot \Delta h \cdot V \tag{D.25}$$

where ρ is the density of water, Δh is the elevation change and V is the volume of water.

D.1.7 Implementation

The optimization model is written in the GNU Mathematical Programming Language (GMPL) and solved with the CPLEX barrier method.

D.2 Input data

D.2.1 Electricity generation technologies

The electricity generation technologies included in the model are listed in Table (D.1). The implemented cost and performance data for electricity generation are provided in Table (D.2). Power generation costs and heat rates for 2010 are estimated from [218, 219]. Cost multipliers for the different power plant cooling technology costs are used to generate future projections (section S2.4). Cost and efficiency impacts of operating the unit flexibly are estimated from [208]. Water performance of the different power generation technologies are taken from [20]. Costs for the different power plant cooling technologies are distinguished following an analysis with a power plant cost model [20]. Load control technology costs are estimated from the supply curves in [123], with the capacity constrained to be less than 10% of the total electricity demand in each time period. Cost uncertainty for load control is included by considering the range in supply curves reported in [123] and a similar range in cost reductions are assumed for storage. Technology vintages and locations, as well as committed investments (future capacity installations) are estimated from [174, 195–197] and are included in Table (D.3).

Carbon emissions from fossil fuel combustion are tracked and constrained in the model. We use the Intergovernmental Panel on Climate Change's default values for crude oil (73.3 kg / GJ) and natural gas (56.1 kg / GJ) [324].

D.2.2 Water supply technologies

The implemented cost and performance data for water supply technologies are provided in Table (D.4). The water supply technologies included are reverse osmosis (RO) desalination, multi-stage flash (MSF) desalination, rainwater harvesting, groundwater withdrawals, and surface water withdrawals. Desalination energy costs are taken from [181], and for RO, include enhanced energy recovery. Costs for rainwater harvesting are estimated using the data reported for a multifamily unit in [205]. Average available rainfall in each region is then used to identify a monthly capacity factor. Wastewater treatment costs are estimated from [217]. The electricity intensity of rainwater harvestng systems is estimated

Energy Carrier	Fuel	Technology	Cooling System	Model Name
Urban Electricity	Natural Gas	Combined-cycle	Once-through - Freshwater	NGCC OT
			Once-through - Seawater	NGCC SW
			Closed-loop - Freshwater	NGCC CL
			Air-cooled	NGCC AC
		Single-cycle	Once-through - Freshwater	NGST OT
			Once-through - Seawater	NGST SW
			Closed-loop - Freshwater	NGST CL
			Air-cooled	NGST AC
		Combustion turbine	-	NGGT
	Oil	Combined-cycle	Once-through - Freshwater	OLCC OT
			Once-through - Seawater	OLCC SW
			Closed-loop - Freshwater	OLCC CL
			Air-cooled	OLCC AC
		Single-cycle	Once-through - Freshwater	OLST OT
			Once-through - Seawater	OLST SW
			Closed-loop - Freshwater	OLST CL
			Air-cooled	OLST AC
		Combustion turbine	-	OLGT
	Nuclear		Once-through - Freshwater	NC OT
			Once-through - Seawater	NC SW
			Closed-loop - Freshwater	NC CL
	Geothermal		Once-through - Freshwater	GEO OT
			Once-through - Seawater	GEO SW
	Solar	Concentrating w/o thermal storage	Once-through - Freshwater	CSP OT
			Once-through - Seawater	CSP SW
			Closed-loop - Freshwater	CSP CL
			Air-cooled	CSP AC
		Concentrating w/ thermal storage	Once-through - Freshwater	CSPTS OT
			Once-through - Seawater	CSPTS SW
			Closed-loop - Freshwater	CSPTS CL
			Air-cooled	CSPTS AC
		Photovoltaic	-	PV
	Wind	Onshore	-	WND
	-	Load Control	-	LC
		Short-term Electricity storage	-	ELS
Rural Electricity	Oil	Combustion Turbine	-	Rural OLGT
	Solar	Photovoltaic	-	Rural PV
	-	Short-term Electricity storage	-	Rural ELS

Table D.1: Electricity supply technologies considered in the analysis.

Model name	Capital cost [\$/kW]	Fixed cost [\$/kW-yr]	Variable cost [\$/MWh]	Flexible cost [\$/MWh]	Baseload Heat rate [btu/kWh]	Flexible heat-rate [btu/kWh]	Load factor	ELCC	Water withdrawal [m^3/MWh]	Return flow [m^3/MWh]	Lifetime
NGCC OT	1023	15.37	3.27	2.17	6430	6816	0.85	0.9	39.8	39.3	30
NGCC CL	1064	15.98	3.40	2.17	6564	6958	0.85	0.9	0.7	0.1	30
NGCC AC	1105	16.60	3.53	2.17	6591	6986	0.85	0.9	-	-	30
NGCC SW	1023	15.37	3.27	2.17	6430	6816	0.85	0.9	-	-	30
NGGT	676	7.04	10.37	1.61	9750	10335	0.92	0.9	-	-	30
NGST OT	1159	16.18	3.27	2.05	10850	11501	0.85	0.9	132.8	131.2	30
NGST CL	1205	16.83	3.40	2.05	11033	11695	0.85	0.9	2.4	0.3	30
NGST AC	1251	17.47	3.53	2.05	12045	12767	0.85	0.9	-	-	30
NGST SW	1159	16.18	3.27	2.05	10850	11501	0.85	0.9	-	-	30
OLCC OT	1023	15.37	3.27	2.17	6430	6816	0.85	0.9	39.7	39.4	30
OLCC CL	1064	15.98	3.40	2.17	6564	6958	0.85	0.9	0.6	0.1	30
OLCC AC	1105	16.60	3.53	2.17	6591	6986	0.85	0.9	-	-	30
OLCC SW	1023	15.37	3.27	2.17	6430	6816	0.85	0.9	-	-	30
OLGT	676	7.04	10.37	1.61	9750	10335	0.92	0.9	-	-	30
OLST OT	1159	16.18	3.27	2.05	10850	11501	0.85	0.9	132.5	131.4	30
OLST CL	1205	16.83	3.40	2.05	11033	11695	0.85	0.9	2.1	0.4	30
OLST AC	1251	17.47	3.53	2.05	12045	12767	0.85	0.9	-	-	30
OLST SW	1159	16.18	3.27	2.05	10850	11501	0.85	0.9	-	-	30
NC OT	5530	93.28	2.14	2.05	-	-	0.90	0.9	176.6	175.0	30
NC CL	5751	97.01	2.23	2.05	-	-	0.90	0.9	5.7	1.2	30
NC SW	5530	93.28	2.14	2.05	-	-	0.90	0.9	-	-	30
GEO OT	6243	132.00	0.00	2.05	-	-	0.90	0.9	71.27	70.56	30
GEO SW	6243	132.00	0.00	2.05	-	-	0.90	0.9	-	-	30
CSP OT	5067	67.26	0.00	2.05	-	-	0.35	0.1	206.4	204.1	30
CSP CL	5270	69.95	0.00	2.05	-	-	0.34	0.1	3.5	3.4	30
CSP AC	5472	72.64	0.00	2.05	-	-	0.31	0.1	-	-	30
CSP SW	5067	67.26	0.00	2.05	-	-	0.35	0.1	-	-	30
CSPTS OT	7286	79.72	0.00	2.05	-	-	0.35	0.9	206.4	204.1	30
CSPTS CL	7577	82.90	0.00	2.05	-	-	0.31	0.9	3.5	3.4	30
CSPTS AC	7869	86.09	0.00	2.05	-	-	0.28	0.9	-	-	30
CSPTS SW	7286	79.72	0.00	2.05	-	-	0.35	0.9	-	-	30
PV	3873	24.69	0.00	0.00	-	-	0.35	0.1	-	-	30
WND	2213	39.55	0.00	0.00	-	-	0.35	0.1	-	-	30
LC	3000	0.01	0.00	0.00	-	-	0.90	0.9	-	-	20
ELS	3000	16.39	0.00	1.50	-	-	0.95	0.9	-	-	20
Rural OLGT	676	7.04	10.37	2.05	9750	10335	0.90	0.9	-	-	30
Rural PV	4183	27.75	0.00	0.00	-	-	0.35	0.9	-	-	30
Rural ELS	935	16.36	0.00	1.50	-	-	0.95	0.9	-	-	20

Table D.2: Cost and performance of electricity supply technologies implemented in the model. Heat rates are used to convert fossil fuel generation output to fuel consumption and emissions. The water requirements for seawater cooled plants are not tracked as there is no constraint on seawater withdrawals beyond coastline accessibility. ELCC = effective load carrying capacity: the fraction of installed capacity allocated to peak load carrying capability of the system.

Province	Power Generation Capacity [MW] NGCC AC	NGCC SW	NGST SW	NGST AC	NGGT	OLCC AC	OLCC SW	OLST SW	OLST AC	OLGT	Rural OLGT
Asir	0	0	0	0	0	0	0	0	0	572	0
Bahah	0	0	0	0	0	0	0	0	0	0	0
N. Borders	0	0	0	0	0	0	0	0	0	629	45
Jawf	0	0	0	0	0	0	0	0	0	214	0
Madinah	0	0	0	0	0	0	0	0	0	202	0
Quassim	0	0	0	0	0	0	0	0	0	493	0
Riyad	1992	0	0	1151	721	0	0	0	0	1296	21
E. Region	0	520	6003	0	916	0	0	0	0	2010	0
Ha'il	0	0	0	0	0	0	0	0	0	210	0
Jizan	0	0	0	0	0	0	0	2400	0	618	20
Makkah	0	0	0	0	0	0	2983	8625	0	1134	0
Najran	0	0	0	0	0	0	0	0	0	289	61
Tabuk	0	0	0	0	0	0	0	0	0	902	70
Total	1992	520	6003	1151	1637	0	2983	11025	0	8568	216

Table D.3: Estimated baseyear distribution of power generation in Saudi Arabia.

from [216]. Investment and fixed costs for groundwater and surface water are excluded as it is assumed that most of this infrastructure is already in place and no further expansion is considered in the model. Additional costs for surface and groundwater are accounted for by tracking the electricity used, which is assumed to be the primary component of supply costs.

The base-year distribution of unconventional water supply and wastewater treatment technologies in Saudi Arabia is provided in Table (D.5), and are estimated from the analysis in [177]. The distribution of surface reservoirs and precipitation by month is provided in Table (D.6) and is also estimated based on the analysis in [177].

D.2.3 Electricity transmission and water conveyance

The electricity transmission and water conveyance data implemented in the mode is summarized in Tables (D.7) and (D.8). Electricity transmission capacity data is difficult to obtain and we alternatively estimated existing and planned capacities between regions based on maps provided by the regional balancing area authority [213, 214]. Water conveyance capacity between regions is estimated from recent regional assessments [177, 180]. Transmission costs are taken from another electricity planning model with a similar representa-

Technology type	Capital cost [$/m^3/day]	Fixed cost [$/m^3/day]	Variable cost [$/m^3]	Electricity Demand [kWh/m^3]	Heat Demand [MJ/m^3]	Lifetime
Groundwater	-	-	0.01	0.3 - 0.8	-	-
Surface water	-	-	0.01	0.1 - 0.3	-	-
Rainwater Harvesting (RWH)	590	15	0	0 - 0.2	-	30
Primary Wastewater Treatment (WWTP)	1000	0	0.04	0.3 - 0.5	-	30
Wastewater Recycling (WWTT)	1500	0	0.04	0.8 - 1	-	30
Multi-stage Flash Desalination (MSF)	1850	0	0.1	10 - 16	200 - 250	30
Reverse Osmosis Desalination (RO)	1700	0	0.1	3 - 5	-	30

Table D.4: Cost and performance of water supply technologies implemented in the model. The range in reported energy intensities is used to parameterize a ”min”, ”mean”, and ”max” water performance scenario. The ”min” scenario is explored in the sensitivity analysis with the ”mean” scenario used in the other cases.

	Water Supply Capacity [MCM/yr]			
Province	MSF	RO	WWTP	Recycling
Asir	0	0	13	6
Bahah	0	0	0	0
N. Borders	0	0	0	0
Jawf	0	0	0	0
Madinah	117	39	59	28
Quassim	0	0	14	6
Riyad	0	0	267	128
E. Region	506	29	371	178
Ha’il	0	0	0	0
Jizan	1	0	0	0
Makkah	356	36	189	91
Najran	0	0	0	0
Tabuk	7	4	0	0
Total	986	108	913	438

Table D.5: Estimated baseyear distribution of unconventional water supply and wastewater treatment technologies in Saudi Arabia. WWTP = Primary wastewater treatment (not suitable for potable reuse).

Province	Precipitation [mm/yr]	Surface Storage [MCM/yr]	Monthly Precipitation Fraction Jan	Feb	Mar	Apr	May	Jun	Jul	Aug	Sep	Oct	Nov	Dec
Asir	278	411	0.06	0.06	0.14	0.22	0.19	0.03	0.07	0.10	0.02	0.02	0.04	0.03
Bahah	81	41	0.10	0.06	0.16	0.30	0.15	0.02	0.02	0.05	0.01	0.02	0.04	0.06
N. Borders	96	21	0.22	0.09	0.17	0.17	0.02	0.02	0.00	0.00	0.00	0.07	0.08	0.16
Jawf	67	0	0.25	0.00	0.09	0.16	0.00	0.03	0.00	0.04	0.11	0.17	0.03	0.12
Madinah	202	85	0.16	0.02	0.17	0.24	0.09	0.01	0.00	0.01	0.00	0.02	0.19	0.08
Quassim	145	6	0.15	0.07	0.18	0.20	0.10	0.00	0.00	0.00	0.00	0.03	0.17	0.11
Riyad	93	92	0.13	0.11	0.26	0.25	0.03	0.00	0.00	0.00	0.00	0.01	0.07	0.14
E. Region	90	0	0.25	0.08	0.06	0.14	0.04	0.00	0.00	0.00	0.00	0.00	0.20	0.24
Ha'il	101	13	0.18	0.19	0.12	0.11	0.05	0.00	0.00	0.00	0.05	0.09	0.13	0.08
Jizan	202	246	0.06	0.02	0.04	0.09	0.08	0.06	0.11	0.16	0.11	0.11	0.07	0.06
Makkah	202	336	0.19	0.01	0.06	0.11	0.01	0.00	0.01	0.05	0.05	0.13	0.20	0.19
Najran	22	90	0.00	0.43	0.02	0.05	0.17	0.15	0.00	0.07	0.00	0.11	0.00	0.00
Tabuk	120	7	0.15	0.24	0.13	0.09	0.05	0.00	0.00	0.00	0.05	0.07	0.11	0.12

Table D.6: Precipitation and surface water storage data implemented in the modeling framework.

tion [221], while water conveyance infrastructure costs are estimated from a recent analysis for Saudi Arabia [212]. No cost improvements for network technologies are considered in the model. Existing interprovincial water conveyance is estimated from [177], and includes a 360 MCM/yr connection between E. Region and Riyad, a 20 MCM/yr connection between E. Region and Qassim, and a 10 MCM/yr line between Makkah and Asir.

Network Technology	Capacity units	Capital cost [\$/capacity-km]	Fixed O&M [\$/capacity-yr]	Lifetime	Efficiency loss [%/km]
Electricity Transmission	kW	1.13	0.01	60	0.006
Freshwater Transfer	m^3/day	6.70	0.03	60	0.03

Table D.7: Estimated costs for network technologies.

D.2.4 Cost projections and senstivity

The long-term cost projections implemented in the model are provided in Table (D.9). An investment cost multplier is used to shift the base-year investment costs in future model

Province Start	Province End	Distance [km]	Elevation Δ [m]	Line Rating	Est. Capacity [MW]	Status
Asir	Riyad	954	-1788	1 X 380 kV	467	E
Asir	Jizan	200	-2360	2 X 380 kV	934	E
Asir	Makkah	600	-2123	1 X 380 kV	467	P
Asir	Najran	249	-1107	1 X 380 kV	467	E
Bahah	Makkah	311	-1878	1 X 380 kV	467	E
N. Borders	Jawf	163	30	1 X 380 kV	467	P
N. Borders	E. Region	966	-526	1 X 380 kV	467	E
Jawf	Ha'il	391	426	1 X 380 kV	467	E
Jawf	Makkah	467	194	1 X 380 kV	467	P
Madinah	Quassim	509	40	1 X 380 kV	467	E
Madinah	Ha'il	481	384	1 X 380 kV	467	P
Madinah	Makkah	441	-331	2 X 380 kV	934	E
Madinah	Tabuk	620	152	2 X 380 kV	934	E
Quassim	Riyad	359	-36	3 X 380 kV	1401	E
Quassim	E. Region	720	-638	1 X 380 kV	467	E
Quassim	Ha'il	269	344	1 X 380 kV	467	E
Riyad	E. Region	478	-602	4 X 380 kV	1868	E
Riyad	Makkah	876	-335	1 X 380 kV	467	P
Jizan	Makkah	702	237	1 X 380 kV	467	E
Jizan	Najran	328	1253	1 X 380 kV	467	E

Table D.8: Estimated baseyear distribution of electricity transmission technologies [213, 214]. Line ratings were converted to estimated transfer capabilities based on the historical transfer capabilities between zones described in [174]. Existing lines (status = E) are assumed to already be available in the baseyear, whereas planned lines (status = P) are assumed available in 2015.

years to reflect anticpated long-term improvements and uncertainties. Future cost changes for electricity generation technology are estimated from the recent projections released by the National Renewable Energy Labratory [220]. We specifically consider the min, mean, and max range projected in the NREL data to generate the cost multipliers. These multipliers are then applied to the costs listed in Table (D.2). For water supply technologies, moderate cost improvements are anticipated [181], and we alternatively vary the base-year captial costs according to the uncertainty ranges reported in [180, 181, 205, 217].

D.2.5 Resource potentials

Renewable energy potentials are derived for each province by defining an average monthly capacity factor (the fraction of total installed capacity that can be produced annually) for each technology. For solar energy, intra-annual geographic diversity is modeled using monthly observations of solar intensity from a number of measurement stations [214]. These data are then calibrated to reflect the anticipated performance of actual solar power systems (average capacity factor of 30%) estimated from a detailed technological assessment [325]. For wind energy, many of the best sites lie on the Western coast [187,214], and we constrain wind expansion to these provinces and assume an average capacity factor of 30%. Similarly, we constrain geothermal expansion to provinces with known geothermal potential [184].

Without connection to a hydrological model tracking surface water availability, the provincial distribution of surface water resources is assumed to follow the distribution of reservoir capacities [177]. We then model the monthly contribution of annual run-off following the historical spatial monthly precipitation distribution. Access to seawater is constrained to provinces with coastlines. For rainwater harvesting, the historical average precipitation is used to identify a monthly capacity factor in each region.

Technology	Scenario	2010	2015	2020	2025	2030	2035	2040	2045	2050
PV	min	1.00	0.50	0.29	0.29	0.29	0.29	0.29	0.29	0.29
	mid	1.00	0.52	0.43	0.36	0.29	0.29	0.29	0.29	0.29
	max	1.00	0.54	0.54	0.54	0.54	0.54	0.54	0.54	0.54
WND	min	1.00	0.71	0.67	0.65	0.63	0.63	0.63	0.63	0.63
	mid	1.00	0.78	0.76	0.74	0.74	0.73	0.73	0.73	0.73
	max	1.00	0.78	0.78	0.78	0.78	0.78	0.78	0.78	0.78
CSPTS	min	1.00	0.93	0.42	0.42	0.42	0.42	0.42	0.42	0.42
	mid	1.00	0.93	0.56	0.49	0.42	0.42	0.42	0.42	0.42
	max	1.00	0.93	0.70	0.70	0.70	0.70	0.70	0.70	0.70
CSP	min	1.00	0.93	0.42	0.42	0.42	0.42	0.42	0.42	0.42
	mid	1.00	0.93	0.56	0.49	0.42	0.42	0.42	0.42	0.42
	max	1.00	0.93	0.70	0.70	0.70	0.70	0.70	0.70	0.70
NGCC / OLCC	min	1.00	0.99	0.93	0.91	0.89	0.88	0.87	0.87	0.87
	mid	1.00	0.99	0.93	0.91	0.89	0.88	0.87	0.87	0.87
	max	1.00	0.99	0.93	0.91	0.89	0.88	0.87	0.87	0.87
NGGT / OLGT	min	1.00	0.92	0.89	0.87	0.85	0.83	0.83	0.83	0.83
	mid	1.00	0.92	0.89	0.87	0.85	0.83	0.83	0.83	0.83
	max	1.00	0.92	0.89	0.87	0.85	0.83	0.83	0.83	0.83
NC	min	1.00	0.97	0.85	0.83	0.80	0.78	0.76	0.76	0.76
	mid	1.00	0.97	0.85	0.83	0.80	0.78	0.76	0.76	0.76
	max	1.00	0.97	0.85	0.83	0.80	0.78	0.76	0.76	0.76
LC / ELS	min	1.00	1.00	0.50	0.33	0.33	0.33	0.33	0.33	0.33
	mid	1.00	1.00	0.67	0.50	0.33	0.33	0.33	0.33	0.33
	max	1.00	1.00	0.92	0.83	0.67	0.67	0.67	0.67	0.67
MSF	min	0.65	0.65	0.65	0.65	0.65	0.65	0.65	0.65	0.65
	mid	1.00	1.00	1.00	1.00	1.00	1.00	1.00	1.00	1.00
	max	1.35	1.35	1.35	1.35	1.35	1.35	1.35	1.35	1.35
RO	min	0.53	0.53	0.53	0.53	0.53	0.53	0.53	0.53	0.53
	mid	1.00	1.00	1.00	1.00	1.00	1.00	1.00	1.00	1.00
	max	1.47	1.47	1.47	1.47	1.47	1.47	1.47	1.47	1.47
RWH	min	0.75	0.75	0.75	0.75	0.75	0.75	0.75	0.75	0.75
	mid	1.00	1.00	1.00	1.00	1.00	1.00	1.00	1.00	1.00
	max	1.42	1.42	1.42	1.42	1.42	1.42	1.42	1.42	1.42
WWTT	min	0.75	0.75	0.75	0.75	0.75	0.75	0.75	0.75	0.75
	mid	1.00	1.00	1.00	1.00	1.00	1.00	1.00	1.00	1.00
	max	1.30	1.30	1.30	1.30	1.30	1.30	1.30	1.30	1.30

Table D.9: Investment cost multipliers for supply technologies.

D.3 Demand models

Demands for electricity and water occurring in the agricultural, domestic, and manufacturing sectors drive capacity expansion requirements and thus represent crucial model inputs. Econometric models are widely used to generate demand projections, and we apply a similar approach to generate demands for Saudi Arabia. We identify semi-logarithmic models between historical per capita GDP and domestic sector electricity and water withdrawal to reflect saturation of useful services with increasing income-level [223, 326]. Historical energy consumption data is obtained from the International Energy Agency [78], historical water data is obtained from the United Nations Food & Agricultural Organization [230], and historical socioeconomic indicators are obtained from the World Bank [170]. Least squares analysis is then used with these data to identify the models included in Table (D.10). Urban and rural income inequalities are estimated by downscaling national GDP following the procedure described in Grübler et al. [294]. Manufacturing demands are estimated with a similar model that treats downscaled provincial GDP as the independent variable, with electricity used for desalination subtracted from the baseyear data using the estimated capacity and energy intensity in 2010. Wastewater (return-flow) from the manufacturing and domestic sectors is estimated based on national consumption efficiencies taken from a recent global analysis [223].

Agricultural demand projections account for the additional relationship observed between irrigation water requirements and national agricultural policy. Historically, cereals were promoted and grown as an export crop, but due to irrigation requirements and the impact on groundwater, Saudi Arabia's agricultural policy recently moved towards phasing out this water intensive crop and in the direction of producing higher value fruits and vegetables for local consumption [227]. It can be expected that as income-levels increase in Saudi Arabia, the demand for higher value food products will as well [327], potentially leading to higher irrigation withdrawals to support cultivation locally. We reflect these anticipated income effects on agricultural water use by first removing the volume applied for cereals from the historical data based on a recent analysis of irrigation water demands [227], and then fitting a semi-logarithmic model between the remaining agricultural water demand and per capita GDP. Irrigation for cereal crops is assumed to stagnate post-2010. The majority of water withdrawn for irrigation is consumed, and for this reason we exclude return-flow from the agricultural sector. For agricultural electricity demand, we find no clear relationship with historical irrigation volumes and alternatively utilize the estimated baseyear agricultural water-energy intensity (kWh/m^3) for future projections.

For the demand projections, we utilize population, urbanization, and GDP projections aligned with the shared socioeconomic pathways (SSP) [172, 173, 224, 225]; the most recent socioeconomic scenarios put forward by the international global change research community. We specifically focus on the SSP2 scenario, a mid-range case reflecting a continuation of current trends (moderate sustainability policy and technology shifts). Although SSP2 is a moderate scenario (globally), in the specific case of Saudi Arabia it corresponds to substantial population and economic activity growth [172, 173].

We utilize the quantitative scenario data to generate a single national-level electricity and freshwater demand trajectory for each sector out to 2050, with the aggregated results depicted in Figure (D.5). Moderate levels of end-use technological change are included (1 % per year compound annual reduction), and reflect expected efficiency improvements driven by technological innovation. Positive growth coefficients are stipulated for electricity (1 % per year compound annual increase) due to the anticipated growth in electrified end-uses (e.g., air conditioning and electric vehicles). It is important to note that the resulting electricity demand trajectory is somewhat conservative to other recent projections [189]. The estimated national domestic and industrial demands are downscaled to the provincial level based on the population distribution, whereas agricultural demands are disaggregated following the historical distribution [230]. Monthly domestic electricity demands are decomposed based on historical trends [189]. Domestic and irrigation water demands are broken into monthly components based on the estimated moisture deficit, calculated across 1/4 degree grid cells and weighted based on population for domestic demands [231]. The distribution across each region is summarized in Table (D.11).

D.3.1 Sensitivity scenarios

Although the reference demand trajectories include improvements in energy efficiency, advanced conservation scenarios are defined to reflect uncertainties surrounding techno-

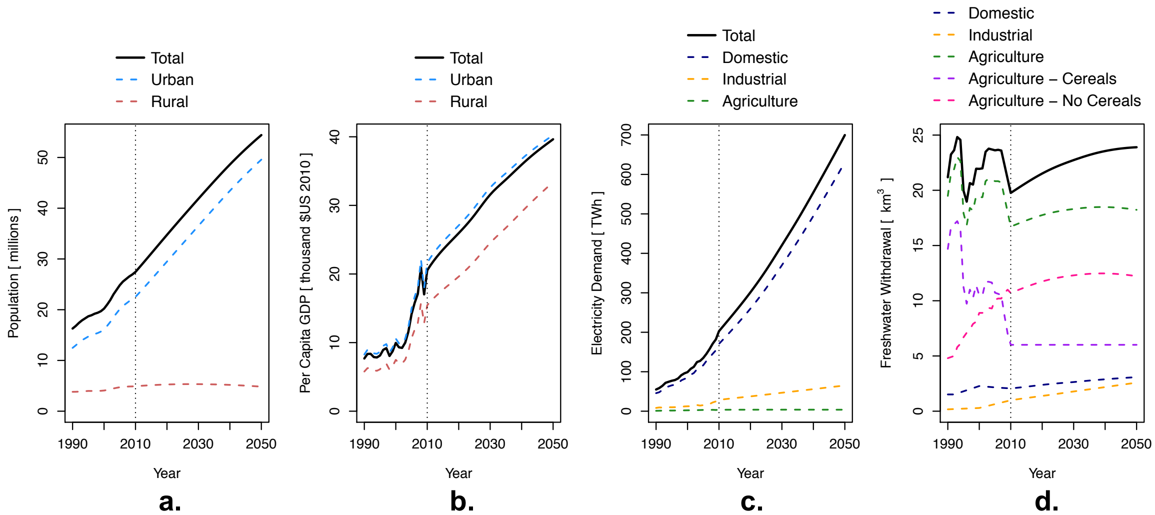

Figure D.1: National socioeconomic and demand projections for the SSP2 scenario. a. Population; b. Per capita GDP; c. Electricity demand; and d. Freshwater withdrawal. Industrial demands exclude electricity for desalination and cooling water for thermoelectric generation.

Sector	Resource	Demand Equation	Units	Model Parameters		
				a	b	λ
Domestic	Freshwater	$(a+b\cdot\ln g)\cdot\phi\cdot\lambda^y$	m^3/capita	356.96	-28.71	1.00
	Electricity	$(a+b\cdot\ln g)\cdot\phi\cdot\lambda^y$	kWh/capita	-15745.75	2194.47	1.01
Industrial	Freshwater	$(a+b\cdot\ln G)\cdot\phi\cdot\lambda^y$	km^3	-12.89	0.51	0.99
	Electricity	$(a+b\cdot\ln G)\cdot\phi\cdot\lambda^y$	km^3	-222.15	9.04	0.99
Agriculture	Freshwater	$(a+b\cdot\ln g)\cdot\phi\cdot\lambda^y$	m^3/capita	692.73	-29.16	0.99
	Electricity	$a\cdot\lambda^y$	kWh/m^3	0.22	-	0.99

Table D.10: Identified demand models for the domestic, industrial, and agricultural sectors. The parameter ϕ represents the base-year model error, and decays to unity along an exponential trajectory to represent convergence over time. Agriculture water requirements exclude irrigation for cereal crops, which is assumed to stagnate over future periods. G = GDP, and g = per capita GDP. Positive technological change parameters λ are stipulated for electricity due to the anticipated growth in electrified end-uses (e.g., air conditioning and electric vehicles) that may outpace autonomous efficiency improvements. Least-squares analysis is applied to identify model coefficients with data from IEA [78], FAO [230], and the World Bank [170].

Province	% Total	Monthly Demand Fraction Jan	Feb	Mar	Apr	May	Jun	Jul	Aug	Sep	Oct	Nov	Dec
Asir	1.9	0.075	0.077	0.079	0.086	0.089	0.096	0.09	0.087	0.089	0.084	0.075	0.074
Bahah	0.2	0.077	0.078	0.078	0.085	0.089	0.095	0.091	0.087	0.087	0.084	0.076	0.073
N. Borders	0.0	0.065	0.072	0.075	0.083	0.093	0.101	0.102	0.099	0.092	0.082	0.069	0.066
Jawf	8.8	0.067	0.071	0.076	0.083	0.093	0.101	0.101	0.099	0.092	0.081	0.069	0.066
Madinah	2.4	0.070	0.075	0.081	0.087	0.092	0.097	0.094	0.091	0.090	0.082	0.072	0.070
Quassim	18.8	0.068	0.073	0.078	0.088	0.092	0.097	0.097	0.093	0.091	0.083	0.071	0.069
Riyad	24.0	0.070	0.074	0.077	0.085	0.091	0.097	0.096	0.092	0.090	0.084	0.073	0.070
E. Region	9.2	0.071	0.075	0.078	0.086	0.092	0.097	0.094	0.091	0.089	0.083	0.074	0.070
Ha'il	10.8	0.068	0.072	0.077	0.086	0.093	0.099	0.098	0.096	0.091	0.082	0.071	0.067
Jizan	15.1	0.074	0.079	0.080	0.087	0.088	0.096	0.089	0.088	0.089	0.083	0.075	0.074
Makkah	3.8	0.073	0.077	0.081	0.086	0.090	0.095	0.091	0.088	0.090	0.083	0.074	0.073
Najran	1.1	0.073	0.077	0.080	0.086	0.089	0.097	0.089	0.088	0.088	0.083	0.075	0.073
Tabuk	4.0	0.069	0.073	0.077	0.086	0.092	0.099	0.098	0.095	0.090	0.081	0.071	0.068

Table D.11: Regional and monthly breakdown of irrigation requirements. Regional distribution is taken from FAO [230]. The percent total is used to disaggregate the national agricultural sector electricity and water demand projections to the provincial level, and is held constant over future periods. The monthly distribution is assumed to follow the moisture deficit, which is calculated across 1/4 degree grid cells and averaged across regions following the procedure described in [231].

logical change, price response, and end-use behaviour. The alternative scenarios are generated by varying the technological change parameter λ in Table 10 such that the demands decrease by 40% in the year 2050 relative to the reference scenario. This represents a potential for water and electricity conservation similar to that identified in recent analyses [39, 234]. The potential impacts of alternative food import policies on national irrigation withdrawals are also important to consider due to the fraction of total freshwater demand applied for irrigation. We explore a scenario investigating the potential for increased food imports to displace unconventional water resource expansion by simulating a 50% reduction in irrigation withdrawals by 2050. Finally, we combine all conservation measures to generate an *Optimistic* development scenario. The alternative demand scenarios are depicted in Figures 2 to 5 below.

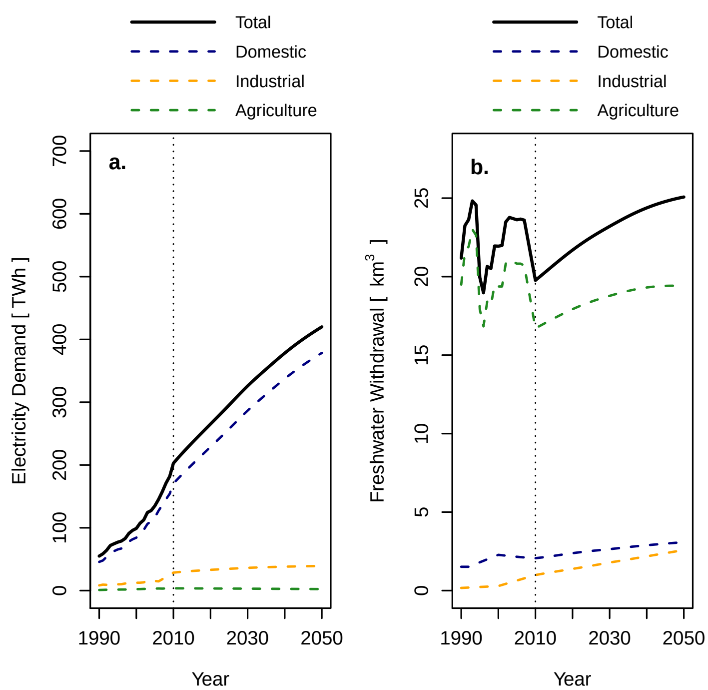

Figure D.2: Demand projections for the ”Electricity conservation” scenario. a. Electricity demand; and b. Freshwater withdrawal.

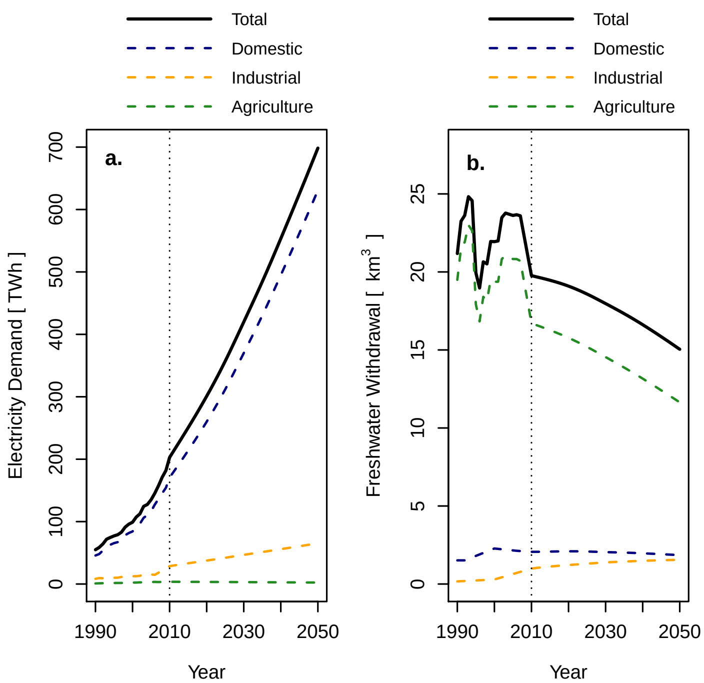

Figure D.3: Demand projections for the "Water conservation" scenario. a. Electricity demand; and b. Freshwater withdrawal.

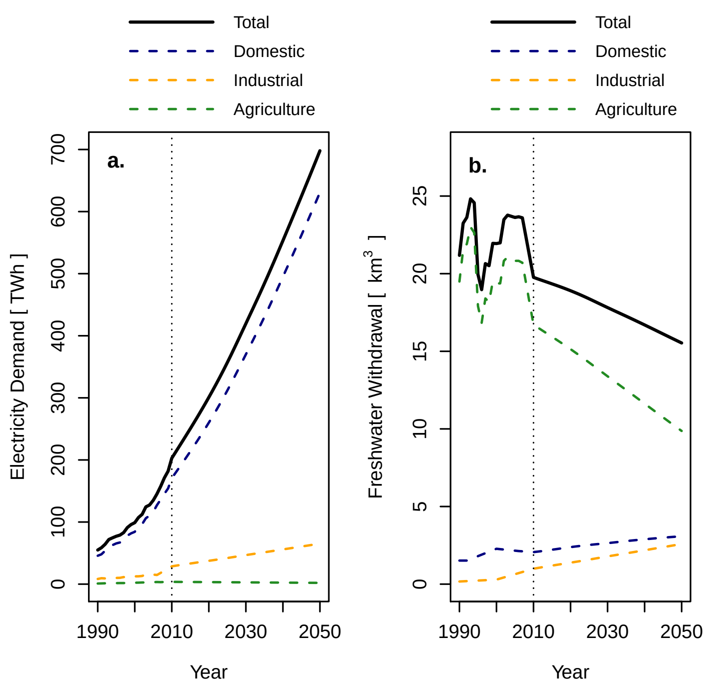

Figure D.4: Demand projections for the "Increased food imports" scenario. a. Electricity demand; and b. Freshwater withdrawal.

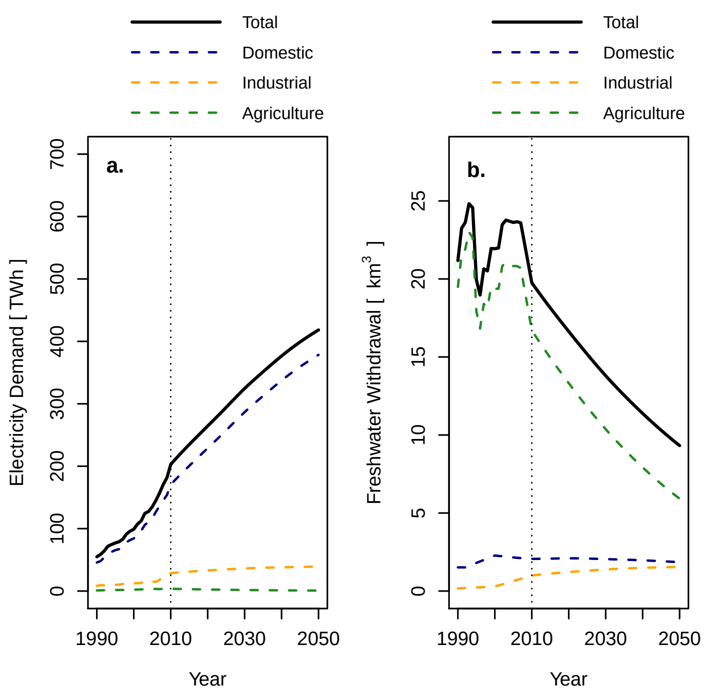

Figure D.5: Demand projections for the "Optimistic" scenario. a. Electricity demand; and b. Freshwater withdrawal.

D.4 Supplementary figures

D.4.1 Provincial delineation

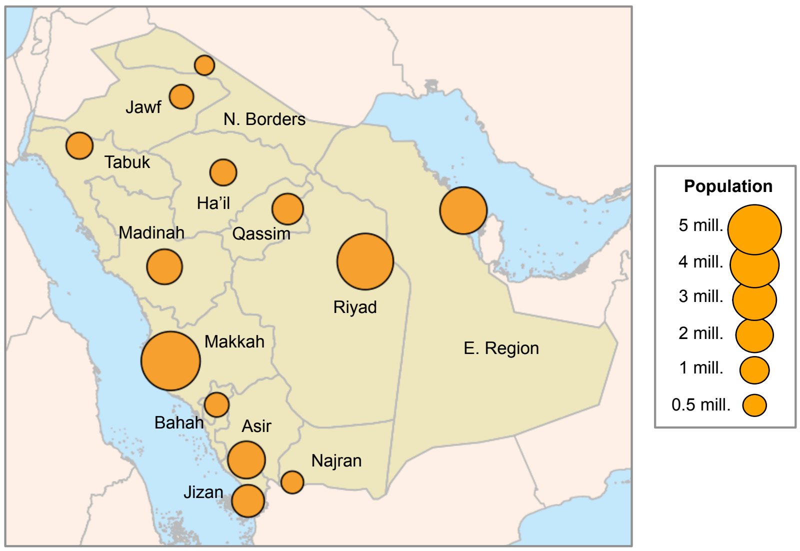

Figure D.6: Spatial extent of subnational regions considered in the model align with provincial administrative boundaries. The locations of provincial capital cities are used to estimated network parameters, and are depicted along with the estimated 2010 provincial population distribution.

D.4.2 Provincial technology distributions in 2050

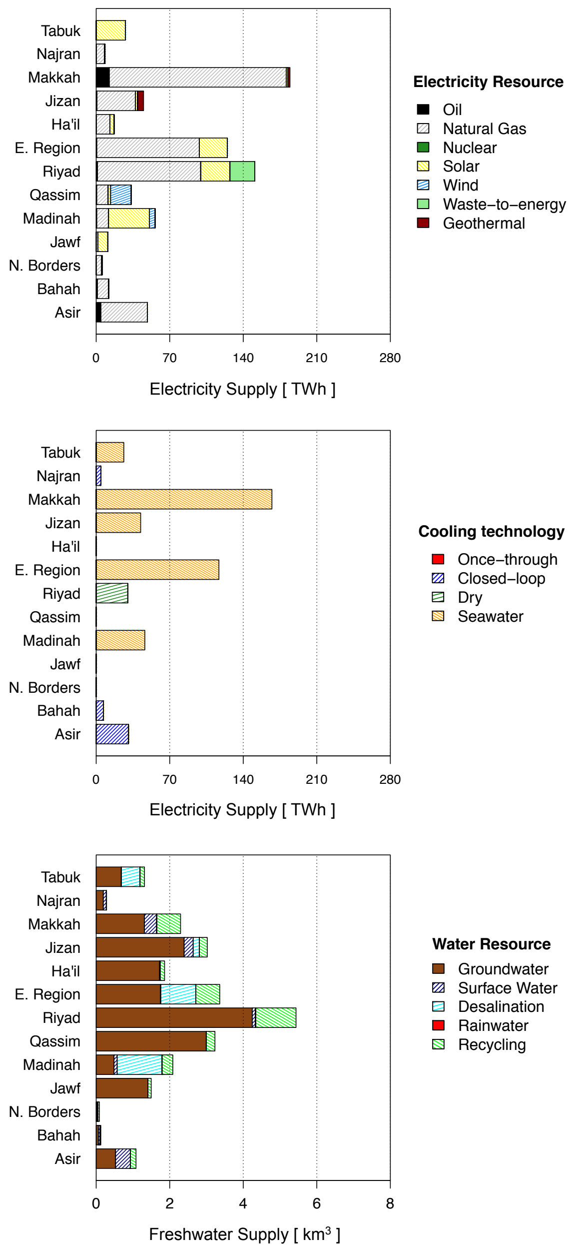

Figure D.7: **0% reduction in groundwater withdrawals, and 0% reduction in cumulative CO2 emissions**. Optimal supply technology distributions in 2050. Top: electricity supply by resource. Middle: electricity supply by cooling technology. Bottom: water supply by source.

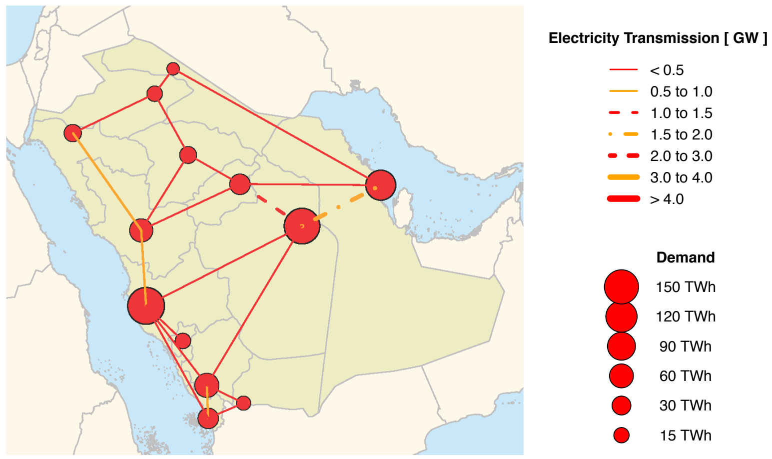

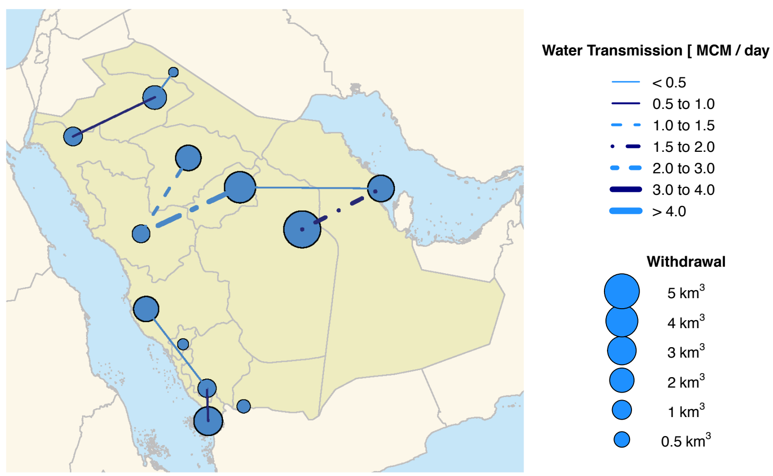

Figure D.8: **0% reduction in groundwater withdrawals, and 0% reduction in cumulative CO2 emissions**. Optimal network technology distributions in 2050. Top: interprovincial electricity network. Bottom: interprovincial freshwater network.

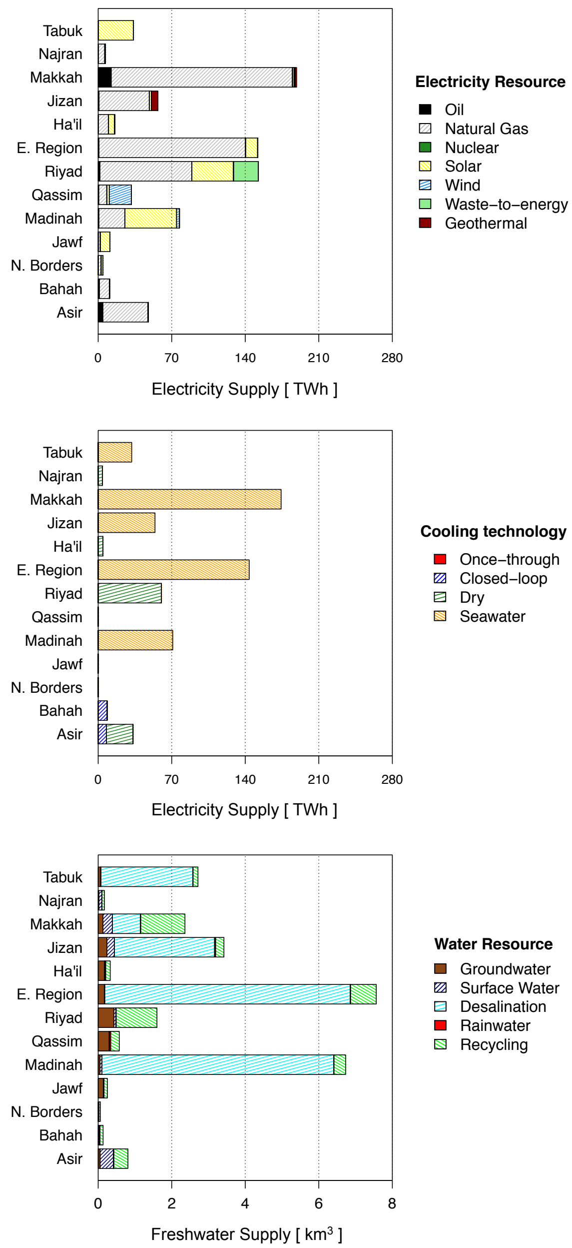

Figure D.9: **90% reduction in groundwater withdrawals, and 0% reduction in cumulative CO2 emissions**. Optimal supply technology distributions in 2050. Top: electricity supply by resource. Middle: electricity supply by cooling technology. Bottom: water supply by source.

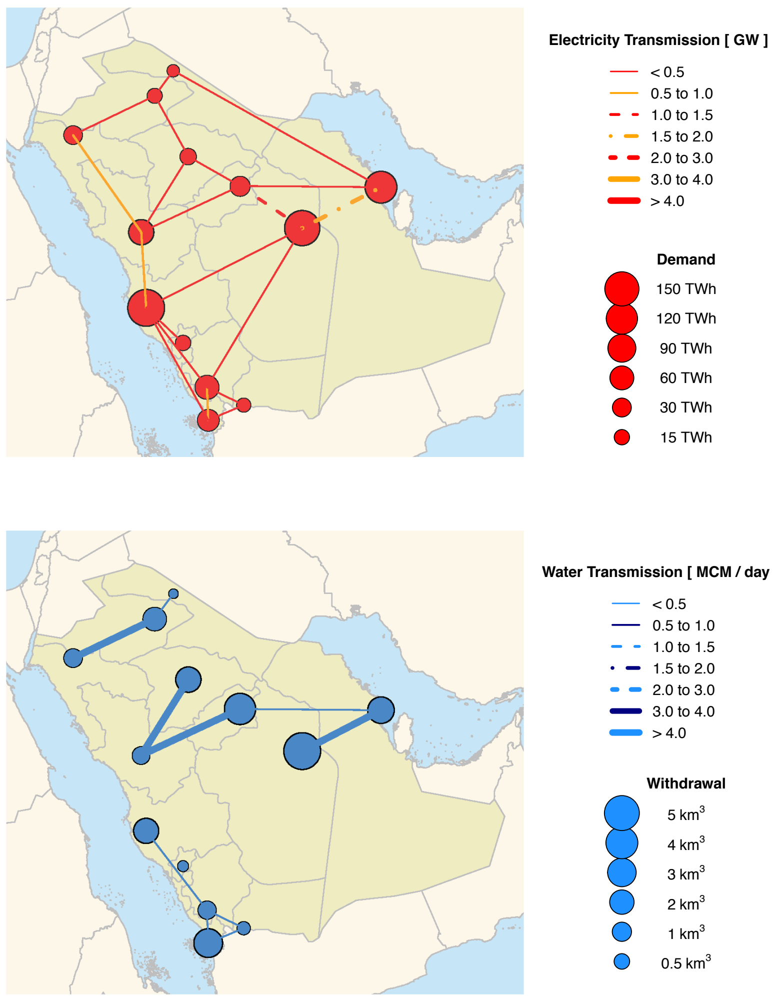

Figure D.10: **90% reduction in groundwater withdrawals, and 0% reduction in cumulative CO2 emissions**. Optimal network technology distributions in 2050. Top: interprovincial electricity network. Bottom: interprovincial freshwater network.

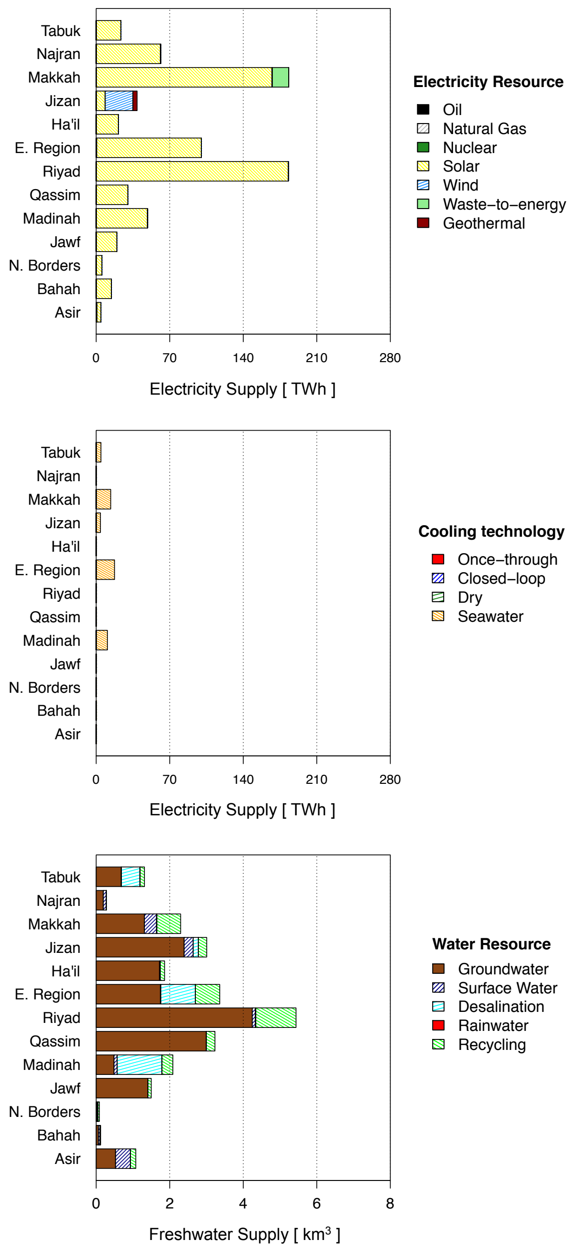

Figure D.11: **0% reduction in groundwater withdrawals, and 80% reduction in cumulative CO2 emissions**. Optimal supply technology distributions in 2050. Top: electricity supply by resource. Middle: electricity supply by cooling technology. Bottom: water supply by source.

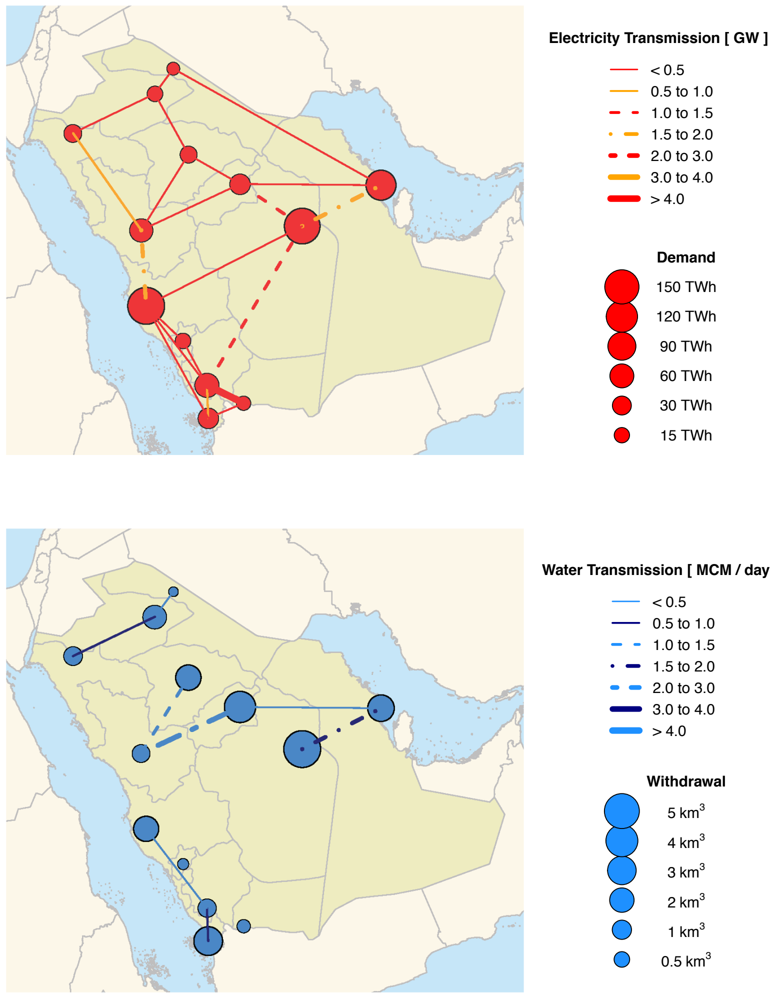

Figure D.12: **0% reduction in groundwater withdrawals, and 80% reduction in cumulative CO2 emissions**. Optimal network technology distributions in 2050. Top: interprovincial electricity network. Bottom: interprovincial freshwater network.

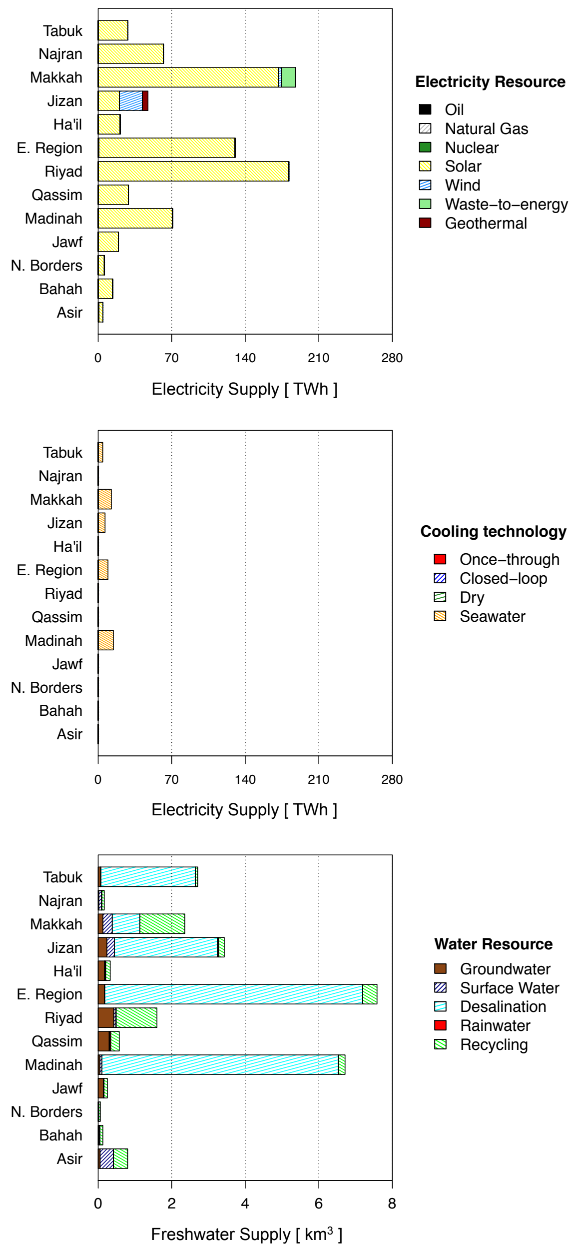

Figure D.13: **90% reduction in groundwater withdrawals, and 80% reduction in cumulative CO2 emissions**. Optimal supply technology distributions in 2050. Top: electricity supply by resource. Middle: electricity supply by cooling technology. Bottom: water supply by source.

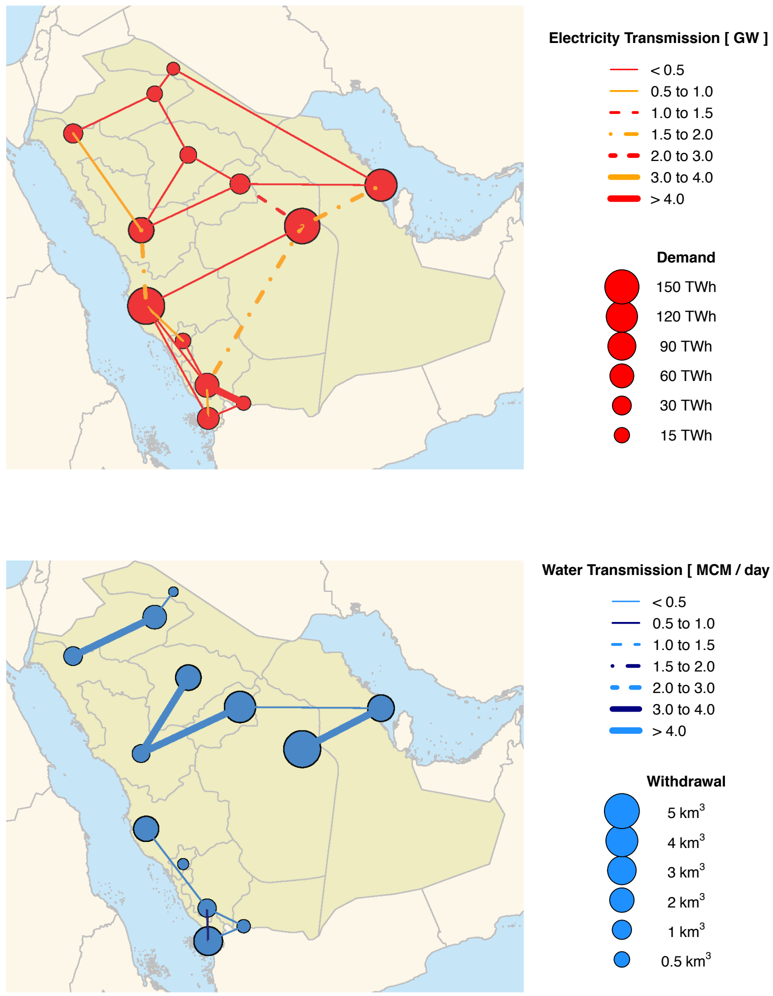

Figure D.14: **90% reduction in groundwater withdrawals, and 80% reduction in cumulative CO2 emissions**. Optimal network technology distributions in 2050. Top: interprovincial electricity network. Bottom: interprovincial freshwater network.

Appendix E

Supplementary material: Multi-criteria infrastructure planning for integrated water-energy systems

E.1 MCA process and implementation

This supplementary material describes in greater detail the MCA procedure applied in this paper and its implementation as an integrated software tool. This framework is embedded in the modular web-based tool for multiple criteria model analysis (MCMA) [254].

E.1.1 Process

Specification of the MCA starts with uploading the core model provided either in the standard mathematical programming system (MPS) format or as a General Algebraic Modeling System (GAMS) format model. In this paper, the core model is written in the GNU mathematical prgramming language and converted to MPS format. The names of the core model variables are presented to the user, who selects those to be used as criteria, and defines the corresponding criterion name and type (either minimization or maximization). The uploaded core model together with the criteria specification constitutes the MCA problem instance, definition of which triggers a set of optimization tasks necessary for computing the pay-off table, i.e., the values of utopia components and an approximation of the nadir. Computation of the pay-off table requires $4 \cdot K$ optimizations, where K is the number of selected criteria. After these computations are completed, the MCA problem instance is ready for interactive analysis. An option for defining more than one analysis instance is used in diverse situations, e.g., when problems are analyzed by several users or if a user wants to make several analyses each with a different focus. The initial analysis instance is generated automatically. Subsequent instances are optionally created by the users whenever desired.

MCA is an iterative process supporting the user in the Pareto set exploration that aims at finding subsets of solutions with desired properties (e.g., cheap, or moderately priced, or expensive). Therefore each analysis is composed of iterations. To provide an initial view on the Pareto-set, several iterations are generated automatically. First, efficient solutions corresponding to each utopia component are generated by selfish optimization of the corresponding criterion, i.e., all other criteria are set to be inactive. Finally, an example of balanced preferences is generated by setting for each criterion the same relative (to the utopia/nadir range) levels of aspiration and reservation.

With the above summarized background information the user takes full control of further iterations. For each iteration the user analyzes the Pareto-solutions obtained in previous iterations, and considers which criteria he/she wants to improve and which should be compromised, and then sets values for each criterion of aspiration and reservation aiming at obtaining an efficient solution that fits their preferences (desired trade-offs between criteria values) better. At each iteration the multi-criteria problem is converted into an auxiliary parametric single-objective problem using the achievement scalarizing function given by (5.10), the solution of which provides a Pareto solution hopefully having a better trade-off between criteria than the previous solution.

Typically, the MCA users explore various areas of the Pareto frontier (e.g., cheap and expensive having the corresponding bad and good values of environmental criteria) before deciding which compromises between the criteria values fit best their preferences. Examples of this process are provided in Section 5.3, and more methodological background in [76, 243, 252, 253].

E.1.2 Implementation

The MCA of the model described in Section 5.2.2 was done with the MCMA, modular web-based tool for multiple criteria model analysis [254]. The MCMA tool implements the methodology described in Section 5.2.2 and enables analysis of models provided in either the standard MPS format for linear programming (LP) models or models specified in GAMS. In order to enable a proper MCA the core models should conform to specific requirements on the core model (i.e., outcome variables defined, no constraints due to preferences, optimization criterion ignored, etc.).

The workflow of the MCA implementation is actually hidden from the MCA users, who are guided through the MCA process (described in E.1.1) by a typical Graphical User Interface (GUI). The SEWP core model described in Section 5.2.3 is initially generated in the standard MPS format in the same way as for the traditional single-criterion optimization; only the constraints for objectives other than cost are not generated. Then the MCMA tool is used for the MCA process described in E.1.1. For each iteration (i.e., specification of aspiration and reservation values for each criterion) the following actions are executed:

- The interactively specified values of $\bar{q}_k$ and $\underline{q}_k$ are stored in a common data-base (DB).

- The GUI calls the multi-criteria (MC)-solver, which generates the MC-part of the MCA, and queues the corresponding Optimization Task (OT).

- A dedicated utility called Task Manager (TM) distributes the OTs over the workstations with the available optimizers (same solvers as used for the single criterion model optimization).

- A dedicated MC optimization-solver merges the MC-part with the core model into either the MPS standard file or a GAMS format model, and invokes the relevant solver for solving the corresponding LP problem. For the MCA of the SEWP model, the CPLEX solver is used.

- After the LP problem is solved, the MCO-solver extracts from the provided solution file values of criteria and uploads them into the DB.

- After the solution is uploaded into the DB, the MC-solver computes the elements of the graphical solution representation, and marks in the DB as available for the user.

- The status of computations related to each MCA iteration is updated in the DB by each software component. The GUI checks this status whenever the user wants to explore the results of the corresponding iteration, and provides the user with access to the relevant selected iteration of efficient solutions or to the information about the computation status of the iteration.

- In addition to the analysis in the criteria space typically supported by the GUI of the MCA tools, the user has access to full solutions provided by the solver of the optimization task. These solution can therefore be used for model-specific analysis (a sample of such analysis is shown in Section 5.3).

Bibliography

[1] IEA, "Chapter 17: Water for Energy," in *World Energy Outlook*, pp. 1–33, International Energy Agency, 2012.

[2] S. G. Rothausen and D. Conway, "Greenhouse-gas emissions from energy use in the water sector," *Nature Climate Change*, vol. 1, no. 4, pp. 210–219, 2011.

[3] IPCC, "Summary for Policy-makers," in *Climate Change 2013: The Physical Science Basis. Contribution of Working Group I to the Fifth Assessment Report of the Intergovernmental Panel on Climate Change*, pp. 1–33, Cambridge University Press, 2013.

[4] C. Paskal, "The vulnerability of energy infrastructure to environmental change," in *China and Eurasia Forum Quarterly*, vol. 8, pp. 149–163, 2010.

[5] R. Schaeffer, A. S. Szklo, A. F. Pereira de Lucena, B. S. Moreira Cesar Borba, L. P. Pupo Nogueira, F. P. Fleming, A. Troccoli, M. Harrison, and M. S. Boulahya, "Energy sector vulnerability to climate change: a review," *Energy*, vol. 38, no. 1, pp. 1–12, 2012.

[6] L. Schrattenholzer, A. Miketa, K. Riahi, and R. A. Roehrl, *Achieving a sustainable global energy system: Identifying possibilities using long-term energy scenarios*. Edward Elgar Publishing, 2004.

[7] S. Messner and M. Strubegger, "Users Guide for MESSAGE III," *Rep. WP-95-69, International Institute for Applied Systems Analysis, Laxenburg, Austria*, vol. 14, 1995.

[8] A. J. Seebregts, G. A. Goldstein, and K. Smekens, "Energy/environmental modeling with the MARKAL family of models," in *Operations Research Proceedings 2001*, pp. 75–82, Springer, 2002.

[9] M. Howells, H. Rogner, N. Strachan, C. Heaps, H. Huntington, S. Kypreos, A. Hughes, S. Silveira, J. DeCarolis, M. Bazillian, *et al.*, "OSeMOSYS: The open source energy modeling system: An introduction to its ethos, structure and development," *Energy Policy*, vol. 39, no. 10, pp. 5850–5870, 2011.

[10] V. Krey, "Global energy-climate scenarios and models: a review," *Wiley Interdisciplinary Reviews: Energy and Environment*, vol. 3, no. 4, pp. 363–383, 2014.

[11] D. L. McCollum, V. Krey, K. Riahi, P. Kolp, A. Grubler, M. Makowski, and N. Nakicenovic, "Climate policies can help resolve energy security and air pollution challenges," *Climatic Change*, vol. 119, no. 2, pp. 479–494, 2013.

[12] M. Bonsch, F. Humpenöder, A. Popp, B. Bodirsky, J. P. Dietrich, S. Rolinski, A. Biewald, H. Lotze-Campen, I. Weindl, D. Gerten, *et al.*, "Trade-offs between land and water requirements for large-scale bioenergy production," *GCB Bioenergy*, 2014.

[13] W. Gerbens-Leenes, A. Y. Hoekstra, and T. H. van der Meer, "The water footprint of bioenergy," *Proceedings of the National Academy of Sciences*, vol. 106, no. 25, pp. 10219–10223, 2009.

[14] M. I. Hejazi, N. Voisin, L. Liu, L. M. Bramer, D. C. Fortin, J. E. Hathaway, M. Huang, P. Kyle, L. R. Leung, H.-Y. Li, *et al.*, "21st century United States emissions mitigation could increase water stress more than the climate change it is mitigating," *Proceedings of the National Academy of Sciences*, vol. 112, no. 34, pp. 10635–10640, 2015.

[15] J. Macknick, S. Sattler, K. Averyt, S. Clemmer, and J. Rogers, "The water implications of generating electricity: Water use across the United States based on different electricity pathways through 2050," *Environmental Research Letters*, vol. 7, no. 4, p. 045803, 2012.

[16] E. A. Byers, J. W. Hall, and J. M. Amezaga, “Electricity generation and cooling water use: UK pathways to 2050,” *Global Environmental Change*, vol. 25, pp. 16–30, 2014.

[17] C. Cameron, W. Yelverton, R. Dodder, and J. J. West, “Strategic responses to CO2 emission reduction targets drive shift in US electric sector water use,” *Energy Strategy Reviews*, vol. 4, pp. 16–27, 2014.

[18] E. G. Davies, P. Kyle, and J. A. Edmonds, “An integrated assessment of global and regional water demands for electricity generation to 2095,” *Advances in Water Resources*, vol. 52, pp. 296–313, 2013.

[19] P. Kyle, E. G. Davies, J. J. Dooley, S. J. Smith, L. E. Clarke, J. A. Edmonds, and M. Hejazi, “Influence of climate change mitigation technology on global demands of water for electricity generation,” *International Journal of Greenhouse Gas Control*, vol. 13, pp. 112–123, 2013.

[20] O. Fricko, S. C. Parkinson, N. Johnson, M. Strubegger, M. T. van Vliet, and K. Riahi, “Energy sector water use implications of a 2 degree C climate policy,” *Environmental Research Letters*, vol. 11, no. 3, p. 034011, 2016.

[21] V. C. Tidwell, J. Macknick, K. Zemlick, J. Sanchez, and T. Woldeyesus, “Transitioning to zero freshwater withdrawal in the US for thermoelectric generation,” *Applied Energy*, vol. 131, pp. 508–516, 2014.

[22] EIA, “State Electricity Profiles 2014: `www.eia.gov/electricity/state/`; accessed august 2016.”

[23] M. Webster, P. Donohoo, and B. Palmintier, “Water-CO2 trade-offs in electricity generation planning,” *Nature Climate Change*, vol. 3, no. 12, pp. 1029–1032, 2013.

[24] S. Bouckaert, E. Assoumou, S. Selosse, and N. Maïzi, “A prospective analysis of waste heat management at power plants and water conservation issues using a global TIMES model,” *Energy*, vol. 68, pp. 80–91, 2014.

[25] A. Santhosh, A. M. Farid, and K. Youcef-Toumi, “Real-time economic dispatch for the supply side of the energy-water nexus,” *Applied Energy*, vol. 122, pp. 42–52, 2014.

[26] A. S. Stillwell, M. E. Clayton, and M. E. Webber, “Technical analysis of a river basin-based model of advanced power plant cooling technologies for mitigating water management challenges,” *Environmental Research Letters*, vol. 6, no. 3, p. 034015, 2011.

[27] A. Miara, C. J. Vörösmarty, R. J. Stewart, W. M. Wollheim, and B. Rosenzweig, “Riverine ecosystem services and the thermoelectric sector: Strategic issues facing the Northeastern United States,” *Environmental Research Letters*, vol. 8, no. 2, p. 025017, 2013.

[28] N. Buras, “Integration of Water Resource Constraints in Energy Models,” tech. rep., Systems Optimization Laboratory, Department of Operations Research, Stanford University, 1979.

[29] J. Matsumoto and L. W. Mays, “Capacity expansion model for large-scale water-energy systems,” *Water Resources Research*, vol. 19, no. 3, pp. 593–607, 1983.

[30] M. T. van Vliet, S. Vögele, and D. Rübbelke, “Water constraints on European power supply under climate change: Impacts on electricity prices,” *Environmental Research Letters*, vol. 8, no. 3, p. 035010, 2013.

[31] S. M. Cohen, K. Averyt, J. Macknick, and J. Meldrum, “Modeling climate-water impacts on electricity sector capacity expansion,” in *ASME 2014 Power Conference*, pp. 1–8, American Society of Mechanical Engineers, 2014.

[32] S. J. Pereira-Cardenal, H. Madsen, K. Arnbjerg-Nielsen, N. Riegels, R. Jensen, B. Mo, I. Wangensteen, and P. Bauer-Gottwein, “Assessing climate change impacts on the Iberian power system using a coupled water-power model,” *Climatic Change*, pp. 1–14, 2014.

[33] E. Ibanez, T. Magee, M. Clement, G. Brinkman, M. Milligan, and E. Zagona, "Enhancing hydropower modeling in variable generation integration studies," *Energy*, vol. 74, pp. 518–528, 2014.

[34] W. Mo, R. Wang, and J. B. Zimmerman, "Energy–Water Nexus Analysis of Enhanced Water Supply Scenarios: A Regional Comparison of Tampa Bay, Florida, and San Diego, California," *Environmental Science & Technology*, vol. 48, no. 10, pp. 5883–5891, 2014.

[35] A. Dubreuil, E. Assoumou, S. Bouckaert, S. Selosse, and N. Maızi, "Water modeling in an energy optimization framework–The water-scarce middle east context," *Applied Energy*, vol. 101, pp. 268–279, 2013.

[36] N. Al-Qattan, M. Ross, and A. K. Sunol, "A multi-period mixed integer linear programming model for water and energy supply planning in Kuwait," *Clean Technologies and Environmental Policy*, vol. 17, no. 2, pp. 485–499, 2015.

[37] W. Huang, D. Ma, and W. Chen, "Connecting water and energy: Assessing the impacts of carbon and water constraints on China's power sector," *Applied Energy*, vol. In Press, pp. 1–11, 2016.

[38] Y. Zhou and R. S. Tol, "Evaluating the costs of desalination and water transport," *Water Resources Research*, vol. 41, no. 3, 2005.

[39] M. D. Bartos and M. V. Chester, "The conservation nexus: Valuing interdependent water and energy savings in Arizona," *Environmental Science & Technology*, vol. 48, no. 4, pp. 2139–2149, 2014.

[40] A. S. Stillwell and M. E. Webber, "Geographic, technologic, and economic analysis of using reclaimed water for thermoelectric power plant cooling," *Environmental Science & Technology*, vol. 48, no. 8, pp. 4588–4595, 2014.

[41] D. J. Sailor and A. Pavlova, "Air conditioning market saturation and long-term response of residential cooling energy demand to climate change," *Energy*, vol. 28, no. 9, pp. 941–951, 2003.

[42] M. Isaac and D. P. Van Vuuren, "Modeling global residential sector energy demand for heating and air conditioning in the context of climate change," *Energy Policy*, vol. 37, no. 2, pp. 507–521, 2009.

[43] A. F. Hamlet, S.-Y. Lee, K. E. Mickelson, and M. M. Elsner, "Effects of projected climate change on energy supply and demand in the Pacific Northwest and Washington State," *Climatic Change*, vol. 102, no. 1-2, pp. 103–128, 2010.

[44] J. A. Dirks, W. J. Gorrissen, J. H. Hathaway, D. C. Skorski, M. J. Scott, T. C. Pulsipher, M. Huang, Y. Liu, and J. S. Rice, "Impacts of climate change on energy consumption and peak demand in buildings: A detailed regional approach," *Energy*, vol. 79, pp. 20–32, 2015.

[45] R. Bierkandt, M. Auffhammer, and A. Levermann, "US power plant sites at risk of future sea-level rise," *Environmental Research Letters*, vol. 10, no. 12, p. 124022, 2015.

[46] S. Bergstrom, B. Carlsson, M. Gardelin, G. Lindstrom, A. Pettersson, and M. Rummukainen, "Climate change impacts on runoff in Sweden-assessments by global climate models, dynamical downscaling and hydrological modelling," *Climate research*, vol. 16, no. 2, pp. 101–112, 2001.

[47] B. Lehner, G. Czisch, and S. Vassolo, "The impact of global change on the hydropower potential of europe: a model-based analysis," *Energy Policy*, vol. 33, no. 7, pp. 839–855, 2005.

[48] B. Schaefli, B. Hingray, A. Musy, *et al.*, "Climate change and hydropower production in the Swiss Alps: Quantification of potential impacts and related modelling uncertainties," *Hydrology and Earth System Sciences Discussions*, vol. 11, no. 3, pp. 1191–1205, 2007.

[49] H. Koch and S. Vögele, "Dynamic modelling of water demand, water availability and adaptation strategies for power plants to global change," *Ecological Economics*, vol. 68, no. 7, pp. 2031–2039, 2009.

[50] H. Förster and J. Lilliestam, "Modeling thermoelectric power generation in view of climate change," *Regional Environmental Change*, vol. 10, no. 4, pp. 327–338, 2010.

[51] M. T. van Vliet, J. R. Yearsley, F. Ludwig, S. Vögele, D. P. Lettenmaier, and P. Kabat, "Vulnerability of US and European electricity supply to climate change," *Nature Climate Change*, vol. 2, no. 9, pp. 676–681, 2012.

[52] H. Koch, S. Vögele, F. Hattermann, and S. Huang, "Hydro-climatic conditions and thermoelectric electricity generation–Part II: Model application to 17 nuclear power plants in Germany," *Energy*, vol. 69, pp. 700–707, 2014.

[53] M. D. Bartos and M. V. Chester, "Impacts of climate change on electric power supply in the Western United States," *Nature Climate Change*, vol. 5, no. 8, pp. 748–752, 2015.

[54] C. Zhang, L. D. Anadon, H. Mo, Z. Zhao, and Z. Liu, "Water-carbon trade-off in China's coal power industry," *Environmental Science & Technology*, vol. 48, no. 19, pp. 11082–11089, 2014.

[55] S. Pryor and R. Barthelmie, "Climate change impacts on wind energy: A review," *Renewable and Sustainable Energy Reviews*, vol. 14, no. 1, pp. 430–437, 2010.

[56] J. A. Crook, L. A. Jones, P. M. Forster, and R. Crook, "Climate change impacts on future photovoltaic and concentrated solar power energy output," *Energy & Environmental Science*, vol. 4, no. 9, pp. 3101–3109, 2011.

[57] T. Cheng, D. Hill, J. Beamer, and G. García-Medina, "Climate change impacts on wave and surge processes in a Pacific Northwest (USA) estuary," *Journal of Geophysical Research: Oceans*, vol. 120, no. 1, pp. 182–200, 2015.

[58] J. A. Sathaye, L. L. Dale, P. H. Larsen, G. A. Fitts, K. Koy, S. M. Lewis, and A. F. P. de Lucena, "Estimating impacts of warming temperatures on California's electricity system," *Global Environmental Change*, vol. 23, no. 2, pp. 499–511, 2013.

[59] S. C. Nierop, “Envisioning resilient electrical infrastructure: A policy framework for incorporating future climate change into electricity sector planning,” *Environmental Science & Policy*, vol. 40, pp. 78–84, 2014.

[60] J. T. Payne, A. W. Wood, A. F. Hamlet, R. N. Palmer, and D. P. Lettenmaier, “Mitigating the effects of climate change on the water resources of the Columbia River basin,” *Climatic Change*, vol. 62, no. 1-3, pp. 233–256, 2004.

[61] S. K. Tanaka, T. Zhu, J. R. Lund, R. E. Howitt, M. W. Jenkins, M. A. Pulido, M. Tauber, R. S. Ritzema, and I. C. Ferreira, “Climate warming and water management adaptation for California,” *Climatic Change*, vol. 76, no. 3-4, pp. 361–387, 2006.

[62] M. Jeuland, “Economic implications of climate change for infrastructure planning in transboundary water systems: An example from the Blue Nile,” *Water Resources Research*, vol. 46, no. 11, 2010.

[63] C. R. Connell-Buck, J. Medellín-Azuara, J. R. Lund, and K. Madani, “Adapting Californias water system to warm vs. dry climates,” *Climatic Change*, vol. 109, no. 1, pp. 133–149, 2011.

[64] P. Dowling, “The impact of climate change on the european energy system,” *Energy Policy*, vol. 60, pp. 406–417, 2013.

[65] R. Golombek, S. A. Kittelsen, and I. Haddeland, “Climate change: Impacts on electricity markets in Western Europe,” *Climatic change*, vol. 113, no. 2, pp. 357–370, 2012.

[66] Z. Khan, P. Linares, and J. García-González, “Adaptation to climate-induced regional water constraints in the spanish energy sector: An integrated assessment,” *Energy Policy*, vol. 97, pp. 123–135, 2016.

[67] A. F. P. de Lucena, R. Schaeffer, and A. S. Szklo, “Least-cost adaptation options for global climate change impacts on the Brazilian electric power system,” *Global Environmental Change*, vol. 20, no. 2, pp. 342–350, 2010.

[68] NWPPC, “Appendix L: Climate Change and Power Planning,” in *Sixth Northwest Conservation and Electric Power Plan*, pp. 1–20, Northwest Power Planning & Conservation Council, 2010.

[69] V. Taseska, N. Markovska, and J. M. Callaway, “Evaluation of climate change impacts on energy demand,” *Energy*, vol. 48, no. 1, pp. 88–95, 2012.

[70] M. Welsch, S. Hermann, M. Howells, H. H. Rogner, C. Young, I. Ramma, M. Bazilian, G. Fischer, T. Alfstad, and D. Gielen, “Adding value with CLEWS: Modelling the energy system and its interdependencies for Mauritius,” *Applied Energy*, vol. 113, pp. 1434–1445, 2014.

[71] L. L. Dale, N. Karali, D. Millstein, M. Carnall, S. Vicuña, N. Borchers, E. Bustos, J. OHagan, D. Purkey, C. Heaps, *et al.*, “An integrated assessment of water-energy and climate change in Sacramento, California: How strong is the nexus?,” *Climatic Change*, vol. 132, no. 2, pp. 223–235, 2015.

[72] Z. Khan, P. Linares, and J. García-González, “Integrating water and energy models for policy driven applications: A review of contemporary work and recommendations for future developments,” *Renewable and Sustainable Energy Reviews*, vol. 67, pp. 1123–1138, 2017.

[73] K. Calvin, M. Wise, L. Clarke, J. Edmonds, P. Kyle, P. Luckow, and A. Thomson, “Implications of simultaneously mitigating and adapting to climate change: Initial experiments using GCAM,” *Climatic Change*, vol. 117, no. 3, pp. 545–560, 2013.

[74] S. Hallegatte, “Strategies to adapt to an uncertain climate change,” *Global Environmental Change*, vol. 19, no. 2, pp. 240–247, 2009.

[75] S. Li, D. W. Coit, S. Selcuklu, and F. A. Felder, “Electric power generation expansion planning: Robust optimization considering climate change,” in *Industrial and Systems Engineering Research Conference*, pp. 1–8, 2014.

[76] A. Wierzbicki, M. Makowski, J. Wessels, *et al.*, *Model-based decision support methodology with environmental applications*. Kluwer Academic Publishing, 2000.

[77] D. Jornada and V. J. Leon, "Robustness methodology to aid multiobjective decision making in the electricity generation capacity expansion problem to minimize cost and water withdrawal," *Applied Energy*, vol. 162, pp. 1089–1108, 2016.

[78] IEA, "International Energy Agency Statistics: Saudi Arabia." `http://www.iea.org/countries/non-membercountries/saudiarabia/`, 2014. Last accessed: 2015-06-10.

[79] T. Gleeson, Y. Wada, M. F. Bierkens, and L. P. van Beek, "Water balance of global aquifers revealed by groundwater footprint," *Nature*, vol. 488, no. 7410, pp. 197–200, 2012.

[80] IPCC, "Summary for Policy-makers," in *Climate Change 2014: Impacts, Adaptation, and Vulnerability. Part A: Global and Sectoral Aspects. Contribution of Working Group II to the Fifth Assessment Report of the Intergovernmental Panel on Climate Change*, pp. 1–31, Cambridge University Press, 2014.

[81] S. N. Chandramowli and F. A. Felder, "Impact of climate change on electricity systems and markets: A review of models and forecasts," *Sustainable Energy Technologies and Assessments*, vol. 5, pp. 62–74, 2014.

[82] J.-C. Ciscar and P. Dowling, "Integrated assessment of climate impacts and adaptation in the energy sector," *Energy Economics, In Press*, pp. 1–10, 2014.

[83] N. Miller, J. Jin, K. Hayhoe, and M. Auffhammer, "Climate Change, Extreme Heat, and Electricity Demand in California," tech. rep., California Energy Commission, 2007.

[84] K. Madani, M. Guégan, and C. B. Uvo, "Climate change impacts on high-elevation hydroelectricity in California," *Journal of Hydrology*, vol. 510, pp. 153–163, 2014.

[85] R. Loulou, G. Goldstein, K. Noble, *et al.*, "Documentation for the MARKAL Family of Models," *Energy Technology Systems Analysis Programme*, pp. 65–73, 2004.

[86] M. Welsch, M. Howells, M. Bazilian, J. DeCarolis, S. Hermann, and H. Rogner, "Modelling elements of Smart Grids: Enhancing the OSeMOSYS (Open Source Energy Modelling System) code," *Energy*, vol. 46, no. 1, pp. 337–350, 2012.

[87] K. Hunter, S. Sreepathi, and J. F. DeCarolis, "Modeling for insight using Tools for Energy Model Optimization and Analysis (Temoa)," *Energy Economics*, vol. 40, pp. 339–349, 2013.

[88] M. R. Allen, P. A. Stott, J. F. Mitchell, R. Schnur, and T. L. Delworth, "Quantifying the uncertainty in forecasts of anthropogenic climate change," *Nature*, vol. 407, no. 6804, pp. 617–620, 2000.

[89] A. W. Wood, L. R. Leung, V. Sridhar, and D. Lettenmaier, "Hydrologic implications of dynamical and statistical approaches to downscaling climate model outputs," *Climatic change*, vol. 62, no. 1-3, pp. 189–216, 2004.

[90] N. S. Christensen, D. P. Lettenmaier, *et al.*, "A multimodel ensemble approach to assessment of climate change impacts on the hydrology and water resources of the colorado river basin," *Hydrology and Earth System Sciences Discussions*, vol. 11, no. 4, pp. 1417–1434, 2007.

[91] H. Fowler, S. Blenkinsop, and C. Tebaldi, "Linking climate change modelling to impacts studies: recent advances in downscaling techniques for hydrological modelling," *International Journal of Climatology*, vol. 27, no. 12, pp. 1547–1578, 2007.

[92] S. Hagemann, C. Chen, J. O. Haerter, J. Heinke, D. Gerten, and C. Piani, "Impact of a statistical bias correction on the projected hydrological changes obtained from three gcms and two hydrology models," *Journal of Hydrometeorology*, vol. 12, no. 4, pp. 556–578, 2011.

[93] M. Schnorbus, K. Bennett, A. Werner, and A. Berland, "Hydrologic impacts of climate change in the Peace, Campbell and Columbia watersheds, British Columbia, Canada," tech. rep., Pacific Climate Impacts Consortium, University of Victoria, 2011.

[94] N. Nakicenovic and R. Swart, "Special Report on Emissions Scenarios," *Special Report on Emissions Scenarios, Edited by Nebojsa Nakicenovic and Robert Swart, pp. 612. Cambridge, UK: Cambridge University Press.*, vol. 1, 2000.

[95] D. P. Van Vuuren, J. Edmonds, M. Kainuma, K. Riahi, A. Thomson, K. Hibbard, G. C. Hurtt, T. Kram, V. Krey, J.-F. Lamarque, *et al.*, "The representative concentration pathways: an overview," *Climatic Change*, vol. 109, pp. 5–31, 2011.

[96] S. Messner, A. Golodnikov, and A. Gritsevskii, "A stochastic version of the dynamic linear programming model MESSAGE III," *Energy*, vol. 21, no. 9, pp. 775–784, 1996.

[97] J. E. Bistline and J. P. Weyant, "Electric sector investments under technological and policy-related uncertainties: A stochastic programming approach," *Climatic Change*, vol. 121, no. 2, pp. 143–160, 2013.

[98] R. Loulou and A. Kanudia, "Minimax regret strategies for greenhouse gas abatement: Methodology and application," *Operations Research Letters*, vol. 25, no. 5, pp. 219–230, 1999.

[99] S. Fuss, J. Szolgayova, M. Obersteiner, and M. Gusti, "Investment under market and climate policy uncertainty," *Applied Energy*, vol. 85, no. 8, pp. 708–721, 2008.

[100] Y. Cai, G. Huang, Z. Yang, and Q. Tan, "Identification of optimal strategies for energy management systems planning under multiple uncertainties," *Applied Energy*, vol. 86, no. 4, pp. 480–495, 2009.

[101] J. M. Mulvey, R. J. Vanderbei, and S. A. Zenios, "Robust optimization of large-scale systems," *Operations research*, vol. 43, no. 2, pp. 264–281, 1995.

[102] R. H. Moss, J. A. Edmonds, K. A. Hibbard, M. R. Manning, S. K. Rose, D. P. Van Vuuren, T. R. Carter, S. Emori, M. Kainuma, T. Kram, *et al.*, "The next generation of scenarios for climate change research and assessment," *Nature*, vol. 463, no. 7282, pp. 747–756, 2010.

[103] A. Sopinka and G. C. van Kooten, “Is BC a net power importer or exporter,” 2012.

[104] BCHydro, “Appendix 6B-2: Addendum to the Greenhouse Gas Reduction Scenarios of the Western Interconnection: (2010-2050),” in *BC Hydro 2013 Integrated Resource Plan*, BC Hydro, 2013.

[105] G. A. Meehl, C. Covey, K. E. Taylor, T. Delworth, R. J. Stouffer, M. Latif, B. McAvaney, and J. F. Mitchell, “The WCRP CMIP3 multimodel dataset: A new era in climate change research,” *Bulletin of the American Meteorological Society*, vol. 88, no. 9, pp. 1383–1394, 2007.

[106] A. Werner, “BCSD downscaled transient climate projections for eight select GCMs over British Columbia, Canada,” tech. rep., Pacific Climate Impacts Consortium, University of Victoria, 2011.

[107] X. Liang, E. F. Wood, and D. P. Lettenmaier, “Surface soil moisture parameterization of the vic-2l model: Evaluation and modification,” *Global and Planetary Change*, vol. 13, no. 1, pp. 195–206, 1996.

[108] BCHydro, “Appendix 2C: Hydrologic Impacts of Climate Change,” in *BC Hydro 2013 Integrated Resource Plan*, BC Hydro, 2013.

[109] BCHydro, “Columbia River Project Water Use plan,” tech. rep., BC Hydro, 2007.

[110] BCHydro, “Peace River Project Water Use plan,” tech. rep., BC Hydro, 2007.

[111] BCHydro, “Seven Mile River Project Water Use plan,” tech. rep., BC Hydro, 2007.

[112] BCHydro, “Campbell River Project Water Use plan,” tech. rep., BC Hydro, 2012.

[113] BCHydro, “Bridge River Project Water Use plan,” tech. rep., BC Hydro, 2007.

[114] Alcan, “Working with water: BC operations,” tech. rep., Rio Tinto Alcan, 2010.

[115] BCHydro, “Alcan/BC Hydro 2007 long-term electricity purchase agreement,,” tech. rep., BC Hydro, 2007.

[116] BCHydro, "BC Hydro Balancing Area Load Data, accessed March 2014, `http://transmission.bchydro.com/transmission_system/balancing_authority_load_data/`."

[117] BCHydro, "BC Station Data PCDS, Pacific Climate Impacts Consortium, accessed March 2014, `http://tools.pacificclimate.org/dataportal/`."

[118] D. J. Sailor and J. R. Muñoz, "Sensitivity of electricity and natural gas consumption to climate in the usa: Methodology and results for eight states," *Energy*, vol. 22, no. 10, pp. 987–998, 1997.

[119] B. Kiani, A. Rowe, P. Wild, L. Pitt, A. Sopinka, and T. F. Pedersen, "Optimal electricity system planning in a large hydro jurisdiction: Will British Columbia soon become a major importer of electricity?," *Energy Policy*, vol. 54, pp. 311–319, 2013.

[120] BCHydro, "Chapter 3: Resource Options," in *BC Hydro 2013 Integrated Resource Plan*, BC Hydro, 2013.

[121] T. Jones, "British Columbia electricity supply," tech. rep., Western Wilderness Committee, 2010.

[122] A. Sopinka, G. C. van Kooten, and L. Wong, "Can British Columbia achieve electricity self-sufficiency and meet its renewable portfolio standard?," tech. rep., University of Victoria, Department of Economics, Resource Economics and Policy Analysis Research Group, 2012.

[123] A. Lovins, *Reinventing fire: Bold business solutions for the new energy era*. Chelsea Green Publishing, 2013.

[124] S. C. Parkinson and N. Djilali, "Long-term energy planning with uncertain environmental performance metrics," *Applied Energy*, vol. 147, pp. 402–412, 2015.

[125] "Global Energy Assessment - Toward a Sustainable Future: Key Findings; Summary for Policymakers; Technical Summary," 2012.

[126] W. Moomaw, P. Burgherr, G. Heath, M. Lenzen, J. Nyboer, and A. Verbruggen, "Annex II: Methodology," in *IPCC Special Report on Renewable Energy Sources and Climate Change Mitigation*, pp. 974–998, IPCC, 2011.

[127] V. Fthenakis and H. C. Kim, "Land use and electricity generation: A life-cycle analysis," *Renewable and Sustainable Energy Reviews*, vol. 13, no. 6, pp. 1465–1474, 2009.

[128] M. Pehnt, "Dynamic life cycle assessment (lca) of renewable energy technologies," *Renewable energy*, vol. 31, no. 1, pp. 55–71, 2006.

[129] M. Hauck, Z. Steinmann, I. Laurenzi, R. Karuppiah, and M. Huijbregts, "How to quantify uncertainty and variability in life cycle assessment: the case of greenhouse gas emissions of gas power generation in the US," *Environmental Research Letters*, vol. 9, no. 7, p. 074005, 2014.

[130] N. Johnson, V. Krey, D. L. McCollum, S. Rao, K. Riahi, and J. Rogelj, "Stranded on a low-carbon planet: Implications of climate policy for the phase-out of coal-based power plants," *Technological Forecasting and Social Change*, vol. 90, pp. 89–102, 2015.

[131] V. Krey, D. Martinsen, and H.-J. Wagner, "Effects of stochastic energy prices on long-term energy-economic scenarios," *Energy*, vol. 32, no. 12, pp. 2340–2349, 2007.

[132] W. Usher and N. Strachan, "Critical mid-term uncertainties in long-term decarbonisation pathways," *Energy Policy*, vol. 41, pp. 433–444, 2012.

[133] B. D. Leibowicz, "Evaluation of post-Fukushima Japanese electricity strategies: A stochastic simulation model," *International Journal of Energy Research*, 2014.

[134] A. Gritsevskyi and N. Nakićenovic, "Modeling uncertainty of induced technological change," *Energy policy*, vol. 28, no. 13, pp. 907–921, 2000.

[135] E. Shittu, "Energy technological change and capacity under uncertainty in learning," *IEEE Transactions on Engineering Management*, vol. PP, no. 99, pp. 1–13, 2013.

[136] H. Chen and T. Ma, "Technology adoption with limited foresight and uncertain technological learning," *European Journal of Operational Research*, 2014.

[137] S. J. Stoyan and M. M. Dessouky, "A stochastic mixed-integer programming approach to the energy-technology management problem," *Computers & Industrial Engineering*, vol. 63, no. 3, pp. 594–606, 2012.

[138] M. Yang, W. Blyth, R. Bradley, D. Bunn, C. Clarke, and T. Wilson, "Evaluating the power investment options with uncertainty in climate policy," *Energy Economics*, vol. 30, no. 4, pp. 1933–1950, 2008.

[139] L. Fan, B. F. Hobbs, and C. S. Norman, "Risk aversion and CO2 regulatory uncertainty in power generation investment: Policy and modeling implications," *Journal of Environmental Economics and Management*, vol. 60, no. 3, pp. 193–208, 2010.

[140] S. Syri, A. Lehtilä, T. Ekholm, I. Savolainen, H. Holttinen, and E. Peltola, "Global energy and emissions scenarios for effective climate change mitigation: Deterministic and stochastic scenarios with the TIAM model," *International Journal of Greenhouse Gas Control*, vol. 2, no. 2, pp. 274–285, 2008.

[141] R. Loulou, M. Labriet, and A. Kanudia, "Deterministic and stochastic analysis of alternative climate targets under differentiated cooperation regimes," *Energy Economics*, vol. 31, pp. S131–S143, 2009.

[142] T. Ekholm, "Hedging the climate sensitivity risks of a temperature target," in *Risks, costs and equity: Modelling efficient strategies for climate and energy policy*, VTT Technical Research Centre of Finland, 2013.

[143] A. Kanudia and R. Loulou, "Robust responses to climate change via stochastic MARKAL: The case of Quebec," *European Journal of Operational Research*, vol. 106, no. 1, pp. 15–30, 1998.

[144] M.-C. Hu and B. F. Hobbs, "Analysis of multi-pollutant policies for the US power sector under technology and policy uncertainty using MARKAL," *Energy*, vol. 35, no. 12, pp. 5430–5442, 2010.

[145] F. Babonneau, A. Haurie, R. Loulou, and M. Vielle, “Combining stochastic optimization and Monte Carlo simulation to deal with uncertainties in climate policy assessment,” *Environmental Modeling & Assessment*, vol. 17, no. 1-2, pp. 51–76, 2012.

[146] E. De Cian and T. Massimo, “Mitigation portfolio and policy instruments when hedging against climate policy and technology uncertainty,” *Environmental Modeling & Assessment*, vol. 17, no. 1-2, pp. 123–136, 2012.

[147] L. Fan, C. S. Norman, and A. G. Patt, “Electricity capacity investment under risk aversion: A case study of coal, gas, and concentrated solar power,” *Energy Economics*, vol. 34, no. 1, pp. 54–61, 2012.

[148] M. Labriet, A. Kanudia, and R. Loulou, “Climate mitigation under an uncertain technology future: A TIAM-World analysis,” *Energy Economics*, vol. 34, pp. S366–S377, 2012.

[149] I. Keppo and B. van der Zwaan, “The impact of uncertainty in climate targets and CO2 storage availability on long-term emissions abatement,” *Environmental Modeling & Assessment*, vol. 17, no. 1-2, pp. 177–191, 2012.

[150] V. Krey and K. Riahi, “Risk hedging strategies under energy system and climate policy uncertainties,” in *Handbook of Risk Management in Energy Production and Trading*, pp. 435–474, Springer, 2013.

[151] Y. Li, G. Huang, and X. Chen, “Planning regional energy system in association with greenhouse gas mitigation under uncertainty,” *Applied Energy*, vol. 88, no. 3, pp. 599–611, 2011.

[152] A. Kanudia, M. Labriet, and R. Loulou, “Effectiveness and efficiency of climate change mitigation in a technologically uncertain world,” *Climatic Change*, pp. 1–16, 2012.

[153] G. Heinrich, L. Basson, B. Cohen, M. Howells, and J. Petrie, "Ranking and selection of power expansion alternatives for multiple objectives under uncertainty," *Energy*, vol. 32, no. 12, pp. 2350–2369, 2007.

[154] J. E. Bistline, "Electric sector capacity planning under uncertainty: Shale gas and climate policy in the US," in *31st USAEE/IAEE North American Conference. Austin, TX*, 2012.

[155] G. B. Dantzig, "Linear programming under uncertainty," *Management science*, vol. 1, no. 3-4, pp. 197–206, 1955.

[156] P. B. Hazell, "A linear alternative to quadratic and semivariance programming for farm planning under uncertainty," *American Journal of Agricultural Economics*, vol. 53, no. 1, pp. 53–62, 1971.

[157] J. A. Wicks and J. W. Guise, "An alternative solution to linear programming problems with stochastic input-output coefficients," *Australian Journal of Agricultural and Resource Economics*, vol. 22, no. 1, pp. 22–40, 1978.

[158] B. A. McCarl and T. H. Spreen, "Applied Mathematical Programming Using Algebraic Systems," 1997.

[159] A. Sopinka, G. Cornelis van Kooten, and L. Wong, "Reconciling self-sufficiency and renewable energy targets in a hydro dominated system: The view from British Columbia," *Energy Policy*, vol. 61, pp. 223–229, 2013.

[160] S. C. Parkinson and N. Djilali, "Robust response to hydro-climatic change in electricity generation planning," *Climatic Change*, vol. 130, no. 4, pp. 475–489, 2015.

[161] T. W. Hudiburg, B. E. Law, C. Wirth, and S. Luyssaert, "Regional carbon dioxide implications of forest bioenergy production," *Nature Climate Change*, vol. 1, no. 8, pp. 419–423, 2011.

[162] E.-D. Schulze, C. Körner, B. E. Law, H. Haberl, and S. Luyssaert, "Large-scale bioenergy from additional harvest of forest biomass is neither sustainable nor greenhouse gas neutral," *GCB Bioenergy*, vol. 4, no. 6, pp. 611–616, 2012.

[163] "B.C. Best Practices Methodology for Quantifying Greenhouse Gas Emissions," tech. rep., Government of Britich Columbia, Ministry of Environment, 2013.

[164] A. Brandt, G. Heath, E. Kort, F. OSullivan, G. Pétron, S. Jordaan, P. Tans, J. Wilcox, A. Gopstein, D. Arent, *et al.*, "Methane leaks from North American natural gas systems," *Science*, vol. 343, no. 6172, pp. 733–735, 2014.

[165] R. W. Howarth, R. Santoro, and A. Ingraffea, "Methane and the greenhouse-gas footprint of natural gas from shale formations," *Climatic Change*, vol. 106, no. 4, pp. 679–690, 2011.

[166] T. M. Wigley, "Coal to gas: The influence of methane leakage," *Climatic change*, vol. 108, no. 3, pp. 601–608, 2011.

[167] A. T. Dale, V. Khanna, R. D. Vidic, and M. M. Bilec, "Process based life-cycle assessment of natural gas from the Marcellus shale," *Environmental science & technology*, vol. 47, no. 10, pp. 5459–5466, 2013.

[168] C. L. Weber, P. Jaramillo, J. Marriott, and C. Samaras, "Life cycle assessment and grid electricity: What do we know and what can we know?," *Environmental science & technology*, vol. 44, no. 6, pp. 1895–1901, 2010.

[169] "Appendix 5B-2: Addendum Report Greenhouse Gas Price Forecast - Additional Scenarios," in *BC Hydro 2013 Integrated Resource Plan*, BC Hydro, 2013.

[170] World Bank, "World Bank Indicators." `http://data.worldbank.org/indicator`, 2014. Last accessed: 2015-10-11.

[171] Food and Agriculture Organization of the United Nations, "Groundwater Management in Saudi Arabia: Draft Synthesis Report," 2009.

[172] K. Samir and W. Lutz, "The human core of the shared socioeconomic pathways: Population scenarios by age, sex and level of education for all countries to 2100," *Global Environmental Change*, 2014.

[173] R. Dellink, J. Chateau, E. Lanzi, and B. Magne, "Long-term economic growth projections in the Shared Socioeconomic Pathways," *Global Environmental Change*, 2015.

[174] Center for Engineering Research, "Updated Generation Planning for the Saudi Electricity Sector," tech. rep., Electricity & Cogeneration Regulatory Authority, 2006.

[175] MEP, "Ministry of Economics and Planning, Saudi Arabia Ninth National Development Plan," 2009.

[176] G. Joodaki, J. Wahr, and S. Swenson, "Estimating the human contribution to groundwater depletion in the Middle East, from GRACE data, land surface models, and well observations," *Water Resources Research*, vol. 50, no. 3, pp. 2679–2692, 2014.

[177] S. Chowdhury and M. Al-Zahrani, "Characterizing water resources and trends of sector wise water consumptions in Saudi Arabia," *Journal of King Saud University-Engineering Sciences*, vol. 27, no. 1, pp. 68–82, 2015.

[178] P. Gleick, *The World's Water*. Pacific Institute, 2009.

[179] W. M. Zahid, "Wastewater Treatment Technologies For Water Reuse In Saudi Arabia, The 2nd Saudi International Water Technology Conference, King Abdulaziz City for Science and Technology," 2014.

[180] A. Kajenthira, A. Siddiqi, and L. D. Anadon, "A new case for promoting wastewater reuse in saudi arabia: Bringing energy into the water equation," *Journal of Environmental Management*, vol. 102, pp. 184–192, 2012.

[181] N. Ghaffour, T. M. Missimer, and G. L. Amy, "Technical review and evaluation of the economics of water desalination: current and future challenges for better water supply sustainability," *Desalination*, vol. 309, pp. 197–207, 2013.

[182] S. Rehman and A. Ahmad, "Assessment of wind energy potential for coastal locations of the Kingdom of Saudi Arabia," *Energy*, vol. 29, no. 8, pp. 1105–1115, 2004.

[183] F. Trieb and H. Müller-Steinhagen, "Concentrating solar power for seawater desalination in the Middle East and North Africa," *Desalination*, vol. 220, no. 1, pp. 165–183, 2008.

[184] H. Taleb, "Barriers hindering the utilisation of geothermal resources in Saudi Arabia," *Energy for Sustainable Development*, vol. 13, no. 3, pp. 183–188, 2009.

[185] K. Ummel, "Global prospects for utility-scale solar power: toward spatially explicit modeling of renewable energy systems," *Center for Global Development Working Paper*, no. 235, 2010.

[186] A. M. Bilton, R. Wiesman, A. Arif, S. M. Zubair, and S. Dubowsky, "On the feasibility of community-scale photovoltaic-powered reverse osmosis desalination systems for remote locations," *Renewable Energy*, vol. 36, no. 12, pp. 3246–3256, 2011.

[187] S. Shaahid, L. Al-Hadhrami, and M. Rahman, "Economic feasibility of development of wind power plants in coastal locations of Saudi Arabia: A review," *Renewable and Sustainable Energy Reviews*, vol. 19, pp. 589–597, 2013.

[188] M. T. Hussein, A. Lashin, A. Al Bassam, N. Al Arifi, and I. Al Zahrani, "Geothermal power potential at the western coastal part of Saudi Arabia," *Renewable and Sustainable Energy Reviews*, vol. 26, pp. 668–684, 2013.

[189] KACARE, "King Abdullah City for Atomic and Renewable Energy, Saudi Arabia's Renewable Energy Strategy and Solar Energy Deployment Roadmap," 2012.

[190] A. Dipaola, "Saudi Arabia Delays $109 Billion Solar Plant by 8 Years." `http://www.bloomberg.com/news/articles/2015-01-20/saudi-arabia-\delay-109-billion-solar-plant-by-8-years`, 2015. Last accessed: 2015-07-21.

[191] M. Al-Nory and M. El-Beltagy, "An energy management approach for renewable energy integration with power generation and water desalination," *Renewable Energy*, vol. 72, pp. 377–385, 2014.

[192] D. Letto, S. Snowling, R. George, C. Morrissey, H. Andres, and C. Fox, "Creating new revenue with existing processes: Evaluating grid balance with demand-side loads at wastewater treatment plants using dynamic modeling," *Proceedings of the Water Environment Federation*, vol. 2012, no. 12, pp. 4301–4322, 2012.

[193] T. Novosel, B. Ćosić, T. Pukšec, G. Krajačić, N. Duić, B. V. Mathiesen, H. Lund, and M. Mustafa, "Integration of renewables and reverse osmosis desalination: Case study for the Jordanian energy system with a high share of wind and photovoltaics," *Energy*, vol. 92, pp. 270–278, 2015.

[194] K. T. Sanders, "Critical review: Uncharted waters? The future of the electricity-water nexus," *Environmental Science & Technology*, vol. 49, no. 1, pp. 51–66, 2014.

[195] Alstom, "Alstom Case Study: Gas Product Solutions, Riyadh 12 - Saudi Arabia," 2013.

[196] "ACWA Power International, Combined Qurayyah IPP1 and 2: Addendum to Social and Environmental Assessment Report," 2011.

[197] "MAC Construction, PP9 1200 MW Combined-cycle Power Station," 2012.

[198] K. Gerdes and C. Nichols, "Netl: Water requirements for existing and emerging thermoelectric plant technologies," tech. rep., DOE/NETL, 2009.

[199] C. Turchi, M. Wagner, and C. Kutscher, "Water Use in Parabolic Trough Power Plants: Summary Results from WorleyParsons' Analyses," *NREL*, pp. 1–25, 2010.

[200] C. Zhang, L. D. Anadon, H. Mo, Z. Zhao, and Z. Liu, "Water-carbon trade-off in China's coal power industry," *Environmental Science & Technology*, vol. 48, no. 19, pp. 11082–11089, 2014.

[201] S. Atilhan, A. B. Mahfouz, B. Batchelor, P. Linke, A. Abdel-Wahab, F. Nápoles-Rivera, A. Jiménez-Gutiérrez, and M. M. El-Halwagi, "A systems-integration approach to the optimization of macroscopic water desalination and distribution networks: a general framework applied to Qatar's water resources," *Clean Technologies and Environmental Policy*, vol. 14, no. 2, pp. 161–171, 2012.

[202] S. C. Bhattacharyya and G. R. Timilsina, "A review of energy system models," *International Journal of Energy Sector Management*, vol. 4, no. 4, pp. 494–518, 2010.

[203] J. Swisher, G. Martino-Jannuzzi, and R. Redlinger, "Tools and Methods for Integrated Resource Planning: Improving Energy Efficiency and Protecting the Environment," tech. rep., United Nations Environment Programme, 1997.

[204] C. A. Scott, "The water-energy-climate nexus: Resources and policy outlook for aquifers in Mexico," *Water Resources Research*, vol. 47, no. 6, 2011.

[205] L. Domènech and D. Saurí, "A comparative appraisal of the use of rainwater harvesting in single and multi-family buildings of the Metropolitan Area of Barcelona (Spain): Social experience, drinking water savings and economic costs," *Journal of Cleaner Production*, vol. 19, no. 6, pp. 598–608, 2011.

[206] N. Nada, "Desalination in Saudi Arabia: An Overview," in *Water Arabia Conference & Exhibition*, pp. 1–44, Saudi Arabian Water Environment Association, 2013.

[207] P. Sullivan, V. Krey, and K. Riahi, "Impacts of considering electric sector variability and reliability in the MESSAGE model," *Energy Strategy Reviews*, vol. 1, no. 3, pp. 157–163, 2013.

[208] N. Kumar, P. Besuner, S. Lefton, and D. Agan, "Power Plant Cycling Costs," tech. rep., Inertek APTECH and National Renewable Energy Laboratory, 2012.

[209] S. C. Parkinson and N. Djilali, "Robust response to hydro-climatic change in electricity generation planning," *Climatic Change*, vol. 130, no. 4, pp. 475–489, 2015.

[210] B. R. Phillips and R. S. Middleton, "SimWIND: A geospatial infrastructure model for optimizing wind power generation and transmission," *Energy Policy*, vol. 43, pp. 291–302, 2012.

[211] A. S. Stillwell, C. W. King, and M. E. Webber, "Desalination and Long-Haul Water Transfer as a Water Supply for Dallas, Texas: A Case Study of the Energy-Water Nexus in Texas," *Texas Water Journal*, vol. 1, no. 1, pp. 33–41, 2010.

[212] T. M. Missimer, R. G. Maliva, N. Ghaffour, T. Leiknes, and G. L. Amy, "Managed Aquifer Recharge (MAR) Economics for Wastewater Reuse in Low Population Wadi Communities, Kingdom of Saudi Arabia," *Water*, vol. 6, no. 8, pp. 2322–2338, 2014.

[213] SEC, "Saudi Electricity Company Annual Report 2013," tech. rep., Saudi Electricity Company, 2013.

[214] King Abdullah City for Atomic and Renewable Energy, "Renwable Energy Resource Atlas." `https://rratlas.kacare.gov.sa/RRMMPublicPortal/`, 2014. Last accessed: 2015-06-10.

[215] M. T. Al-Nory, A. Brodsky, B. Bozkaya, and S. C. Graves, "Desalination supply chain decision analysis and optimization," *Desalination*, vol. 347, pp. 144–157, 2014.

[216] A. S. Vieira, C. D. Beal, E. Ghisi, and R. A. Stewart, "Energy intensity of rainwater harvesting systems: A review," *Renewable and Sustainable Energy Reviews*, vol. 34, pp. 225–242, 2014.

[217] H. E. Muga and J. R. Mihelcic, "Sustainability of wastewater treatment technologies," *Journal of Environmental Management*, vol. 88, no. 3, pp. 437–447, 2008.

[218] Black and Veatch, "Cost and Performance Data for Power Generation Technologies," tech. rep., National Renewable Energy Laboratory, 2013.

[219] EIA, "Updated Capital Cost Estimates for Utility Scale Electricity Generating Plants," tech. rep., United States Energy Information Association, 2013.

[220] "NREL, Annual Technology Baseline (ATB) workbook, October 2015."

[221] J. Johnston, A. Mileva, J. Nelson, and D. Kammen, "SWITCH-WECC: Data, Assumptions, and Model Formulation," tech. rep., Renewable and Appropriate Energy Laboratory, University of California Berkeley, 2013.

[222] K. Riahi, F. Dentener, D. Gielen, A. Grubler, J. Jewell, Z. Klimont, V. Krey, D. McCollum, S. Pachauri, and S. Rao, “Global Energy Assessment Chapter 17: Energy pathways for sustainable development,” 2012.

[223] M. Flörke, E. Kynast, I. Bärlund, S. Eisner, F. Wimmer, and J. Alcamo, “Domestic and industrial water uses of the past 60 years as a mirror of socio-economic development: A global simulation study,” *Global Environmental Change*, vol. 23, no. 1, pp. 144–156, 2013.

[224] B. C. O’Neill, E. Kriegler, K. Riahi, K. L. Ebi, S. Hallegatte, T. R. Carter, R. Mathur, and D. P. van Vuuren, “A new scenario framework for climate change research: the concept of shared socioeconomic pathways,” *Climatic Change*, vol. 122, no. 3, pp. 387–400, 2014.

[225] L. Jiang and B. C. O’Neill, “Global urbanization projections for the Shared Socioeconomic Pathways,” *Global Environmental Change*, 2015.

[226] J. M. Beltrán and S. Koo-Oshima, “Water desalination for agricultural applications,” *FAO Land and water discussion paper*, vol. 5, p. 48, 2006.

[227] O. K. Ouda, “Impacts of agricultural policy on irrigation water demand: A case study of Saudi Arabia,” *International Journal of Water Resources Development*, vol. 30, no. 2, pp. 282–292, 2014.

[228] U. Yermiyahu, A. Tal, A. Ben-Gal, A. Bar-Tal, J. Tarchitzky, and O. Lahav, “Rethinking desalinated water quality and agriculture,” *Science*, vol. 318, no. 5852, pp. 920–921, 2007.

[229] S. Assouline, D. Russo, A. Silber, and D. Or, “Balancing water scarcity and quality for sustainable irrigated agriculture,” *Water Resources Research*, 2015.

[230] FAO, “Food and Agriculture Organization of the United Nations, AQUASTAT - Saudi Arabia Profile.” `http://www.fao.org/nr/water/aquastat/main/index.stm`, 2014. Last accessed: 2015-06-10.

[231] S. C. Parkinson, N. Johnson, B. Jones, M. T. van Vliet, N. D. Rao, O. Fricko, K. Riahi, M. Florke, and N. Djilali, “Climate and human development impacts on municipal water demand: A spatially-explicit global modeling framework,” *Environmental Modelling & Software, In Press*, pp. 1–12, 2016.

[232] K. Frenken, “Irrigation in the middle east region in figures aquastat survey-2008.,” *Water Reports*, no. 34, 2009.

[233] J. D. Bredehoeft, “The water budget myth revisited: why hydrogeologists model,” *Groundwater*, vol. 40, no. 4, pp. 340–345, 2002.

[234] H. M. Taleb and S. Sharples, “Developing sustainable residential buildings in Saudi Arabia: A case study,” *Applied Energy*, vol. 88, no. 1, pp. 383–391, 2011.

[235] M. A. McNeil, V. E. Letschert, and J. Ke, “Bottom–Up Energy Analysis System (BUENAS): An international appliance efficiency policy tool,” *Energy Efficiency*, vol. 6, no. 2, pp. 191–217, 2013.

[236] IEA, “Chapter 17: Water for Energy,” in *World Energy Outlook*, pp. 1–33, International Energy Agency, 2012.

[237] M. Fripp, “Switch: a planning tool for power systems with large shares of intermittent renewable energy,” *Environmental science & technology*, vol. 46, no. 11, pp. 6371–6378, 2012.

[238] E. H. Beh, G. C. Dandy, H. R. Maier, and F. L. Paton, “Optimal sequencing of water supply options at the regional scale incorporating alternative water supply sources and multiple objectives,” *Environmental Modelling & Software*, vol. 53, pp. 137–153, 2014.

[239] M. Bekchanov, C. Ringler, A. Bhaduri, and M. Jeuland, “How would the Rogun Dam affect water and energy scarcity in Central Asia?,” *Water International*, vol. 40, no. 5-6, pp. 856–876, 2015.

[240] S. J. Pereira-Cardenal, B. Mo, A. Gjelsvik, N. D. Riegels, K. Arnbjerg-Nielsen, and P. Bauer-Gottwein, "Joint optimization of regional water-power systems," *Advances in Water Resources*, vol. 92, pp. 200–207, 2016.

[241] S. C. Parkinson, N. Djilali, V. Krey, O. Fricko, N. Johnson, Z. Khan, K. Sedraoui, and A. H. Almasoud, "Impacts of groundwater constraints on Saudi Arabia's low-carbon electricity supply strategy," *Environmental Science & Technology*, vol. 50, no. 4, pp. 1653–1662, 2016.

[242] D. L. McCollum, V. Krey, and K. Riahi, "An integrated approach to energy sustainability," *Nature Climate Change*, vol. 1, no. 9, pp. 428–429, 2011.

[243] M. Makowski, "Management of attainable tradeoffs between conflicting goals," *Journal of Computers*, vol. 4, no. 10, pp. 1033–1042, 2009.

[244] L. Duckstein and S. Opricovic, "Multiobjective optimization in river basin development," *Water Resources Research*, vol. 16, no. 1, pp. 14–20, 1980.

[245] M. Makowski, L. Somlyódy, and D. Watkins, "Multiple criteria analysis for water quality management in the Nitra basin," *Journal of the American Water Resources Association*, vol. 32, no. 5, pp. 937–951, 1996.

[246] S. Pohekar and M. Ramachandran, "Application of multi-criteria decision making to sustainable energy planning: A review," *Renewable & Sustainable Energy Reviews*, vol. 8, no. 4, pp. 365–381, 2004.

[247] M. Lehtveer, M. Makowski, F. Hedenus, D. McCollum, and M. Strubegger, "Multi-criteria analysis of nuclear power in the global energy system: Assessing trade-offs between simultaneously attainable economic, environmental and social goals," *Energy Strategy Reviews*, vol. 8, pp. 45–55, 2015.

[248] S. Sattler, J. Macknick, D. Yates, F. Flores-Lopez, A. Lopez, and J. Rogers, "Linking electricity and water models to assess electricity choices at water-relevant scales," *Environmental Research Letters*, vol. 7, no. 4, p. 045804, 2012.

[249] S. M. Lele, "Improved algorithms for reservoir capacity calculation incorporating storage-dependent losses and reliability norm," *Water Resources Research*, vol. 23, no. 10, pp. 1819–1823, 1987.

[250] N. Johnson, M. Strubegger, M. McPherson, S. C. Parkinson, V. Krey, and P. Sullivan, "A reduced-form approach for representing the impacts of wind and solar PV deployment on the structure and operation of the electricity system," *Energy Economics*, vol. In Press, pp. 1–11, 2016.

[251] A. P. Wierzbicki, "The use of reference objectives in multiobjective optimization," in *Multiple Criteria Decision Making Theory and Application*, pp. 468–486, Springer, 1980.

[252] J. Granat and M. Makowski, "Interactive specification and analysis of aspiration-based preferences," *European Journal of Operational Research*, vol. 122, no. 2, pp. 469–485, 2000.

[253] M. Makowski and A. P. Wierzbicki, "Modeling knowledge: Model-based decision support and soft computations," in *Applied Decision Support with Soft Computing*, pp. 3–60, Springer, 2003.

[254] M. Makowski and H. Ren, "IIASA Integrated Modeling Environment Project - Multiple Criteria Model Analysis (MCMA)." www.iiasa.ac.at/∼marek/mca_doc/mcma.html, 2016. Last accessed: 2016-06-12.

[255] B. C. ONeill, E. Kriegler, K. L. Ebi, E. Kemp-Benedict, K. Riahi, D. S. Rothman, B. J. van Ruijven, D. P. van Vuuren, J. Birkmann, K. Kok, *et al.*, "The roads ahead: Narratives for shared socioeconomic pathways describing world futures in the 21st century," *Global Environmental Change*, 2015.

[256] M. I. Hejazi, J. Edmonds, L. Clarke, P. Kyle, E. Davies, V. Chaturvedi, M. Wise, P. Patel, J. Eom, and K. Calvin, "Integrated assessment of global water scarcity over the 21st century under multiple climate change mitigation policies," *Hydrology and Earth System Sciences*, vol. 18, no. 8, pp. 2859–2883, 2014.

[257] N. Johnson, P. Burek, S. Parkinson, P. Havlik, N. Nakicenovic, K. Riahi, and D. Wiberg, "Modeling the energy-water-land nexus: A review of opportunities and challenges for integrated assessment modeling," in *Annual Meeting of the Integrated Assessment Modeling Consortium (IAMC), November 17, 2015*, pp. 1–15, 2015.

[258] C. J. Vörösmarty, P. Green, J. Salisbury, and R. B. Lammers, "Global water resources: Vulnerability from climate change and population growth," *Science*, vol. 289, no. 5477, pp. 284–288, 2000.

[259] J. Alcamo, P. Döll, T. Henrichs, F. Kaspar, B. Lehner, T. Rösch, and S. Siebert, "Development and testing of the WaterGAP 2 global model of water use and availability," *Hydrological Sciences Journal*, vol. 48, no. 3, pp. 317–337, 2003.

[260] N. W. Arnell, D. P. van Vuuren, and M. Isaac, "The implications of climate policy for the impacts of climate change on global water resources," *Global Environmental Change*, vol. 21, no. 2, pp. 592–603, 2011.

[261] Y. Wada, L. van Beek, D. Viviroli, H. H. Dürr, R. Weingartner, and M. F. Bierkens, "Global monthly water stress: 2. Water demand and severity of water stress," *Water Resources Research*, vol. 47, no. 7, 2011.

[262] I. Haddeland, J. Heinke, H. Biemans, S. Eisner, M. Flörke, N. Hanasaki, M. Konzmann, F. Ludwig, Y. Masaki, J. Schewe, *et al.*, "Global water resources affected by human interventions and climate change," *Proceedings of the National Academy of Sciences*, vol. 111, no. 9, pp. 3251–3256, 2014.

[263] G. van Drecht, A. Bouwman, J. Harrison, and J. Knoop, "Global nitrogen and phosphate in urban wastewater for the period 1970 to 2050," *Global Biogeochemical Cycles*, vol. 23, no. 4, 2009.

[264] R. I. McDonald, K. Weber, J. Padowski, M. Flörke, C. Schneider, P. A. Green, T. Gleeson, S. Eckman, B. Lehner, D. Balk, *et al.*, "Water on an urban planet: Urbanization and the reach of urban water infrastructure," *Global Environmental Change*, vol. 27, pp. 96–105, 2014.

[265] M. Hejazi, J. Edmonds, L. Clarke, P. Kyle, E. Davies, V. Chaturvedi, M. Wise, P. Patel, J. Eom, K. Calvin, *et al.*, "Long-term global water projections using six socioeconomic scenarios in an integrated assessment modeling framework," *Technological Forecasting and Social Change*, vol. 81, pp. 205–226, 2014.

[266] N. Hanasaki, S. Fujimori, T. Yamamoto, S. Yoshikawa, Y. Masaki, Y. Hijioka, M. Kainuma, Y. Kanamori, T. Masui, K. Takahashi, *et al.*, "A global water scarcity assessment under shared socio-economic pathways–Part 1: Water use," *Hydrology and Earth System Sciences*, vol. 17, no. 7, pp. 2375–2391, 2013.

[267] C. W. Howe and F. P. Linaweaver, "The impact of price on residential water demand and its relation to system design and price structure," *Water Resources Research*, vol. 3, no. 1, pp. 13–32, 1967.

[268] P. W. Mayer, W. B. DeOreo, E. M. Opitz, J. C. Kiefer, W. Y. Davis, B. Dziegielewski, and J. O. Nelson, *Residential end uses of water*. AWWA Research Foundation and American Water Works Association Denver, CO, 1999.

[269] J. Thompson, *Drawers of Water II: 30 years of change in domestic water use & environmental health in east Africa. Summary*, vol. 3. IIED, 2001.

[270] L. A. House-Peters and H. Chang, "Urban water demand modeling: Review of concepts, methods, and organizing principles," *Water Resources Research*, vol. 47, no. 5, 2011.

[271] S. J. Cohen, "Projected increases in municipal water use in the great lakes region due to CO2 induced climatic change," *JAWRA Journal of the American Water Resources Association*, vol. 23, no. 1, pp. 91–101, 1987.

[272] G. Dandy, T. Nguyen, and C. Davies, "Estimating residential water demand in the presence of free allowances," *Land Economics*, pp. 125–139, 1997.

[273] T. Downing, R. Butterfield, B. Edmonds, J. Knox, S. Moss, B. Piper, and E. Weatherhead, "Climate change and the demand for water," *DETR*, 2003.

[274] D. S. Gutzler and J. S. Nims, “Interannual variability of water demand and summer climate in Albuquerque, New Mexico,” *Journal of Applied Meteorology*, vol. 44, no. 12, pp. 1777–1787, 2005.

[275] T. C. Brown, R. Foti, and J. A. Ramirez, “Projected freshwater withdrawals in the United States under a changing climate,” *Water Resources Research*, vol. 49, no. 3, pp. 1259–1276, 2013.

[276] A. Thebo, P. Drechsel, and E. Lambin, “Global assessment of urban and peri-urban agriculture: irrigated and rainfed croplands,” *Environmental Research Letters*, vol. 9, no. 11, p. 114002, 2014.

[277] M. G. Badami and N. Ramankutty, “Urban agriculture and food security: A critique based on an assessment of urban land constraints,” *Global Food Security*, vol. 4, pp. 8–15, 2015.

[278] P. Gober, A. Brazel, R. Quay, S. Myint, S. Grossman-Clarke, A. Miller, and S. Rossi, “Using watered landscapes to manipulate urban heat island effects: how much water will it take to cool phoenix?,” *Journal of the American Planning Association*, vol. 76, no. 1, pp. 109–121, 2009.

[279] S. H. Kim, M. Hejazi, L. Liu, K. Calvin, L. Clarke, J. Edmonds, P. Kyle, P. Patel, M. Wise, and E. Davies, “Balancing global water availability and use at basin scale in an integrated assessment model,” *Climatic Change*, vol. 136, no. 2, pp. 217–231, 2016.

[280] D. Laucelli, L. Berardi, and O. Giustolisi, “Assessing climate change and asset deterioration impacts on water distribution networks: Demand-driven or pressure-driven network modeling?,” *Environmental Modelling & Software*, vol. 37, pp. 206–216, 2012.

[281] M. W. Jenkins, J. R. Lund, and R. E. Howitt, “Using economic loss functions to value urban water scarcity in california,” *Journal (American Water Works Association)*, vol. 95, no. 2, pp. 58–70, 2003.

[282] M. A. Cole, “Economic growth and water use,” *Applied Economics Letters*, vol. 11, no. 1, pp. 1–4, 2004.

[283] Y. Shen, T. Oki, N. Utsumi, S. Kanae, and N. Hanasaki, “Projection of future world water resources under SRES scenarios: Water withdrawal,” *Hydrological Sciences Journal*, vol. 53, no. 1, pp. 11–33, 2008.

[284] M. Hejazi, J. Edmonds, V. Chaturvedi, E. Davies, and J. Eom, “Scenarios of global municipal water-use demand projections over the 21st century,” *Hydrological Sciences Journal*, vol. 58, no. 3, pp. 519–538, 2013.

[285] B. Guo, Y. Chen, Y. Shen, W. Li, and C. Wu, “Spatially explicit estimation of domestic water use in the arid region of northwestern China: 1985–2009,” *Hydrological Sciences Journal*, vol. 58, no. 1, pp. 162–176, 2013.

[286] X. Cirera and E. Masset, “Income distribution trends and future food demand,” *Philosophical Transactions of the Royal Society B: Biological Sciences*, vol. 365, no. 1554, pp. 2821–2834, 2010.

[287] F. Cowell, *Measuring inequality*. Oxford University Press, 2011.

[288] J. Aitchison and J. A. Brown, *The Lognormal Distribution*. Cambridge University Press, 1966.

[289] B. J. van Ruijven, D. P. van Vuuren, B. J. de Vries, M. Isaac, J. P. van der Sluijs, P. L. Lucas, and P. Balachandra, “Model projections for household energy use in India,” *Energy Policy*, vol. 39, no. 12, pp. 7747–7761, 2011.

[290] U. A. Amarasinghe and V. Smakhtin, “Global water demand projections: past, present and future.,” tech. rep., International Water Management Institute (IWMI), 2014.

[291] A. Young, “Inequality, the urban-rural gap and migration,” *The Quarterly Journal of Economics*, p. qjt025, 2013.

[292] I. Koutiva and C. Makropoulos, "Modelling domestic water demand: An agent based approach," *Environmental Modelling & Software*, vol. 79, pp. 35–54, 2016.

[293] R. Koenker, "quantreg: Quantile Regression. R package version 4.10," 2007.

[294] A. Grübler, B. O'Neill, K. Riahi, V. Chirkov, A. Goujon, P. Kolp, I. Prommer, S. Scherbov, and E. Slentoe, "Regional, national, and spatially explicit scenarios of demographic and economic change based on SRES," *Technological Forecasting and Social Change*, vol. 74, no. 7, pp. 980–1029, 2007.

[295] A. Grübler, *Technology and global change*. Cambridge University Press, 2003.

[296] M. Smith, *CROPWAT: A computer program for irrigation planning and management*, vol. 46. UN FAO, 1992.

[297] P. Döll, "Impact of climate change and variability on irrigation requirements: a global perspective," *Climatic change*, vol. 54, no. 3, pp. 269–293, 2002.

[298] J. J. Boland, "Assessing urban water use and the role of water conservation measures under climate uncertainty," *Climatic Change*, vol. 37, no. 1, pp. 157–176, 1997.

[299] T. D. Johnson and K. Belitz, "A remote sensing approach for estimating the location and rate of urban irrigation in semi-arid climates," *Journal of Hydrology*, vol. 414, pp. 86–98, 2012.

[300] E. Domene and D. Saurí, "Urbanisation and water consumption: Influencing factors in the metropolitan region of Barcelona," *Urban Studies*, vol. 43, no. 9, pp. 1605–1623, 2006.

[301] L. Fan, G. Liu, F. Wang, V. Geissen, and C. J. Ritsema, "Factors affecting domestic water consumption in rural households upon access to improved water supply: Insights from the Wei River Basin, China," *PloS one*, vol. 8, no. 8, p. e71977, 2013.

[302] A. K. Marinoski, A. S. Vieira, A. S. Silva, and E. Ghisi, "Water end-uses in low-income houses in Southern Brazil," *Water*, vol. 6, no. 7, pp. 1985–1999, 2014.

[303] H. H. Zhang and D. F. Brown, "Understanding urban residential water use in Beijing and Tianjin, China," *Habitat International*, vol. 29, no. 3, pp. 469–491, 2005.

[304] W. Farmer, K. Strzepek, C. A. Schlosser, P. Droogers, and X. Gao, "A Method for Calculating Reference Evapotranspiration on Daily Time Scaler," tech. rep., MIT Joint Program on the Science and Policy of Global Change, 2011.

[305] M. S. Johnson, M. J. Lathuillière, T. R. Tooke, and N. C. Coops, "Attenuation of urban agricultural production potential and crop water footprint due to shading from buildings and trees," *Environmental Research Letters*, vol. 10, no. 6, p. 064007, 2015.

[306] B. Jones and B. ONeill, "Spatially explicit global population scenarios consistent with the Shared Socioeconomic Pathways," *Environmental Research Letters*, vol. 11, no. 8, p. 084003, 2016.

[307] B. Jones, "Assessment of a gravity-based approach to constructing future spatial population scenarios," *Journal of Population Research*, vol. 31, no. 1, pp. 71–95, 2014.

[308] K. E. Taylor, R. J. Stouffer, and G. A. Meehl, "An overview of CMIP5 and the experiment design," *Bulletin of the American Meteorological Society*, vol. 93, no. 4, pp. 485–498, 2012.

[309] S. Hempel, K. Frieler, L. Warszawski, J. Schewe, and F. Piontek, "A trend-preserving bias correction–the isi-mip approach," *Earth System Dynamics*, vol. 4, no. 2, pp. 219–236, 2013.

[310] ISI-MIP, "ISI-MIP database." http://esg.pik-potsdam.de, 2014. Last accessed: 2015-03-10.

[311] A. Kay, A. Rudd, H. Davies, E. Kendon, and R. Jones, "Use of very high resolution climate model data for hydrological modelling: baseline performance and future flood changes," *Climatic Change*, vol. 133, no. 2, pp. 193–208, 2015.

[312] M. Flörke, S. Eisner, N. Hanasaki, Y. Masaki, Y. Wada, and M. Bierkens, “A multi-model ensemble for identifying future water stress hotspots,” in *Impacts World 2013, International Conference on Climate Change Effects*, 2013.

[313] K. Riahi, S. Rao, V. Krey, C. Cho, V. Chirkov, G. Fischer, G. Kindermann, N. Nakicenovic, and P. Rafaj, “RCP 8.5: A scenario of comparatively high greenhouse gas emissions,” *Climatic Change*, vol. 109, no. 1-2, pp. 33–57, 2011.

[314] D. P. van Vuuren, E. Stehfest, M. G. den Elzen, T. Kram, J. van Vliet, S. Deetman, M. Isaac, K. K. Goldewijk, A. Hof, A. M. Beltran, *et al.*, “RCP2. 6: Exploring the possibility to keep global mean temperature increase below 2 degrees C,” *Climatic Change*, vol. 109, no. 1-2, pp. 95–116, 2011.

[315] W. Nordhaus, Q. Azam, D. Corderi, K. Hood, N. M. Victor, M. Mohammed, A. Miltner, and J. Weiss, “The G-Econ database on gridded output: Methods and data,” *Yale University, New Haven*, 2006.

[316] A. Sen, *Poverty and inequality in India: Getting closer to the truth.* New Delhi: Macmillan, 2003.

[317] L. Shi, “Changes in income inequality in China in the last three decades,” 2010.

[318] R. Kanbur and J. Zhuang, “Urbanization and inequality in Asia,” *Asian Development Review*, vol. 30, no. 1, pp. 131–147, 2013.

[319] G. H. Griffiths and E. William, “Pareto-Lognormal Income Distributions: Inequality and Poverty Measures, Estimation and Performance,” tech. rep., The University of Melbourne, 2012.

[320] PCIC, “Plan2adapt regional climate change database, accessed March 2014.”

[321] BCHydro, “Independent Power Producer List,” tech. rep., BC Hydro, 2011.

[322] A. Makhorin, “Modeling language GNU Mathprog,” *Relatório Técnico, Moscow Aviation Institute*, 2008.

[323] B. . Veatch, "Cost and Performance Data for Power Generation Technologies," tech. rep., Black & Veatch, Prepared for the National Renewable Energy Laboratory, 2012.

[324] "2006 IPCC Guidelines for National Greenhouse Gas Inventories," 2006.

[325] A. M. Al-Nasser, "Performance and economics of a solar thermal power generation plant in Jubail, Saudi Arabia: Parabolic trough collector," in *Energy Conference and Exhibition (EnergyCon), 2010 IEEE International*, pp. 752–757, IEEE, 2010.

[326] J. Eom, L. Clarke, S. H. Kim, P. Kyle, and P. Patel, "China's building energy demand: Long-term implications from a detailed assessment," *Energy*, vol. 46, no. 1, pp. 405–419, 2012.

[327] U. A. Schneider, P. Havlík, E. Schmid, H. Valin, A. Mosnier, M. Obersteiner, H. Böttcher, R. Skalskỳ, J. Balkovič, T. Sauer, *et al.*, "Impacts of population growth, economic development, and technical change on global food production and consumption," *Agricultural Systems*, vol. 104, no. 2, pp. 204–215, 2011.